

Northumbria Research Link

Citation: Bowe, Catherine (2015) Viability assessment of the probiotic spore former *B. Subtilis*: An investigation into the effect of in-vitro pig gastric conditions. Doctoral thesis, Northumbria University.

This version was downloaded from Northumbria Research Link:
<http://nrl.northumbria.ac.uk/id/eprint/27266/>

Northumbria University has developed Northumbria Research Link (NRL) to enable users to access the University's research output. Copyright © and moral rights for items on NRL are retained by the individual author(s) and/or other copyright owners. Single copies of full items can be reproduced, displayed or performed, and given to third parties in any format or medium for personal research or study, educational, or not-for-profit purposes without prior permission or charge, provided the authors, title and full bibliographic details are given, as well as a hyperlink and/or URL to the original metadata page. The content must not be changed in any way. Full items must not be sold commercially in any format or medium without formal permission of the copyright holder. The full policy is available online: <http://nrl.northumbria.ac.uk/policies.html>

VIABILITY ASSESSMENT OF THE
PROBIOTIC SPORE FORMER *B.*
SUBTILIS: AN INVESTIGATION INTO
THE EFFECT OF *IN-VITRO* PIG
GASTRIC CONDITIONS

C. BOWE

PhD

2015

VIABILITY ASSESSMENT OF THE
PROBIOTIC SPORE FORMER *B.*
SUBTILIS: AN INVESTIGATION INTO
THE EFFECT OF *IN-VITRO* PIG
GASTRIC CONDITIONS

CATHERINE BOWE

A thesis submitted in partial fulfilment of
the requirements of the University of
Northumbria at Newcastle for the degree
of Doctor of Philosophy Research
undertaken in the School of Applied
Sciences and in collaboration with The
School of Agriculture and Rural
development at Newcastle University

June 2015

Abstract

Probiotics are bacteria which have the capacity to exert a beneficial effect upon the host when consumed in sufficient numbers. However, in order for these bacteria to colonise the gut, they need to survive the harsh conditions of the upper gastrointestinal tract (GIT). In this project, the probiotic spore former *Bacillus subtilis* has been investigated upon exposure to simulated pig gastric conditions. The main aim of this work was to elucidate what phenomena influence the perceived decline in viable count observed in gastric conditions by exploring the impact of acidified medium on the physiological state and viability of spores. It was anticipated that the main cause of spore death would either be a germination-induced death, or a direct sporicidal effect.

The primary part of this project involved developing a methodology to assess these physiological states. Flow cytometry (FCM) was selected for this role based on its potential to rapidly analyse and enumerate high numbers of single cells. Furthermore, germination levels were measured *via* release of dipicolinic acid (DPA) from the spore core.

The results indicated that surprisingly high levels of spore death occurred despite very little DPA release. Whilst this initially supported the direct sporicidal hypothesis, a more detailed examination of the forces at work within the system studied eluded to the fact that aggregation was a key driver behind the perceived decline in counts. This conclusion was only possible due to the fact that FCM enabled an analysis of the total spore and cell count within each sample.

As was hypothesised, pre-germinated spores became far more susceptible to acidic conditions than dormant spores. Crucially, the loss in viability was only confirmed through the use of propidium iodide staining in FCM.

Aggregation in the stomach environment has not been mentioned before in probiotic research, and also explains the unusual results shown by previous researchers, where significant losses in viability were reported in the stomach of animals, only to be rapidly recovered in the other parts of the GIT.

The findings of this work highlight the need to find better methods to assess bacterial numbers, as current methods may give misleading data into probiotic survival in the host. The advantage of using a method such as FCM is also highlighted, given its ability to assess sub-populations of bacteria, rather than being limited to assessing culturability. Furthermore, the need for precise dosing instructions with regards to probiotics should also be considered.

Contents

List of Figures	xi
1 Chapter One: Introduction	1
1.1 Introduction to Probiotics.....	1
1.1.1 Probiotic properties	2
1.1.2 Probiotic challenges	4
1.1.3 Probiotics in agriculture	5
1.1.4 Diet.....	7
1.1.5 Intra-gastric variation	8
1.2 <i>Bacillus subtilis</i>	9
1.2.1 Sporulation	10
1.2.2 Germination	16
1.2.3 Function and composition of bacterial spore structures.....	20
1.2.4 Alternative responses to changes in the environment	22
1.2.5 Viability assessment of <i>B. subtilis</i> cells and spores in the GIT.....	23
1.2.6 Current Microbial Enumeration Methods	24
1.3 Flow cytometry principles	30
1.3.1 FCM data acquisition strategies.....	32
1.4 Aims and Objectives	40
2 Chapter Two: Developing a FCM methodology to analyse <i>B. subtilis</i> cells and spores	42
2.1 Introduction.....	42
2.1.1 Fluorochrome selection.....	42
2.1.2 Staining concentrations	44

2.1.3	Setting compensation	44
2.1.4	Staining temperature analysis	46
2.2	Materials and Methods.....	47
2.2.1	Cell and Spore preparation.....	47
2.2.2	FCM settings and operation	48
2.2.3	Visualising dead from dormant spores.....	49
2.2.4	Assessing germination <i>via</i> DPA release	50
2.3	Results: Selection and optimization of FCM data acquisition strategies	51
2.3.1	Towards Standardisation using Giga Beads.....	51
2.3.2	Setting FCM acquisition	56
2.3.3	Developing the Staining Protocol	63
2.3.4	Setting compensation	72
2.3.5	Visualising Dead from Dormant Spores	77
2.3.6	Assessing levels of germination <i>via</i> UV spectrophotometry	82
2.3.7	FCM servicing and re-alignment	88
2.4	Concluding remarks on the development of a FCM methodology	89
3	Chapter Three: Optimising spore yields and purity	90
3.1	Introduction.....	90
3.1.1	Methods for sporulation.....	90
3.1.2	Methods for purification	93
3.1.3	Aims and Objectives	94
3.2	Materials and Methods.....	94
3.2.1	Spore production.....	94

3.2.2	FCM	95
3.2.3	Fluorescent Microscopy	96
3.3	Results	97
3.3.1	Effect of multiple washing steps	98
3.3.2	Exploring the effect of filtering on spore purity	105
3.3.3	Manganese supplementation	108
3.3.4	Comparison between spore harvesting methods	112
3.3.5	Alternative sporulation media	114
3.4	Conclusion	118
3.4.1	Selection of sporulation medium	119
3.4.2	Supplementation with Manganese	119
3.4.3	Assessment of spore purity	119
4	Chapter Four: Assessment of the impact of antimicrobials and other microbiocidal treatments on <i>B. subtilis</i> cells and spores.....	121
4.1	Introduction.....	121
4.1.1	Enumeration using counting beads	121
4.1.2	EtOH as a method of cell killing without activating spore germination	122
4.1.3	Antimicrobials used and their effect on <i>Bacillus subtilis</i>	123
4.1.4	Aims and Objectives	126
4.2	Materials and Methods.....	126
4.2.1	Antimicrobial treatments.....	126
4.2.2	Plating	127
4.2.3	Petroff-Hausser counting chamber.....	127

4.2.4	FCM Enumeration.....	127
4.2.5	Effect of EtOH on cells and spores.....	128
4.2.6	Statistical analysis of the data collected.....	129
4.3	Results.....	129
4.3.1	Antimicrobial assessment	129
4.3.2	EtOH as method of cell killing without activating spore germination.....	133
4.4	Discussion	140
4.4.1	Antimicrobial investigations	140
4.4.2	EtOH as a method of cell killing without activating spore germination.....	142
4.5	Concluding Remarks.....	143
5	Chapter Five: Assessing germination in <i>B. subtilis</i> spores	144
5.1	Introduction.....	144
5.1.1	DPA release of acid treated spores.....	145
5.1.2	FCM Cell sorting	150
5.1.3	Aims and Objectives	151
5.2	Materials and Methods.....	151
5.2.1	Spore production.....	151
5.2.2	Analysis of DPA release from spores	152
5.2.3	DPA release and viability of spores following different HCl treatments.....	154
5.2.4	Cell Sorting	156
5.3	Results.....	157
5.3.1	Determining the magnitude of DPA release following an extreme acid treatment	157

5.3.2	DPA release and viability of spores following different Hydrochloric acid treatment	159
5.3.3	Cell sorting	163
5.4	Discussion	178
5.4.1	DPA release studies	178
5.4.2	Cell sorting	183
6	Chapter Six: <i>In vitro</i> modelling of Pig stomach conditions	185
6.1	Introduction	185
6.1.1	<i>In vitro</i> conditions	185
6.1.2	Heat activation	187
6.1.3	Aims and objectives	188
6.2	Materials and Methods	188
6.2.1	FCM settings	188
6.2.2	FCM Enumeration	189
6.2.3	Plating	190
6.2.4	Viability of spores in simulated gastric conditions	190
6.2.5	Statistics	191
6.3	Results	191
6.3.1	FCM output from acid treated spores	191
6.3.2	Effect of 40mM HCl on spores in LB broth	192
6.3.3	Effect of 55mM HCl on spores in LB broth	195
6.3.4	Effect of 100mM HCl on spores in LB broth	197
6.3.5	Assessment of total counts	198

6.3.6	Assessing FCM sub-populations.....	203
6.4	Conclusion	209
6.4.1	Comparison of methodologies	209
6.4.2	Effect of simulated feeding and gastric conditions on spores.....	209
6.4.3	Assessment of total counts.....	210
6.4.4	FCM sub-population analysis	211
7	Investigating the impact of aggregation on <i>B. subtilis</i> viability enumeration.....	212
7.1	Introduction.....	212
7.1.1	Bacterial aggregation and intermolecular forces.....	212
7.1.2	Models for determining adhesion	218
7.1.3	The importance of aggregation in probiotics	220
7.1.4	External factors inducing aggregation	221
7.1.5	Aims and objectives	222
7.2	Material and Methods	223
7.2.1	Effect of heating-induced aggregation on total counts.....	223
7.2.2	Effect of surfactant on total spore counts exposed immersed in LB at different pH ranges	223
7.2.3	Assessment of total counts in acidified PBS.....	224
7.2.4	Assessment of viable spore counts in LB and PBS.....	224
7.2.5	Assessment of spore counts in 100mM HCl acidified pig feed	225
7.2.6	Enumeration.....	225
7.2.7	Particle size analysis	225
7.2.8	Measuring zeta potential	226

7.2.9	Statistical analysis.....	226
7.3	Results.....	226
7.3.1	Exploring the effect of heating on total counts using FCM.....	226
7.3.2	Comparison of total numbers of spores in LB broth at different pH's with and without 1% Tween using two methods.....	229
7.3.3	Comparison of total numbers of spores in PBS at different pH's with and without 1% Tween.....	231
7.3.4	Exploring the effect of surfactant on plate count.....	232
7.3.5	Application of 1% Tween 20 to spores immersed in simulated fed stomach conditions.....	234
7.3.6	Spore particle size analysis.....	237
7.3.7	Zeta potential.....	240
7.4	Conclusion.....	241
7.4.1	Conclusions relating to the addition of 1% Tween 20.....	241
7.4.2	Particle size distribution and zeta potential.....	243
7.4.3	Concluding remarks.....	244
8	Chapter Eight: Discussion and Conclusion.....	246
8.1	Selection and optimisation of FCM settings.....	246
8.1.1	Setting FCM acquisition.....	246
8.1.2	Staining procedure.....	247
8.1.3	OD ₂₇₀ measurements.....	248
8.2	Spore generation and purification.....	248
8.2.1	The impact of manganese on sporulation.....	249
8.3	FCM assessment of antimicrobials on cells of <i>B. subtilis</i>	249

8.4	FCM assessment of germination and cell sorting	250
8.4.1	Monitoring the release of DPA via UV spectroscopy.....	250
8.4.2	FCM analysis of spore germination	251
8.5	<i>In vitro</i> porcine gastric conditions	252
8.6	Bacterial spore aggregation.....	253
8.7	Conclusion	254
8.7.1	Future Work	257
9	Appendices.....	258
	Appendix 1.....	258
	BBL™ AK Agar #2	258
	Ethanol treatment.....	260
	Appendix 2.....	262
	Appendix 3.....	272
	References.....	274

List of Figures

Figure 1.1	Diagram showing the four main compartments of the pig stomach. From the oesophagus: pars nonglandularis, cardia, fundus and pylorus leading to the duodenum (Möβeler <i>et al.</i> 2010).	8
Figure 1.2	Diagram showing the movement of ions across the mucosal layer and lumen of the stomach (Allen and Garner 1980).	9
Figure 1.3	Overview of the stages of sporulation in <i>B. subtilis</i> from González-Pastor (2011)	11

Figure 1.4 Electron microscopy images showing stages I, II and III of sporulation. A and B= wild type *B. subtilis* cell (168) undergoing asymmetric septation, C and D= early stage forespore engulfment. Scale bar = 200nm. Electron microscopy images taken from Thompson *et al.* (2006)..... 13

Figure 1.5 Stages of Sporulation visualised by electron microscopy a = Mature *B. subtilis* spore within a mother cell from Catalano *et al.* (2001) where scale bar =500nm. b = mature free spore. Scale bar = 125nm from Silvaggi *et al.* (2004)..... 14

Figure 1.6 A: Example of scanning electron microscopy (SEM) cross section of *Bacillus* spore and B, schematic diagram of radial spore layers. Scale bar represents 0.2µm (Henriques and Moran 2000). 15

Figure 1.7 Outline of nutrient germination of *Bacillus* spores. The germ cell wall is not shown but it expands as the cortex is hydrolysed in stage II of germination. Image and text from Setlow (2014)..... 17

Figure 1.8 Imaging of *B. anthracis* spore germination through TEM at (a) 0 hour, (b) 1 hour, (c) 2 hours, and (d) 3 hours. A, spore coat; B, outer spore membrane; C, spore cortex; D, germ cell wall; E, inner spore membrane; F, spore core; G, cell wall; H (Zaman *et al.* 2005). 19

Figure 1.9 Diagram of cross section of a dormant spore, illustrating layers of the spore coat. The outer forespore membrane covers the cortex (PGCW), and this is surrounded by the basement layer (blue), followed by the inner coat (orange), then the outer coat (purple) and finally the crust (red). Coloured boxes underneath indicate where important germinant receptors are located in each layer. 21

Figure 1.10 a) FCM output of *B. subtilis* cells and spores, (stained with 1.5µM Syto 16 and 48µM PI) with SpheroTech fluorescent counting beads on a forward scatter (FSC) vs side scatter (SSC) density plot. b) The same sample, displayed on a far red (FL4) vs Red (FL3) fluorescent density plot. Region A is drawn around the fluorescent counting beads 28

Figure 1.11 Gated FCM density plot of *B. subtilis* cells and spores, (stained with 1.5µM Syto 16 and 48µM PI, a) FSC vs SSC with region B drawn around the main cells and spore

population, b) Gated plot of region B with Green (FL1) vs Red (FL3) density plot (of the same sample), showing the fluorescence emission of this stained sample. Region C: dormant spores, Region D: germinating spores, Region E: Live cells and outgrown spores, Region F: dead cells and spores, Region G: double stained cells and spores, and/or cell doublets. 29

Figure 1.12 Diagram of inner flow cytometry system showing the position of the laser in relation to the cell stream and the fluorescent detectors (Invitrogen 2014). 30

Figure 2.1 Emission spectra of Syto 16 and PI the 530/30 filter/bandpass is the FL1 channel and the 670/0 long pass filter is the FL3 channel. Graph constructed using Fluorescence Spectra Viewer (Life Technologies). Bandwidth windows at 530/30 45

Figure 2.2 a) FL1 (green) fluorescence against FL3 (red) fluorescence showing density profile of cells and spores of *B. licheniformis* from Mathys *et al.* (2007) (0 = noise), 1 = dormant, 2 = germinated, 3 = unknown, 4 = inactivated. b) Results of flow cytometric assessment (density plots) (Baier *et al.* 2010) Regions: R1: dormant spores, R2: germinated spores, R3: unknown state, R4: inactivated spores, R5: noise, V1: vegetative cells, V2: vegetative cells inactivated by thermal effects..... 46

Figure 2.3 Representative dual parameter density plot showing SSC vs FL1 of the Giga bead mix. a) Our own trial b) results from the Giga bead mix protocol. Regions are constructed so that: Region A: 380nm beads (far red fluorescence), region B: 525nm, region C: 3000nm, region D: 190nm, region E: 380nm, region F: 450nm, region G: 660nm and region H: 1000nm. n=3. 52

Figure 2.4 (From previous page) Dual parameter density plots showing green fluorescence (FL1) vs side scatter (SSC) density plots of Giga bead mix. Regions are assigned such that: Region I: 380nm beads (far red fluorescence), region J: 525nm, region P: 3000nm, region K: 190nm, region L: 380nm, region M: 450nm, region N: 660nm and region O: 1000nm. a) Results from protocol (percentages not clear) b) Results from a high concentration of beads run on 'high' flow rate setting, c) low concentration of beads run on the 'high' flow rate setting, d) high concentration of beads run on the 'low' flow rate setting, e) low concentration of beads run on the 'low' flow rate setting..... 54

Figure 2.5 a) Establishment of a triggering criterion using a preliminary FCM analysis of *B. subtilis* cells and fluorescent beads. Cells and beads (6µm, Calibrite, Invitrogen) were suspended and surveyed in filtered PBS. Events were logged using the FSC trigger channel (a) and the same sample using the SSC channel (b). Region A (green) shows the beads and region B (blue) denotes the cell population and region C (orange) denotes the ‘noise’ and debris. Data collection set to 10,000 events..... 57

Figure 2.6 Optimisation of SSC voltages for simultaneous detection of cells and beads in filtered PBS. FSC set to E02. a) SSC voltage 233 V, b) SSC voltage at 620V and c) SSC voltage at 340V. Region A (green): bead population, Region B (blue:) cell and spore population, Region C (orange): ‘noise’ and debris. 60

Figure 2.7 FSC voltage analysis of cell and bead sample. a) E00 setting, b) E01 setting, c) E02 setting and d) E03 setting. Region A (green): beads Region B (blue): Cell and spore population, Region C (orange): ‘noise’ and debris. 61

Figure 2.8 Single parameter histogram showing green fluorescence of cells stained with Syto 16 at varying concentrations. Red: 0.1µM, Green: 0.5µM, Blue: 1µM, Turquoise: 1.5µM, Orange: 2µM, Pink: 2.5µM, Burgundy: 3µM and Lilac: 5µM..... 65

Figure 2.9 Single parameter histogram of red fluorescence (FL3-Height) Heated cells stained with PI. No dilution upon FCM analysis. Red: 12µM, Green: 24µM, Blue: 48µM, Turquoise: 60µM and Orange: 100µM..... 65

Figure 2.10 Single parameter histograms of green fluorescence (FL1-Height) versus frequency of events. a) cells and spores at a concentration of 1×10^6 counts/ml and b) cells and spores at a concentration of 5×10^5 counts/ml. 66

Figure 2.11 Dual parameter density plots of green fluorescence (FL1) against red fluorescence (FL3). Region E (green) = vegetative cells, region D (lilac) = spores. Spores stained at a) 1µM b) 2µM c) 2.5µM, d) 3µM and e) 6µM with Syto 16 67

Figure 2.12 Dual parameter density plots of green fluorescence (FL1) against red fluorescence (FL3). Region E (green) = vegetative cells, region D (lilac) = spores. Cells and

spores at 5×10^5 counts/ml stained at a) $1 \mu\text{M}$ b) $2 \mu\text{M}$ c) $2.5 \mu\text{M}$, d) $3 \mu\text{M}$ and e) $6 \mu\text{M}$ with Syto 16.	68
Figure 2.13 Dual parameter density plots of green fluorescence (FL1-Height) as a function of red fluorescence (FL3-Height). Results are left ungated to see the effect of staining concentration on the debris. Cells and spores at a concentration of 1×10^6 counts/ml stained with Syto 16 at the following concentrations a) $1 \mu\text{M}$, b) $2 \mu\text{M}$, c) $2.5 \mu\text{M}$, d) $3 \mu\text{M}$, e) and $6 \mu\text{M}$	69
Figure 2.14 Green (FL1-Height) versus red (FL3-Height) fluorescence density plot showing filtered PBS with the following concentrations of Syto 16. a) $2 \mu\text{M}$, b) $2.5 \mu\text{M}$, c) $3 \mu\text{M}$ and d) $5 \mu\text{M}$	70
Figure 2.15 a) Dual parameter density plot of forward scatter (FSC) vs side scatter (SSC) of unstained cells in PBS. Region B indicates the cell population. b) Ungated dual parameter density plot of green fluorescence (FL1-Height) against red fluorescence (FL3-Height). Quadrants set so that the lower left quadrant encompasses the first decade denoting unstained material. This shows the corresponding FL1 vs FL3 density plot of the sample. No compensation or threshold set.....	73
Figure 2.16 Dual parameter density plot showing green fluorescence (FL1-Height) against red fluorescence (FL3-Height) of a) Heated cells stained with $48 \mu\text{M}$ PI and b) Cells stained with $2 \mu\text{M}$ Syto 16). Quadrants set so that the lower left quadrant encompasses the first log. No compensation set.....	73
Figure 2.17 Dual parameter density plot of green (FL1) versus red (FL3) fluorescence. Cells and spores stained with Syto 16. Quadrants set so that the lower left quadrant encompasses the first decade denoting unstained material. Voltage Settings: FL1= 551, FL2= 580, FL3= 608; Compensation: FL2- FL1 =40.0%; FL3 to FL2 = 23.8%	74
Figure 2.18 Dual parameter density plot of green (FL1) versus red (FL3) fluorescence. Quadrants set so that the lower left quadrant encompasses the first decade denoting unstained material. Showing a) Living cells double stained, b) mixture of living and dead	

cells double stained, and c) Living cells, dead cells and spores double stained. Purple region: dormant spores, orange region, dead cells and blue region: live cells.	75
Figure 2.19 Gated FCM plot using equation AND A to examine only the cell and spore region. a) An FL1 (green) fluorescence (x axis) against FL3 (red) fluorescence (y axis) a) Heated cells and dormant spores stained with 48uM PI to form a PI positive population (top left) and PI negative population (bottom left). B) Live cells and dormant spore stained with 1uM Syto 16. F1: upper left quadrat, F2: upper right quadrat, F3 bottom left quadrat, F4 bottom right quadrat. NB. ERROR notice indicates no events in that region.....	76
Figure 2.20 Temperature analysis of water in autoclave	77
Figure 2.21 Dual parameter density plots of green fluorescence (FL1) versus red fluorescence (FL3) Spores stained at 4°C a) Dead spores b) Dormant spores	78
Figure 2.22 Dual parameter density plots of green fluorescence (FL1) versus red fluorescence (FL3) Spores stained at 28°C for 5 minutes a) Dead spores b) Dormant spores.	79
Figure 2.23 Dual parameter density plots of green fluorescence (FL1) versus red fluorescence (FL3) Spores stained at 28°C for 10 minutes a) Dead spores and b) Dormant spores.	79
Figure 2.24 Dual parameter density plots of green fluorescence (FL1) versus red fluorescence (FL3) Spores stained at 28°C for 15 minutes a) Dead spores and a) Dormant spores.	80
Figure 2.25 Dual parameter density plot showing green fluorescence (FL1) as a function of red fluorescence (FL3)a) Cells incubated for 30 minutes at 28°C b) a mix of cells, dead cells, dead spores and dormant spores. Incubated at 28°C for 30 minutes. Region A (Red) = Living cells, Region B (Green)= dead cells, Region C (Dark blue) = Damaged cells, Region D (Orange) = dormant spores, Region E (Turquoise) = dead spores.....	81
Figure 2.26 Percent DPA release from <i>B. subtilis</i> spores incubated in PBS at 4, 28 and 37°C. Error bars represent the 95% confidence interval and n=3	83

Figure 2.27 Spores suspended in PBS and kept in ice water. Error bars represent the 95% confidence interval and n=3.....	84
Figure 2.28 Amended DPA release from spores in PBS. The ‘blank’ was set using the supernatant of the spores kept at 0°. Error bars show the 95% confidence interval where n=3.	85
Figure 2.29 Representative FSC vs SSC density plots of a sample of dormant spores run through the FCM. Region B (blue) shows the spore and cell area and region C (orange) shows the debris. Left panel a) shows the profile before servicing, and right, b) shows the optimised conditions after the service. FCM acquisition settings as follows for both plots: FSC E01 and SSC 425. n=4.....	88
Figure 3.1. Representative FSC and SSC analysis of spores produced on AK sporulating agar (sample A), incubated for 10 days and harvested by flooding with sterile filtered water, treated with EtOH and then re-suspended in water. Spores were analysed by FCM in sterile filtered PBS. Panels a) single parameter histogram describing Forward scatter and b) single parameter histogram describing Side scatter. n=10.	97
Figure 3.2 Double stained spore sample A analysed by FCM on a) FSC vs SSC density plot. Region B (green): cells and spores. b) Gated (using equation B) fluorescence plot where FL1-Height represents green fluorescence and FL3-Height red fluorescence. Region C (orange): dormant spores, region D (turquoise): germinating spores, region E (pink): Live cells, region F (burgundy): dead spores, region G (light blue): double stained cells.....	98
Figure 3.3 FCM output for spores from centrifuged spores sample A, double stained with Syto 16 and PI a) FSC vs SSC density plot of spore sample A, where Region B (blue): cells and spores. b), Gated (using equation B) fluorescence plot where FL1-Height represents green fluorescence and FL3-Height red fluorescence. Region C (orange): dormant spores, region F (burgundy): dead spores, region D (turquoise): germinating spores, region E (pink): Live cells, region G (light blue): double stained cells.	99
Figure 3.4 DIC image of <i>B. subtilis</i> spores sample A under 40x objective lens.....	100

Figure 3.5 a) DIC image of *B. subtilis* spores sample A taken under 63x objective lens. b) Blue circles highlight spores (phase bright) which are in focus, and red circles indicate dormant spores which are still phase bright, but appear dark owing to the fact these are not in the plane of view..... 101

Figure 3.6 I3 (blue) light image of double stained (1.5µM Syto 16 and 48µM PI) *B. subtilis* spores sample A. Taken under the 63x objective..... 102

Figure 3.7 Fluorescent microscope output and FCM output of *B. subtilis* spore sample B, showing effect of filtering. a) Top row, left, DIC image using 63x objective before 0.2µm filter and right, FCM FSC vs SSC profile of the same sample, with Region B drawn around the cells and spore population. b) Bottom row, DIC image at 63x magnification post 0.2µm filter and right, FCM FSC vs SSC density profile, with Region B drawn around the cell and spore population for sample B. 106

Figure 3.8 Examples of FCM density plot of FSC vs SSC, region A (red) corresponds to debris and region B (green) is the cell and spore location. Column a) *B. subtilis* spores harvested from a normal AK sporulating agar plate and column b) *B. subtilis* spores harvested from a MnSO₄ supplemented AK agar plate. 109

Figure 3.9 Effect of manganese supplementation on the amount of debris present in spore stocks. Debris corresponds to region A on the FCM FSC vs SSC plots and spores correspond to region B of Figure 3.8. White bars show spores grown on AK agar without additional manganese and shaded bars are spores grown on AK agar with 100µl 3.4mM MnSO₄. Error bars represent the 95% CI where n =10. 110

Figure 3.10 DIC image under 100x objective lens of *B. subtilis* spores grown on AK sporulating agar without additional Mn. Representative frame where n=10. 111

Figure 3.11 DIC image under 100x objective lens of *B. subtilis* spores grown on AK sporulating agar, supplemented with an additional 100µl 3.4mM MnSO₄. Representative frame where n=10. 111

Figure 3.12 Representative FCM density output of manganese supplemented spores on a FSC vs SSC plot. Region A (red) is drawn around the debris or 'noise' population and region B (green) corresponds to the cell and spores area on the plot..... 112

Figure 3.13 The percentage of events that correspond to either debris or spores as shown by FCM FSC vs SSC profiles for non-Mn supplemented samples. White bars indicate flooded samples and shaded bars are scraped plates. Error bars represent the 95% CI where n=4. . 113

Figure 3.14 The percentage of events that correspond to either debris or spores as shown by FCM FSC vs SSC profiles for Mn supplemented samples. White bars indicate flooded samples and shaded bars are scraped plates. Error bars represent the 95% CI where n=7. . 113

Figure 3.15 Typical example of FCM profiles for spores produced in DSM broth. a) shows density plots of FSC vs SSC where Region B (blue): cell and spores region b): Gated on Region B, region C (orange): dormant spores, region D (turquoise): germinating spores, region E (pink): Live cells, region F (burgundy): dead spores and cells, region G (light blue) cell doublets. 114

Figure 3.16 An example of typical FCM profiles for spores produced *via* AK sporulating agar. a) shows density plots of FSC vs SSC where Region B: cell and spores region, b) Gated on Region B, region C (orange): dormant spores, region D (turquoise): germinating spores, region E (pink): Live cells, region F (burgundy): dead spores and cells, region G (light blue) cell doublets. 115

Figure 3.17 *B. subtilis* spores produced using DSM medium. DIC light under 63x objective lens. Representative image where n=7..... 116

Figure 3.18 Double stained *B. subtilis* spores produced using DSM medium. I3 light under the 63x objective lens. Representative image where n=7. 116

Figure 3.19 *B. subtilis* spores produced using DSM medium. DIC light under the 63x objective lens. Representative image where n=7..... 117

Figure 3.20 Double stained *B. subtilis* spores produced using DSM medium. I3 light under the 63x objective lens. Representative image where n=7. 117

Figure 3.21 VenturiOne output for *B. subtilis* spores produced on manganese supplemented agar, following 50% EtOH treatment and multiple washes, a) density plot of FSC vs SSC, region A (red) drawn around the cell/spore area. b) density plot gated on region A of FL1 (Green) fluorescence vs FL3 (Red) fluorescence, Region A (red): cells and spores, region B (green): dormant spores, region C (blue): dead spores, region D (orange): germinating spores, region E (turquoise) dead cells, region F (pink): Live cells. Region G: double stained cells. Representative output where n=5. 118

Figure 4.1 FCM density plots showing The FL1 – Height (green fluorescence) parameter against the FL3-Height (red fluorescence) parameter are shown as density plots of *B. subtilis* cells treated with a) untreated, b) Green Tea, c) PAA and d) chlorine. Regions assigned showing dead cells: Region F (burgundy), damaged cells: Region G (light blue), Living cells: Region E (pink), Germinating spores: Region D (turquoise) and Dormant spores (or unstained debris): Region C (orange). All plots gated using equation NOT A to remove beads followed by AND B to examine cells only and omit debris. Representative plots where n=3..... 130

Figure 4.2 Log plate count and FCM count comparisons of various treatments shown in Table 4.1 132

Figure 4.3 FCM density plot of Green fluorescence (FL1-Height) vs Red fluorescence (FL3-Height). Mixture of dormant spores, dead spores, live cells and dead cells. Gated on Region B (not shown, cell and spore region), region C (orange): dormant spores, region D (turquoise): germinating spores, region E (pink): Live cells, region F (burgundy): dead spores and cells, region G (light blue) cell doublets (one live and one dead cell joined together, Representative plot where n=3..... 133

Figure 4.4 FCM density profiles of double stained *B. subtilis* spores. The FL1 – Height (green fluorescence) parameter against the FL3-Height (red fluorescence) parameter are shown as density plots of a) dead spores stained at 28°C and b) Dormant spores stained at 28°C, showing a smaller region of dead spores. Region H (lilac) indicates living cells, region C (orange) dead cells, (high PI staining indicating high DNA content) region D (turquoise)

dead cells, region E (pink) Dormant spores, region F (burgundy) dead spores and region G (light blue) unknown sub-population. Representative plot where n=3. 134

Figure 4.5 a) The FL1 – Height (green fluorescence) parameter against the FL3-Height (red fluorescence) parameter are shown as density plots of a) Heat activated EtOH treated cells and spores, and b) EtOH treated cells and spores (no heat activation). Region B: beads, Region C (orange): Dead cells (high DNA content), Region D (turquoise): Dead cells, Region E (pink): Dormant spores, Region F (burgundy): Dead spores, Region G (light blue): unknown sub-population. Region H (lilac): Live cells and germinating spores. Representative FCM plot where n=3. 135

Figure 4.6 Representative forward scatter (FSC) versus side scatter (SSC) density plot of cells and spores heat activated and treated with EtOH. Region L (blue) corresponds to the spores region and region M (Orange) corresponds to the cell region. (Region I in green shows us the bead population) and region A encompasses the cell and spore population. Where n=3..... 136

Figure 4.7 Heat activated EtOH treated cells and spores displayed on a) FL1 vs FL3 density plot of gated on the cell region M in Figure 4.6. Where Region N (orange): dead cells, Region O (turquoise) dead cells, Region P (pink): dormant spores, Region Q (burgundy): dead spores, Region R (light blue): Dead spores. b) FL1 vs FL3 density plots, gated on the spore region L from Figure 4.6. Where Region S (orange): dead cells, Region U (turquoise) dead cells, Region T (pink): dormant spores, Region V (burgundy): dead spores, Region W (light blue): Dead spores. Representative FCM profiles where n=3..... 137

Figure 4.8 Correlation of viable counts shown in Table 4.2 *via* plating (x axis), Petroff-Hausser haemocytometer and FCM after staining at 4°C and 28°C. n=3..... 138

Figure 5.1 %DPA release of spore samples. Plain: showing the sample heated at 96°C for 90 minutes, Shaded: showing the sample treated with 0.1M HCl (pH 0.8) at 37°C for 1 hour in water, Dotted: Dashed: spores kept at 37°C in dd H₂O for one hour. Error bars showing the 95% CI where n=3. 158

Figure 5.2 shows the percentage decrease in viability of spores subject to the conditions described in the table below. Spotted bar indicates spores in water, empty bars indicate spores in PBS only and shaded bars show spores in PBS with germinants. Error bars represent the 95% CI where n=6..... 159

Figure 5.3 The percentage attributed to direct sporicidal effects is the total lethality minus the percent germination. Sporicidal effect implies the amount of death without release of DPA. Error bars represent the 95% CI where n=6. Sample codes as per Figure 5.2..... 161

Figure 5.4 Cells grown in LB broth, then re-suspended in PBS a) FCM profile of side scatter (SSC) vs forward scatter (FSC) where five sub-populations are apparent on the density plot. Region A (red): cell doublets in chains, Region B (green): single cells, Region C (blue): cell doublets (width ways), Region D (orange): single cells, width ways, Region E (turquoise): debris. b) FACS sorted LB agar plate, in columns A and B) Region E (turquoise) is sorted at rates of 1, 3, 10, 30 and 50 droplets per well. Cell regions (A-D) in columns C-F sorted at one drop per well. n=1 164

Figure 5.5 FCM profiles for live cells stained with, the Syto 16 only. Density plots created using WinMDI software. a) FL1 vs Forward scatter (FSC), Region L: small Syto positive particles, Region U: Outgrown spores, Region W: Germinating spores, Region X: Phase dark spores, or possibly spore aggregates, Region AH: dormant spores. b) FL3 vs FSC, region O: outgrown dead spores or dead cells, region S: germinating spores, Region Y: dead cells. n=1 166

Figure 5.6 Sorted plate of cells grown in LB broth overnight and stained with Syto 16 (only) 167

Figure 5.7 Representative FCM output on density plots created using VenturiOne software. a) FCM profiles for sorted plate 2 of side scatter SSC vs forward scatter FSC. Region D: all spores, Region J: Large particles (possibly germinating spores), Region N: small spores, Region M: small spores, region V: debris. b) FCM profiles for sorted plate 3. FL1 vs FSC, region L: small green particles, region E: Dormant spores, region U: large bright green

particles, region W: germinating spores, Region X: germinating spores. c) FL3 vs FSC, region O: very small red particles, Region S: main cells/spores region. n=3. 169

Figure 5.8 Representative sorted plate of spores immersed in LB broth, then re-suspended in PBS and stained with Syto 16 and PI. Region V (Figure 5.7a) in columns A and B: debris, sorted at rates of 1, 3, 10, 30 and 50 droplets per well shown in the grid. Cell and spores regions D, J, M, N from Figure 5.7a in columns C-F sorted at one drop per well. Representative sorted plate where n=3. 170

Figure 5.9 FCM profiles for spores immersed in LB broth for 30 minutes, then treated with 55mM HCl for one hour. Density plots created using VenturiOne software. a) Side scatter (SSC) vs forward scatter (FSC), Region F (green): all spores. b) FL1 vs FSC, region G (blue): small green particles, region I (turquoise): germinating spores. c) FL3 vs FSC, region H (orange): very small red particles, Region J (pink): main spore region, K (purple): germinated dead spores. n=1..... 173

Figure 5.10 Spores immersed in LB broth for 30 minutes, than treated with 55mM HCl for 1 hour. Re-suspended in PBS and stained with Syto 16 and PI. All sorted at rates of 1, 3, 10, and 30 droplets per well. n=1..... 174

Figure 5.11 FCM profiles for sorted plate 4. Density plots created using VenturiOne software. a) Side scatter (SSC) vs forward scatter (FSC), Region F (green): all spores. b) FL3 vs FSC, region H (orange) very small red particles, Region J (pink): main spore region, K (purple): germinated dead spores. c) FL1 vs FSC, region G (blue): small green particles, region I (turquoise): germinating spores (phase dark). Region L (pale blue): germinating spores and Region M (lilac): outgrown spores and cells. 175

Figure 5.12 Spores immersed in LB broth to initiate germination, then shocked with 55mM HCl. a) Plated double stained spores, germinated in LB broth then shocked with 55mM HCl for 30 seconds at room temperature (analysed in PBS). Sorted at rates of 1, 3, 10 and 30 . 176

Figure 5.13 Structure of DPA from Yardimci and Setlow (2010)..... 181

Figure 6.1 a) FSC vs SSC density plot of heat activated spores immersed in 55mM HCl for two hours, Region B denotes the cell and spore population. b) FL1 vs FL3 density plot gated

on region B. Region C (orange) Dormant spores, Region D (turquoise) germinating spores, Region E (pink) outgrown spores/live cells, Region F (Burgundy) Dead cells and dead spores and Region G, double stained cells and/or cell doublets.	192
Figure 6.2 40mM HCl on dormant spores of <i>B. subtilis</i> , showing log (10) transformed data a) plating and b) viable FCM counts. Error bars represent the 95% CI where n=3. Shaded bars refer to heat activated (HA) spores and white bars denote the non-heat activated (NHA) spores.	193
Figure 6.3 40mM HCl on pre-germinated spores, showing log 10 transformed a) plating counts and b) viable FCM counts. Error bars represent the 95% CI where n=3. Shaded bars refer to heat activated (HA) spores and white bars denote the non-heat activated (NHA) spores.	193
Figure 6.4 55mM HCl (pH 2.6) on dormant spores, showing log (10) transformed viable counts by plating (a) and by FCM (b). Error bars represent the 95% CI, where n=3. Shaded bars refer to heat activated (HA) spores and white bars denote the non-heat activated (NHA) spores.	195
Figure 6.5 55mM HCl on pre-germinated spores, showing log (10) transformed viable counts by plating (a) and FCM (b). Error bars represent the 95% CI, where n=3. Shaded bars refer to heat activated (HA) spores and white bars denote the non-heat activated (NHA)..	195
Figure 6.6 100mM HCl on dormant spores, showing log 10 transformed viable counts by plating (a) and FCM (b). Error bars represent the 95% CI, where n=3. Shaded bars refer to heat activated (HA) spores and white bars denote the non-heat activated (NHA) spores. ..	197
Figure 6.7 100mM HCl on pre-germinated spores, showing log 10 transformed viable counts by plating (a) and FCM (b). Error bars represent the 95% CI, where n=3. Shaded bars refer to heat activated (HA) spores and white bars denote the non-heat activated (NHA) spores	197
Figure 6.8 a) FL3 vs FL4 density plot for HA sample subject to 40mM HCl for 60 minutes, region A is drawn around the bead population b) Gated FSC vs SSC density plot using equation NOT A to remove beads. Region B denotes the cell and spore population.	199

Figure 6.9 Percentage of total count for each sample in relation to the total count at time 0 for NHA spores. Error bars represent the 95% CI. a) Shows the dormant spores and b) the pre-germinated spores..... 200

Figure 6.10 FCM output for size calibration beads on a single parameter histogram of Forward scatter (FSC) vs number of events. Region A: 1µm beads, Region B: 2µm beads, Region C: 4 µm beads, and Region D 6µm beads. (Displayed using WinMDI software). . 203

Figure 6.11 FCM analysis of a NHA sample of dormant spores subject to 55mM HCl for 120 minutes a) Gated FSC vs SSC density plot using equation NOT A to remove beads. Region B denotes the cell and spore population. b) Single parameter histogram of FSC vs number of events where Region L incorporates particles of ≤ 1 µm, Region M approximately 2 µm, and Region N particles greater than 4µm. 204

Figure 6.12 Representative FCM analysis of pre-germinated spores immersed in 55mM HCl in LB broth displayed on FL1 vs FL3 density plot at a) time 0 and b) 120 minutes. Region C: dormant spores, Region D: Germinating spores, Region E: Live cells and outgrown spores, Region F: Dead spores and cells, Region G: Cell doublets. 206

Figure 6.13 Percentage increase in PI positive events of a) dormant spores immersed in 40, 55 and 100mM HCl in LB broth and b) Pre-germinated spores immersed in 40, 55 and 100mM HCl. Error bars represent the 95% CI where n=3. 207

Figure 7.1 Total interaction between a bacterial cell and surface depending on ionic strength (Hori and Matsumoto 2010)..... 218

Figure 7.2 Representative FCM analysis of spores immersed in PBS with 1% Tween 20 displayed on a FSC vs SSC density plot. The plots have been gated to remove beads. I) Left, region B (blue) is drawn around the main cells and spore position. b) all high FSC and SSC events region E (pink) on the FCM profile. Other regions are C (pink)= dormant spores and cells, D (turquoise) = Large aggregates. n=3. 227

Figure 7.3 Total counts for heat activated and non-heat activated spores in different conditions, prepared according to method 1. a) the log counts/ml are from region B containing cells and spores, on the FCM profile above (Figure 7.2.). b) Counts for ‘large

events' shown as all high FSC and SSC events region E (pink) in Figure 7.2. Error bars represent the 95% CI where n=3..... 227

Figure 7.4 Representative FCM analysis of spores immersed in LB broth presented on a FL1 vs FL3 density plot (a) and region A (red) drawn around beads. b) regions drawn on a gated plot using equation NOT A to remove beads from the FSC vs SSC plot. Region E (pink): all spore events (including large aggregates), Other regions are C (orange)= dormant spores and cells, D (turquoise) = Large aggregates. n=3. 229

Figure 7.5 Comparison of log spore counts in LB over a range of pHs, showing a) run one according to method 1 (top) and b) run two according to method 2 (bottom). White bars indicate spores in LB broth only and red bars show spores in LB broth supplemented with 1% Tween. Values are based on the number of events in region E (burgundy). Error bars represent the 95% CI where n=2 in run one and n=3 in run two. 230

Figure 7.6 Comparison of total spore FCM counts in PBS over a range of pHs. White bars indicate spores in PBS only and red bars show spores in PBS supplemented with 1% Tween. Values are based on the total number of cells and spores according to FCM. Error bars represent the 95% CI where n=3..... 232

Figure 7.7 Plate counts of spores immersed in acidified LB broth. Error bars represent the 95% CI where n=3 233

Figure 7.8 Comparison of plating counts for PBS alone and PBS with 1% Tween 20. White bars indicate spores immersed in PBS without Tween 20 and shaded bars represent spores immersed in PBS with 1% Tween 20. Error bars represent the 95% CI where n=3..... 234

Figure 7.9 Spores immersed in 100mM PBS in Servapore dialysis tubing (time 0) displayed on a representative FCM density plot a) FSC vs SSC density plot gated to remove beads where region B (blue) is drawn around the total cell and spore region, b) FL1 vs FL3 fluorescent density plot gated on region B (blue), where region C (orange): dormant spores, Region D (turquoise): germinating spores, Region E (pink): Live cells and outgrown spores, Region F (burgundy): Dead spores and cells, and region G (light blue): double stained cells and spores. n=3. 235

Figure 7.10 Total FCM counts of dormant spores immersed in 100mM HCl in pig pellet feed, based on Region B. Error bars denote the 95% CI where n=3.....	235
Figure 7.11 Dormant spores immersed in 100mM HCl in pellet pig feed. White bars denote samples analysed with no Tween and shaded bars with 1% Tween 20. a) Plating and b) viable FCM counts. Error bars denote the 95% CI where n=3.	236
Figure 7.12 Particle size distribution of spores in PBS (100mM) at different pH levels. Values represent the average of three samples. Red line pH 7, green line pH 5, blue line pH 3, black line pH 1	237
Figure 7.13 Analysis of average particle size of dormant spores immersed in PBS at pH 7 and 3, analysed at a) 1000rpm, b) 1500 rpm, and c) 2000 rpm. Error bars denote the 95% CI where n=3.	239
Figure 7.14 Zeta potential for spores immersed in PBS at pH 1, 3, 5 and 7. Data represent the average of 9 measurements and error bars represent the 95% CI.	240
Figure 9.1 FCM output for spore samples B, C and D and E following multiple washing steps. Left column) density plot of FSC vs SSC, region A (red) drawn around the cell/spore area of a) sample B, c) Sample C, e) Sample D and g) Sample E. Region B (blue): cells and spores. Right column) density plot gated on region B of FL1 (Green) fluorescence vs FL3 (Red) fluorescence, region C (orange): dormant spores, region D (turquoise): germinating spores, region E (pink): live cells, region F (burgundy): dead spores and cells, region G (light blue): double stained cells. b) Sample B, d) Sample C, f) Sample D and h) Sample E.	263
Figure 9.2 Fluorescent microscopy image of <i>B. subtilis</i> spore sample B, taken using the 63x objective lens. Stained with Syto 16 and PI under a) DIC light and b) I3 (blue) light	264
Figure 9.3 Fluorescent microscopy image of <i>B. subtilis</i> spore sample C, taken using the 63x objective lens. Stained with Syto 16 and PI under a) DIC light and b) I3 (blue) light	265
Figure 9.4 Fluorescent microscopy image of <i>B. subtilis</i> spore sample D, taken using the 63x objective lens. Stained with Syto 16 and PI under a) DIC light and b) I3 (blue) light	266

Figure 9.5 Double stained *B. subtilis* spores sample E under the 63x objective lens a) DIC light image b) I3 light image..... 267

Figure 9.6 Sample A of *B. subtilis* spores. a) Top row, left, DIC image using the 63x objective lens before 0.2µm filter and right, FCM FSC vs SSC profile of the same sample with Region B drawn around the cell and spore population. b) Bottom row, DIC image at 63x magnification post 0.2um filter and right, FCM FSC vs SSC density profile with Region B drawn around the cell and spore population..... 268

Figure 9.7 Sample C of *B. subtilis* spores. a) Top row, left, DIC image at 63x magnification before 0.2µm filter and right, FCM FSC vs SSC profile of the same sample with Region B drawn around the cell and spore population. b) Bottom row, DIC image at 63x magnification post 0.2um filter and right, FCM FSC vs SSC density profile with Region B drawn around the cell and spore population. 269

Figure 9.8. Sample D of *B. subtilis* spores. a) Top row, left, DIC image using 63x objective lens before 0.2µm filter and right, FCM FSC vs SSC profile of the same sample with Region B drawn around the cell and spore population. b) Bottom row, DIC image at 63x magnification post 0.2um filter and right, FCM FSC vs SSC density profile with Region B drawn around the cell and spore population. 270

Figure 9.9 Sample E of *B. subtilis* spores. a) Previous page, left, DIC image under the 63x objective lens before 0.2µm filter and right, FCM FSC vs SSC profile with Region B drawn around the cell and spore population. b) DIC image under the 63x objective lens post 0.2µm filter and right, FCM FSC vs SSC density profile with Region B drawn around the cell and spore population..... 271

Figure 9.10 Spores immersed in LB broth for 30 minutes, then re-suspended in PBS and stained with Syto 16 and PI. All sorted at rates of 1, 3, 10, and 30 droplets per well as shown in the grid on the right..... 272

Figure 9.11 Spores immersed in LB broth for 30 minutes, then re-suspended in PBS and stained with Syto 16 and PI. All sorted at rates of 1, 3, 10, and 30 droplets per well as shown in the grid on the right. 273

Acknowledgments

The work that has gone into producing this thesis would not have been possible first and foremost without the aid of my supervisor, Dr. Nikos Mavroudis, whose constant guidance, support and patience has meant that this work has been an enriching experience.

I would also like to thank my other supervisors, Prof. Olivier Sparagano, and Dr. Lynn Dover for their input and advice during the project. A thank you to Prof. Sandra Edwards at Newcastle University for her knowledge and expertise which has been a big help during the PhD.

Thank you to Professor Stephen Harding and Dr. Richard Gillis at the National Centre for Macromolecular Hydrodynamics at Nottingham University for their help and advice on the zeta potential measurements also.

In particular, Dr. Gerhard Nebe-von-Caron deserves a huge thank you, without whom it is quite possible the flow cytometry would not have taken off as it has. For his vast expertise in this area, I am extremely grateful.

This project would not have been possible without the Northumbria University Research Development Fund and the funding received from the Yorkshire Agricultural Society, both of which have been essential to the PhD.

Peter Nobes at VenturiOne software must also get a thanks for his assistance with the Flow cytometry software.

A final thank you to everyone else who has helped me out over the years in the labs, the technicians, staff and students working at Northumbria have helped to make this a rewarding and enjoyable experience.

Declaration

I declare that the work contained in this thesis has not been submitted for any other award and that it is all my own work. I also confirm that this work fully acknowledges opinions, ideas and contributions from the work of others. The work was done in collaboration with The School of Agriculture and Rural development at Newcastle University.

I declare that the Word Count of this Thesis is 59,515 words

Name:

Signature:

Date: 12/06/2015

List of abbreviations:

ATP: Adenine tri-phosphate

a_w : water activity

BWG: Body weight gain

ca: circa

C. E.: Competitive exclusion

cF: Carboxyfluorescein

cFDA: Carboxyfluorescein diacetate

cfu: Colony forming unit

CLE: Cortex lytic enzyme

ddH₂O: double distilled water

DGGE: Denaturing Gradient Gel Electrophoresis

DIC: Differential interference contrast

DPA: pyridine-2,6-dicarboxylic acid or dipicolinic acid

ENS: Enteric nervous system

EPS: Extracellular polysaccharide

EtOH: Ethanol

FCM: Flow cytometry

FISH: Fluorescent *in situ* hybridisation

FL1: green fluorescence channel

FL2: orange fluorescence channel

FL3: red fluorescence channel

FM: Fluorescent microscopy

FSC: Forward scatter

GFK: Glucose, fructose and potassium (germinant mix)

GIT: Gastro-intestinal tract

GR: Germinant receptor

GTP: Guanine tri-phosphate

HCl: Hydrochloric acid

I3: blue light

LAB: Lactic acid bacteria

LB: Luria Bertani (broth)

MAL: Muramic acid- δ -lactam

MCP: Mother cell proximal pole

MIC: Minimum inhibitory concentration

NAD(H): Nicotinamide adenine dinucleotide

NADP(H): Nicotinamide adenine dinucleotide phosphate

PBS: Phosphate Buffered Saline

PCR: Polymerase chain reaction

PH: Petroff-Hausser

qPCR: Real time-quantitative PCR

RT-PCR: Reverse transcriptase PCR

SCFA: Short Chain fatty acids

SSC or RALS: side scatter or right angle light scatter (interchangeable)

TEM: Transmission electron microscopy

VBNC: Viable but non-culturable

1 Chapter One: Introduction

1.1 Introduction to Probiotics

The application of some non-pathogenic bacteria as probiotics has become a widely studied area of current research in food and nutritional sciences, and also veterinary and medical sciences. Probiotics are defined as ‘A preparation of or a product containing viable, defined microorganisms in sufficient numbers, which alter the microflora (by implantation or colonization) in a compartment of the host and by that exert beneficial health effects in this host’ (Schrezenmeir and de Vrese 2001). This definition applies to the use of probiotics in any accessible compartment of the host. In this research, issues relating to the use of probiotics in the porcine gastrointestinal tract (GIT) will be investigated.

The health benefits associated with probiotics have been known for thousands of years; Genesis 18: 8 implies that the effect of drinking sour milk is associated with longevity and Hippocrates and other ancient scientists reported that drinking fermented milk could cure disorders of the digestive system (Ranadheera *et al.* 2010). In 1907, the Russian scientist Élie Metchnikoff first proposed a scientifically valid assumption on the benefits of drinking sour milk, whereby health could be improved by manipulating the host microbiome through the consumption of host-friendly bacteria (Anukam and Reid 2007; Ranadheera *et al.* 2010; Mackowiak 2013). This principle still encompasses the kernel of probiotic research today. However, it wasn't until 1965 that the name ‘probiotic’ was first coined as an antonym to antibiotics (Lilly and Stillwell 1965). Since then, it has been shown that probiotics work by improving the balance of favourable microflora in the gut (Ibrahim and Bezkorovainy 1993). This might occur through a variety of mechanisms mediated by bacterial and host factors. According to the FAO/WHO (2002) the essential properties a bacterium should have to be classed as a probiotic are:

- Resistance to gastric acidity

- Bile acid resistance
- Adherence to mucus and/or human epithelial cells and cell lines
- Antimicrobial activity against potentially pathogenic bacteria
- Ability to reduce pathogen adhesion to surfaces
- Bile salt hydrolase activity

There are several extensive reviews which highlight the known and theoretical advantages probiotics may impart (Cutting 2011; Novik *et al.* 2014), though a probiotic may not necessarily meet all of these properties.

1.1.1 Probiotic properties

Firstly, the probiotic organism might produce bacteriocins, which are small peptides, lethal to other bacteria but not the producing strain (Józefiak *et al.* 2013) meaning they could help eliminate a subset of other micro-organisms, including pathogens (Kleerebezem *et al.* 2004). Bacteriocins such as nisin have been shown to be produced *in situ* (i.e. in the GIT) (Bogovič-Matijašić and Rogelj 2011) and Józefiak *et al.* (2013) have shown that the levels of short chain fatty acids (SCFA) generated by bacterial fermentation were lowest in diets supplemented with nisin or salinomycin and body weight gain (BWG) was highest when broilers received nisin above 900 and 2700 IU nisin/g feed respectively. This believed to be attributed to modification of the host's GIT microbial ecology, resulting in the modulation of host immunity or improved nutrient absorption and utilisation. Whilst the lactic acid bacteria (LAB) usually have a narrow target spectrum, capable of killing only closely related bacteria, *Bacillus* spp. have been shown to produce bacteriocins with a broader spectra of inhibition (Khochamit *et al.* 2015).

With reference to *Bacillus subtilis*, strain W42 produces bacteriocin W42, shown to have bactericidal activity against *Listeria monocytogenes* (Kindoli *et al.* 2012). The *B. subtilis* strain KKU213 has been shown to have antimicrobial action against *L. monocytogenes*, *Staphylococcus aureus*, *Bacillus cereus* and *Micrococcus luteus* owing to

the production of subtilisin A. The genes responsible for this are identical to those found in *B. subtilis* 168, the most commonly used strain in *B. subtilis* research. Given this information, it is likely that many *B. subtilis* strains will be capable of producing antimicrobials (Khochamit *et al.* 2015).

Another popular principle is that the probiotic could prevent colonisation by harmful bacteria in the gut *via* competitive exclusion (C.E.), following the principle that the adherence of probiotic bacteria to the intestinal wall will limit the availability of adherence sites for opportunistic pathogens reducing the risk of infection (Larsen *et al.* 2007). In support of this hypothesis, over the past few decades, research has proven that probiotics can colonise the GIT, at least on a temporary basis (Alander *et al.* 1999; Casula and Cutting 2002; Sheth *et al.* 2012).

Aside from these mechanisms which alter or buffer GIT microflora community structure through microbe-microbe interactions, others have been proposed which influence host biology. One such mechanism to improve the health of the recipient organism is *via* the production of vitamins, and others have been suggested involving the triggering of non-specific immune interactions thus heightening the host's immune responses (Isolauri *et al.* 2001; Walker and Buckley 2006). Isolauri *et al.* (2001) states, 'a potential mechanism of probiotic therapy is improvement of the intestine's immunologic barrier, particularly through intestinal immunoglobulin A responses and alleviation of intestinal inflammatory responses, which produce a gut-stabilizing effect'. In support of this possibility is *B. subtilis* recent use as adjuvants in vaccine delivery (de Souza *et al.* 2014).

The combination of these findings, has led to the notion that probiotic consumption will give the host greater protection against pathogenic organisms, a lowered chance of contracting colonic cancer, and can attenuate the effect of gastro-intestinal diseases such as irritable bowel syndrome, Crohn's disease and lactose intolerance (Liong 2008; Ranadheera *et al.* 2010). In relation to cancers, previous research has suggested probiotics may be capable of reducing bacteria responsible for mediating the conversion of pro-carcinogens to

carcinogens, though it is acknowledged that further studies are needed to elucidate the exact mechanism behind these promising results (Salminen *et al.* 1993; Orrhage *et al.* 1995; Uccello *et al.* 2012).

However, the current opinion on probiotics from the European Food Safety Authority (EFSA 2010a) is that there is insufficient evidence to prove immune-stimulation occurs and that other potential effects have not been investigated long enough to form any significant proof (Binnendijk and Rijkers 2013). Given this verdict, it is important to investigate probiotics further and more rigorously, thus aiming to generate new insights on their modes of action and therefore provide sufficient evidence for their potential effects.

1.1.2 Probiotic challenges

In order for the viable components of a probiotic preparation to impart a beneficial effect on the recipient they must be able to survive a series of quite different hostile environments. The first challenge the probiotic faces is the preparation and storage conditions of the food matrix in which it is delivered. For example, yoghurts are frequently used as vehicles for probiotic delivery however they undergo a series of heat treatments and retain a low pH, therefore it is essential that the probiotic can survive these treatments too. The next hurdle a probiotic must be able to survive is passage through the strongly acidic environment of the stomach. Not only this, but the stomach also contains the protease pepsin, which is known to have broad spectrum antimicrobial properties against both Gram positive and Gram negative bacteria (Holzapfel *et al.* 1998; Zhu *et al.* 2006).

Once the bacteria have passed through the stomach they are then exposed to the bile salts in the duodenum. This will break apart any clumps or aggregates that have formed and then expose the bacteria to a highly alkaline environment. Finally, the probiotic must be able to adhere to the mucosal wall of the large intestine to be able to act as a C. E. agent (Liu *et al.* 2011) and colonise the intestines, at least on a transient basis. Considering all these factors, the probiotics must then be able to survive in large enough numbers to be able to

colonize the intestine and assert a beneficial effect on the host. Given the multiple junctures at which attritional losses might occur, the magnitude of the initial inoculum dose is critical. However reported dosages required vary, for example Khan (2014) notes that the minimum therapeutic dose is 10^5 cells/ml (for liquid food), however the Fermented Milks and Lactic Acid Bacteria Beverages Association in Japan state that at least 10^7 cells/ml need to be present to be labelled as probiotic. Previously, it was recommended that bacterial numbers should range between 10^7 and 10^9 cells/ml in the product for this to be achieved (Gordon *et al.* 1957). Khan (2014) stresses that in general, there is no clear minimum dose required to assert a probiotic effect. These values are reported for commonly used probiotic species such as *Lactobacilli* and *Bifidobacteria*. In agriculture, there has been a shift towards using spore forming bacteria as probiotics, aiming to use them in the dormant spore form, rather than administering the vegetative form. In particular *Bacillus licheniformis* and *B. subtilis* are now commercially available from companies such as Chr. Hansen (Hansen 2014) and ORFFA (ORFFA 2010). Similarly to the vegetative cell probiotics, the recommended dosage for the spore forming probiotics also varies according to the manufacturers. Chr Hansen, have recommended a minimum dose of 1.28×10^9 spores/kg feed of their product BioPlus 2B (Commission 2000) which contains *B. subtilis* and *B. licheniformis*, whereas Orffa recommend 3×10^8 spores/kg feed of *B. subtilis* as Calsporin (EFSA 2010b).

1.1.3 Probiotics in agriculture

Probiotics are an extremely popular constituent of health foods, with a global market value of \$24.23 billion in 2011 (Pedretti 2013). A significant part of this market is in agriculture, where probiotics are used to improve the quality of life, and therefore productivity, of many commonly farmed animals such as cows, broiler chickens and pigs (Link and Kováč 2006; Chiquette 2009; Capcarová *et al.* 2011). The need for probiotics stems from the banning of antibiotics as prophylactics, in an attempt to prevent the emergence of antibiotic resistant pathogenic bacteria (Šabatková *et al.* 2008). The vast majority of products available for animals are spore-forming bacilli, with *B. subtilis* being a

common species used. Since the legislative ban on antibiotic usage in animal husbandry, probiotic spores are now commonly fed to animals as a disease preventative measure (Vondruskova *et al.* 2010). *B. subtilis* probiotic spores are currently used in commercial brands of feed supplement such as BioPlus 2B (from Chr. Hansen) and Calsporin (from ORFFA).

Sporulation occurs upon deprivation of available nutrients, leading to the formation of dormant endospores which are extremely resilient to external stresses. They will germinate once they return to more favourable conditions for outgrowth. However, it is widely acknowledged that vegetative cells will die very quickly in both stomach and duodenal conditions (Clavel *et al.* 2004; Ceuppens *et al.* 2012).

There is sufficient evidence in the current scientific literature to substantiate the beneficial effects of ingested probiotic spores (Alexopoulos *et al.* 2004). In recent years there have been studies involving pigs to indicate that the enteric nervous system (ENS) contains chemically coded neurons that serve specific functions for the control of the gastrointestinal tract. Intriguingly, di Giancamillo *et al.* (2010) has shown that luminal changes in the gut of piglets administered probiotics instigated a response in the ENS that altered the neuronal and glial (non- electrical brain cells (Fields 2013)) chemical codes thus creating a 'larger number of galanin- and calcitonin gene related peptide (CGRP)-immunoreactive neurons' and also 'glial fibrillary acidic protein positive enteric glial cells were significantly higher in the inner and outer submucosal plexuses of treated animals'.

Nutritional advantages are also proven to be related to gut microflora. In a study by Torrallardona *et al.* (2003), pigs were given ¹⁵N and ¹⁴C isotopes from dietary ¹⁵NH₄Cl and ¹⁴C-polyglucose respectively. These were assimilated by bacteria in the gut to make essential amino acids such as lysine. This lysine (with the heavier isotope) was found to persist in the piglet faeces and gut contents. As mammals are unable to assimilate lysine into amino acids themselves, the lysine must be from bacterial origin. This highlights the importance of having a good balance of microflora in the gut.

However, it is not clear yet what exactly happens to the ingested spores while travelling across the animal GIT tract (Leser *et al.* 2008; Ceuppens *et al.* 2010), which may be due in part, to the complexities of *in vivo* modelling (Sumeri *et al.* 2008). Although it is now generally acknowledged that spores can indeed germinate in the GIT, (Casula and Cutting 2002; Cartman *et al.* 2008) the extent of germination is still not known (Hong *et al.* 2005; Ripamonti *et al.* 2009). Whilst there is great ambiguity in this area, one of the most financially important questions would be to query the viability of the spores. This question would be vital for farmers and those in the animal husbandry sectors and can be answered by evaluating the physiological states exhibited by the probiotic bacteria (administered as spores) as they travel along the gastrointestinal tract (GIT) (Hong *et al.* 2005; Huyghebaert *et al.* 2011; Kenny *et al.* 2011). Before such studies can be undertaken, it is essential that a thorough understanding of the organism's life cycle is obtained, and the challenges it will face in the GIT are understood.

1.1.4 Diet

The conditions of the pig stomach are incredibly variable, but the first and most significant cause of changes in composition and pH of stomach fluids will be the diet (Kararli 1995; Partanen *et al.* 2006; Merchant *et al.* 2011). Any food given to a pig will cause an initial increase in pH (caused by the food directly) to reported values of pH 4.94 (Möbeler *et al.* 2010). The stomach then reaches a pH of around 3.5 shortly after eating (Kararli 1995; Canibe and Jensen 2003; Canibe *et al.* 2005; Yang *et al.* 2005; Marcinakova *et al.* 2010; Möbeler *et al.* 2012). An interesting factor to also consider is that the size of the particles of food will also impact the pH in the stomach. This was studied in detail by Möbeler *et al.* (2010), where it was found that a finely ground diet would cause less variation in the separate regions of the stomach compared to a coarsely ground diet (See Figure 1.1 for areas of the stomach). This finding is probably due to the increased surface area in a finely ground meal, compared with a coarsely ground meal, where the particles would obviously take longer to be broken down.

Testament to the differences seen in stomach conditions at different times is that 'gastric juice has a high Na^+ and a low H^+ concentration at low secretory rates (when the stomach is nearly empty), while at high secretory rates (post meal) the reverse is found.' Noted by Allen and Garner (1980).

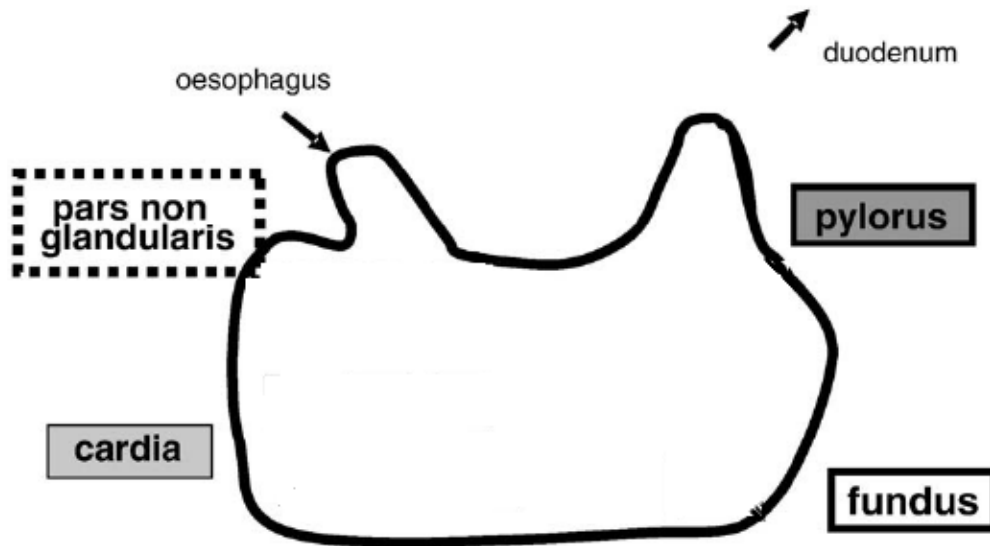


Figure 1.1 Diagram showing the four main compartments of the pig stomach. From the oesophagus: pars nonglandularis, cardia, fundus and pylorus leading to the duodenum (Möβeler *et al.* 2010).

1.1.5 Intra-gastric variation

The study carried out by Möβeler *et al.* (2010) illustrates that the first part of the stomach, (pars nonglandularis) has the highest pH (up to 4.94) and the penultimate part of the stomach (fundus) typically has the lowest pH (to pH 3.07).

Ion movement across the mucosal layer of the stomach

Given the very low pH of the stomach, the thick layer of mucus in the stomach is vital in protecting the epithelial layer (Allen and Garner 1980).

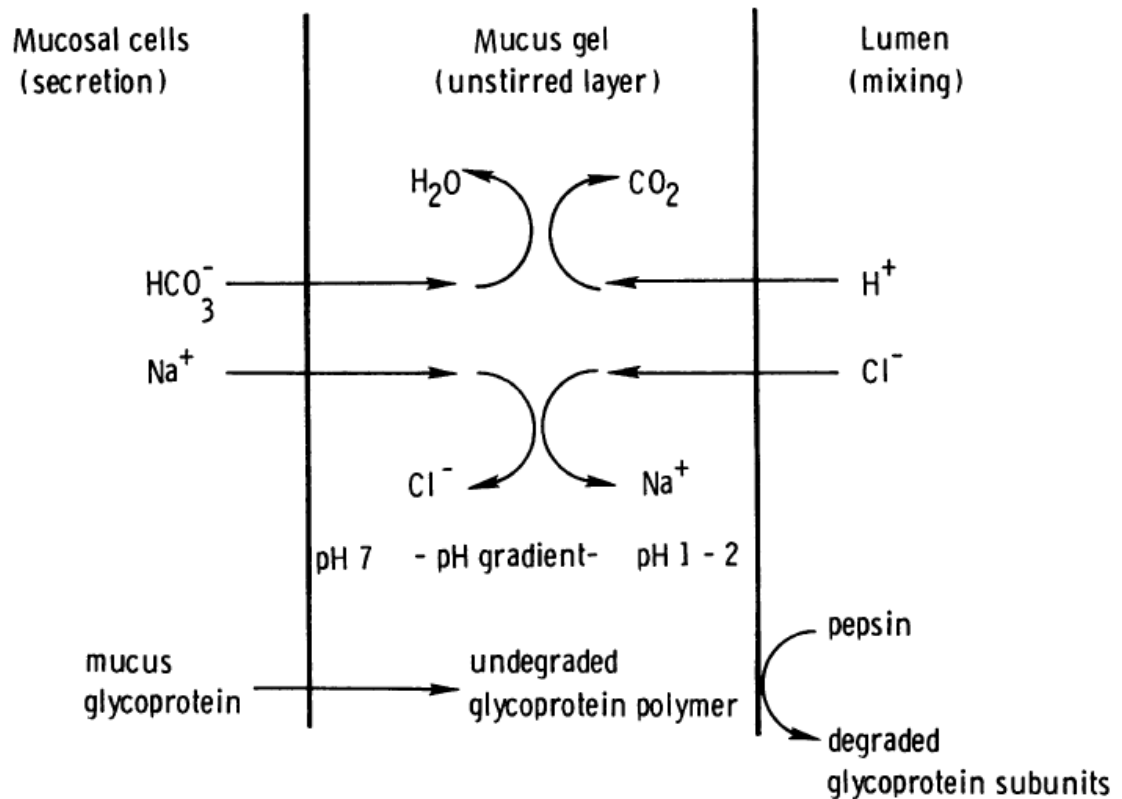


Figure 1.2 Diagram showing the movement of ions across the mucosal layer and lumen of the stomach (Allen and Garner 1980).

Figure 1.2 illustrates that the mucus layer remains unstirred, giving protection to the mucosal cells. This mucus gel is where the HCl from the stomach is neutralised by HCO_3^- secreted by the surface epithelial cells to produce CO_2 and H_2O .

This constant neutralisation of HCl by HCO_3^- will mean that HCl is secreted constantly to ensure a low lumen pH is maintained (Allen and Garner 1980)

1.2 *Bacillus subtilis*

B. subtilis is a Gram positive facultative anaerobe from the family *Bacillaceae* (Traag et al. 2013). Originally found in soil, it is one of the most widely studied organisms, largely owing to its potential as a model for *Bacillus anthracis* and other pathogenic spore formers (*B. cereus*, *Clostridium difficile*) and also as a means to investigate industrial

decontamination processes. Furthermore, its' genome was fully sequenced in 1997 (Kunst *et al.* 1997), meaning it is the best characterised Gram positive bacteria. Domestic strains of *B. subtilis* can be traced back to the original Marburg strain, which gave rise to the tryptophan-requiring auxotroph *B. subtilis* 168 (Zeigler *et al.* 2008).

It has recently been hypothesised that it has specifically adapted to life in the GIT (Tam *et al.* 2006). Their purported efficacy as probiotics rests in the dormant spores' resistance to external stresses, meaning they are less susceptible to the harsh conditions encountered in the GIT (Cutting 2011). Since it is generally believed that the lower GIT is an anaerobic environment (oxygen concentration at 2–7% of air saturation) (He *et al.* 1999), *B. subtilis*' ability to grow in anaerobic conditions is another attribute that makes it suitable for both colonisation of the GIT and its suitability as a probiotic. *B. subtilis* cells will use nitrate as the terminal electron acceptor under anaerobic conditions and since this is abundant in the GIT, the organism should be able to undergo anaerobic respiration in these conditions (Sorokulova 2013).

1.2.1 Sporulation

Spore forming Firmicutes bacteria generally fall under the genera of *Bacillus* and *Clostridia*. Sporulation occurs as a response to insufficient nutrients in the environment, typically carbon and nitrogen, and in some cases phosphorous. This starvation is usually caused by harsh environmental conditions (Piggot and Hilbert 2004; Cutting 2011). Sporulation can be induced in a laboratory setting through the use of Difco Sporulation Medium (DSM) or AK sporulating agar detailed in Appendix 1, in which the vegetative cells are starved of nutrients and therefore begin the sporulation process early in culture.

Typically, the changes that result in spore formation begin in the cytoplasm of the vegetative cell. The cell will divide asymmetrically (shown in Figure 1.4 A and B) and the smaller compartment will ultimately form the dormant spore and the resulting spore houses the DNA of the original bacterium, whilst the larger segment is mainly responsible for the formation of the spore coat (McKenney and Eichenberger 2012). As a general rule, spores

are non-motile and one bacterium forms one spore, similarly as one spore germinates, it germinates into one vegetative cell originally (Muir and Kitchie 1961).

Sporulation takes between six to eight hours and involves the formation of a proteinaceous coat *via* a cascade of four mother cell-specific transcription factors as well as protein-protein cross linking and proteolytic events (Henriques and Moran 2000). Sporulation has previously been broken down into six key stages (labelled O to V) (McKenney and Eichenberger 2012). However more recently, eight stages are described, though as Tan and Ramamurthi (2014) state, the process of sporulation does not occur in distinct stages, as there may be considerable overlap in defined stages as the events occur in a continuum. An overview of the general process of sporulation is shown below in Figure 1.3

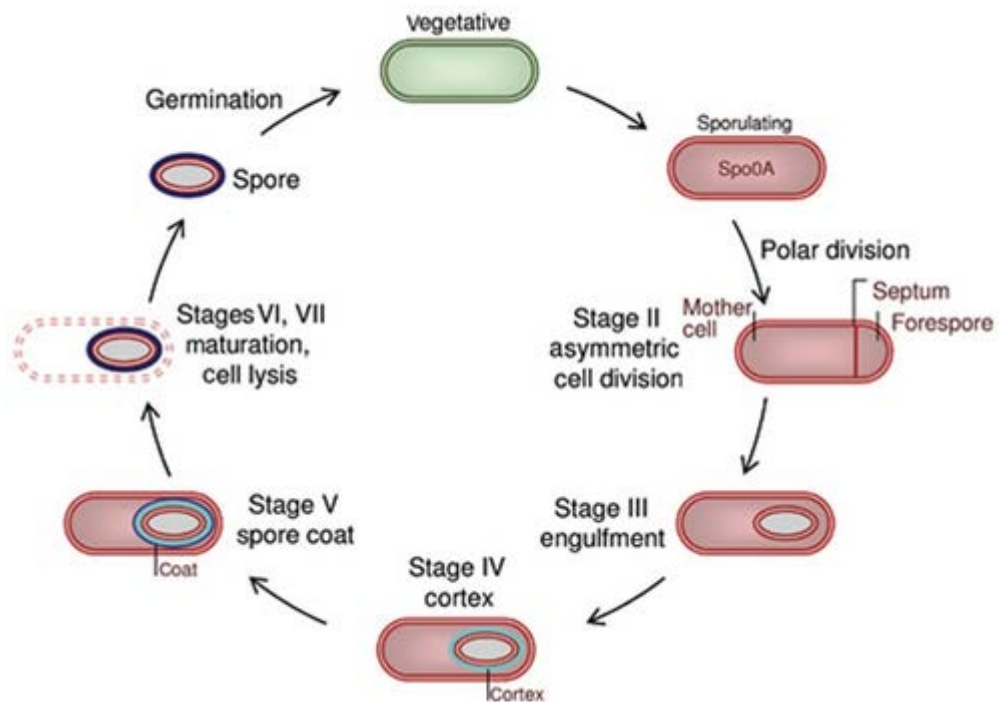


Figure 1.3 Overview of the stages of sporulation in *B. subtilis* from González-Pastor (2011)

Stage O relates to the spore decision to sporulate. Whilst there is no known specific molecular signal that initiates sporulation, a combination of factors are known to play a role

in triggering sporulation (McKenney *et al.* 2013). Nutrient depletion is of course one of the primary factors involved, though initially a sub-population of the spores will begin cannibalistic behaviour, in which the neighbouring spores are broken down to provide nutrients for the toxin-producing sub-population (González-Pastor 2011). However, when starvation conditions become clearer, the spores commit to sporulation through the activation of histidine sensor kinases (Kin A, Kin B and Kin C) which shuttle phosphate through a phosphorelay system leading to phosphorylation of the Spo0A transcription factor (McKenney *et al.* 2013).

Stage I: axial filamentation and ensuring correct chromosome copy number. Sporulation begins when initiation signals activate the master transcription regulator Spo0A. The commencement of spore forming manifests visually as small granules in the protoplasm that eventually join together to assume an oval shape which is shorter but broader than the original bacterium. The granule is highly refractile and will not stain by ordinary methods (Henriques and Moran 2000; Cutting 2011). At this stage, the cell harbours two chromosomes, one for the mother cell and another for the forespore, though the pattern of transcription in the two genomes are different and the structures of the nucleoids in each compartment are very different also (Ragkousi *et al.* 2000). This stage involves early spore engulfment, where the septum shows curvature seen in Figure 1.4 A.

Stage II is known as asymmetric septation. In this stage, temporary genetic asymmetry arises because the polar septum bisects the axial filament resulting in only about a third of the chromosome being harboured by the forespore. The enzyme DNA translocase (found in the mother cell) is responsible for pumping the remaining DNA into the forespore (Tan and Ramamurthi 2014).

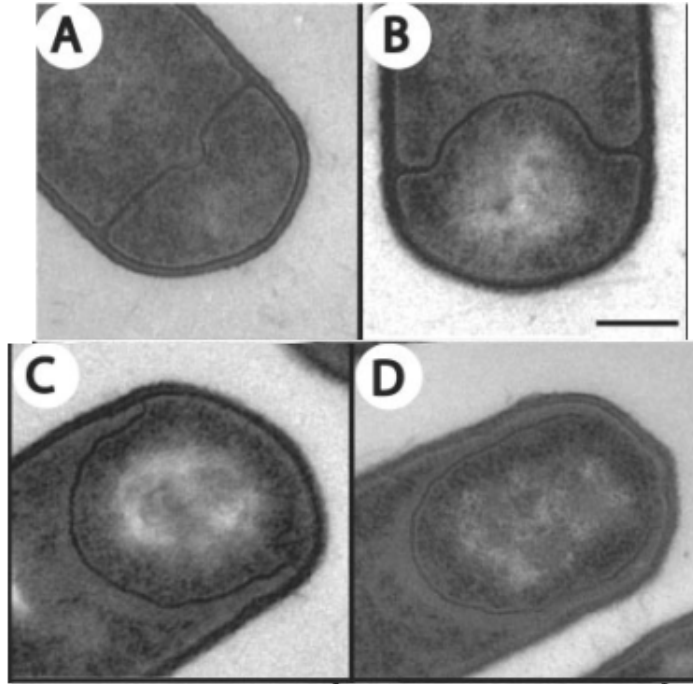


Figure 1.4 Electron microscopy images showing stages I, II and III of sporulation. A and B= wild type *B. subtilis* cell (168) undergoing asymmetric septation, C and D= early stage forespore engulfment. Scale bar = 200nm. Electron microscopy images taken from Thompson *et al.* (2006)

Stage III, is known as engulfment. It is at this point that the mother cell engulfs the forespore as the polar septum curves around the forespore forming a double membrane around the forespore within the mother cell cytosol. To finish engulfment, ‘the membranes must undergo membrane fission to pinch off and release the forespore’ (Tan and Ramamurthi 2014).

Stage IV and V refer to the cortex and coat assembly. Some researchers have denoted stage IV as cortex formation and stage V as coat formation (Errington 2003; González-Pastor 2011), though there is considerable overlap between the two processes (Tan and Ramamurthi 2014). At stage IV, (late sporulation) the spore is still phase dark. Coat formation begins with a scaffold that it comprised of half of the coat proteins on the mother cell side of the forespore (known as the mother cell proximal pole, MCP). The sigma factor σ^E controls the assembly of the basement layer, though this is under the control of three

morphogenic proteins: SpoIVA, SafA and CotE (de Francesco *et al.* 2012). The inner and outer coat layers are reliant on SafA and CotE (McKenney *et al.* 2013).

Stage V is late sporulation where the spore becomes phase bright, this occurs approximately six hours after the initiation of sporulation.

Stage VI is the release of the dormant spore from the mother cell. This is shown in Figure 1.5 a. The larger mother cell, which is required for spore formation, is eventually lysed. The prespore is then released within the mother cell as a protoplast (Piggot and Hilbert 2004)

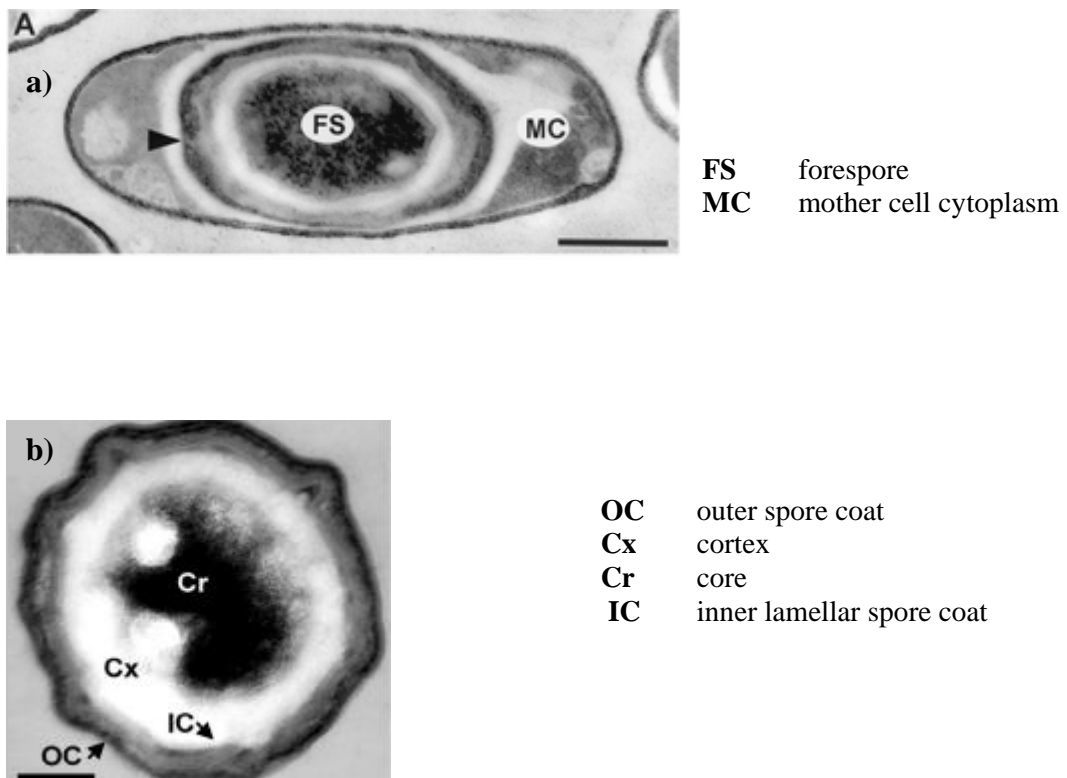
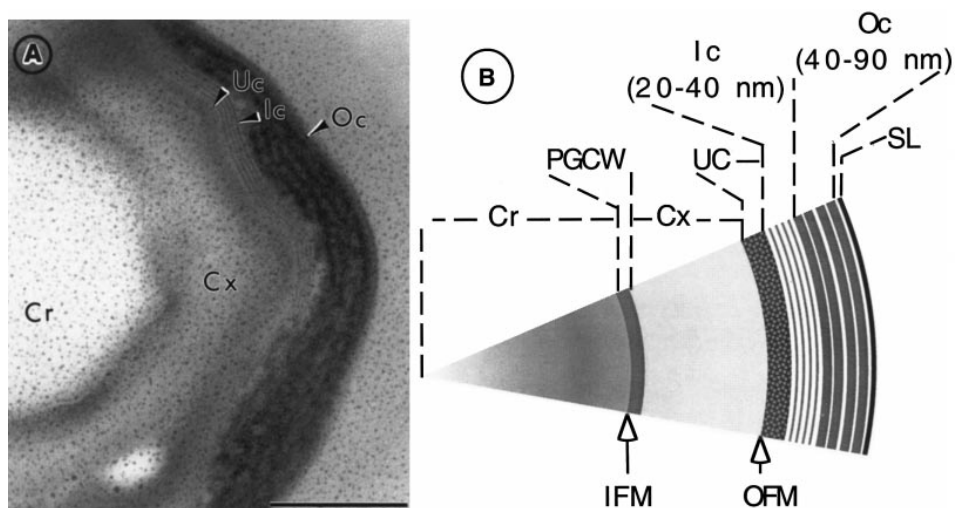


Figure 1.5 Stages of Sporulation visualised by electron microscopy a = Mature *B. subtilis* spore within a mother cell from Catalano *et al.* (2001) where scale bar =500nm. b = mature free spore. Scale bar = 125nm from Silvaggi *et al.* (2004).

Stage VII is sometimes used to refer to the completed lysis of the mother cell and the released spore in Figure 1.5 b (Reineke 2013).

The spore itself is composed of various different layers (see Figure 1.6), the outer most layer is known as the surface layer (SL), then the coat is formed of the outer (OC), inner (IC) and a stained amorphous layer known as the under coat (UC) which separates the coat from the cortex (Cx). The outer forespore membrane (OFM) also separates the cortex from the undercoat. The cortex is a key factor in protecting the spore from heat resistance and lysozyme enzymes. Separating the cortex from the spore core (Cr) is the Inner forespore membrane (IFM) which is surrounded by the primordial germ cell wall (PGCW). It is inside the spore core that the chromosome is situated, protected by many barriers from harsh conditions. This spore core is composed of several fine lamellae (Carroll *et al.* 2008).



Cr Core
PGCW primordial germ cell wall
Cx Cortex
UC Under coat
Ic Inner cortex
Oc Outer Coat
SL Surface Layer or exosporium
IFM Inner Forespore membrane
OFM outer forespore membrane

Figure 1.6 A: Example of scanning electron microscopy (SEM) cross section of *Bacillus* spore and B, schematic diagram of radial spore layers. Scale bar represents 0.2 μ m (Henriques and Moran 2000).

1.2.2 Germination

The transition of a spore into a dividing vegetative cell is now referred to in two different stages; germination and outgrowth. Germination refers to the first stage and outgrowth is the transformation of the germinated spore into the vegetative cell (Hitchins *et al.* 1963).

With regards to the germination of spores in the gastrointestinal tract, it is acknowledged that this is triggered through nutrient germinants of low molecular weight such as sugars, amino acids or purine derivatives (Paredes-Sabja *et al.* 2011). The most commonly named germinants are L-alanine, glucose, fructose, potassium (GFK) and L-asparagine. L-alanine interacts with the nutrient germinant receptor GerA whereas GerB and GerK are thought to interact with L-asparagine and GFK (Atluri *et al.* 2006). As most of these compounds are found in abundance in the GIT it can be assumed that they are key factors in germination of *Bacillus* in gastric conditions. Furthermore, germination of *B. subtilis* spores can be induced by acid treatment at pH 3 for 30 minutes (Leser *et al.* 2008). This suggests that ingested spores may start to germinate during stomach passage.

The process of germination occurs in two stages and takes approximately 25 minutes (Hitchins *et al.* 1963), though there is a highly variable lag time from the addition of germinants to the onset of germination between spores in a given population (Setlow 2014). A diagram detailing the basic process is shown below in Figure 1.7

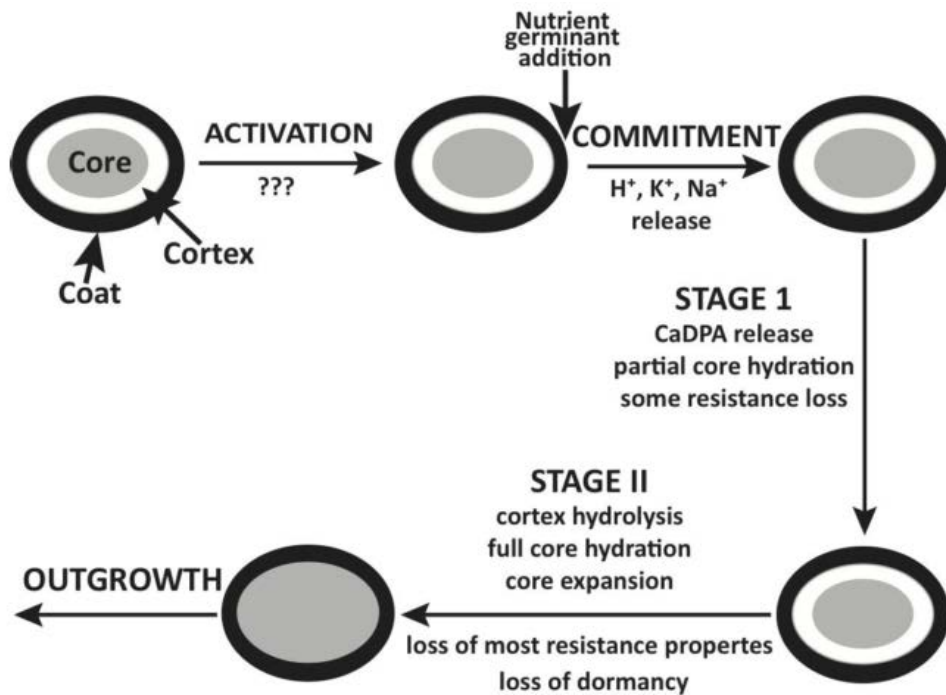


Figure 1.7 Outline of nutrient germination of *Bacillus* spores. The germ cell wall is not shown but it expands as the cortex is hydrolysed in stage II of germination. Image and text from Setlow (2014)

Stage I.

- Nutrient germinants bind to specific receptors, known as germinant receptors (GRs) located in the spore's inner membrane, (IFM) as shown on Figure 1.6 which initiates spore commitment to germination (Yi and Setlow 2010). This is associated with a change in the permeability of the inner membrane (Setlow 2014).
- This triggers the release of core small molecules, including dipicolinic acid (DPA). DPA is assumed to be released *via* channels made of SpoVA proteins (Setlow 2014). It is at this point in germination that the spore will lose its resistance to stresses.
- The small molecules released are replaced by water.

Stage II.

- DPA release triggers hydrolysis of the peptidoglycan cortex.

- Cortex hydrolysis is catalysed by either of two cortex-lytic enzymes (CLEs) (CwlJ and SleB) which recognise muramic acid- δ -lactam (MAL) – a component of the cortex PG (Setlow 2014).
- Cortex hydrolysis then allows core expansion and further water uptake followed by spore outgrowth (Kong *et al.* 2010).

Outgrowth

Rehydration of the spore (when water reaches approximately 80% of wet weight) allows metabolism to begin in the core, followed by macromolecular synthesis. This leads to the conversion of the germinating spore to a growing cell (Setlow 2014). Outgrowth takes around 95 minutes and is divided into four stages: swelling, emergence from the spore coat, elongation of the emergent organism, and finally division of the elongated organism (Hitchins *et al.* 1963). Zaman *et al.* (2005) illustrated this process using transmission electron microscopy (TEM) in Figure 1.8.

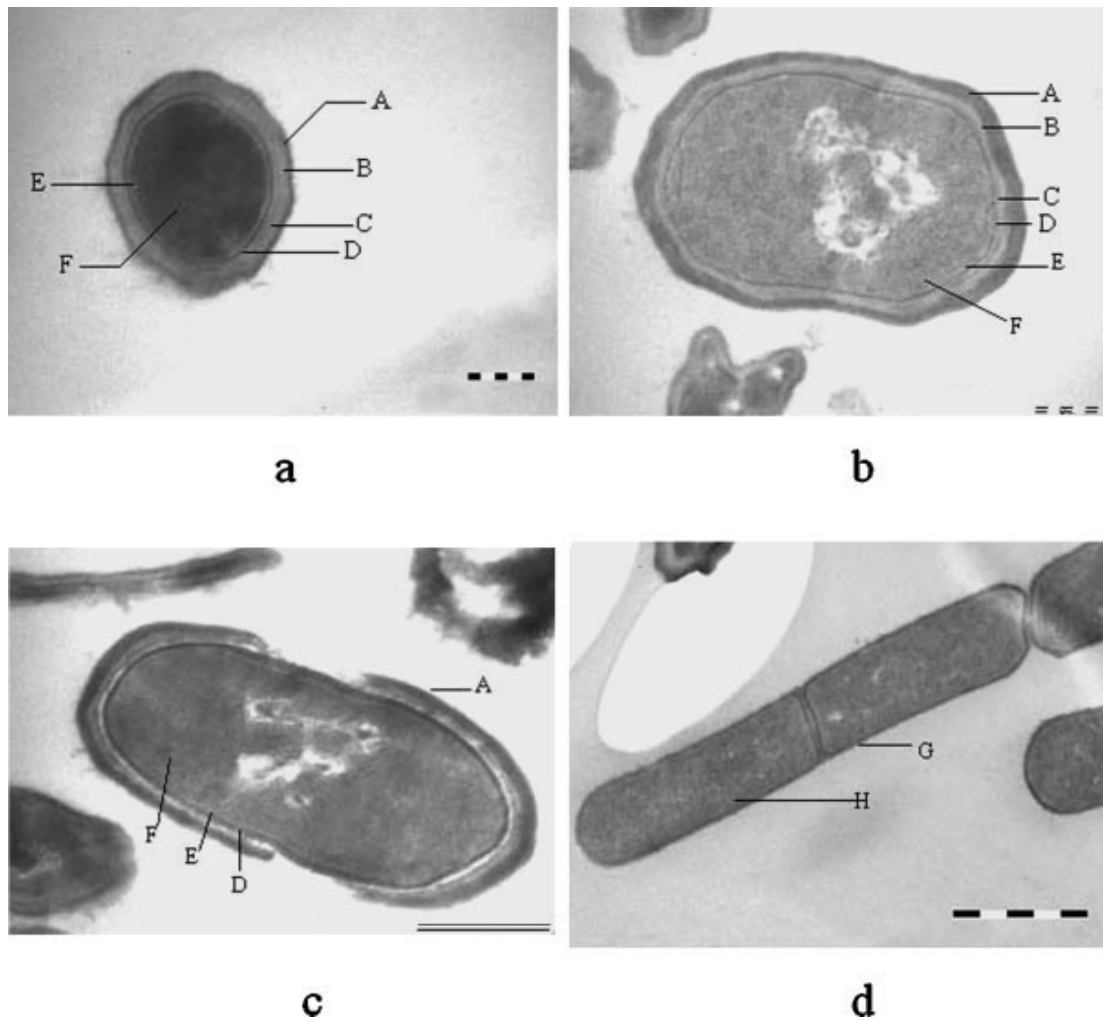


Figure 1.8 Imaging of *B. anthracis* spore germination through TEM at (a) 0 hour, (b) 1 hour, (c) 2 hours, and (d) 3 hours. A, spore coat; B, outer spore membrane; C, spore cortex; D, germ cell wall; E, inner spore membrane; F, spore core; G, cell wall; H (Zaman *et al.* 2005).

In Figure 1.8 a) the *B. anthracis* spore is in its dormant state. *Bacillus* spores either have a smooth or ridged surface. The difference is thought to be due to the loss of the exosporium in the bumpy or ridged spores during cultivation or sampling. This fact is intriguing as most non-pathogenic Bacilli do not possess a well formed exosporium, therefore this feature is linked with infection (Swiecki *et al.* 2006).

Figure 1.8 b. Illustrates the beginning of germination, there is a small increase in length as well as volume of the spores. This change may be a result of the increase in hydration levels of the spore.

In Figure 1.8 c. a further increase in length but a decrease in width is seen. The spore coat begins to break and the germ wall becomes the outer layer which later forms the cell wall.

Figure 1.8 d. illustrates two distinct vegetative cells in the typical *Bacillus* rod form (Zaman *et al.* 2005).

Once the final stage is reached, vegetative growth can resume, assuming conditions are favourable and there are sufficient nutrients to meet the needs of the organism.

Bacterial spores are one of the most durable life forms on Earth, owing to their resistance to extreme heat, desiccation, radiation, and various chemicals (Setlow 2006). Understandably, they are a common topic in biological research, however there are still many aspects of the dormant spore's structure to function relationship that are poorly understood. Of primary importance, is to understand what the spore is composed of and how these structures aid the spore's resistance.

1.2.3 Function and composition of bacterial spore structures.

The structure of the spore has been studied in great detail, as shown in Section 1.2.1 (sporulation). In the following section, the most relevant functions and compositions of spore structures are highlighted in the context of the research project executed herein.

The core

It is acknowledged that the spore core, where the DNA is located, is semi-dehydrated by replacing water with Ca^{2+} - dipicolinic acid (CaDPA), a 1:1 chelate of pyridine-2,6-dicarboxylic acid (DPA) with divalent cations, predominantly Calcium. DPA is present at >800mM in the spore core, well above the level of solubility (Huang *et al.* 2007). This dehydration plays a large role in spore resistance to external stresses. Only when the DPA has been dissolved by water and exits the spore can outgrowth be achieved. It is surrounded by the inner forespore membrane (McKenney *et al.* 2013).

The PG cortex

The cortex is a peptidoglycan layer encasing the core, it is composed of a thin layer called the primordial germ cell wall (PGCW) and the thicker outer layer referred to as the cortex. The PGCW is so named because it is believed to form the basis for the vegetative cell wall (Atrih *et al.* 1996). The main cortex is composed of the same amino acids and sugars found in the vegetative cell peptidoglycan, however around 50% of disaccharides in the spore peptidoglycan are substituted with muramic acid δ -lactam residues (Warth and Strominger 1969). Muramic acid δ -lactam is produced by enzymatic removal of a peptide side chain from the N-acetylmuramic acid residue (a disaccharide) (Gilmore *et al.* 2004). Its main purpose is to assist in core dehydration, and is believed to contribute to heat resistance (Meador-Parton and Popham 2000).

Spore coat

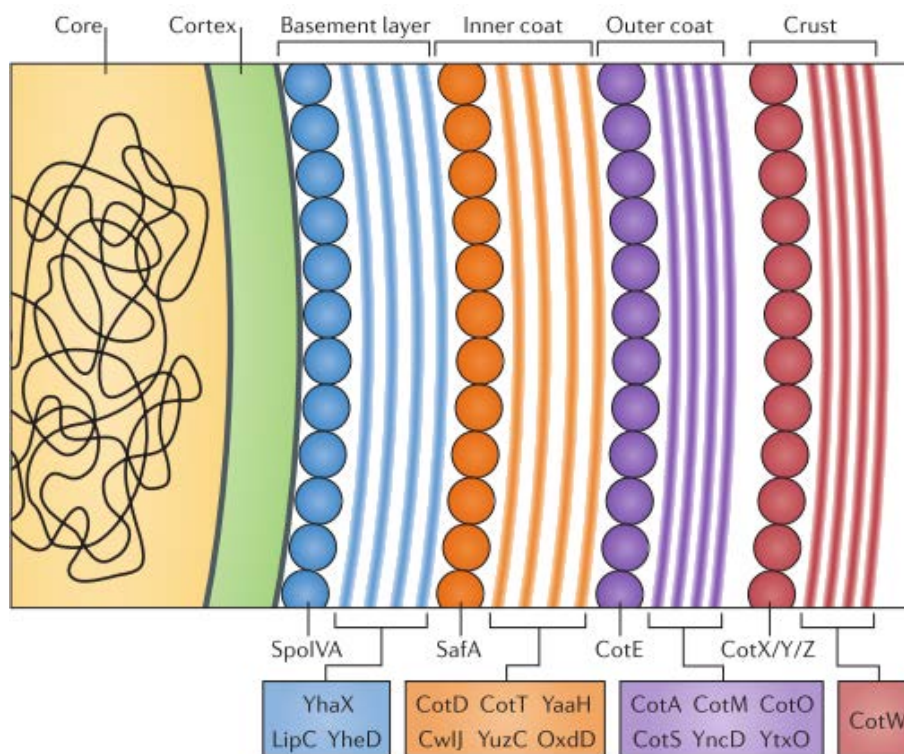


Figure 1.9 Diagram of cross section of a dormant spore, illustrating layers of the spore coat. The outer forespore membrane covers the cortex (PGCW), and this is surrounded by the basement layer (blue),

followed by the inner coat (orange), then the outer coat (purple) and finally the crust (red). Coloured boxes underneath indicate where important germinant receptors are located in each layer.

The coat is largely comprised of proteins, which are assembled by the mother cell during sporulation. The first layer, known as the basement layer, or the under coat (Huang *et al.* 2008) is the first to be assembled, by the cascading mother cell genes. The inner coat and outer coat are constructed in layers. The full sequence of events in coat formation are explained in a recent review from McKenney and Eichenberger (2012). Within the coat are enzymes, of particular note is the presence of alanine racemase YncD, which converts L-alanine to D-alanine: a germination inhibitor. It is thought to play a role in preventing germination when conditions are unfavourable to cell survival (Chesnokova *et al.* 2009).

1.2.4 Alternative responses to changes in the environment

As well as sporulation, some *B. subtilis* strains may react to a depletion of nutrients by changing their motility, secreting extracellular enzymes, undergoing competence for genetic transformation (Dubnau 1991) or producing antibiotics. One particularly well studied bioactive compound is surfactin (Carvalho *et al.* 2010). This acts as a surfactant and an antimicrobial.

Biofilm formation is another key response to certain environmental conditions. A bacterial biofilm consists of aggregates of bacteria, stabilised by an extracellular polysaccharide matrix (EPS) produced by the cells (Winkelman *et al.* 2009). Bacterial motility initially promotes the formation of biofilms, but once the bacteria start to adhere, this motility is inhibited by EpsE, a protein that inhibits flagellar rotation. Biofilms arise due to a complex series of regulatory proteins, which alter the *B. subtilis* from the planktonic individual cell, to the cell aggregate state (Guttenplan *et al.* 2010). Surfactin is considered to be one of the signals that induces the expression of matrix genes in the population (Vlamakis *et al.* 2013) though biofilm formation is primarily dependent on the adhesion of cells to a

surface. Ultimately, the biofilm structure provides increased antibiotic resistance to the bacterial population as well as resistance to other stressors in the environment, making them a clear alternative survival strategy for *B. subtilis* (Stanley and Lazazzera 2004).

1.2.5 Viability assessment of *B. subtilis* cells and spores in the GIT

Understandably, given the potential for *Bacillus subtilis* as a probiotic, a lot of studies have been focused on the transit of spores through the GIT. *In vivo* mice models are a convenient means of exploring spore behaviour in GIT conditions (Hoa *et al.* 2001). Casula and Cutting (2002) inoculated mice with spores of *B. subtilis* and tracked their passage through the murine GIT. In some examples, faecal spore numbers exceed the inoculum suggesting that germinated spores, after a few limited rounds of growth and division, re-sporulate to escape the hostile environment in the GI tract. Re-sporulation of *B. subtilis* can occur in the ileum and large intestine of mice; however, the author notes that these figures are quite unusual, given the timescale for the spores to undergo germination, outgrowth as well as survive the acid and bile stress across the GIT (Casula and Cutting 2002). No other explanations are offered for this increase in spore count in this paper.

As probiotics are geared towards use in agriculture, another *in vivo* model to use is pigs. Leser *et al.* (2008) illustrate that in nutrient-rich medium, germination of *B. licheniformis* CH200 and *B. subtilis* CH20 occurs within 60–90 minutes. Given that the stomach passage time for a solid meal is 3–12 hours in growing pigs, a fraction of the spores most likely germinated in the stomach. Indeed Leser *et al.* (2008) go on to partially assess spore behaviour in a pig GIT using spores encased in a dialysis membrane of molecular weight cut off from 12,000 to 14,000 Daltons. This allows complete transport of GIT liquids but not microorganisms (Leser *et al.* 2008). This experimental approach has the inherent limitation of not allowing direct interaction between the spores and other microbial communities in the gut, confining the study to the assessment of the influence of the abiotic conditions on the spores. However it should be noted that antimicrobial peptides, such as those produced by LAB may pass through these membranes since they are usually in the

range of 5-10kD (Dirix *et al.* 2004). Similarly, one cannot exclude the fact that small diffusible chemical signals, known as quorum sensing molecules may also pass through these membranes which can influence multicellular behaviours such as germination and biofilm formation (Sifri 2008). It was noted in the study that the numbers of bacteria drop quite dramatically in the stomach, but recover very quickly in the jejunum. As with the murine study by Casula and Cutting (2002), this rapidly changing count seems quite unusual, though again, no explanation is offered for this phenomenon. Furthermore, there was a lack of a rigorous assessment on the physiological states of the ingested bacterial spores.

However, another merit of the study from Leser *et al.* (2008) is the deployment of a basic microbial flow cytometric (FCM) analysis to simply identify general numbers of vegetative cells and spores. Their FCM protocol lacked the ability to verify viability, meaning the ability to cross reference the FCM data with the plating data was limited. Despite the limitations, their idea of spore encasement provides a unique and effective way of systematic monitoring of the spore physiological status across the GIT. Provided that a more advanced FCM analysis was applied to their experimental approach, more light could be shed on which areas of the GIT may cause probiotic spore outgrowth, death or sporulation. Within this idea lies the opportunity to obtain more detailed and insightful knowledge that could be directly applicable for enhancing probiotic viability, whilst generating information in an area that is not well investigated as acknowledged in the current literature (Casula and Cutting 2002; Cartman *et al.* 2008)

1.2.6 Current Microbial Enumeration Methods

Aside from FCM, viability has been conventionally studied *via* plating/culturing. The use of plating as a means to count bacteria rests on the assumption that one cell will produce one colony, therefore colony forming unit counts (cfu/ml) can be used as a method of cell counting (Stopa 2000). Whilst information on the culturability of probiotics can be readily achieved through these traditional microbiological techniques, they do not indicate

how damaged or in what physiological state the spores are. A large problem with any technique involving the measurement of viability is the fact that viable or 'living' cells can be defined in a number of different ways. For methods such as plating, viability simply refers to an organisms' ability to grow in the presence of nutrients (Khan *et al.* 2010). There are a number of drawbacks associated with this assumption, primarily, if a cell was stressed or sub-lethally damaged, the organism may be resuscitated in the appropriate conditions, for example Kong *et al.* (2004) illustrated how bacteria may be resuscitated in anaerobic conditions. A standard plating method, performed in aerobic conditions would therefore not include bacteria which could possibly be recovered in anaerobic conditions. Similarly, there are several bacterial species cells which can enter a viable but non-culturable state (VBNC). This is a strategy employed by some species which enables them to enter a state of very low metabolic activity, allowing them to achieve long-term survival in unfavourable conditions. However this prevents them from being able to form colonies, and accordingly, bacteria in this state will not be viewed under plating techniques (Ramamurthy *et al.* 2014). Furthermore, an extensive study by Jongenburger *et al.* (2010) highlights the large variation in plate count data. It may be that issues such as bacterial aggregation or chains of cells affect these plate counts. For example, a clump of cells would only be viewed as a single colony, where in actual fact there could be several viable bacteria.

It is possible to gain an approximate number of spores to germinating/vegetative cells within a sample. The most common method is to heat samples to 80°C for 20 minutes to destroy vegetative cells and germinating spores, therefore leaving the dormant spores only. Another method of eliminating vegetative cells is to grow *Bacillus* in DSM and treat with lysozyme (Spinosa *et al.* 2000) as previously noted, the spores are resistant to lysozyme therefore only the vegetative cells and germinating spores will be killed. The spores can then be germinated and counted on a suitable medium. Another method for determining spore counts in a mixture of spores and cells, is to kill vegetative cells with Renografin (used to destroy vegetative cells in *B. anthracis*) (Wang *et al.* 2009).

Owing to the nature of cultivation it is known that this technique, whilst useful, does not give a very accurate account of microflora of the GIT. This has resulted in the use of molecular techniques, such as Fluorescent *in situ* hybridisation (FISH) Denaturing Gradient Gel Electrophoresis (DGGE) and reverse transcriptase polymerase chain reaction (RT-PCR) and real time-quantitative PCR (qPCR). The benefits of such techniques are that they eliminate the need for culturing of bacteria. This is particularly relevant when one considers the number of uncultivable bacteria known to exist. A significant body of bacterial research takes advantage of molecular techniques to measure species richness and microbial diversity in samples (Thanantong *et al.* 2006; Baxter and Cummings 2008; Hajela *et al.* 2012). These culture-independent methods are reviewed extensively by Davis (2014), the main benefits of such molecular methods being that high numbers of different bacterial species can be detected based on their DNA or RNA.

In particular, FISH has been covered quite extensively in probiotic research. Usually rRNA targeted fluorescently labelled oligonucleotides are used, which have the advantage of being able to identify species at the sub-species level owing to the wide availability of rRNA sequence data (Wallner *et al.* 1993). Typically, 16s rRNA sequences are retrieved from online databases such as Genbank, or EMBL. These sequences are analysed and potential target regions for the hybridisation probes are selected (Langendijk *et al.* 1995). These fluorescently labelled bacteria can then be analysed using a direct imaging technique, such as confocal microscopy, or can be enumerated using flow cytometry (FCM) (Davis 2014).

Measuring metabolic activity of cells is another common way of determining counts of viable cells. The dye carboxyfluorescein diacetate (cFDA) can be used to detect the cytoplasmic esterase-catalysed hydrolysis of cFDA to carboxyfluorescein (cF) and two acetate molecules. As cF is strongly fluorescent this can be used as a marker for metabolic activity (Shen *et al.* 2009).

To visualise this dye, microscopic techniques can be employed. A haemocytometer is regularly employed in microscopic research to enumerate cells, however specially

designed bacterial counting chambers are preferential, as these have a smaller depth and hence there is less space for bacteria to flow over each other and eliminates the issue of multiple planes of view. Typically a Petroff-Hausser (PH) counting chamber is 0.02mm in depth, as opposed to a standard haemocytometer depth of 0.1mm, (some may be further specialised to 0.01mm in depth) (Guillard and Sieracki 2005). The main issue associated with microscopic techniques are the time consuming nature of this analysis. Whilst there are new software that can enumerate or 'count' fluorescent bacteria, such as Image Pro and ImageJ, these programs require an advanced level of IT knowledge and hence a great deal of time to set up for efficiently accurate enumeration. Furthermore, these programs require a high quality image to work effectively; therefore when an image is of poor quality (for example if the background was unevenly lit), these programs would not function. Without the use of advanced software, the only other option available in these cases is to count bacteria manually, though to gain accurate PH counts, a high concentration of cells is required (at least 10^6 - 10^7 cells/ml) (Carlberg 1995). Suffice to say the time taken to count hundreds, or perhaps thousands of bacteria renders microscopic enumeration unsuitable for experimental work involving millions of bacteria (Bakker *et al.* 2007).

One main drawback of the above mentioned methodologies is that they do not equip the investigator with the required insights into the physiological states of the organism. This is particularly relevant when investigating an organism such as *B. subtilis* which has multiple physiological states. From this perspective flow cytometry has much more potential as a tool provided that a suitable FCM protocol is applied for quantification of the different physiological microbial states. Whilst there has been a moderate amount of data generated as to total counts of bacteria by FCM (Paulse *et al.* 2007), to date, there is very little quantitative data concerning specific sub-populations of bacteria. It was found that Khan *et al.* (2010) provides some detailed insights into the viability of *Escherichia coli* O157:H7, *Pseudomonas aeruginosa*, *Pseudomonas syringae*, and *Salmonella enterica*, through staining with Syto 9 and PI. However, the information derived from their study was to assess

VBNC organisms, by identifying cells with a compromised membrane. As such, the study by Khan *et al.* (2010) was not applied to the study of spores and their intermittent states. Leser *et al.* (2008) have also used counting beads to enumerate *Bacillus* in the GIT, but they have not extended their studies to enumerate the amount of dead cells present or the number of dead spores present. While it is evident from the wider current literature that FCM has not been used to its full potential in the area of quantification of bacterial physiological states, it appears that there is a significant volume of knowledge/findings already available (Comas-Riu and Vives-Rego 2002; Black *et al.* 2005; Cronin and Wilkinson 2007; Mathys *et al.* 2007; Leser *et al.* 2008; Nebe-von-Caron 2008) which endorse the potential of flow cytometry (FCM) as a useful tool to assess quantitatively the state of *B. subtilis* spores exposed in different environments provided that is optimised for this objective (Abee *et al.* 2011; Reineke *et al.* 2012). An example is given below in Figure 1.10 of the standard FCM outputs expected and how these can be manipulated to assess and enumerate physiological states of *B. subtilis*. These are displayed using the software VenturiOne.

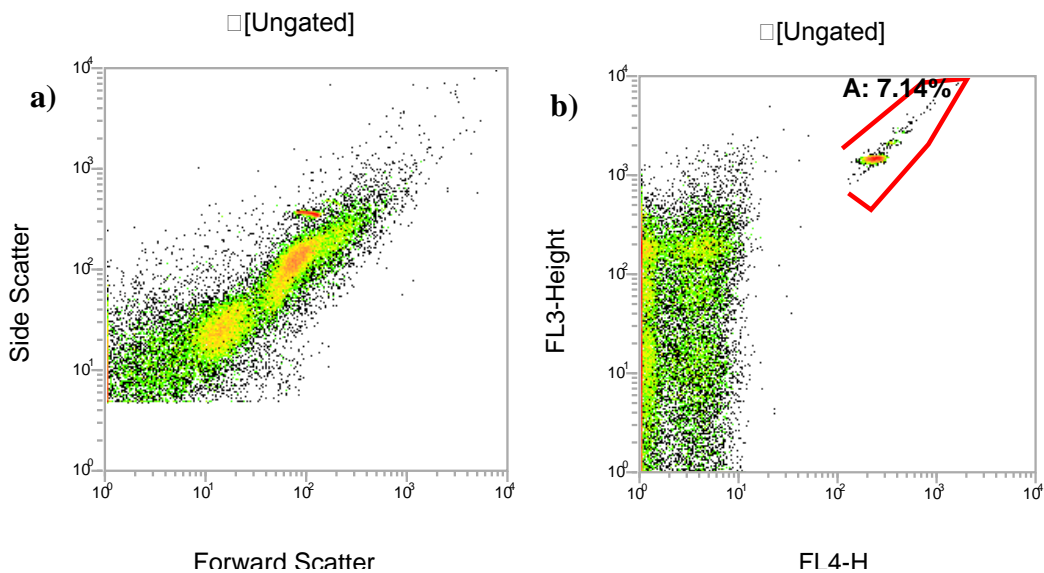


Figure 1.10 a) FCM output of *B. subtilis* cells and spores, (stained with 1.5 μ M Syto 16 and 48 μ M PI) with SpheroTech fluorescent counting beads on a forward scatter (FSC) vs side scatter (SSC) density plot. b) The same sample, displayed on a far red (FL4) vs Red (FL3) fluorescent density plot. Region A is drawn around the fluorescent counting beads

Figure 1.10 illustrates the typical output of *B. subtilis* spores and cells obtained from a FCM analysis. The counting beads fluoresce on all channels meaning they can be separated from the general population by viewing on a fluorescent channel that the other dyes will not fluoresce on (in this example the FL4 channel). A region is drawn around these beads (region A) which are then removed from the general population using Boolean theory to create gates, where the equation NOT A will remove anything in this region from the following gated plots in Figure 1.11.

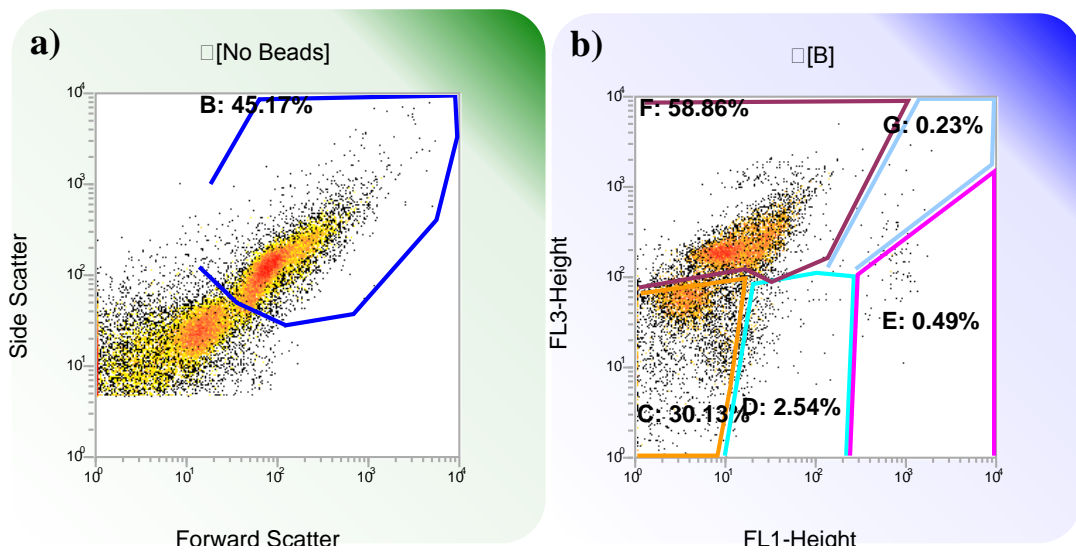


Figure 1.11 Gated FCM density plot of *B. subtilis* cells and spores, (stained with 1.5 μ M Syto 16 and 48 μ M PI, a) FSC vs SSC with region B drawn around the main cells and spore population, b) Gated plot of region B with Green (FL1) vs Red (FL3) density plot (of the same sample), showing the fluorescence emission of this stained sample. Region C: dormant spores, Region D: germinating spores, Region E: Live cells and outgrown spores, Region F: dead cells and spores, Region G: double stained cells and spores, and/or cell doublets.

Figure 1.11 demonstrates a gated plot of a stained sample of *B. subtilis* cells and spores. Region B is drawn around the main cells and spore population and this region is then selected and presented in b) where the sub-populations are assigned (based on previous standards). Thus sub-population enumeration can be achieved using the number of events from each of these regions and combining this with number of counting beads events in region A. This process is detailed further in Chapter 2.

1.3 Flow cytometry principles

Flow cytometry (FCM) uses laser light to characterise cells, determining either their shape or complexity. If specific stains are used fluorescence emitted by stained cells (Shapiro 2003; Mathys *et al.* 2007; Nebe - von - Caron 2009) can reveal structural integrity or compositional information. Commonly applied stains and their utility are described in Table 1.1.

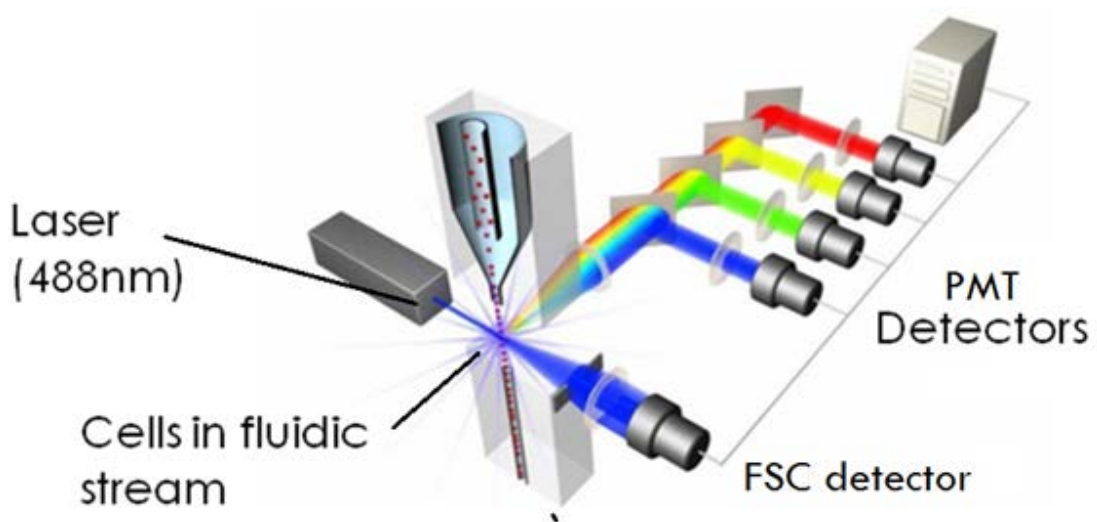


Figure 1.12 Diagram of inner flow cytometry system showing the position of the laser in relation to the cell stream and the fluorescent detectors (Invitrogen 2014).

Flow cytometry uses hydrodynamic focusing of a sample suspension of particles (Figure 1.12), allowing them to pass sequentially through a beam of laser light. The first option in collecting data from a FCM is which trigger channel to collect from. Triggering the collection of data can be from a less sensitive photodiode detector that is linked with the forward scattered light (the FSC trigger). Alternatively triggering of data collection can take advantage of the more sensitive photomultiplier (PMT) detectors. These are linked to either the Side Scattered light (SSC trigger) or to the fluorescent channels (FL trigger). In all cases, the photodetectors can quantify the effect of the spores/cells on the scattering of light emitted by the laser. This yields information on the size and complexity of the particles. The

fluorescent photodetectors allow a flow cytometer to measure emission of fluorescent light, by laser excitation of fluorophores used in dyes (Hernlem and Ravva 2007).

The FCM can distinguish between different sized cells and also determine cell complexity through light scatter. As a cell passes through the beam of light, the light is scattered and the FCM measures both forward scatter and side scatter to determine shape/complexity. Forward scatter relates to cell size, and more specifically diameter, whereas side scatter is indicative of cell complexity, i.e. how many organelles are in the cell, or spore roughness (Vives-Rego *et al.* 2003; Cronin and Wilkinson 2007). The forward scatter is detected as a voltage pulse by a receptor in front of the laser beam. A large forward scatter is indicative of a larger cell and vice versa. The side scatter is detected through a different channel to the right of the beam. For this reason side scatter is sometimes referred to as right angle light scatter (RALS) and is caused by the light from the laser ‘bouncing’ off granules in the cell. A high side scatter therefore indicates a high cell complexity (Díaz *et al.* 2010).

1.3.1 FCM data acquisition strategies

Settings analysis

Whilst bacterial flow cytometry has become far more prominent in microbial research over the past two decades, it remains that little if any, standardisation has taken place (Nebe-von-Caron 2008). One possible reason for this may be the differences in Flow cytometer models, not only across different makes, but also variations within each FCM model. For example, Reineke *et al.* (2012) used the BD FACSCalibur to analyse *B. subtilis* using the E01 setting for forward scatter (FSC) and set the side scatter (SSC) amplification to 721V. Another study using the same model and the same organism (*B. subtilis*) used the FSC E01 setting but set the SSC amplification to 427V (Zahavy *et al.* 2003). Another reason individual settings must be analysed is due to the size of different bacterial species and strains. For example even different species within the same genus have significant differences in cell size, such as *B. cereus*, which typically measures around 1µm in width (Senesi and Ghelardi 2010), whereas *B. subtilis* is usually around 0.5µm in width (Hayhurst 2008). Such differences will have a significant impact on the FCM profile, not only on the FSC and SSC signals, but also in terms of the fluorescent signals. As such, the staining conditions will also need to be manipulated to suit each species of bacteria.

Given the variation in FCM settings used in the literature an investigation into FCM settings might be required to find the optimum settings for a particular model, and microorganism of interest. Further to this, suitable stains will need to be used to meet the needs of the aims of the particular investigation. Table 1.1 details some of the typical stains used for bacterial FCM.

Table 1.1 Commonly used stains for bacterial flow cytometry and their uses

Stain	Function	Properties	Emission wavelength (nm)	Excitation wavelength (nm)
Acridine orange	Stains nucleic acids	Permeable nucleic acid stain (Ueckert <i>et al.</i> 1995)	460 for RNA and 500 for DNA	650 RNA and 526 for DNA
Biscarboxyethyl-carboxyfluorescein (BCECF)	Indicates metabolically active cells.	Properties like cFDA, but more easily loaded. Very pH-sensitive (Ueckert <i>et al.</i> 1995)		

Stain	Function	Properties	Emission wavelength (nm)	Excitation wavelength (nm)
Carboxyfluorescein -diacetate (cFDA)	The fluorescence intensity of cF is often considered to be a relative measure of cellular metabolic activity. Can be used as an indicator of metabolically active cells (Shen <i>et al.</i> 2009).	Non-fluorescent cFDA is taken up by diffusion & converted <i>via</i> a cytoplasmic esterase catalysed hydrolysis to carboxyfluorescein (cF) & 2 molecules of acetate neutral esterase substrate. Crosses even intact membranes, and is retained by these cells, therefore denotes vitality. Extruded by cells of certain strains with specific translocation mechanism(Ueckert <i>et al.</i> 1995).	493	(FL1)
DAPI	Useful for cell cycle studies	Blue membrane impermeant stain	358	461

Stain	Function	Properties	Emission wavelength (nm)	Excitation wavelength (nm)
DHPE	Used for fluorescence activated cell sorting (FACS)	Lipid specific green fluorescent dye. Binds to phospholipid head. pH sensitive (Park <i>et al.</i> 2005)	496	519 (FL1)

Stain	Function	Properties	Emission wavelength (nm)	Excitation wavelength (nm)
DiBAC ₄ (Bis-oxonol)	Dead cells and spores. It is an oxonol – anionic dye	Distributional membrane-potential probe enters depolarized cells, binds to lipid-rich components. Excluded from cells that exhibit a membrane potential (Nebe-von-Caron <i>et al.</i> 1998). However irradiated & controlled populations of endospores were positive for the dye, therefore, unable to distinguish viable from nonviable endospores Cronin and Wilkinson 2007) Stains intracellular proteins or membrane.	490	516 – (Red spectral shift) to 590 depended on the specific bis-oxonol used

Stain	Function	Properties	Emission wavelength (nm)	Excitation wavelength (nm)
DiOC18	Used for FACS on a range of different bacteria (Park <i>et al.</i> 2005)	Green. Stains cell membranes and lipids	475	510 (FL1)
Ethidium Bromide	Indicates de-energised or depolarised cells (Ueckert <i>et al.</i> 1995)	Positively charged dye, intercalates RNA and DNA. Slow penetration of intact membranes (Nebe-von-Caron <i>et al.</i> 1998).	488	575 (FL2)
Fluorescein isothiocyanate (FITC)	Tags various biological molecules, eg. Antibodies	Binds with neutral amino acids to form protein-fluorescein conjugates (McClatchey 2002).	490	525

Stain	Function	Properties	Emission wavelength (nm)	Excitation wavelength (nm)
Propidium Iodide (PI)	Count vegetative cells and spores that are dead/have damaged membranes (Cronin and Wilkinson 2008)	Properties like ethidium bromide (EB), but more membrane-impermeable. Enters cells with compromised membranes (Shapiro 2003). Stains cytoplasm & cytosol – does not penetrate intact membranes due to its additional charge. Will not stain endospores with depolarized cytoplasmic membranes though will stain non-viable spores (Cronin and Wilkinson 2007)	535 optimum. Can be excited with 488nm argon laser (Invitrogen)	617 (FL2 channel – 585nm) can be collected at 675nm (Comas-Riu and Vives-Rego 2002)
Rhodamine 123	Shows cells with a membrane potential.	Cationic lipophilic RH123 passes membranes, but is only retained in cells with a membrane potential.	505	525

Stain	Function	Properties	Emission wavelength (nm)	Excitation wavelength (nm)
SYTO-16	Indicates completion of spore germination. It has been shown to have the biggest difference in fluorescence of dormant and germinating spores (Black <i>et al.</i> 2005) (Mathys <i>et al.</i> 2007)	Nucleic acid, DNA & RNA. Shown to give the biggest difference in fluorescence between dormant and germinating cells (Black <i>et al.</i> 2005). Stains only cortex hydrolysed/ germinating spores.	488	518-525 collected by FL1 specifically 515

Towards standardisation of FCM

The Flow Cytometry UK organisation (Davies *et al.* 2006) initiated a study into flow cytometry standardisation; this involved the participation of several labs across the UK. This research involved dispensing samples of ‘Giga beads’ to many different laboratories. These Giga beads consist of seven different sized nano bead populations, ranging in diameter from 190nm to 3,000nm. This is a comparative study set up by the small particle interest group of Flow Cytometry UK. The aim of these studies was to provide general guidelines for troubleshooting in flow cytometry, with the objective to study differences in FCM equipment across the UK. This gives flow cytometrists across the UK, the opportunity to see how their acquired flow cytometry data would compare with the indicative picture across different UK/EU FCM laboratories.

Given the fact that current literature indicates that people use different settings on each machine it remains likely that for anyone wishing to embark upon a FCM methodology an analysis of all the settings must be done. This is covered in Chapter 2. Furthermore, it would be unrealistic to use FCM as the sole means to analyse data given the relative infancy of the method. Accordingly, most researchers employ at least one other methodological tool while carrying out research, though by adding FCM to current procedures, a greater amount of information can be gained (Díaz *et al.* 2010).

1.4 Aims and Objectives

Given the state of the art in current literature, the following aim was proposed for this project:

Investigate the fate of ingested spores in *in vitro* pig gastric conditions as a means of delineating the phenomena involved with the reported loss of viability of probiotic spores.

This in turn, required the following objectives to be met:

- Develop a bacterial FCM methodology to accurately assess and enumerate the sub-populations of *B. subtilis*
- Assess the effect of different treatments on *B. subtilis* cells and spores *via* FCM and plating
- Determine the extent of germination in *in vitro* GIT conditions

With the information to hand, the following hypotheses have been suggested:

- Spores will germinate in the presence of nutrients and moisture and hence become more susceptible to the harsh conditions of the stomach
- Spore death in the gastric compartment will either be due to germination induced death or a direct sporicidal affect

2 Chapter Two: Developing a FCM methodology to analyse *B. subtilis* cells and spores

2.1 Introduction

The primary focus of this chapter is to detail the steps taken to determine whether a rapid and accurate flow cytometric methodology (FCM) to assess physiological states of *B. subtilis* could be devised. This would be a useful means to study the effects of simulated gastric conditions on *B. subtilis* spores and cells.

2.1.1 Fluorochrome selection

Recent research shows a great deal of variation in staining protocols used for FCM analysis of bacteria (Ananta *et al.* 2005; Cronin and Wilkinson 2007; Khan *et al.* 2010; van Melis *et al.* 2011b; Reineke *et al.* 2012), see Chapter 1 Table 1.1 for full details regarding staining]. It is unclear whether these large variations are due to different preferences in method, or simply a necessity owing to inherent differences in the experimental set-up of the different laboratories (stains used, microorganism/strain, flow cytometer model, etc). Whatever the route of this, it is certain that there is a significant level of variation in terms of the duration of staining, the temperature of staining and also in terms of the type of dye and the dye concentrations.

There are a number of dyes that can be used to assess viability of bacteria (Table 1.1). Among them is the commercially available dual stain: *Baclight* comprised of Syto 9 and propidium iodide (PI), used by Stocks (2004). Syto 13, was used by Leser *et al.* (2008) for *B. subtilis* and *B. licheniformis*. It has also been used extensively with aquatic organisms and *E. coli* (Guindulain *et al.* 1997; Comas-Riu and Vives-Rego 1999; Troussellier *et al.* 1999). Syto 16 has been used by Black *et al.* (2005), Mathys *et al.* (2007); and more recently by Reineke *et al.* (2012) for studying germination of *B. subtilis* spores. For the purpose of this study, the dye would need to be used on mixtures of cells and spores, as it seems likely

that the gastric challenges the spores will face in this project will cause different physiological states to arise.

The Syto dyes belong to a class of cyanine dyes. They are thought to have multiple binding modes, including intercalation and charge interactions with the phosphate backbone and binding to the groove of the DNA double helix. Once they bind to the nucleic acid this causes a vast increase in fluorescence as they become rigid (Shapiro 2003). They will permeate virtually all cell membranes (Tárnok 2008). The differences in the Syto dye family comes from modifying a number of side groups of the molecules. This changes the permeability to live cells. They are based on a heterocyclic ring structure whose permeancy properties are dependent on the nature of various ring substituents (Shapiro 2003). The dyes passively diffuse through cell membranes but only fluoresce once bound to nucleic acid. The PI dye will displace the cyanine dyes when used together (Díaz *et al.* 2010).

PI is a red dye that binds to DNA. However, its usefulness in FCM comes from the fact that it cannot cross an intact cytoplasmic membrane (Díaz *et al.* 2010). This means that only cells which have a damaged membrane will stain with this dye. For this reason it can be used to identify dead cells.

Other stains used to identify dead cells via mechanisms such as membrane depolarisation, are indicators of damage rather than death as illustrated by Nebe-von-Caron *et al.* (1998). In this study, cells that took up Bis-oxonol (BOX) and ethidium bromide (EB) denoting depolarisation, recovered moderately well on agar plates after sorting. The cells stained with PI showed no recovery on agar plates, indicating this is a more efficient way to detect dead cells.

Given that a high number of Syto dyes are available it is important to find which Syto stain is most appropriate. Most of these stains can be used in combination with PI to stain cells of *B. subtilis*. Syto 13 has been used to differentiate cells from spores of *B. licheniformis* and *B. subtilis* subjected to *in vivo* piglet GIT conditions (Leser *et al.* 2008). Whilst this is a significant finding, the stain was not used in conjunction with PI. Comas-Riu and Vives-Rego (2002) have used Syto 13 with PI to study spores, though the organism of

interest in this study was *Paenibacillus polymyxa*. A key study by Black *et al.* (2005) investigated a range of Syto dyes (9, 11,12, 13, 14, 15, 16) and found Syto 16 to show the largest difference in fluorescence between dormant spores and germinated spores of *B. subtilis*. Syto 16 has also been used frequently for *B. subtilis* in combination with PI (Mathys *et al.* 2007; Kong *et al.* 2010; Reineke *et al.* 2012). As such, it was thought that Syto16 was the most appropriate dye to use.

The FCM model used in these studies is the BD FACSCalibur, equipped with a 15 mW, 488 nm air-cooled argon ion laser. BD CellQuest Pro software was used for setting and acquiring data.

2.1.2 Staining concentrations

A rigorous approach to staining analysis involves a number of factors. Temperature, time, cell concentration and optimising the staining concentrations are all key parameters to consider (Longworth 1954). Of key importance is to ensure that the staining protocol conditions are not limited by the staining concentration. For example Stocks (2004) highlights the issue of having inappropriate staining concentrations. In his study, it was illustrated that when the dye Syto 9 was in excess, DNA which should have stained with PI, was shown to fluoresce on the green channel instead, indicating that the PI was not in sufficient enough quantities to displace the Syto stain.

2.1.3 Setting compensation

The phenomenon of fluorescence involves the excitation of a dye, followed by its emission. The emission spectra of Syto 16 and PI have very little overlap in the fluorescent bands collected by a FCM making them ideal for combining in double staining protocols.

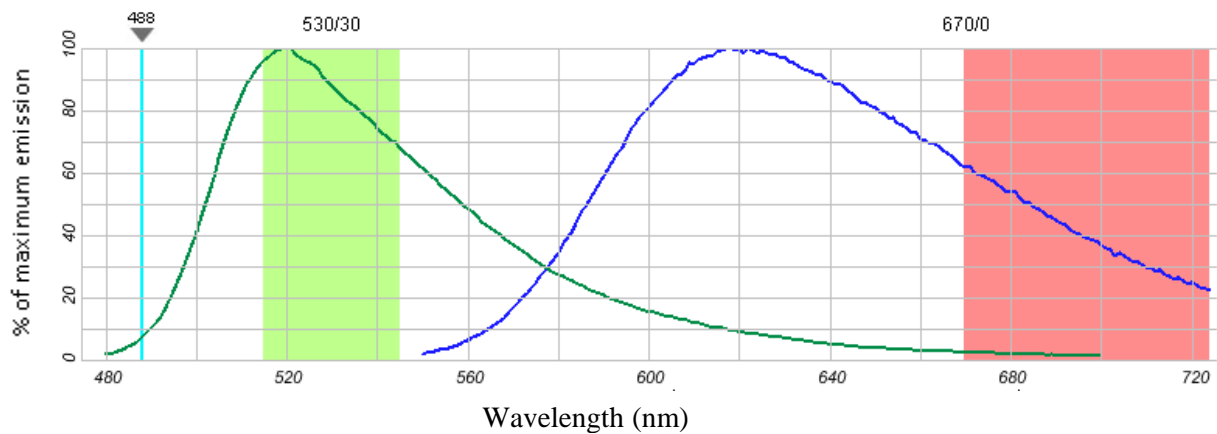


Figure 2.1 Emission spectra of Syto 16— and PI — the 530/30 filter/bandpass is the FL1 channel and the 670/0 long pass filter is the FL3 channel. Graph constructed using Fluorescence Spectra Viewer (Life Technologies). Bandwidth windows at 530/30

In Figure 2.1 the emission spectrum of Syto 16 (green line) and PI (blue line) following excitation with a blue monochromatic light laser beam at 488nm (magenta/cyan line) are shown as a function of their wavelength. The typical collected bandwidths for the FCM fluorescent detectors are also shown. As is clear from the graph, there is no overlap of staining in the FL1 (530/30) channel, however there is a small amount of overlap in the FL3 (670/0) channel. It is important to note, that the stronger the fluorescence of Syto 16, the greater the overlap into the FL3 channel will be. As such, compensation must be set to account for the potential false positive results this could generate. Compensation is set by taking the spectral overlap values and inverting these values using matrix algebra to generate the percentage compensation levels required. More information on this can be found through Bagwell and Adams (1993)

It is a widely held belief that compensation levels could be set with BD Calibrite beads (Invitrogen, UK), which fluoresce on all channels and include a blank set of beads. However, a more advantageous practise is the use of stained populations of cells to set the compensation levels as these would be stained with the actual stains involved in a given study. The emission spectra of stains differ significantly from that of the FITC and PerCP stains used in the BD calibrate beads and execution of calibration assuming an incorrect

emission spectra has the potential of influencing the accuracy of the FCM data particularly when aiming at a quantification objective (Nebe-von-Caron 2012).

2.1.4 Staining temperature analysis

Previous research by Mathys *et al.* (2007) and Baier *et al.* (2010) has shown FCM profiles using Syto 16 and PI to differentiate dead from dormant *B. licheniformis* spores. (see Figure 2.2)

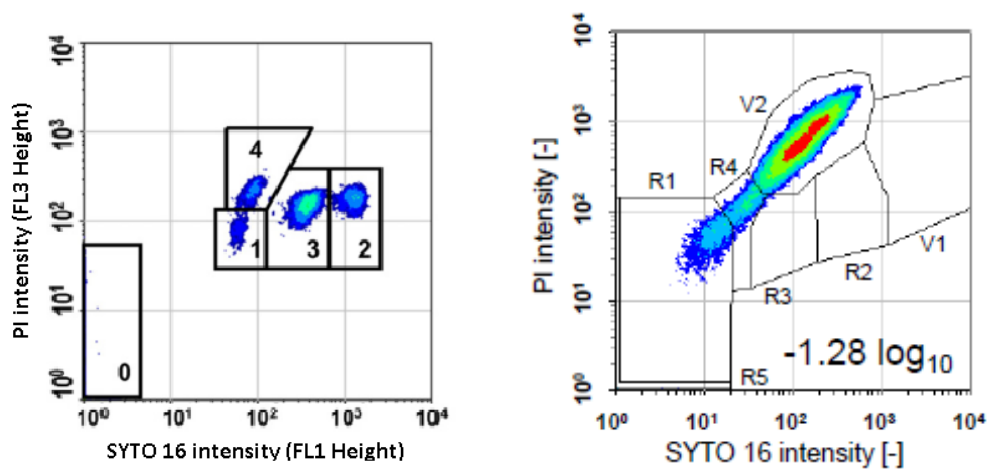


Figure 2.2 a) FL1 (green) fluorescence against FL3 (red) fluorescence showing density profile of cells and spores of *B. licheniformis* from Mathys *et al.* (2007) (0 = noise), 1 = dormant, 2 = germinated, 3 = unknown, 4 = inactivated. b) Results of flow cytometric assessment (density plots) (Baier *et al.* 2010) Regions: R1: dormant spores, R2: germinated spores, R3: unknown state, R4: inactivated spores, R5: noise, V1: vegetative cells, V2: vegetative cells inactivated by thermal effects.

To establish whether it was possible to see this difference meant a highly efficient method of spore killing needed to be found. It was essential to obtain a sample of pure dead spores to use as a standard. Edwards *et al.* (1965) found that heating at 135°C for just over two seconds was sufficient for 99.9999% spore death and 129.4°C for eight seconds was enough

to get almost the same level of spore death. More recently, inactivation has been shown at 19 minutes at 98°C or 95°C for 43 minutes (Jagannath *et al.* 2005).

When these pure populations were acquired, FCM analysis could then take place. A thorough literature search was carried out to look into previous methods used to create clear FCM profiles. It was noted that there was a large variation in staining concentrations used and temperatures (see Table 1.1 in Chapter 1). Experts in the field were consulted on this matter (Cronin 2012) and it was decided that a higher staining temperature could increase the separation between dead spores staining profiles and dormant profiles.

2.2 Materials and Methods

2.2.1 Cell and Spore preparation

Cells of *B. subtilis* (DSM 23776 from the German collection of micro-organisms), a derivative of the 168 strain, were grown overnight at 37°C using 10µl of a frozen spore stock to inoculate a 20ml LB broth. Cells were analysed at stationary phase so that there would be fewer actively growing cells in the mixture, thus avoiding chains of cells. The cells were harvested by centrifuging at 13,000 x *g* for five minutes and re-suspending in 0.2µm filtered PBS (100mM, pH 7.4).

Spores were prepared on AK sporulating agar, (inoculated with 200µl of an overnight culture of cells on each plate) inverted and incubated for seven days at 37°C. After this, the spores were harvested by scraping the plate surface with a sterile loop and placed in a sterile 15ml falcon tube with 10ml sterile water. Based on the method of Zhao *et al.* (2008) these suspensions were washed twice with sterile 0.2µm filtered H₂O at 10,000 x *g* at 4°C (Sorvall RC 5B plus centrifuge, Thermo Scientific, UK), and then re-suspended in 0.2µm filtered 50% EtOH (with H₂O). This mixture was left for 12 hours at 6°C, and then washed three times more in ddH₂O before being stored at 6°C.

2.2.2 FCM settings and operation

The FACSCalibur flow cytometer was initially set up using the E01 setting for FSC, the SSC was set to 300V, and the fluorescent channels were all set at 500V. All sample collection was performed using the 'low' setting, corresponding to $12 \pm 3 \mu\text{l}/\text{min}$. Optimisation of these settings is detailed in Section 2.3. BD Biosciences Sheath fluid (a liquid with a similar composition to PBS) was used in the machine, and 3ml round bottomed FCM tubes (BD biosciences, UK) were installed in the sample injection port containing a 1ml aliquot of the cell suspensions in PBS.

Setting FCM acquisition

The first option in collecting data from the FCM is which trigger channel to collect from. Collection of data can either be activated from the photodiode channel linked with the forward light scattering (known as FSC trigger) or any of the photomultiplier channels linked with the side light scattering or the fluorescent channels (known as SSC or FL trigger). To explore which settings were most appropriate, a range of different voltages were explored:

- FSC voltages: E00, E01, E02 and E03
- SSC voltages: 233, 340, 620V

Using a sample of cells (10 μl) with 50 μl fluorescent Calibrite counting beads, 6 μm in diameter (Invitrogen, UK) suspended in 940 μl PBS (phosphate buffered saline) solution at pH7.4, 100mM the samples were run through the FCM until 10,000 events were collected for each trial. The results were analysed on density plots using the computer software VenturiOne (Applied Cytometry, UK).

Staining concentration analysis

Cells were prepared as previously stated (2.2.1) and 1ml aliquots were taken and centrifuged at 13,000 x g for two minutes. The top 995µl supernatant was discarded and then the cells were re-suspended in sterile filtered PBS (pH 7.4, 100mM). This washing step was repeated again, and in the case of thermally treated cells, this microtube was placed in a water bath set to 85°C and left for 35 minutes. The temperature of the water bath was carefully checked using a microtube filled with 1ml water. A thermocouple was placed into this tube via a small perforation made in the lid of the microtube. The temperature of the water could then be measured over time. The thermocouple was calibrated with a temperature probe before use to ensure accuracy of results.

10µl of the cell suspension was pipetted into a 1ml microtube. Staining concentrations were made up by diluting with the appropriate amount of PBS to a total volume of 500µl.

PI: 12µM, 24µM, 48µM, 60µM and 100µM

Syto 16: 0.1µM, 0.5µM, 1µM, 2µM, 2.5µM, 3µM and 5µM

Samples were vortexed thoroughly after the stains were added and incubated in an ice box for at least 30 minutes before analysis. Prior to FCM, the tubes were vortexed again and then pipetted directly into a fresh FCM tube. For the PBS only samples (Figure 2.14), the same protocol was implemented using the following concentrations of Syto 16: 2, 2.5, 3 and 5µM.

2.2.3 Visualising dead from dormant spores

Dead spores were obtained by placing 1ml of dormant spores in a microtube and autoclaving. For FCM analysis, 1ml aliquots of dead spores and dormant spores were stained with 48µM PI and 2µM Syto 16. One set of samples were kept at <4°C (in an ice box) whereas another set of samples were subjected to 28°C incubation period for a range of times. Depending on the temperature treatment for the sample, the respective microtubes were kept at either 4°C or 28°C for at least 30 minutes before use to minimise the time taken for the sample to reach the desired temperature. All samples were kept in the dark by covering the microtubes with aluminium foil.

2.2.4 Assessing germination via DPA release

Spores with an OD₆₀₀ of 1.0 (approximately 2x10⁸/ml) were suspended in sterile phosphate buffer (100mM, pH 5.5) in aliquots of 1.3ml in DNA free microtubes (Sarstedt, Germany).

Using the UV-Vis spectrophotometer Cary 50, (Varian Inc, USA) equipped with CaryWin UV software to analyse the data, absorbance was measured every 0.5 seconds for 15 seconds. UV transparent plastic disposable cuvettes (Sarstedt, Germany) were filled with 1ml of the supernatant of samples to avoid disturbing the pellet.

DPA release was measured after 15, 30 and 60 minutes at 37°C, 28°C and 4°C (performed in triplicate). Total DPA release was measured from spores which had been heated at 99°C for 37 minutes. This was a modification of the method described by Coleman *et al.* (2007) as it took seven minutes for samples to reach 99°C. To measure the DPA, the samples were centrifuged for two minutes at 13,000 x *g* and the top 1ml supernatant carefully removed and placed in the UV cuvettes. These were then sealed with parafilm to avoid contamination and evaporation.

2.3 Results: Selection and optimization of FCM data acquisition strategies

2.3.1 Towards Standardisation using Giga Beads

A nation-wide study in FCM standardisation has been carried out over the past few years using a selection of different sized beads, with the aim to see how these same beads will appear on various different Flow cytometer models and between different laboratories. A detailed protocol for these experiments can be found in the Giga-bead mix protocol v2.1 (Nebe von Caron and Bongaerts 2012).

To keep in line with the study, this trial was performed using the E00 FSC voltage setting and both the 'high' and 'low' flow rate settings of FCM were investigated. The voltages used in all other parts of this study were optimised for visualisation of *Bacillus subtilis* and counting beads. As such, the voltage of SSC detector was set to a value of 345V, for the Green fluorescence detector [FL1] a value of 551V was used, the red fluorescence [FL2] was set to 580V, and for the Far-Red fluorescence detector [FL3] a value of 608V.

It is important to note that in this section, detector voltages reported were specifically selected for ensuring visualisation of all sizes of beads used in the Giga bead protocol i.e. beads across the range of 190nm to 3000nm. Hence, they are different to those that are used to analyse the bacterial samples.

Figure 2.3 a, b shows a low concentration of Giga beads run in filtered Sheath fluid. The profiles are constructed using the green fluorescence signal (FL1-Height) against the Side scatter. Results of the Giga bead trial are presented here on density plots of SSC vs FL1. Regions were drawn around each sub-population using the data from the Giga bead protocol as a guideline.

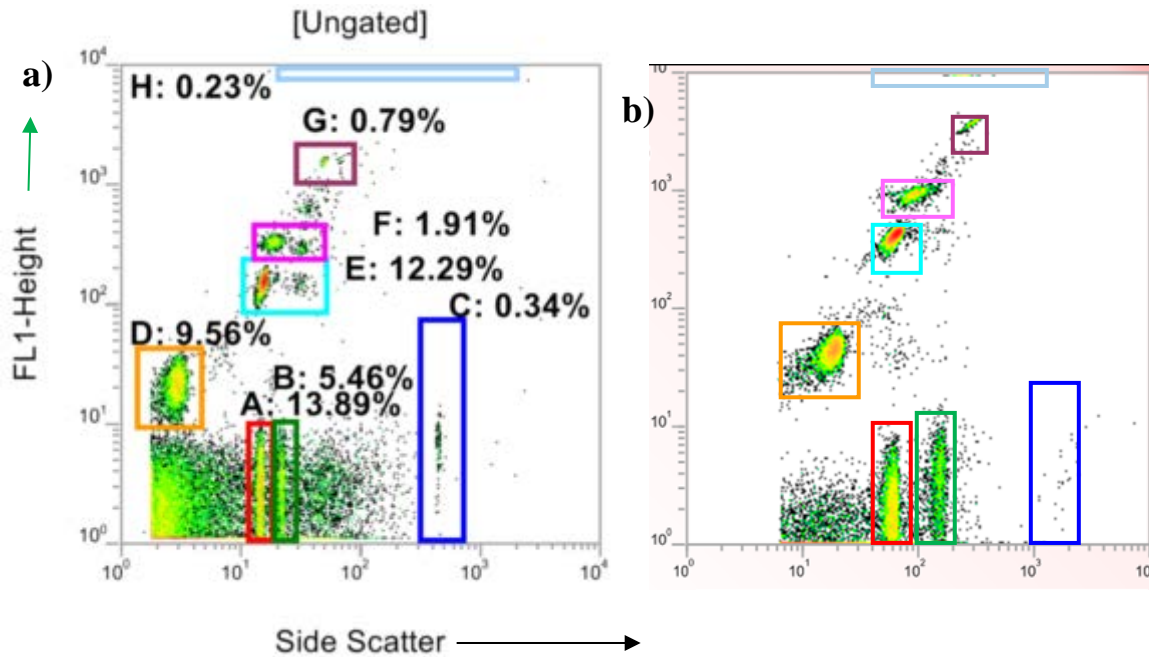


Figure 2.3 Representative dual parameter density plot showing SSC vs FL1 of the Giga bead mix. a) Our own trial b) results from the Giga bead mix protocol. Regions are constructed so that: Region A: 380nm beads (far red fluorescence), region B: 525nm, region C: 3000nm, region D: 190nm, region E: 380nm, region F: 450nm, region G: 660nm and region H: 1000nm. n=3.

The SSC voltage was set so that the larger beads could be seen clearly also (region C). Visually, these results seem to be similar in each instance, though the results from the Giga bead protocol appear to use a higher SSC value, causing the large bead population to become less clear. However to get a better idea of how the results of this study compare with others, it is necessary to compare the values obtained.

In Figure 2.4 a-e the plot of side scatter as a function of green fluorescence [FL1] intensity is presented for all conditions studied with the Giga Beads pack.

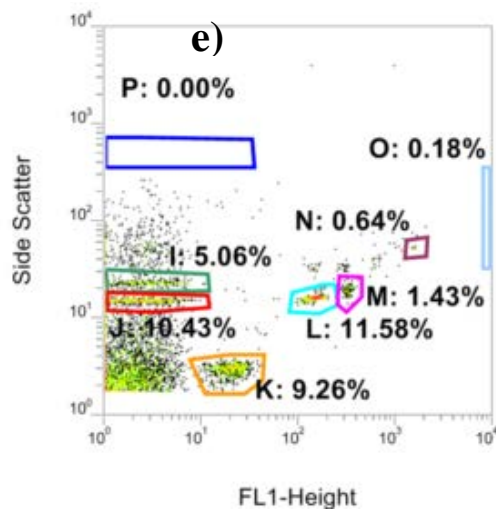
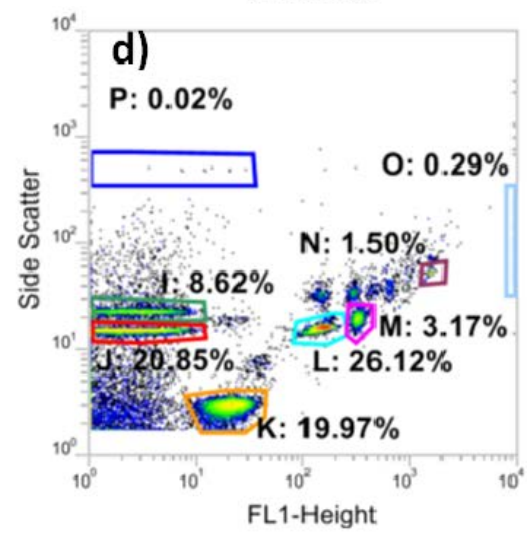
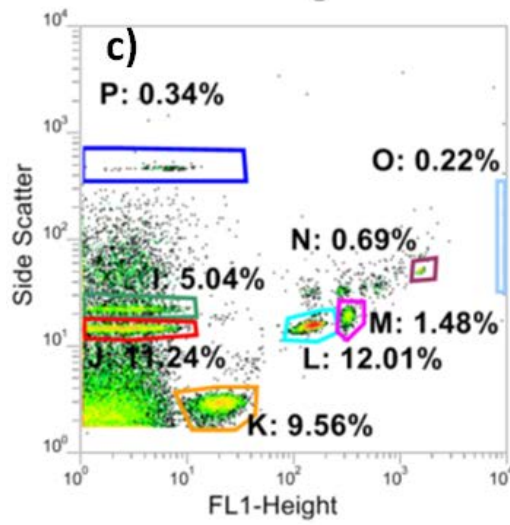
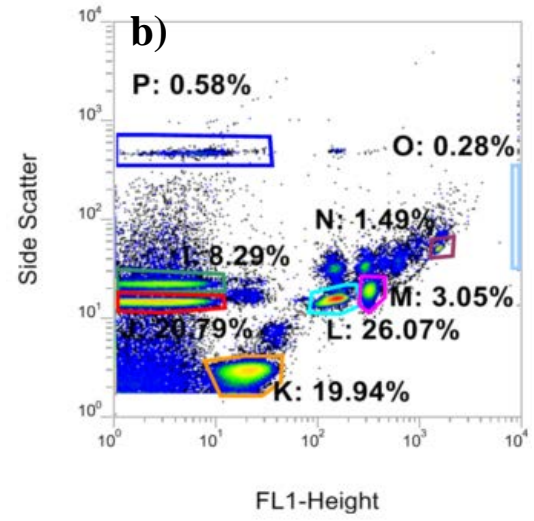
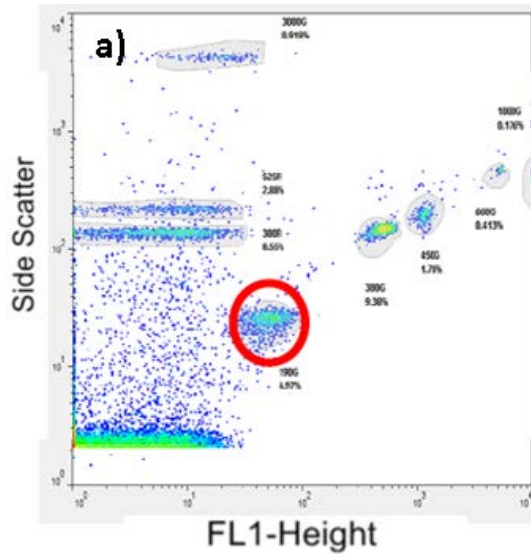


Figure 2.4 (From previous page) Dual parameter density plots showing green fluorescence (FL1) vs side scatter (SSC) density plots of Giga bead mix. Regions are assigned such that: Region I: 380nm beads (far red fluorescence), region J: 525nm, region P: 3000nm, region K: 190nm, region L: 380nm, region M: 450nm, region N: 660nm and region O: 1000nm. a) Results from protocol (percentages not clear) b) Results from a high concentration of beads run on 'high' flow rate setting, c) low concentration of beads run on the 'high' flow rate setting, d) high concentration of beads run on the 'low' flow rate setting, e) low concentration of beads run on the 'low' flow rate setting.

The results from Figure 2.4 a-e indicate a low proportion of the beads are 3000nm. For example, in Figure 2.4 e) there are no beads found in this region, and even in Figure 2.4b) the 3000nm beads only constitute 0.58% of the total events collected.

The percentage of beads in each region was recorded in Table 2.1 using the data from Figure 2.4.

Table 2.1 Relative percentage detection of beads in each mixture under different flow rate settings. a) low concentration of beads and b) a high concentration of beads. Percentages based on regions drawn in Figure 2.4.

Bead		Detection proportions			
diameter nm	Official Giga bead %	Low bead concentration ¹		High bead concentration ²	
		Low Flow Rate ³	High Flow Rate ⁴	Low Flow Rate	High Flow Rate
190	6.97	9.25	9.50	19.88	19.86
300	8.55	10.43	11.24	20.85	20.79
380	9.38	11.58	12.01	26.12	26.07
450	1.78	1.43	1.48	3.17	3.05
525	2.88	5.06	5.04	8.62	8.29
660	0.41	0.70	0.69	1.58	1.59
1000	0.18	0.18	0.22	0.29	0.28
3000	0.92	0.00	0.34	0.02	0.58

1. Low bead concentration = 2µl beads per 1ml 2. High bead concentration =20µl beads per 1ml. 3. Low flow rate =12µl/min 4. High flow rate = 60µl/min

The results indicate that similar to other UK labs participating in the study, our FCM facility is able, upon suitable adjustment of trigger channel and detector voltages, to obtain synchronous acquisition of features ranging from 190 to 3000nm. Being capable of visualising particles across this range of diameter is of particular relevance for our study. Figure 2.4 e illustrates a low concentration and low flow rate may lead to small populations being undetected, given that the region of 3000nm beads (region P) is unpopulated in Figure 2.4 e, with 0% of events recorded, rather than 1% as would be expected based on the values derived from the protocol. Table 2.1 highlights that a higher concentration of beads reduces the signal to noise ratio, this is evident through the fact that the percentage of results in the bead regions are far higher with the high concentration bead mix, than the results for the low concentration bead mix.

The Giga bead experiment has shown us that the flow cytometer available for this study is capable of detecting particles as small as 190nm in diameter. Given that *B. subtilis* will typically have a diameter of 0.5µm (Hayhurst *et al.* 2008) this indicates that the use of FCM is possible for this particular area of research.

The key findings of this part of the study show that switching the FCM from the 'low' to the high setting does not cause a lot of variation in results. This is important to know should it be necessary to use the high setting in future analysis.

With a low concentration of beads, the average increase from the low to high flow rate setting is 5.4%. Interestingly, though the high flow rate gives a visual increase in noise as seen in Figure 2.4 a-e, there is very little difference in the percentages of bead populations in each region. For example, in Table 2.1 with high concentrations of beads, the 'high' setting differed by just 2% to the 'low' setting on average. What was noted was the difference on the large bead population (3000nm Region P, in Figure 2.4). On the 'low' setting, the FCM showed that the largest beads (3000nm) were almost completely undetected (Figure 2.4 e). However, when the FCM was set to the 'high' flow rate setting this region became far more populated (Figure 2.4 c). As has been noted in literature, the high setting can therefore be used for rare event analysis (Nunez 2001).

A closer analysis of the plots in Figure 2.4 (a-e) shows us that there appear to be more clusters of signals than anticipated. Previous literature has suggested that such results are caused by beads which have clumped together during storage (Khan *et al.* 2010). This causes a 'shoulder' to appear on single parameter histograms, as has been seen in the results from this trial.

In general, it appears that our FCM shows a good agreement with the standards expected in flow cytometry. It is interesting that the flow cytometer used in this research appears to have a little more background noise than the example given, (see Figure 2.3 a and b and Figure 2.4 a-e) as the beads were run using a standard filtered sheath fluid (FACSFlow, BD, UK) it is unclear what causes this additional noise.

2.3.2 Setting FCM acquisition

To begin FCM analysis, the FSC voltage was set at E01 and the SSC voltage was set to 340V. Cells were grown as stated in Section 2.2.1 and were analysed under FCM with fluorescent Calibrite counting beads. Results are displayed as density plots where Forward scatter (FSC) is plotted along the x axis and Side scatter (SSC) is plotted as the y-axis. Each dot represents an event and the colour of the dot shows how many events have shown up in the same place. Blue indicates ~0.01% of total events, green indicates low frequency events (~0.03% of the total) yellow, slightly more (0.06%) light orange 0.1% darker orange 0.2% and red 0.5%. Black dots are events that constitute less than 0.005% of total events.

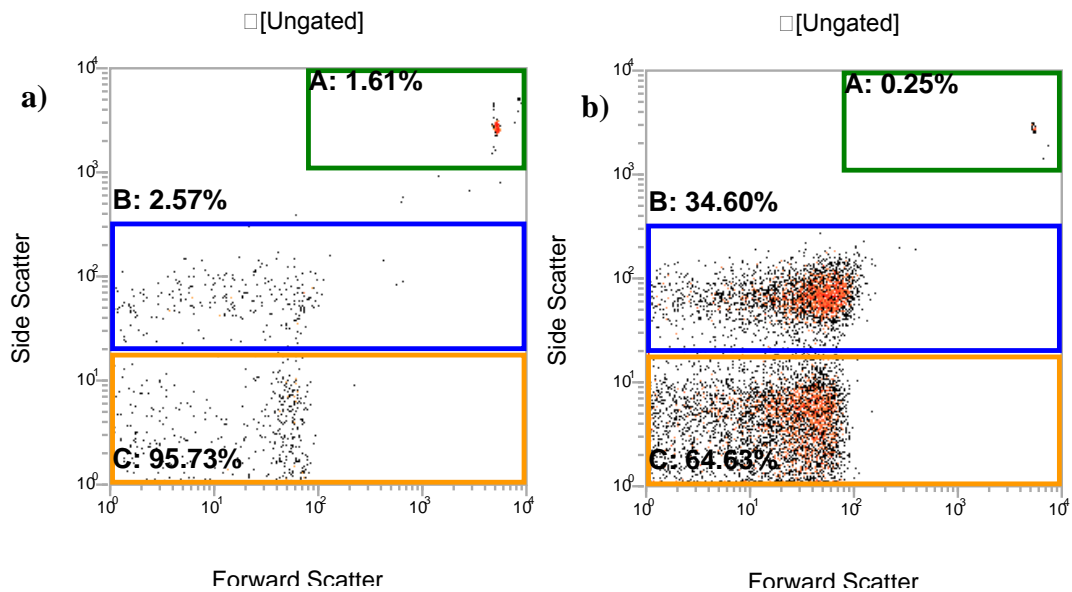


Figure 2.5 a) Establishment of a triggering criterion using a preliminary FCM analysis of *B. subtilis* cells and fluorescent beads. Cells and beads (6 μ m, Calibrite, Invitrogen) were suspended and surveyed in filtered PBS. Events were logged using the FSC trigger channel (a) and the same sample using the SSC channel (b). Region A (green) shows the beads and region B (blue) denotes the cell population and region C (orange) denotes the ‘noise’ and debris. Data collection set to 10,000 events.

Comparison of the results of the survey of the *B. subtilis* overnight culture population using either FSC or SSC as the event trigger (Figure 2.5) reveals strikingly different profiles. Observation of panel a, which describes the data captured using the FSC as an event trigger, reveals that most of the 10,000 recorded events generated an extremely low signal in SSC; this is indicated by the thin red line at the bottom of the profile. Clearly the compression of the data to such an extent allows no possibility of using it to distinguish subtle changes in cellular properties. Of the events that are visible, these cluster into three apparent populations; those with low intensity FSC (< 100) and SSC (<20) signals, those with low intensity FSC and mid intensity SSC (20< SSC <200, region B blue) and those with high intensity signals in both parameters (region A, green). The latter correspond to the detection of the Calibrite beads, their large diameter (6 μ m) generating a strong FSC signal. Their density also generates a strong signal in side scatter. The precision in signal that they generate is indicated by the event density-related colour change. This precision is testament

to their uniform manufacture but is, in part, generated by the use of the logarithmic scaling and our focus on much smaller particles, thus reducing their apparent heterogeneity. The boundaries of region A were established by running a sample of pure beads through the FCM and drawing a square region around this signal, ensuring space was left between these events and the outskirts of the region.

The events described in region B (blue) are associated with intact *B. subtilis* cells and spores, these have a smaller diameter than the beads and generate a lower peak voltage in the FSC photodiode detector that limits at approaching the 10^2 decade. Their granularity also limits signal strength in the much more sensitive photomultiplier detectors of the SSC channels. This region is defined by running a sample of pure PBS through the FCM and comparing this with a sample containing spores, and hence the difference in signal denotes where the cells appear on the FSC vs SSC plot.

Another population of events is detected with a similar distribution of FSC signals strength but with weaker associated SSC responses. These events are likely to be small particles found in the filtered buffer. Whilst it is unusual that the FSC signal is still quite high for these particles, this may indicate a slight issue with the alignment of the laser. This point is covered later in Section 2.3.7.

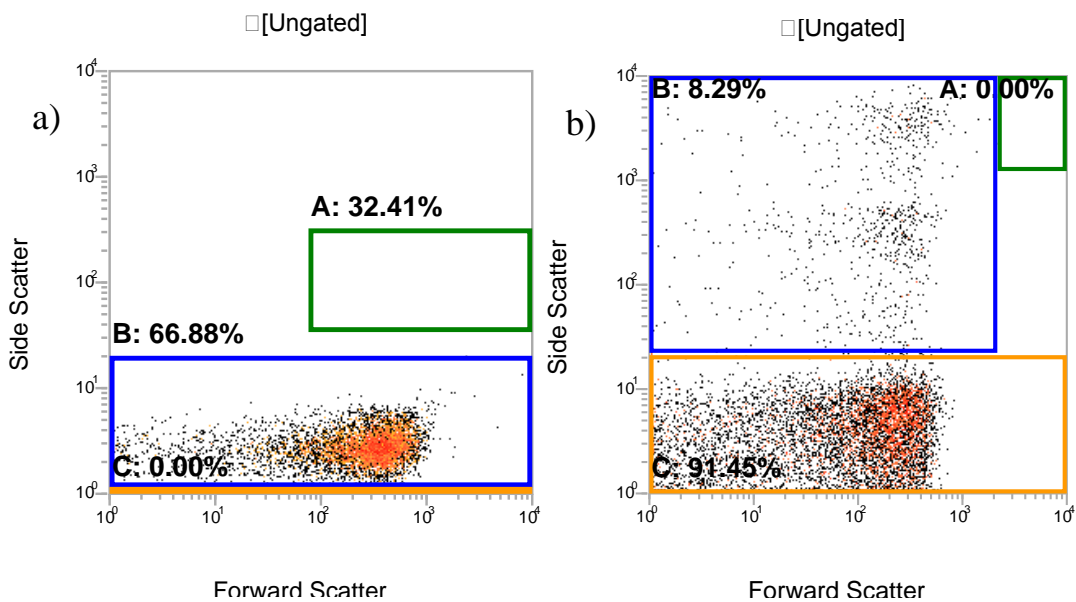
When the same material was surveyed using SSC triggering, only events which provided strong signals for each parameter were recorded. Hence Figure 2.5 b is more populated with events that map the three populations described above. It is clear that the SSC signals related to events recorded in region B do not merge with those events that generate the lower SSC signals; these clearly represent a different population of particulates distinct from intact *B. subtilis* spores and cells. Approximately one-third of the 10,000 surveyed events map to region B attributed to intact *B. subtilis* cells and spores. The beads (region A) were detected at 0.25% of events which is inconsistent with their relative abundance within the *B. subtilis* dominated suspension.

Having established that more robust data collection would be gained using an SSC trigger, the triggering threshold was modified to refine data collection.

According to Nebe-von-Caron (2012), the population of interest has to be clearly separate from the edge of the plot to avoid population artefacts. If the population of interest was placed at the very bottom of the plot, (i.e. close to point 0, 0) there would be a strong chance that electronic noise or other debris might contaminate this region. As such, in previous studies, the cell/spore location is manipulated to establish the region of interest in the middle of the FSC vs SSC plot to achieve maximum resolution of the data set (Bunthof and Abee 2002; Sharpe and Wulff 2005).

With respect to side scatter, the voltage can be set from 150 to 999. By increasing the voltage, the SSC signal is amplified and therefore moves further up the SSC scale.

Therefore, a range of SSC voltages were investigated to achieve this (Figure 2.6).



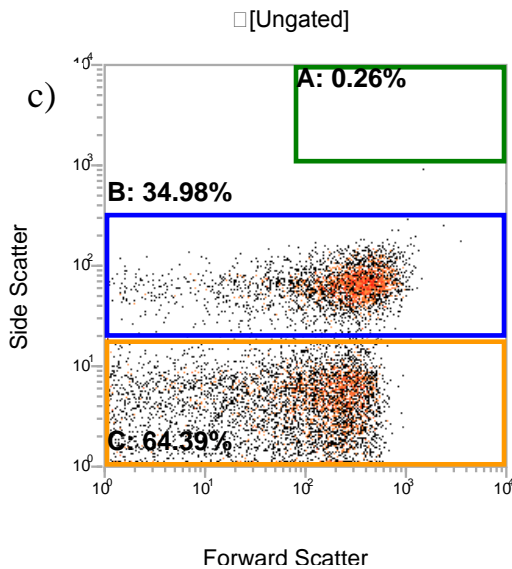


Figure 2.6 Optimisation of SSC voltages for simultaneous detection of cells and beads in filtered PBS. FSC set to E02. a) SSC voltage 233 V, b) SSC voltage at 620V and c) SSC voltage at 340V. Region A (green): bead population, Region B (blue:) cell and spore population, Region C (orange): ‘noise’ and debris.

For this investigation the FSC channel was yet to be set, the E02 setting was used which causes the limit of event FSC magnitude to move from about 100 to about 1000. When a lower voltage (233V) was applied to the SSC PMT detector (Figure 2.6 a) nearly 100% of events collected in the cell and bead regions. Consistent with the lower amplification of signal associated with this reduced voltage, the smaller previously detected particulates were excluded from the data set. In contrast, when the voltage was increased to 620V in Figure 2.6 b), the cell and bead regions become amplified to such an extent that their signals fall off the scale, and the remaining events are simply electronic noise and small debris (based on samples of pure PBS). Therefore the regions cannot be drawn at this voltage. It appears this increased voltage causes the noise signal to be amplified such that these dominate the events on the plot and therefore become the main cause of ‘events’. At 340V shown in Figure 2.6 c) a clear image of cells, beads and noise are shown on scale. The cell and bead regions account for 35% of the total events, though the bead population is at the maximum end of the FSC scale therefore is not visible due to the outline of the bead region. Accordingly, the SSC voltage can be kept at this level, and the FSC channel can then be optimised.

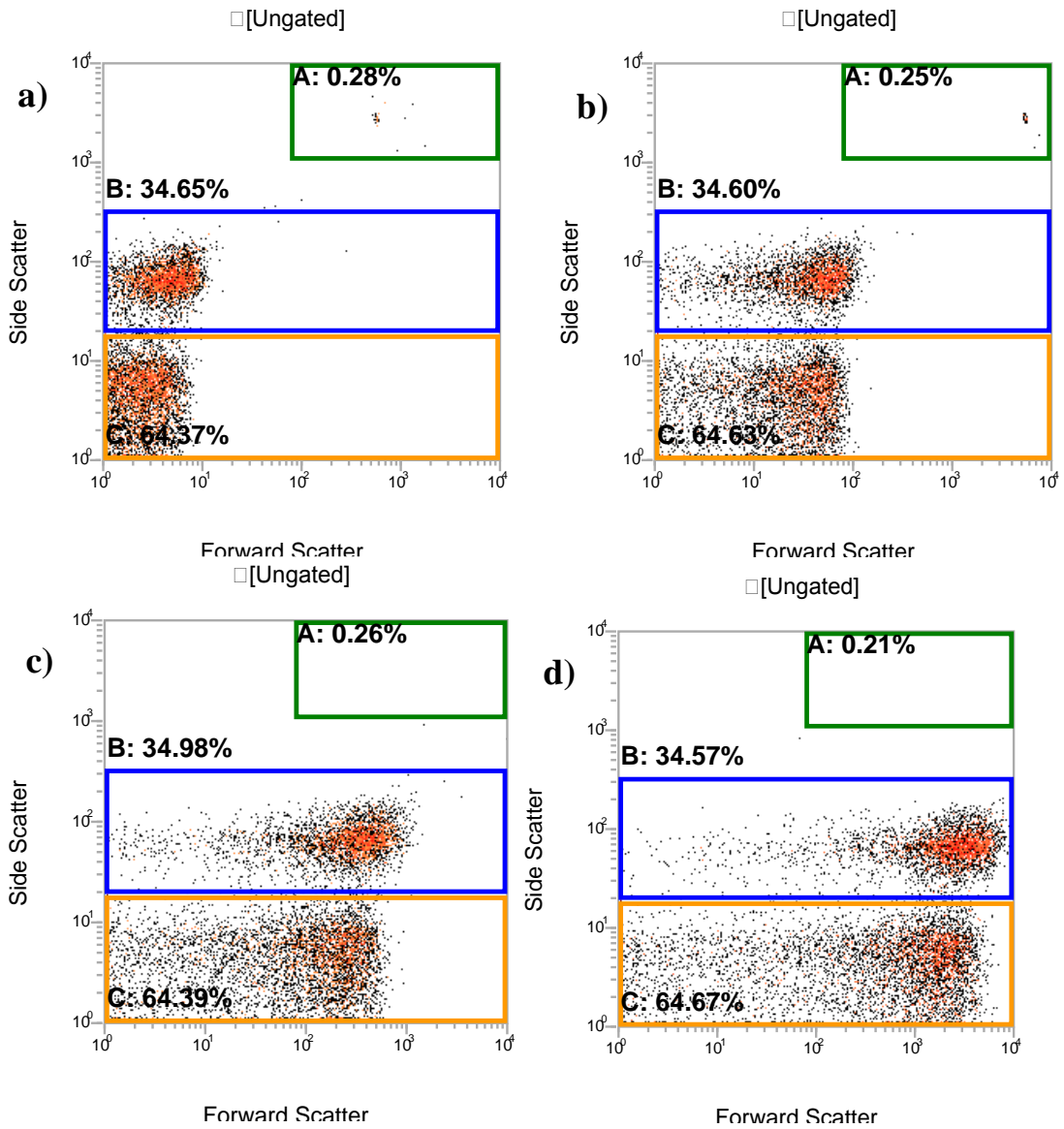


Figure 2.7 FSC voltage analysis of cell and bead sample. a) E00 setting, b) E01 setting, c) E02 setting and d) E03 setting. Region A (green): beads Region B (blue): Cell and spore population, Region C (orange): ‘noise’ and debris.

A similar comparison of survey outcomes was made using different voltage settings applied to the FSC Photodiode detector (Figure 2.7). The cell population is in region B (blue) and the bead population is in region A (green). Values from Figure 2.7 a to d show that there is a poorer detection of beads from the E00 setting to the E03 setting from 0.28% to 0.21%. This corresponds to a 25% reduction in bead number detection. The cell number values differ by very little, indicating they are unaffected by the change in FSC voltage.

In summary, the SSC trigger provides a better signal due to the fact that the SSC trigger is a photomultiplier (PMT) channel, whereas the FSC channel is a photodiode detector. The photomultiplier channels receive significantly lower light levels, but have high gain and far greater signal to noise resolution (Díaz *et al.* 2010). The FSC is more suitable for larger cells, as it is less sensitive (Sharpe and Wulff 2005) therefore does not detect small particles as readily. The results from Figure 2.5 a) show that the bead population becomes far more prominent when the trigger channel is switched from the SSC to FSC, showing a percentage increase from 0.24% to 1.6%. In terms of SSC voltage (Figure 2.6) values around 340 to 360 were optimal for positioning the cell region in the centre of the plot. Whilst the lower SSC voltage gives us a clear image without any debris, it was thought that some background 'noise' could be left in as a control, to show that no valuable data is cut out (Nebe-von-Caron 2012). This excess noise can later be gated out if needed by using the computer software Cell Quest Pro or VenturiOne.

Based on the above mentioned analysis, the E01 channel was found to be optimal for cell analysis as it provides the most centrally placed cell population (Figure 2.7b), whilst still allowing us to see counting beads up to 7µm diameter without compromising their signal. This setting is also reported in literature (Musovic *et al.* 2006; Marbouty *et al.* 2009). It is clear that the E03 setting was inappropriate for this experiment due to the 25% loss in bead number at this voltage. The preliminary FCM investigations into enumeration have suggested that at least 250 events (or 2.5% of total events) are required for the bead enumeration to be accurate. When the bead numbers fell below this level the calculated cell numbers were far higher than expected. This means the bead signal cannot be compromised.

2.3.3 Developing the Staining Protocol

Staining conditions

Before the dye concentrations were investigated, the conditions for the staining were determined based on previous literature. The selection criteria are described in Table 2.2.

Table 2.2 Criteria for selecting a protocol

Parameter	Value	Comments
Temperature	4°C	There was no practical need to investigate temperature effects at this stage. The 4°C was selected to delay/prevent cell proliferation or germination at this temperature. Furthermore, an effective staining concentration at 4°C will be equally if not more effective at higher temperatures. It is known that Diffusion Coefficients of low molecular solutes increase in line with temperature (Longworth 1954).
Time	Up to 30 minutes	Allow stains to fully penetrate but not leave them so long that a.) the cells will pump out the dye, or cause the dyes to fade. b.) the cells/spores might start proliferate/germinate upon abusing the temperature conditions
Stain	Syto 16 and PI	Black <i>et al.</i> (2005) has shown that Syto 16 yields the largest change in fluorescence for germinating to non-germinated <i>B. subtilis</i> . For this reason it was selected as the viable stain. PI is a typical indicator of dead cells, used extensively in this area of research in combination with Syto 16 (Kong <i>et al.</i> 2010; Reineke <i>et al.</i> 2012).
Stain Concentration	2µM and 48µM	Stocks (2004) pointed out that the Syto 16 concentration should be under 8% of the PI concentration. The singly stained dead cells show no further increase in red intensity at 48µM, indicating this concentration is the optimum for staining <i>B. subtilis</i> . Similarly, cells stained with 2µM of Syto 16 show a very high level of staining. This concentration is also below 8% of the PI concentration.
Cell concentration	5x10 ⁵ to 1x 10 ⁶ beads/ml	A cell concentration below 10 ⁴ has been shown to be too low owing to interference with the electronic signal (Khan <i>et al.</i> 2010). A cell concentration which is too high would cause insufficient sampling of the population to occur owing to high event rates. As such it is recommended that event rates remain below 1000 events/s, preferably nearer 200 events/s (Mathys <i>et al.</i> 2007; Shen <i>et al.</i> 2009). For our investigations, a concentration of between 5x10 ⁵ to 1x 10 ⁶ gives us a good flow rate and prevents the dyes from being in excess or too low in concentration (which would mean not all cells were stained).

The staining analysis consisted of using 1ml samples of cells which were stained with the appropriate concentration of dye and then directly analysed (i.e. no further PBS dilution for FCM analysis).

Another set was analysed containing spores (Figure 2.10). This was done to check the staining concentrations did not cause the spore population to interfere with the cell population at high or low concentrations. Two cell concentrations were used in this experiment, one at 1×10^6 (Figure 2.13) and another at 5×10^5 counts/ml (Figure 2.12). In preliminary experiments cell concentrations outside this range have been shown to be either too low to cause a build-up of 'noise' or too high, such that the collection time for 10,000 events was not long enough to obtain an accurate cross section of the entire range of sub-populations in the sample.

The staining kinetics experiments are analysed on single parameter histograms using the overlay function in the VenturiOne software. The fluorescence intensity is related on the x-axis and the frequency of events (height) functions as the y-axis. This allowed us to see both increasing staining intensity, as shown by a shift to right in histogram peaks, and whether there was an increase in the number of events stained, shown through an increase in the height of the histogram peak. These are shown below in Figure 2.8 and Figure 2.9.

Syto 16 staining concentrations

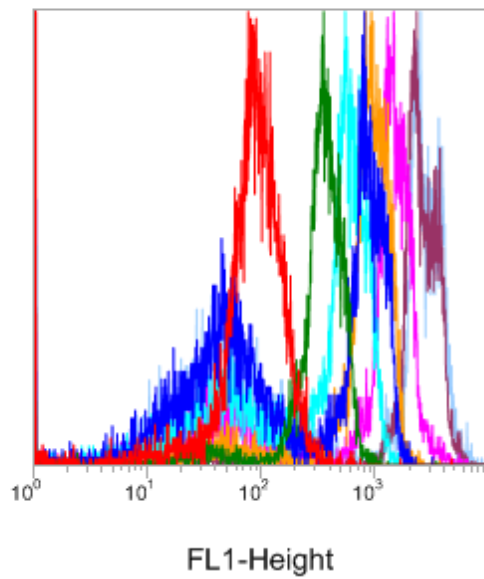


Figure 2.8 Single parameter histogram showing green fluorescence of cells stained with Syto 16 at varying concentrations. Red: 0.1 μ M, Green: 0.5 μ M, Blue: 1 μ M, Turquoise: 1.5 μ M, Orange: 2 μ M, Pink: 2.5 μ M, Burgundy: 3 μ M and Lilac: 5 μ M.

PI staining concentrations

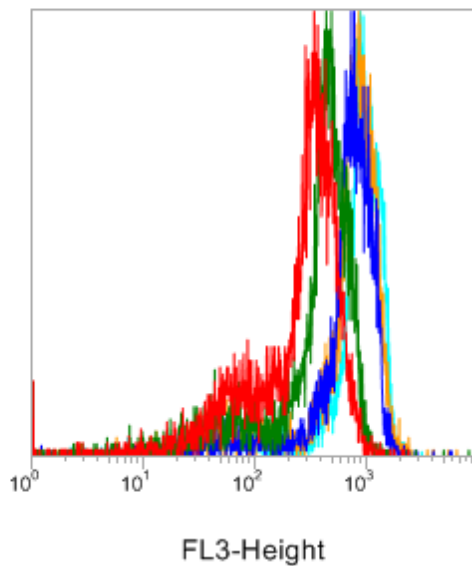


Figure 2.9 Single parameter histogram of red fluorescence (FL3-Height) Heated cells stained with PI. No dilution upon FCM analysis. Red: 12 μ M, Green: 24 μ M, Blue: 48 μ M, Turquoise: 60 μ M and Orange: 100 μ M.

Figure 2.8 shows that the maximum level of intensity in the samples is after the 10^3 decade for the Syto 16 dye at $3\mu\text{M}$ and above, whereas in Figure 2.9 the histogram peaks between the 10^2 and 10^3 mark for the PI stained cells at $48\mu\text{M}$ and above.

Figure 2.10 shows cell and spores singly stained with a range of concentrations Syto 16 from $1\mu\text{M}$ to $6\mu\text{M}$. The results are displayed as single parameter overlay plots of green fluorescence (FL1) versus Height (frequency of events).

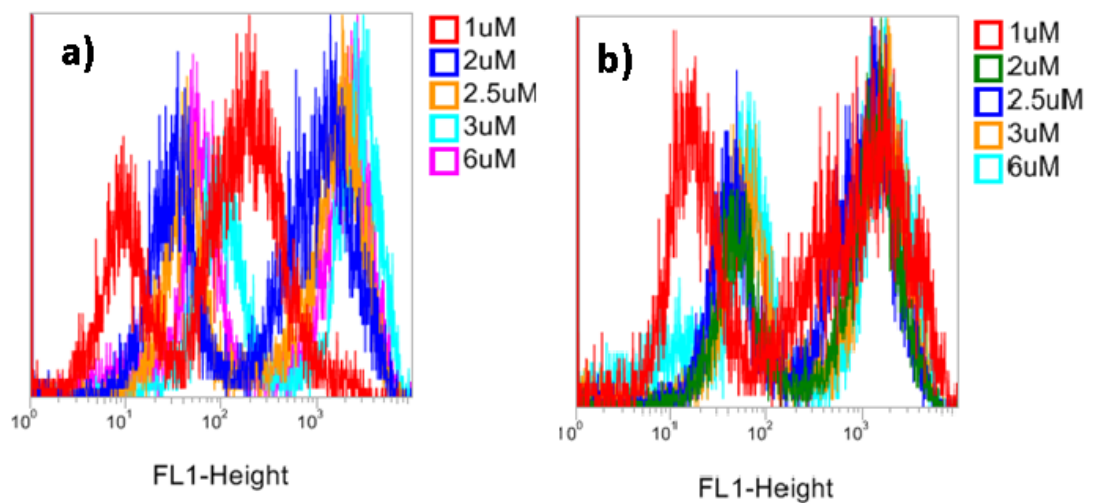


Figure 2.10 Single parameter histograms of green fluorescence (FL1-Height) versus frequency of events. a) cells and spores at a concentration of 1×10^6 counts/ml and b) cells and spores at a concentration of 5×10^5 counts/ml.

Figure 2.10 illustrates the fact that there is a certain level of spore staining around the 10^1 to the 10^2 intensity. The cell populations stain with a higher intensity around the 10^3 log, meaning no overlap of populations is seen. This is clearly conveyed through the fact that the single parameter histograms have two distinct peaks.

The fluorescence intensities of spores and cells stained with Syto 16 were also examined on FL1 vs FL3 density plots to check the dye could adequately separate the dormant spores from the live cells. Spores were stained to check the region assignment in Figure 2.11 and then mixtures of spores and cells were stained. This is shown in Figure 2.12.

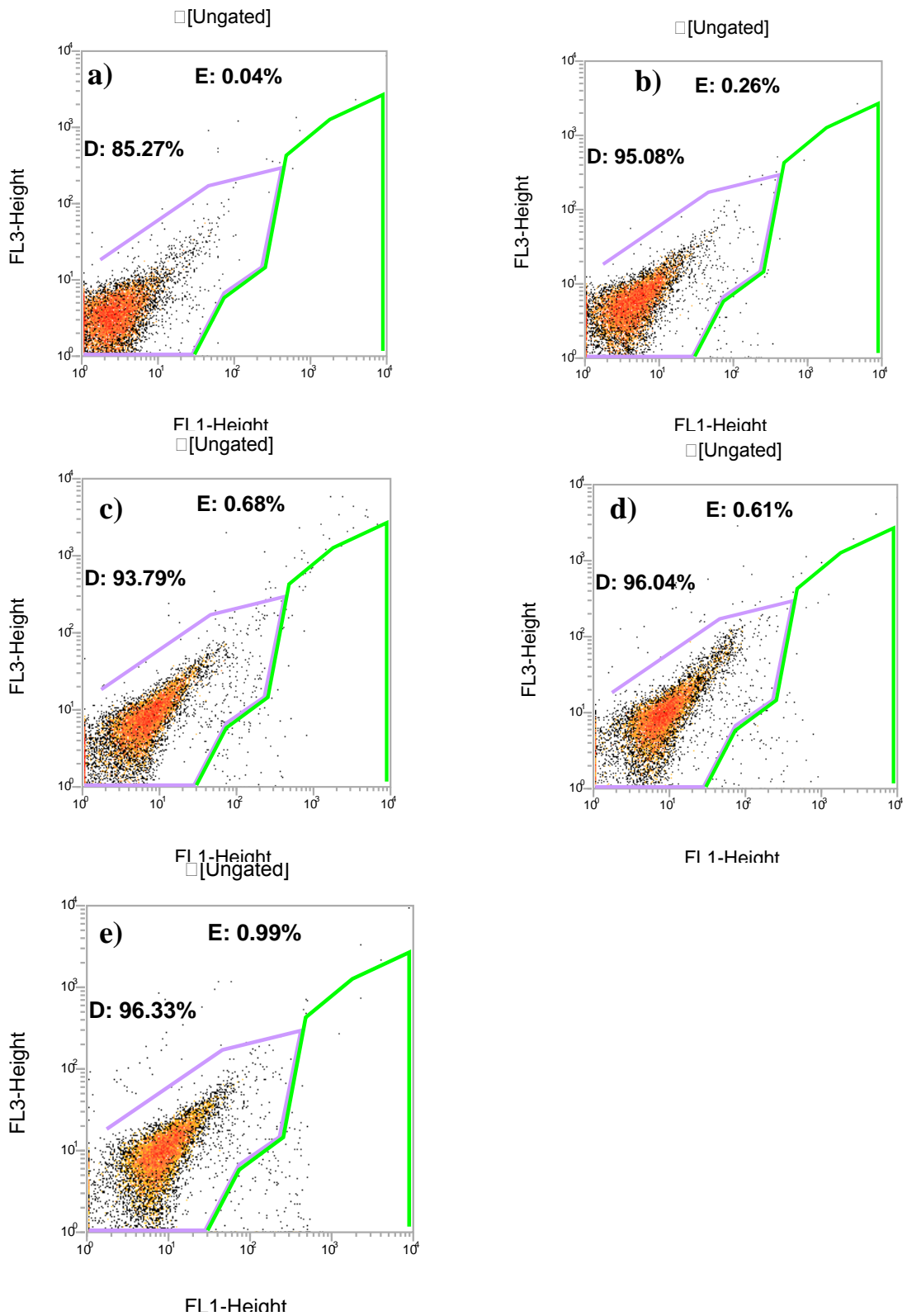


Figure 2.11 Dual parameter density plots of green fluorescence (FL1) against red fluorescence (FL3). Region E (green) = vegetative cells, region D (lilac) = spores. Spores stained at a) 1 μM b) 2 μM c) 2.5 μM, d) 3 μM and e) 6 μM with Syto 16

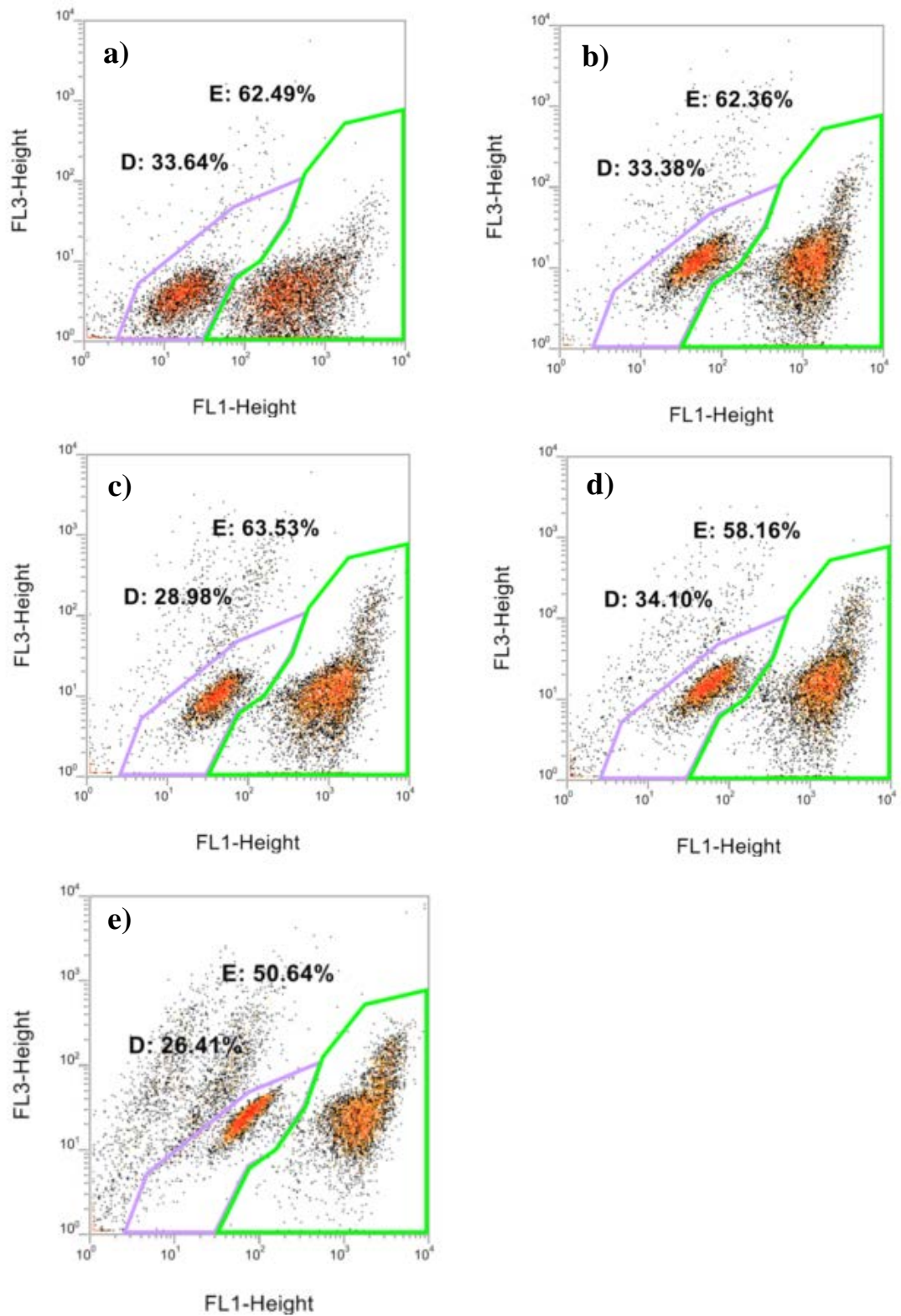


Figure 2.12 Dual parameter density plots of green fluorescence (FL1) against red fluorescence (FL3). Region E (green) = vegetative cells, region D (lilac) = spores. Cells and spores at 5×10^5 counts/ml stained at a) 1 μ M b) 2 μ M c) 2.5 μ M, d) 3 μ M and e) 6 μ M with Syto 16.

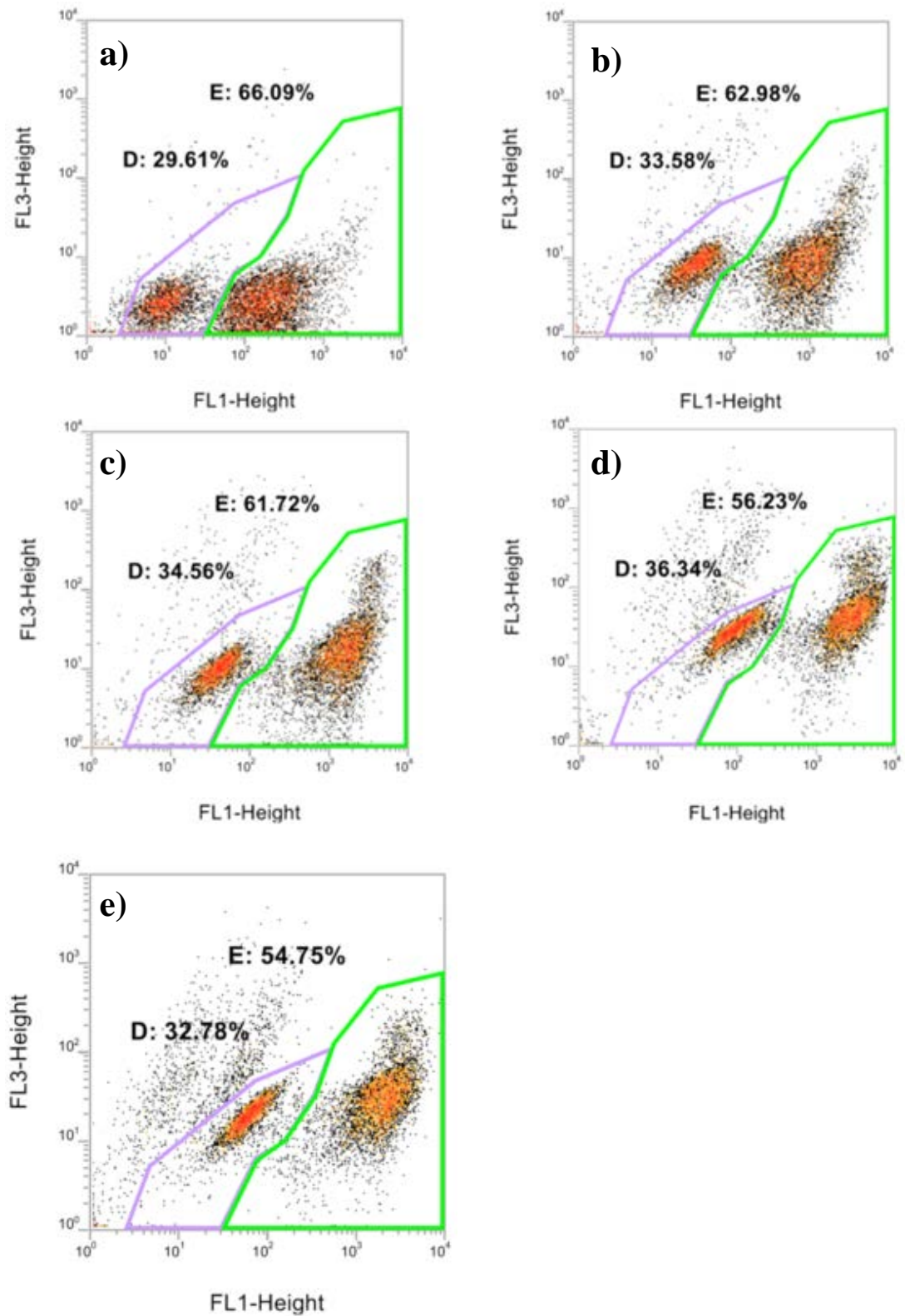


Figure 2.13 Dual parameter density plots of green fluorescence (FL1-Height) as a function of red fluorescence (FL3-Height). Results are left ungated to see the effect of staining concentration on the debris. Cells and spores at a concentration of 1×10^6 counts/ml stained with Syto 16 at the following concentrations a) $1\mu\text{M}$, b) $2\mu\text{M}$, c) $2.5\mu\text{M}$, d) $3\mu\text{M}$, e) and $6\mu\text{M}$

Figure 2.12 shows us the cell population in the green region, with debris still in view (ungated). The spore region is in the lilac shape, verified by running a sample of dormant spores through the FCM alone (Figure 2.11). Increasing the concentration of Syto 16 caused the debris to become stained also (Figure 2.13 a). This phenomenon was investigated further by performing a staining of PBS alone, Figure 2.14 shows the results of this experiment.

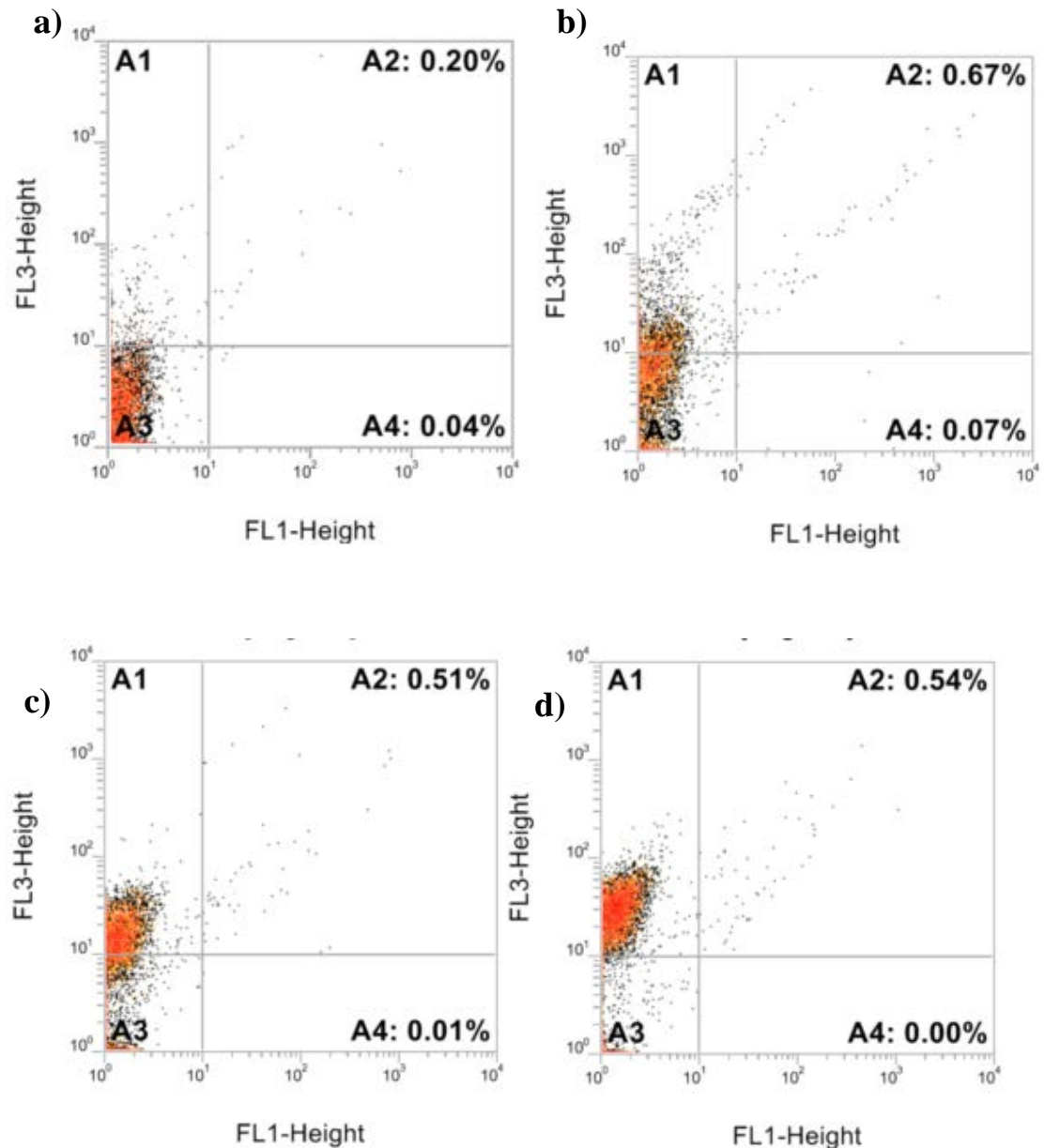


Figure 2.14 Green (FL1-Height) versus red (FL3-Height) fluorescence density plot showing filtered PBS with the following concentrations of Syto 16. a) 2μM, b) 2.5μM, c) 3μM and d) 5μM.

A clear increase in the fluorescence along the FL3 channel is seen as the concentration increases. At 5 μ M almost the entire region has shifted into the second log of intensity.

It was noticed that increasing the staining concentration had no effect on the number of events stained, as shown through the fact that all histogram peaks are at the same height (Figures 2.8 to 2.10). Instead the optimum staining concentration was selected based on the point at which the fluorescent intensity increases no further.

The information derived from the staining concentration investigation was coupled with information from Stocks (2004). This research details how the concentrations of PI and Syto dyes must be in the correct ratios. It was found that the Syto stain must be between 4% and 8% of the PI concentration.

Following this line of reasoning, it can be seen from the graphs that 48 μ M of PI is the point at which the fluorescence intensity increases no further (see Figure 2.9). With this in mind, the correlating concentration of Syto 16 to be between 4 and 8% of the PI concentration is from 2 μ M to 3.5 μ M. However, it was noted that during the staining concentration investigation, after 3 μ M the amount of debris stained increased quite significantly. This is seen clearly as the ungated events in Figure 2.12 e) and Figure 2.13 e). This non-specific staining also shifted from the first decade to the second decade of the FL3 channel as opposed to the central level. As Syto 16 is only meant to stain nucleic acids, one can assume at this concentration, the Syto 16 dye is in excess, and may be staining non nucleic acid components. Based on these assumptions, 48 μ M PI would be a suitable concentration and 2 μ M to 3 μ M of Syto 16 would be a sensible choice of concentration to visualise dead cells and living cells clearly and without too much 'false' staining. When examining the results from the PBS with stain experiment in Figure 2.14, it is evident that as the Syto 16 concentration gets higher, it fluoresces so strongly that the FL3 detector picks up some of this light due to increased spectral overlap. This means that the concentration of Syto 16 should be kept under 3 μ M to avoid conflicting or confusing results.

2.3.4 Setting compensation

Compensation is a tool that can be used to counteract any spectral overlap between dyes. As seen in Figure 2.1. the spectral overlap with PI and Syto 16 appears very low; however, one must take into account that Syto 16 increases its fluorescence intensity upon binding to nucleic acids by a far greater amount than PI. Accordingly, the perceived overlap could be far greater.

Compensation between the FL1 and FL2 channel can be achieved using rainbow fluorescent beads. However, it has been recommended that to gain an accurate level of compensation, the dyes which shall be used in the experimental research should also be used to set the compensation.

As such, to set the compensation correctly, it is necessary to have a Syto 16 positive sample (live cells stained with 2 μ M Syto 16), and a PI positive sample (dead cells stained with 48 μ M PI) and a negative sample, which would be a sample of dormant spores which do not stain with Syto 16 or PI. Additional to this, a sample of unstained cells are also visualised, to determine whether this population exhibits significant auto-fluorescence.

In Figure 2.15 a & b results of unstained cells, presented as a function of green fluorescence [FL1] intensity against red fluorescence intensity (FL3). The FSC and SSC profiles are shown for the cells also. The quadrant tool divides the plots into 4 sections, showing the percentage of events in each sector.

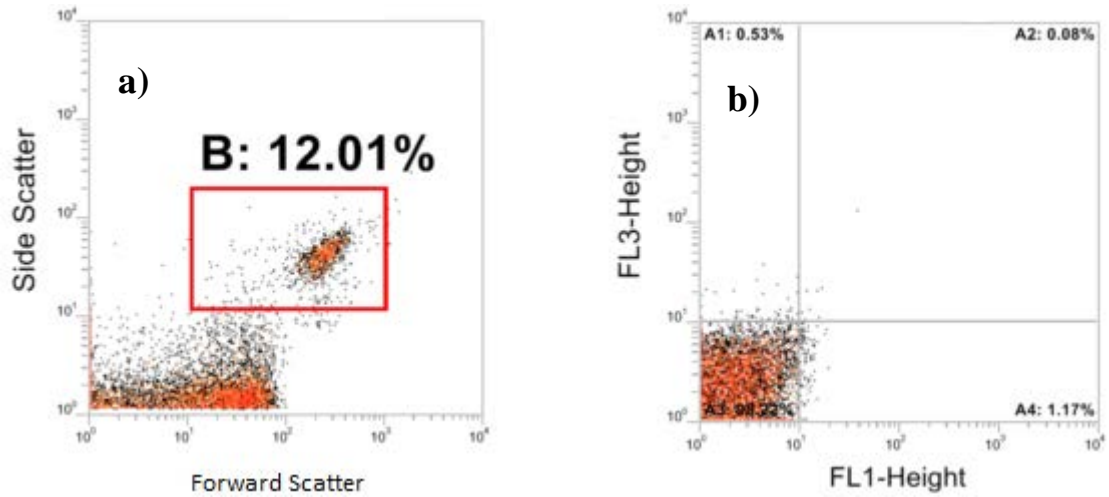


Figure 2.15 a) Dual parameter density plot of forward scatter (FSC) vs side scatter (SSC) of unstained cells in PBS. Region B indicates the cell population. b) Ungated dual parameter density plot of green fluorescence (FL1-Height) against red fluorescence (FL3-Height). Quadrants set so that the lower left quadrant encompasses the first decade denoting unstained material. This shows the corresponding FL1 vs FL3 density plot of the sample. No compensation or threshold set.

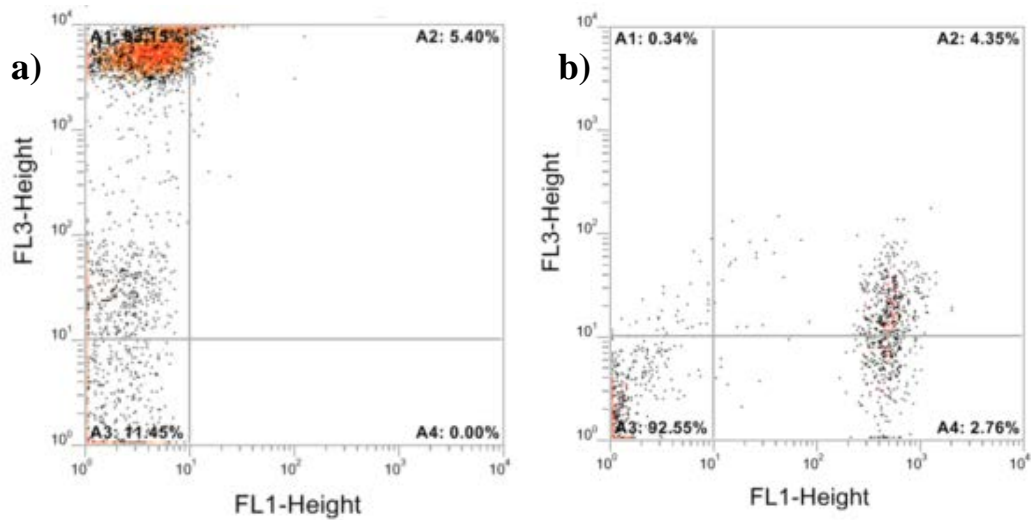


Figure 2.16 Dual parameter density plot showing green fluorescence (FL1-Height) against red fluorescence (FL3-Height) of a) Heated cells stained with 48µM PI and b) Cells stained with 2µM Syto 16). Quadrants set so that the lower left quadrant encompasses the first log. No compensation set

From Figure 2.15 and Figure 2.16 it is clear that the red fluorescence of PI is very high, reaching above the 10^4 decade under the initial settings and the Green fluorescence is under-compensated, due to this population branching into the upper right quadrant. As such the voltages were changed to FL1: 551, FL2: 580, FL3: 608. Compensation can only be adjusted between adjacent channels, therefore to ensure the spectral overlap is removed from the FL3 channel, the compensation must be altered using the FL1-FL2 setting, and then the FL2-FL3 function. The compensation levels were also adjusted such that: FL2- FL1 =40.0%; FL3 to FL2 = 23.8%. These altered settings were tested and their outputs are displayed in Figure 2.17 and Figure 2.18.

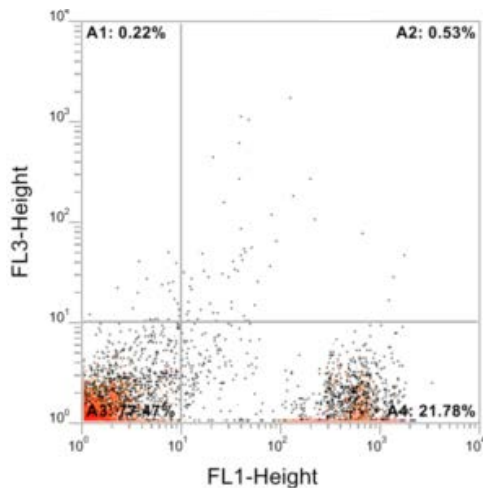


Figure 2.17 Dual parameter density plot of green (FL1) versus red (FL3) fluorescence. Cells and spores stained with Syto 16. Quadrants set so that the lower left quadrant encompasses the first decade denoting unstained material. Voltage Settings: FL1= 551, FL2= 580, FL3= 608; Compensation: FL2- FL1 =40.0%; FL3 to FL2 = 23.8%

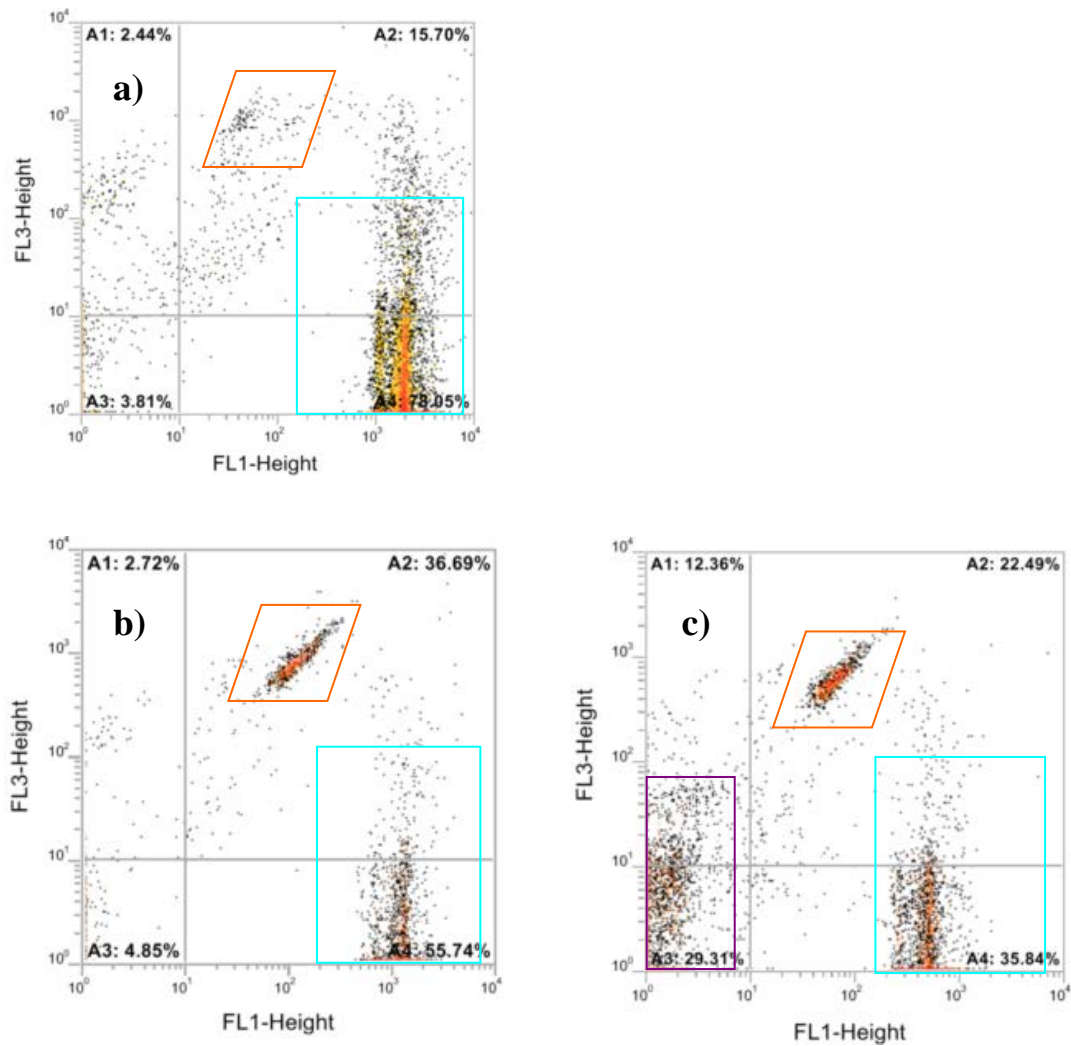


Figure 2.18 Dual parameter density plot of green (FL1) versus red (FL3) fluorescence. Quadrants set so that the lower left quadrant encompasses the first decade denoting unstained material. Showing a) Living cells double stained, b) mixture of living and dead cells double stained, and c) Living cells, dead cells and spores double stained. Purple region: dormant spores, orange region, dead cells and blue region: live cells.

The region assignments in Figure 2.18 show clearly living cells in the turquoise square, stained with Syto 16 only though a slight increase on the FL3 channel owing to the fact that this sample is now double stained. Dead cells are in the orange region, with a strong PI staining and mild Syto 16 staining. The purple region indicates spores which have little to no staining on either fluorescent channel owing to the fact that the stains do not penetrate the

spore to bind nucleic acid. Regions are drawn using samples of pure populations of dormant spores, live cells or dead cells.

It is clear that the negative population still expands outside the bottom left quadrat. With this in mind, the most sensible way to accurately adjust the compensation settings is to look at the mean values for the quadrats and adjust these so the lower left and right quadrats have a similar mean y value, and the lower left and upper left quadrats have a similar x value. The percentage compensation is therefore adjusted so that these values match as closely as possible

Figure 2.19 shows a PI positive population and a PI negative population correctly compensated

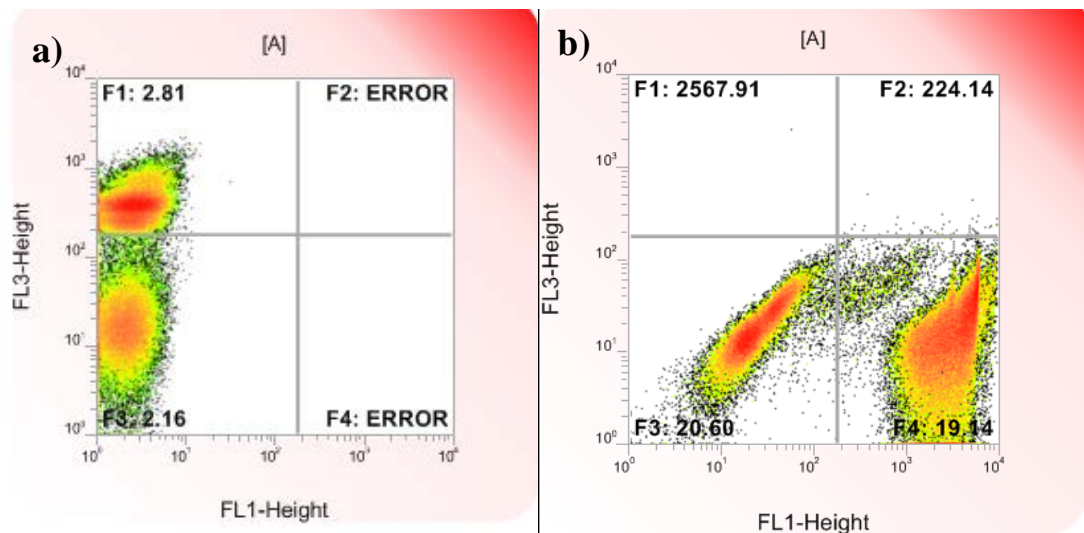


Figure 2.19 Gated FCM plot using equation AND A to examine only the cell and spore region. a) An FL1 (green) fluorescence (x axis) against FL3 (red) fluorescence (y axis) a) Heated cells and dormant spores stained with 48uM PI to form a PI positive population (top left) and PI negative population (bottom left). B) Live cells and dormant spore stained with 1µM Syto 16. F1: upper left quadrat, F2: upper right quadrat, F3 bottom left quadrat, F4 bottom right quadrat. NB. ERROR notice indicates no events in that region.

The x-axis mean for the bottom left is 2.16 and the x-axis mean for the top left is 2.81. As these values are very similar, no compensation is required. The compensation set for the Syto 16 is 40% in the FL2 to FL3 overlap, and 30% in the FL1 to FL2 overlap.

With the voltage and compensation settings as they are in Figure 2.18 (c), dead cells can be easily identified from living cells, and dormant spores from cells. These settings must be checked on a regular basis owing to potential fluctuations in the flow cytometer relating to the strength of the laser. It is recommended that compensation settings are checked before each experimental set (Cronin 2012). The next stage in the development of the methodology is to visualise dead spores from dormant spores.

2.3.5 Visualising Dead from Dormant Spores

As mentioned in Section 2.1.4 the temperature required for at least a 6 log reduction in counts was 129.4°C for eight seconds (Edwards *et al.* 1965). To ensure spores would be killed in the autoclave, a check of the temperature was done using the temperature probe, fitted to a ‘dummy’ microtube, filled with water. The results of the autoclave temperature and the sample temperature are plotted in Figure 2.20

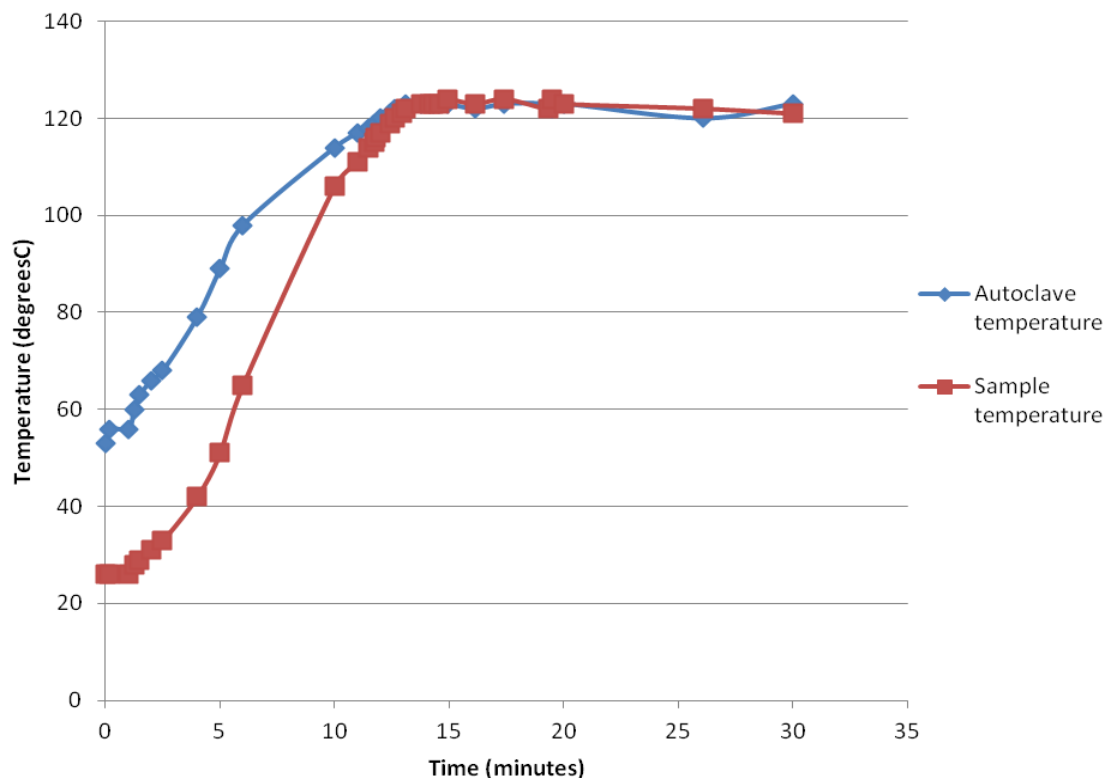


Figure 2.20 Temperature analysis of water in autoclave

Given that the sample temperature is over 100°C for 20 minutes based on the data shown in Figure 2.20 it can be assumed that spores kept in these conditions would definitely reach the required temperatures to induce 100% spore death. (These temperatures were detailed in Section 2.1.4.)

To investigate the effect of temperature on staining profiles of dead spores and dormant spores one set of samples were kept at <4°C whereas another set of samples were subjected to 28°C incubation period for a range of times.

Figure 2.21 to Figure 2.24 compares dormant spores and dead spores staining profiles. As the staining temperature increased and the incubation period increased the dead spores region stained with a higher intensity.

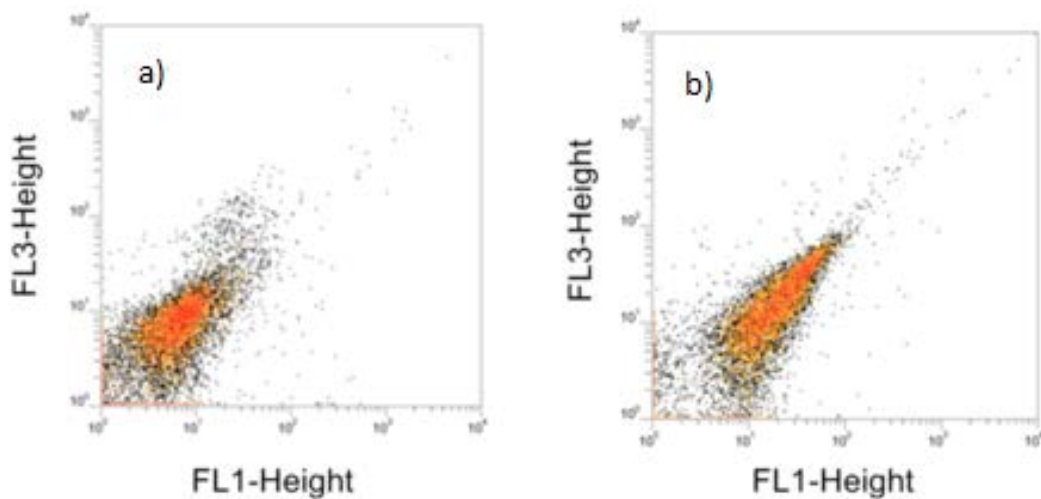


Figure 2.21 Dual parameter density plots of green fluorescence (FL1) versus red fluorescence (FL3) Spores stained at 4°C a) Dead spores b) Dormant spores

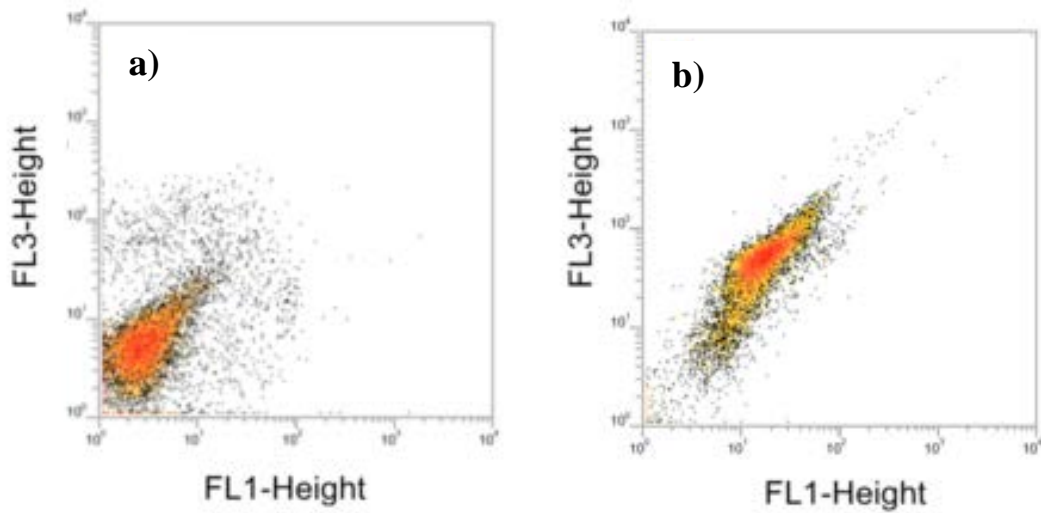


Figure 2.22 Dual parameter density plots of green fluorescence (FL1) versus red fluorescence (FL3) Spores stained at 28°C for 5 minutes a) Dead spores b) Dormant spores.

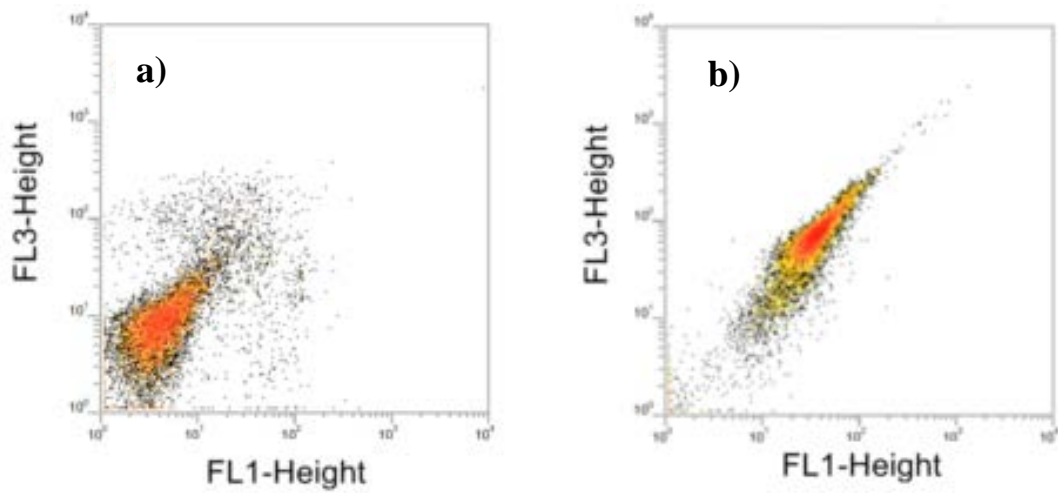


Figure 2.23 Dual parameter density plots of green fluorescence (FL1) versus red fluorescence (FL3) Spores stained at 28°C for 10 minutes a) Dead spores and b) Dormant spores.

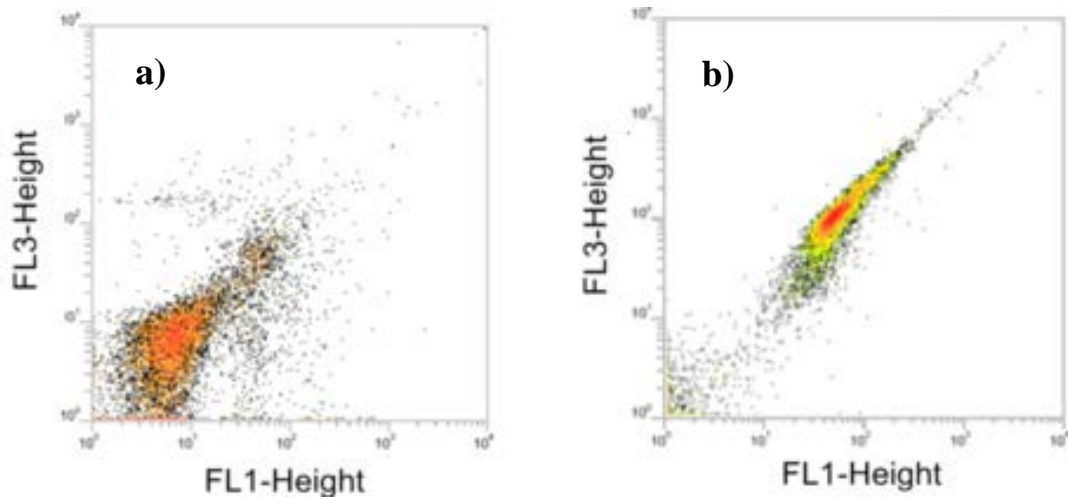


Figure 2.24 Dual parameter density plots of green fluorescence (FL1) versus red fluorescence (FL3) Spores stained at 28°C for 15 minutes a) Dead spores and a) Dormant spores.

The encouraging results from this experiment showed little to no change in the dormant spore profiles despite higher temperature incubation over differing periods of time, but a steady increase in dead spores staining was observed with increased temperature and time.

Following this investigation, the vegetative cells of *B. subtilis* were subject to the same staining procedure to ensure the higher staining temperature did not have a detrimental effect on cell staining. Again, Figure 2.25 shows cells and spore profiles on a FL1 vs FL3 density plot. The regions drawn were suitable for each treatment.

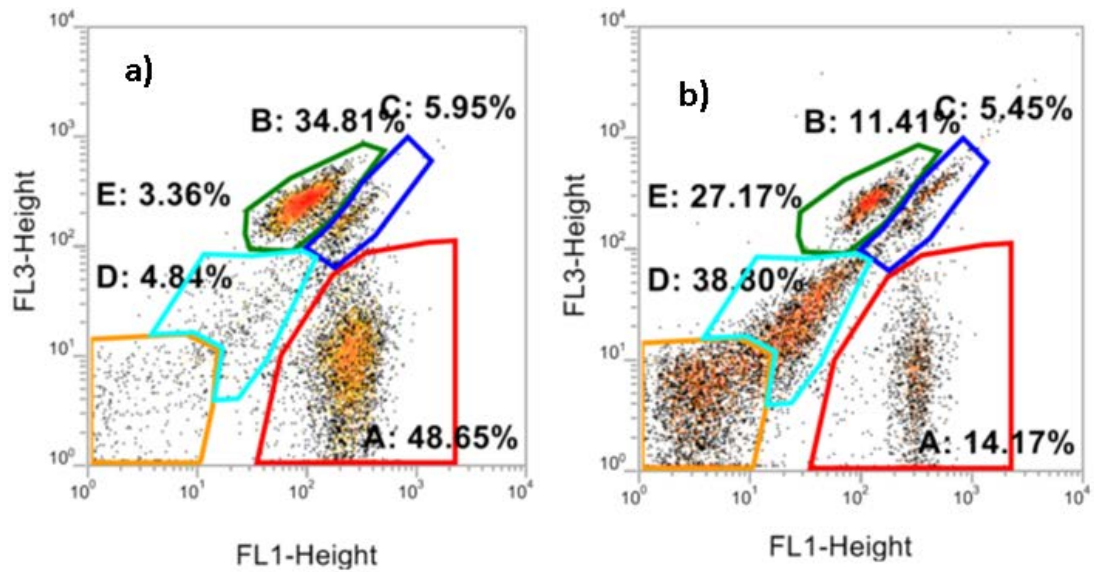


Figure 2.25 Dual parameter density plot showing green fluorescence (FL1) as a function of red fluorescence (FL3) a) Cells incubated for 30 minutes at 28°C b) a mix of cells, dead cells, dead spores and dormant spores. Incubated at 28°C for 30 minutes. Region A (Red) = Living cells, Region B (Green)= dead cells, Region C (Dark blue) = Damaged cells, Region D (Orange) = dormant spores, Region E (Turquoise) = dead spores.

The profiles obtained from the dormant spores and dead spore FCM fluorescent profiles indicate that a staining time above ten minutes should be sufficient to differentiate dead spores from dormant (Figure 2.24) From this data, 15 minutes incubation time was selected for spore staining at 28°C. This time was chosen as it will give us a clear separation in dead and dormant spores, but will not cause the fluorescence signal of dead spores to become so high they would interfere with the cell populations.

2.3.6 Assessing levels of germination via UV spectrophotometry

As detailed in Figure 2.24, to visualise dead spores from dormant, an elevated temperature staining protocol, of 28°C for ten minutes was found to be advantageous. However, it was important to ascertain whether this temperature may cause spore germination.

One of the standard methods for assessing the level of spore germination is to measure the OD₆₀₀ of spores, where a decline in optical density (OD) is indicative of spore germination (van Melis *et al.* 2011a). Specifically, this method measures the change in spore physiology from phase bright to phase dark. However, a more sensitive method is described by Black *et al.* (2007) where the release of pyridine-2,6-dicarboxylic acid (dipicolinic acid, DPA) is measured through an increase in OD at 270nm. This molecule is found solely in the spore cortex and comprises ~20% of core dry weight (Yardimci and Setlow 2010). The advantage of this method is that the onset of germination is detected far more quickly than changes in OD₆₀₀. This is because DPA release occurs in the first stage of germination, before spores turn phase dark (Setlow 2003).

Figure 2.26 shows the % DPA release as a result of incubation times in PBS for 60 minutes at three different temperatures, namely 4, 28 and 37°C. The baseline was set using PBS as the blank.

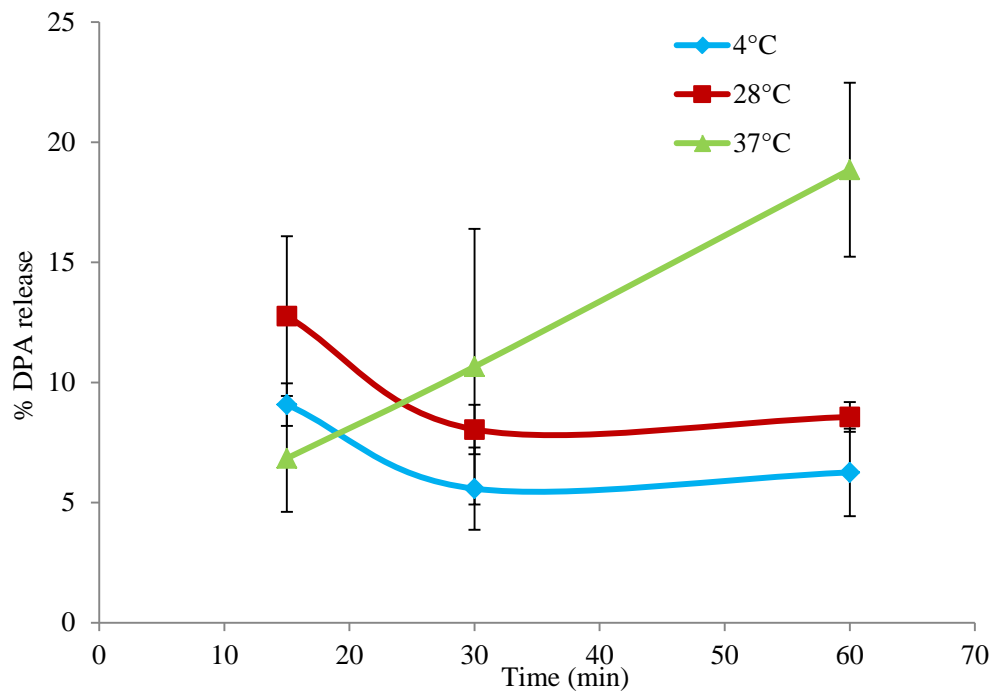


Figure 2.26 Percent DPA release from *B. subtilis* spores incubated in PBS at 4, 28 and 37°C.

Error bars represent the 95% confidence interval and n=3

Figure 2.27 shows DPA release from spores kept in ice water (0°C)

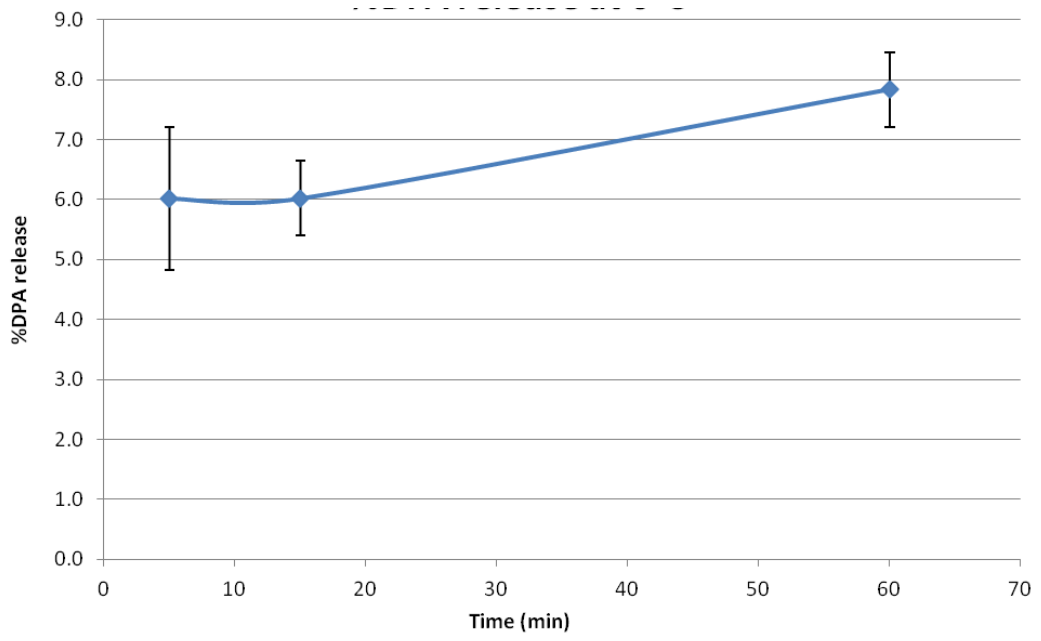


Figure 2.27 Spores suspended in PBS and kept in ice water. Error bars represent the 95% confidence interval and n=3

Upon consultation with Setlow (2012) the baseline was then re-set using the values from the supernatant of spores kept at 0°C. This is shown in Figure 2.28.

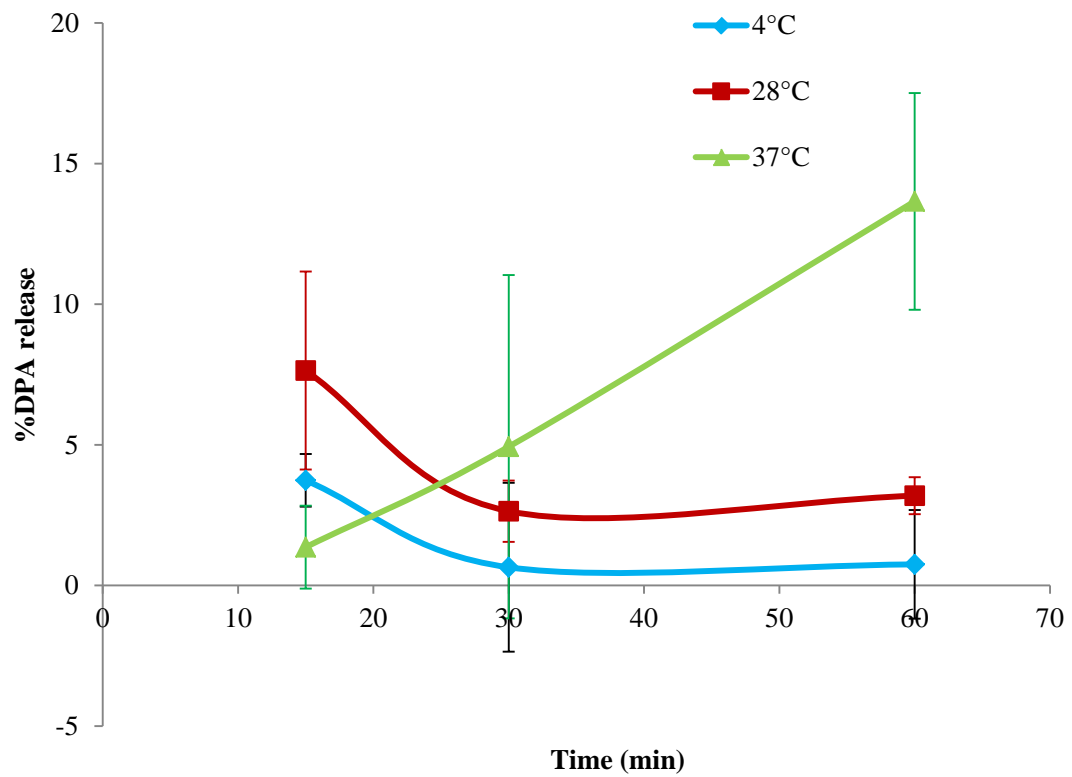


Figure 2.28 Amended DPA release from spores in PBS. The 'blank' was set using the supernatant of the spores kept at 0°. Error bars show the 95% confidence interval where n=3.

Before the results of the UV spectrophotometer were analysed, the Equation 2.1 was created to account for all substances that absorb at 270nm.

Equation 2.1

$$ABS_{270} = ABS_{PBS} + ABS_{non\ GerDPA\ sources} + ABS_{GerDPA} \quad (1)$$

Where:

ABS_{PBS} = absorbance generated by PBS,

$ABS_{non\ GerDPA\ sources}$ = absorbance generated by non-germination related compounds

ABS_{GerDPA} = absorbance generated by DPA released upon germination

However $ABS_{PBS} = 0$ as UV spectrophotometer is set to zero by a PBS blank

Hence

Equation 2.2

$$ABS_{measured} = ABS_{non\ GerDPA\ sources} + ABS_{GerDPA} \quad (2)$$

The $ABS_{non\ GerDPA\ sources}$ refers to other components that may cause an increase in absorbance at this wavelength, not linked with germination. In particular, nucleic acids, proteins and phenols will all cause an increase in absorbance at 270nm (Rosen *et al.* 1975; Wilfinger *et al.* 1997). Nucleic acids and proteins will originate from the *B. subtilis* organism itself, and trace amounts of phenols will arise from the AK sporulation plates used to culture the spores. Previous studies by Igarashi & Setlow (2005) and Vepachedu & Setlow (2007) have shown that DPA is responsible for 85-90% of the absorbance at 270nm. This means that up to 15% of absorbance is due to the non-germination related compounds.

There is also the issue that a small amount of DPA will be present in the surrounding PBS from samples even when no germination has occurred. This is because DPA is synthesised in the mother cell upon sporulation so there will be a small amount of DPA present in all spore samples (Setlow 2006).

To evaluate the potential interference of the ABS value at 270nm from non-germination related compounds, *B. subtilis* spores were incubated in PBS at 0°C for 5, 15 and 60 minutes and their ABS was measured. The apparent % DPA release is presented in Figure 2.26 and Figure 2.27 suggests an unlikely level of germination.

It is known that 0°C temperature inhibits germination, and whilst it would be preferable to check this by measuring whether spores remain phase bright, it was shown in previous studies that spores should remain dormant at this low temperature (Zhao *et al.* 2008; van Melis *et al.* 2011b). All ABS signal obtained from the 0°C experiment should be treated as baseline noise [ABS_{non GerDPA sources}] and hence be subtracted from the ABS values of samples at the other temperatures (4-37 °C). Based on this line of reasoning the percentage DPA release was re-calculated after correcting for the absorbance values from the 0°C spores in PBS. The corrected results are shown in Figure 2.28.

From the corrected % DPA release values at Figure 2.28 it is apparent that there is a high variability of the DPA release values. This is inherent to the methods and has also been reported previously (Paredes-Sabja *et al.* 2008). None-the-less it is possible to confirm that 4°C and 28°C treatments have shown no statistical difference ($p>0.05$) for all three time points indicating a grand average %DPA release value ca 3.1% after 60 minutes. This suggests that possible spore staining treatments at 28°C for up to 60 minutes is unlikely to induce significant levels of germination. On the contrary, incubation at 37°C was found to induce moderate levels of germination, particularly for incubation times exceeding 30 minutes exposure.

It can therefore be concluded that the changes observed in the FCM profiles when elevating the staining protocol temperature from 4°C to 28°C are not due to temperature induced germination. Hence, the sub-population assignments should accurately reflect the

true nature of the samples. Based on this information, it is evident that the staining protocol could be amended to up to 28°C incubation time at 60 minutes, or 30 minutes incubation at 37°C.

2.3.7 FCM servicing and re-alignment

Before our experimentation could begin, the FCM required configuring for bacterial analysis. Little standardisation has been carried out in FCM small particle analysis (Nebevon-Caron 2009) so this involved checking the instrument was in optimum working order. Figure 2.29.a illustrates an example of spores run through the FACSCalibur before and after machine maintenance was carried out, in which the laser alignment was corrected.

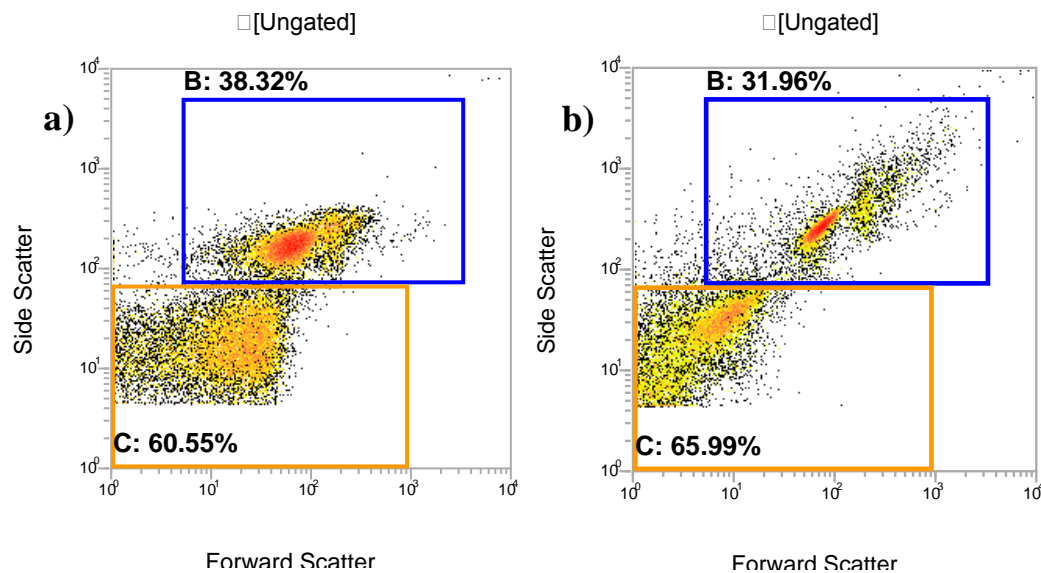


Figure 2.29 Representative FSC vs SSC density plots of a sample of dormant spores run through the FCM. Region B (blue) shows the spore and cell area and region C (orange) shows the debris. Left panel a) shows the profile before servicing, and right, b) shows the optimised conditions after the service. FCM acquisition settings as follows for both plots: FSC E01 and SSC 425. n=4.

Spore samples were run through the machine before and after the re-alignment to monitor changes on the profiles. Before the service, it was noted that the blocking bar for the laser

was misaligned, causing continuous background signal from the laser to be present consistently. Once this was corrected, the spore region became much clearer, and two populations can be clearly distinguished, as opposed to an unclear population before the correction. Such results highlight the importance of good machine maintenance for anyone wishing to carry out small particle analysis on a flow cytometer, to minimise background interference from the laser. As has been shown in the results detailed in this chapter, particular with reference to the Giga bead mixture, this mis-alignment can lead to smaller particles being lost in the noise. It is possible that such problems could deter other researchers from engaging with FCM. Hence by documenting such obstacles, other researchers may be able to better use this multi-parametric tool, since there is currently a paucity of detailed information on bacterial FCM settings (Nebe-von-Caron 2009).

Furthermore, general machine maintenance was employed to prevent the build-up of non-specific noise, both a daily and a monthly cleaning was carried out on the sheath lines and sample tubes. The monthly cleaning consisted of a 10% sodium hypochlorite solution followed by a ddH₂O cleaning of the system. This cleaning regime was kindly suggested by one of our collaborators (Cronin 2012).

2.4 Concluding remarks on the development of a FCM methodology

Based on the observations reported in this section, a bacterial FCM methodology has been developed and adapted to specifically measure the viability and physiology of *B. subtilis* cells and spores. With this methodology now in place it was possible to begin assessing the behaviour of *B. subtilis* in different conditions.

3 Chapter Three: Optimising spore yields and purity

3.1 Introduction

Reliable and reproducible production of dormant *B. subtilis* spores was essential to support experimental work. Several studies have compared the purity of spore preparations using different sporulation strategies, however these papers do not report the best method to check spore purity (Powers 1968; Dragon and Rennie 2001; Monteiro *et al.* 2005; Harrold *et al.* 2011; Tavares *et al.* 2013). To successfully obtain a stock of pure dormant spores it is necessary to have a very high sporulation efficacy, a good method for killing off remaining vegetative cells, whilst keeping the dormant spores unharmed, and for FCM analysis, to have minimal debris left in the mixture.

Not only does the acquisition of a pure dormant spore stock profit researchers, it could also be invaluable to those using spores as probiotics. For commercial probiotic suppliers, obtaining stocks of pure dormant spores should be high on the agenda to produce good quality probiotics.

In this chapter, the development of methods undertaken to create spores with a dormant spore purity of >90% and little cellular debris are detailed.

3.1.1 Methods for sporulation

Sporulation occurs upon the depletion of nutrients in the culture environment, which prevents further cellular replication. Specifically, sporulation can be induced when carbon, nitrogen and sometimes phosphorous are limited (Harrold *et al.* 2011). Whilst there is evidence that a decrease in GTP concentration may be a key trigger in sporulation (Ochi *et al.* 1982; Ratnayake-Lecamwasam *et al.* 2001), Chubukov and Sauer (2014) point out that no single signal (such as NAD(H), NADP(H), ATP or GTP) seems to be responsible for driving the sporulation decision.

However, events surrounding the initiation of sporulation are complicated at the population level as individual cells behave differently (de Jong *et al.* 2011). For example,

previous research has suggested that only a fraction of cells actually undergo sporulation, and the rest lyse, releasing nutrients into the medium that sporulating cells utilise. This is known as ‘cell cannibalism’ and it is intimately linked with the activity of *spo0A* gene (González-Pastor 2011), the master regulator for sporulation. In some cells, this gene is transcriptionally active whereas in others, it remains inactive. Cannibalism is achieved by the release of toxins produced by gene clusters *Skf* and *Sdp* in the cells expressing *spo0A*. *Skf* is responsible for the production and release of a killing factor as well as immunity to it. The *Sdp* gene cluster is responsible for a second killing factor and again the immunity to this bacteriocin, though this bacteriocin also functions as a sporulation delaying protein.

The sporulating cells (with the active *spo0A* gene), therefore break down the non-sporulating cells releasing nutrients. This nutrient release will have one of two possible effects on the Spo0A active cells, depending on their stage in sporulation. If the cells have not yet formed an asymmetric polar septum, then sporulation is arrested and cells resume normal growth (González-Pastor 2011). Alternatively, if septation has been completed, (stage two of sporulation) the additional nutrients will drive the sporulation process (Parker *et al.* 1996). According to González-Pastor (2011), the non-sporulating cells (or Spo0A inactive cells) are affected by these toxins for two known reasons:

a) ‘the *Skf* putative immunity genes and ABC transporters are not transcribed in Spo0A inactive cells’

b) ‘*AbrB* is expressed in Spo0A-inactive cells (*abrB* gene is repressed by Spo0A), and represses transcription of the operon *sdpRI* conferring immunity to the Sdp toxin’ (González-Pastor 2011).

As many of the cells are broken down by the toxins, this leads to a build-up of cellular debris in the sporulating mixture that might not be completely broken down by the cannibalism process. Furthermore, at the final stage of sporulation (Stage five) the mother cell is lysed freeing the mature spore (McKenney and Eichenberger 2012). As such, further cellular debris is present in the environment. This particulate debris can interfere with FCM

analysis of small particles like spores. Accordingly, it is necessary to have a means to prevent or eliminate as many small particles as possible.

To create spores in a laboratory environment, it is necessary to find a means to exhaust nutrients from the cells. Smith *et al.* (2011), in one of the most extensive recent publications on spore production, noted that there is no standard method to produce spores, and the level of dormant spore purity varies considerably between batches whilst using a consistent method. Post-harvest treatments of spores also vary considerably (Smith *et al.* 2011). For example while multiple washes in sterile H₂O are commonly implemented, additional heat, lysozyme, and EtOH treatments are frequently performed in an attempt to achieve higher purity levels (Dragon and Rennie 2001). Importantly, Smith *et al.* (2011) also states that there are no consistent tests for spore dormancy (i.e. resistance to stresses) and spore yield.

One of the most common methods for producing dormant spores is to use specially formulated sporulation media. Difco sporulation medium (DSM) is a liquid sporulation medium developed by Nicholson and Setlow (1990), and includes the key compounds MnCl₂FeSO₄ and Ca(NO₃); Mn²⁺ and Fe²⁺ are essential to sporulation, and calcium is required for the Ca-DPA complex in the spore core (Fleming and Ordal 1964; Fortnagel and Freese 1968).

Production of spores using AK sporulating agar, devised by Arret and Kirshbaum (1959) allows for more direct manipulation of the sporulating environment, since different compounds can be added to the surface of agar plates. The product is available in a powdered form and contains sources of nitrogen, sulphur, amino acids, B vitamins and D-glucose as an energy source, though does not contain additional Fe or Ca sources. This medium contains MnSO₄, vital to the sporulation process, due to its role in proteinase formulation and phosphoglycerate phosphomutase (Charney *et al.* 1951; Oh and Freese 1976)

3.1.2 Methods for purification

Purification of spores involves both the killing and removal of vegetative cells. Lysozyme is commonly used for killing vegetative cells, as outlined by Powers (1968), however this method has been shown to alter the morphology of *B. cereus* spores, and will cause clumping of cells (Zhao *et al.* 2008). As such, gentler methods are often employed. Zhao *et al.* (2008) explored a few methods for *B. cereus* purification. Among these was an ethanol treatment, used to kill off living cells and germinating spores, which was shown to be most effective in terms of spore purity and time efficiency according to a comparison with heat shock, lysozyme and daily washes (for seven days) (Zhao *et al.* 2008) achieving at least 93% purity after a 10 day culturing period. Heat shock will kill off cells, as will lysozyme, and daily washes will help to remove cellular debris. The ethanol washing method was also utilised by Dragon and Rennie (2001) who found it to be just as effective as heat treatment.

Others have used density gradient centrifugation to separate the spores from vegetative cells since spores have a higher density. However, this is a lengthy process, involving several washing steps in ddH₂O. Accordingly, more efficient means of spore purification have been sought out by different researchers (Nicholson and Setlow 1990).

Spore purification to remove cell debris will inevitably involve several washing steps no matter which procedure is followed. Whereas some researchers have used centrifugation at 10,000 x g for 10 minutes to harvest their spore preparations during washing (Goldrick and Setlow 1983), others have centrifuged at 7,000 x g for 20 minutes with the belief that more debris should be removed (Munoz *et al.* 1978). This was based on the fact that fewer cells and debris will be spun down into the pellet, allowing more to be decanted with the supernatant.

The general summary of spore purification is to undertake many washes (in sterile distilled water at 4°C) and to keep examining the solution by phase contrast microscopy until 95%-100% free spores without cells or debris (Keijser *et al.* 2007). It may be that by

spinning at a slightly lower speed (at 7000 x *g* rather than 10000 x *g*) as suggested by Munoz *et al.* (1978) the debris should be eliminated more readily, though since this procedure has not been adopted by a wide range of researchers, this is unlikely to have a large impact on the rates of purification. This is due to the higher density of spores in relation to cells (Dean and Douthit 1974), as a lower G force will mean fewer particles are pelleted, leaving the less dense particles in suspension, which can then be decanted.

3.1.3 Aims and Objectives

The main aim of the research detailed in this chapter was to produce spore stocks with low levels of cellular debris and of high dormant spore purity, i.e. greater than 90% pure dormant spores.

To achieve this, the main parameters investigated were:

- Multiple spore washing steps
- Spore filtration
- Manipulation of the sporulation medium with additional manganese
- Different spore harvesting methods
- Alternative sporulation strategies (i.e. plating vs liquid media)

3.2 Materials and Methods

3.2.1 Spore production

AK sporulation agar was made according to manufacturer's instructions (BBL, UK). *B. subtilis* was cultured in LB broth overnight at 37°C. 1ml samples of cells were centrifuged at 10,000 x *g* for three minutes and re-suspended in 995µl sterile filtered phosphate buffer (100mM, pH7.4). 200µl of this cell suspension was spread on each plate using an EtOH flamed L-shaped glass rod. Plates were left to dry, then inverted and incubated for at least 10 days at 37°C. After this point, spore production was checked daily

by taking a sterile scraping and suspending this in sterile PBS (100M, pH 7.4) and visualising under a microscope using phase contrast, where dormant spores will be phase bright. Incubation was continued until a sample of nearly all free (>90%) dormant spores was seen.

Spores were then harvested by either:

- Flooding the plate with 10ml cold sterile 0.2µm filtered water, then gently agitating the agar surface to dislodge the spores with a sterile glass rod. This spore suspension was then poured into a 15ml falcon tube.
- Scraping the plate with a sterile inoculating loop and shaking this off in a 15ml tube of sterile 0.2µm filtered H₂O.

Post-harvest, the tubes were centrifuged three times at 4080 x *g* for 10 minutes and the supernatant replaced with sterile H₂O. After the third wash, the samples were then suspended in 50% EtOH and refrigerated overnight.

Following this purification step, the samples were centrifuged at 4080 x *g* and re-suspended in H₂O twice more.

All spore samples were kept either refrigerated or on ice, to limit germination.

3.2.2 FCM

Spores stocks were usually at a fairly consistent density (~2 x 10⁸ spores/ml), therefore to analyse the purity of each stock sample, they were diluted 100-fold in 0.2µm filtered phosphate buffer (pH 7.4, 100mM) and double stained with 1.5µM Syto 16 (Life Technologies, UK) and 48µM PI (Sigma Aldrich, UK) for 10 minutes at 28°C. Stained spores were kept on ice until analysed with a BD FACSCalibur flow cytometer (FCM). The SSC channel (a PMT detector) was selected as the trigger and the voltages were set as follows: FSC: E01, SSC 425V, FL1 584V, FL2 641V, FL3 625V. Compensation was set so

that FL2-FL1 41.9% and FL3-FL2 12.6% and SSC threshold was set 160V. At least 10,000 events were recorded for each sample.

3.2.3 Fluorescent Microscopy

Spores were stained with 1.5 μ M Syto 16 and 48 μ M PI then 7 μ l of each spore sample was transferred to the centre of an ethanol-cleaned glass slide and protected by the immediate placing of a cover slip. A Leica DM5000B microscope was used to visualise sample and at least five frames were taken per slide. At each frame both a differential interference contrast (DIC) light image and an I3 (blue) light fluorescent image were captured.

3.3 Results

Spores preparations were analysed by flow cytometry (FCM). The single parameter histogram for FSC (Figure 3.1) appears to suggest a single population of particulates based on the single peak evident; however the SSC histogram illustrates a second incompletely resolved peak suggesting that the debris can be detected within the spore preparation meaning the preparation is not adequately purified for FSC. Thus it is difficult to separate the spore region from debris as shown in the FSC vs SSC density plot below (Figure 3.3).

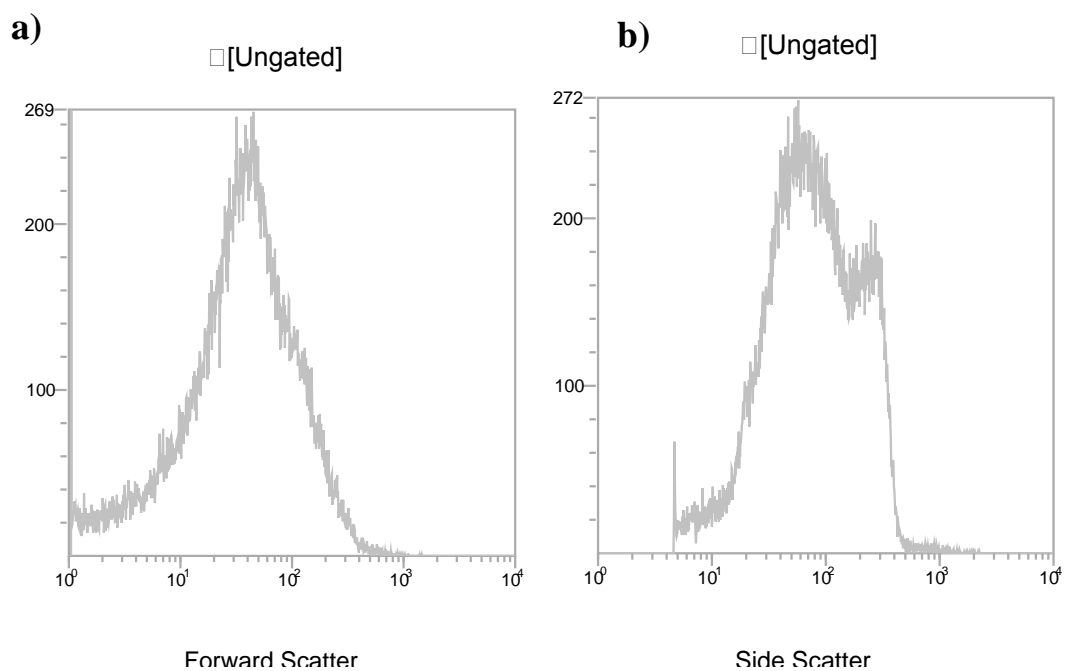


Figure 3.1. Representative FSC and SSC analysis of spores produced on AK sporulating agar (sample A), incubated for 10 days and harvested by flooding with sterile filtered water, treated with EtOH and then re-suspended in water. Spores were analysed by FCM in sterile filtered PBS. Panels a) single parameter histogram describing Forward scatter and b) single parameter histogram describing Side scatter. n=10.

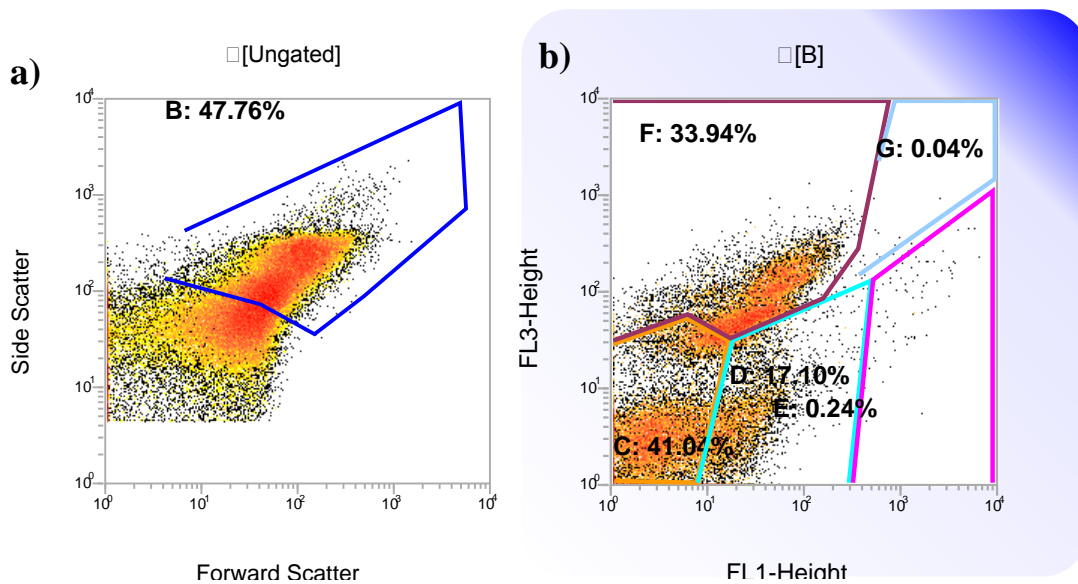


Figure 3.2 Double stained spore sample A analysed by FCM on a) FSC vs SSC density plot. Region B (green): cells and spores. b) Gated (using equation B) fluorescence plot where FL1-Height represents green fluorescence and FL3-Height red fluorescence. Region C (orange): dormant spores, region D (turquoise): germinating spores, region E (pink): Live cells, region F (burgundy): dead spores, region G (light blue): double stained cells.

In Figure 3.3 the region assignments were based on pure samples of live cells, dormant spores, germinating spores, dead spores and dead cells which had been previously defined on this instrument (Chapter 2). It was evident that further purification was necessary in these samples.

3.3.1 Effect of multiple washing steps

In order to reduce the amount of cellular debris retained in the spore sample, a further three (six in total) washing steps were undertaken. Five samples were investigated in this series (labelled A-E), below are representative images and FCM profiles of a typical spore sample. The remaining FCM outputs for samples B-E are presented in Appendix 2.

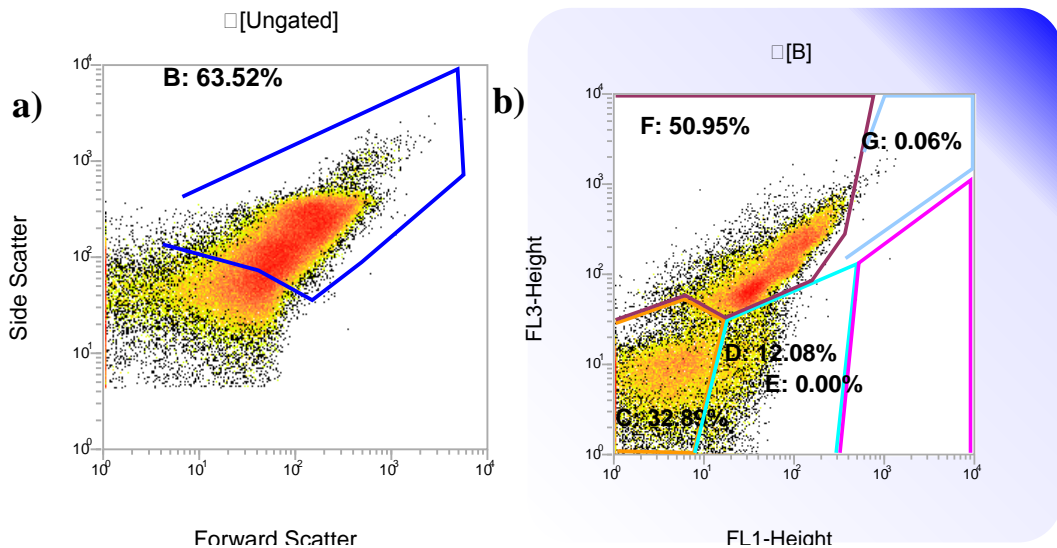


Figure 3.3 FCM output for spores from centrifuged spores sample A, double stained with Syto 16 and PI a) FSC vs SSC density plot of spore sample A, where Region B (blue): cells and spores. b), Gated (using equation B) fluorescence plot where FL1-Height represents green fluorescence and FL3-Height red fluorescence. Region C (orange): dormant spores, region F (burgundy): dead spores, region D (turquoise): germinating spores, region E (pink): Live cells, region G (light blue): double stained cells.

The FCM analysis of spores from Sample A prepared with these extra washes (Figure 3.3) clearly shows the percentage of events in region B (the spore and cell area) rose from 47.76% to 63.52% that indicates a moderate reduction in the contamination of the preparation with debris. However, there appears to have been an increase in the number of dead spores and cells in the sample, characterised by a larger percentage of events populating region F (dead spores region). The unstained region C (dormant spores) constitutes just 32.9% of the total events, this is far lower than reported in previous studies, where $88\% \pm 11\%$ is the average spore yield (Harrold *et al.* 2011).

In an attempt to gain a better understanding of the composition of particulates materials within these preparations they were analysed by fluorescent microscopy as detailed in Section 3.2. Again, the remaining images and FCM profiles of samples (B-E) are given in Appendix 2.

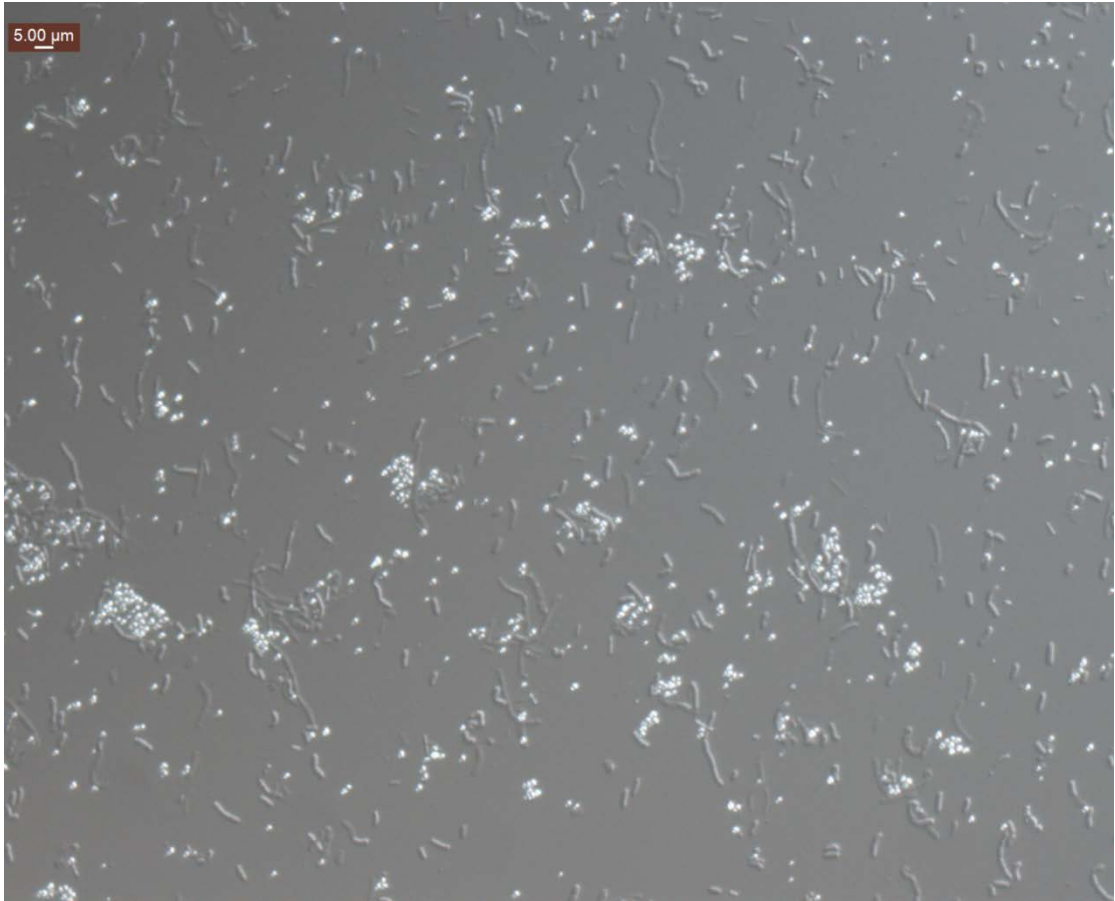


Figure 3.4 DIC image of *B. subtilis* spores sample A under 40x objective lens

On consideration of Figure 3.4, it appears that the majority of organisms in the sample are either intact cells or phase bright dormant spores, the latter are largely clumped together forming aggregates. However, since the FCM profiles (Figure 3.3) suggested a high level of debris was present, the magnification was increased to see if any smaller particles could be seen.

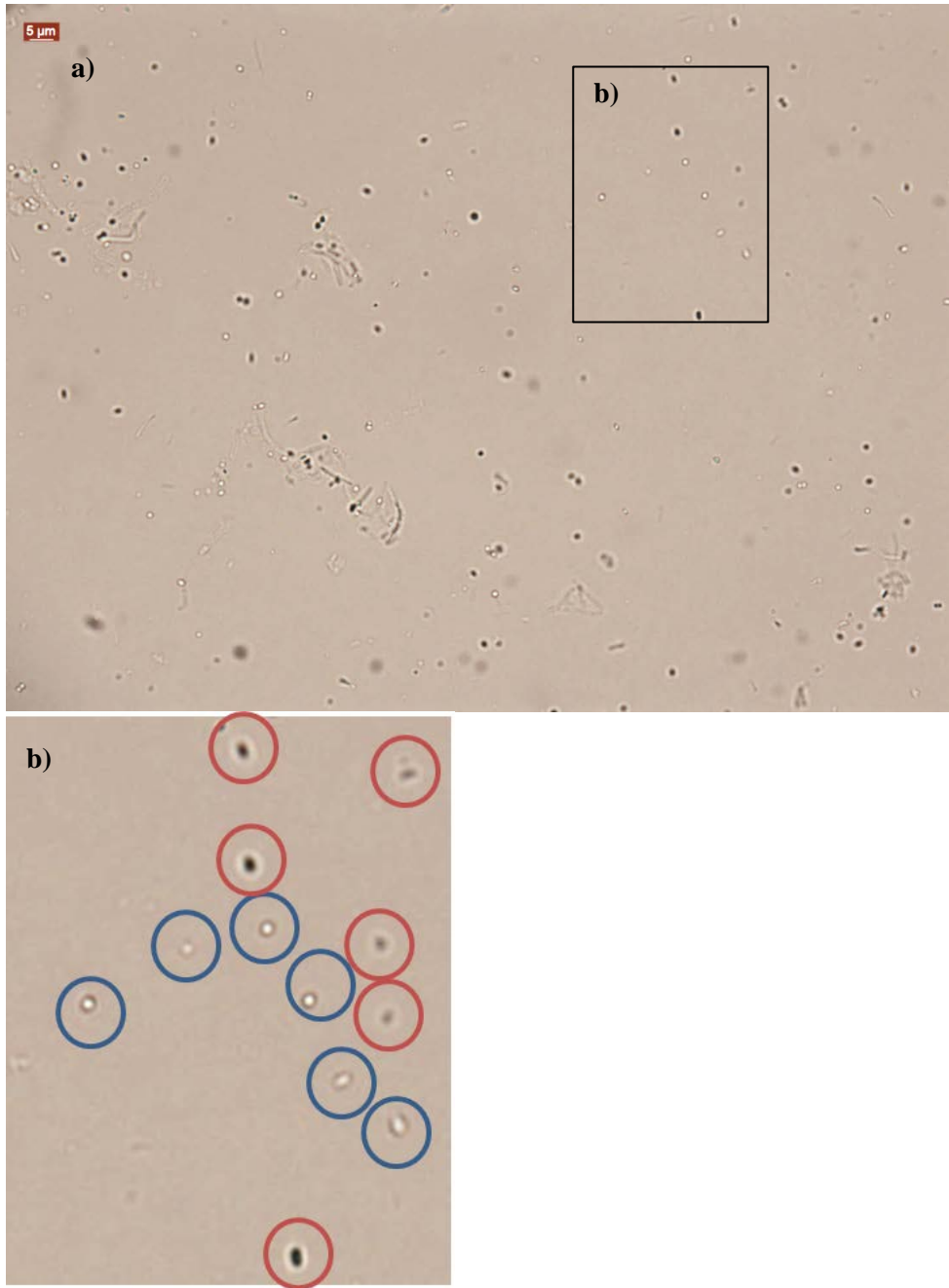


Figure 3.5 a) DIC image of *B. subtilis* spores sample A taken under 63x objective lens. b) Blue circles highlight spores (phase bright) which are in focus, and red circles indicate dormant spores which are still phase bright, but appear dark owing to the fact these are not in the plane of view.

In Figure 3.5 it is evident that there are several intact cells present in the mixture, as well as many other particles of variable sizes. Circular organisms are spores, whether dark or light depends on the plane of view at which these are analysed, though dormant spores in the correct focus should appear brighter, as this corresponds with the amount of DPA present in

the spore core. Conversely spores which have lost their brightness are likely to be germinated spores which have lost their DPA depot (Zhang *et al.* 2010b).

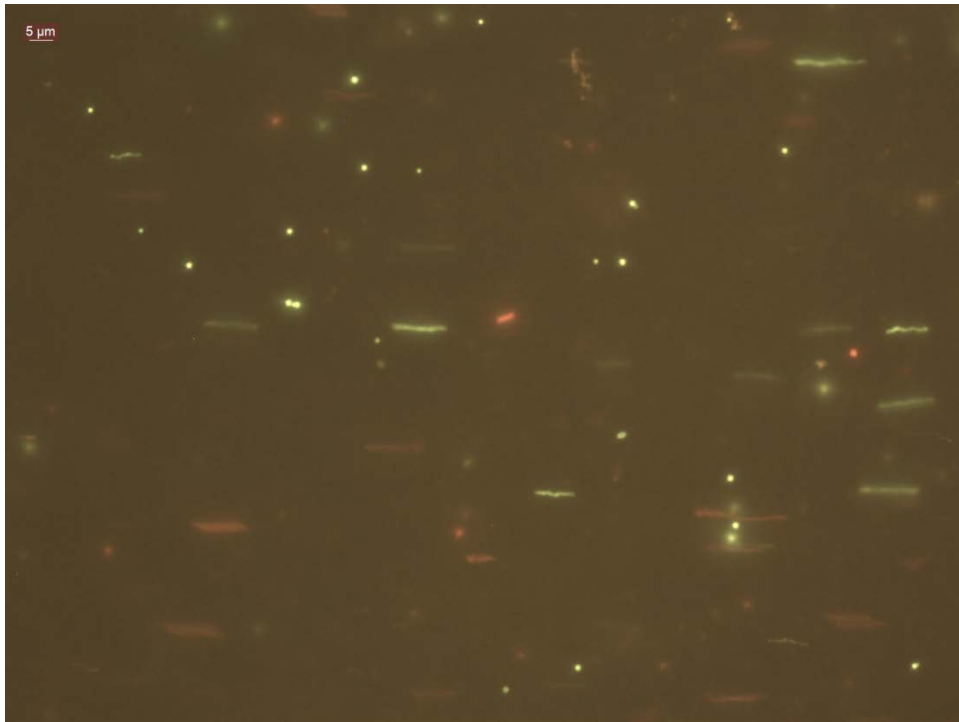


Figure 3.6 I3 (blue) light image of double stained (1.5 μ M Syto 16 and 48 μ M PI) *B. subtilis* spores sample A. Taken under the 63x objective

Green-staining indicates uptake of Syto 16; there were many small circular bright green organisms recorded as (live) immature spores (or possibly germinating spores) and rod shaped green cells, indicating live vegetative cells. A few red-stained rods had taken up PI indicating their loss of viability during processing. Rigorous classification and quantification of these particulates was not carried out to compare to the profiling provided by the FCM analysis. The example shown here illustrates that the excessive washing steps are not sufficient to produce pure spore samples. Significant quantities of intact viable cells and non-viable cells have co-purified with the spores. However, other samples behaved slightly differently under the same conditions.

Fluorescent microscopy was carried out on each sample, to determine how the FCM profiles matched with the microscopy results. Whilst it would be advantageous to enumerate

the samples *via* both FM and FCM, the images produced by FM were not clear enough to accurately define which spores were dormant, germinating, dead live or vegetative cells. Unfortunately, the ImagePro analysis software could not enumerate these samples due to the poor resolution. However, the FM images do provide a rough insight into the state of the samples, therefore these are shown below.

Red circular bodies most likely represent immature spores which have been killed by the EtOH treatment, whilst rod shaped orange/red coloured organisms are dead cells. The I3 light image shows that several spores do appear to be dormant, which corresponds with the FCM profile where 40% of the population sits in the dormant spore region, meaning there is little to no staining with either dye. There are a few red circular spores, indicative of dead spores, which would be representative of the 43% of events in region C of Figure 3.3 b. There are also lots of germinating spores. These are bright green circular points on the I3 light image, corresponding to region D in Figure 3.3.

Table 3.1 Mean values (in bold) for each region from spore samples A-E before and after the multiple washing steps. Regions based on the FCM profile in Figure 3.3, Region B: cells and spores, region C: dormant spores, region D: germinating spores, region E dead cells, region F: Live cells region G: double stained cells,

		Region											
		B		C		D		E		F		G	
		Before	After	Before	After	Before	After	Before	After	Before	After	Before	After
Sample	A	47.76	63.52	41.04	32.89	17.1	12.08	0.24	0	33.94	50.95	0.04	0.06
	B	36.53	63.33	73.63	34.26	12.89	15.73	0.16	0	7.52	45.65	0	0.15
	C	41.61	58.41	65.97	55.43	16.29	26.89	0.19	0.04	11.75	13.26	0.06	0.02
	D	54.5	62.14	30.16	25.4	20.79	16.45	0.78	0.04	44.05	55.01	0.25	0.28
	E	51.77	57.99	40.04	33.01	25.38	27.38	0.16	0.39	27.45	34.36	0.08	0.61
	Mean	46.43	61.08	50.17	36.20	18.49	19.71	0.31	0.09	24.94	39.85	0.09	0.22
	SD	7.36	2.68	18.62	11.31	4.77	6.98	0.27	0.17	15.25	16.76	0.10	0.24

Whilst the washing steps significantly increased the percentage of events in the main region (B) this was still quite low at 61%, indicating large amounts of debris still present and in particular the dormant spore region (C) consisted of just 36% on average. This was deemed unsuitable for bacterial spore work so further purification steps were undertaken.

3.3.2 Exploring the effect of filtering on spore purity

Despite microscopic analysis of the five spore preparations described above showing a composition of mainly spores and cells, the FCM profiles are complex and indicate the presence of significant quantities of debris in the samples, though this debris is not clear *via* microscopy. When these profiles were compared to those of other researchers it was noted that there seemed to be excessive 'noise' in these samples. Accordingly, it was decided that the samples should be passed through a 0.2 μ m pressure filter to eliminate small debris. The remaining cells and spores were retained on the filter paper and these were scraped off and re-suspended in sterile PBS for analysis (Figure 3.7).

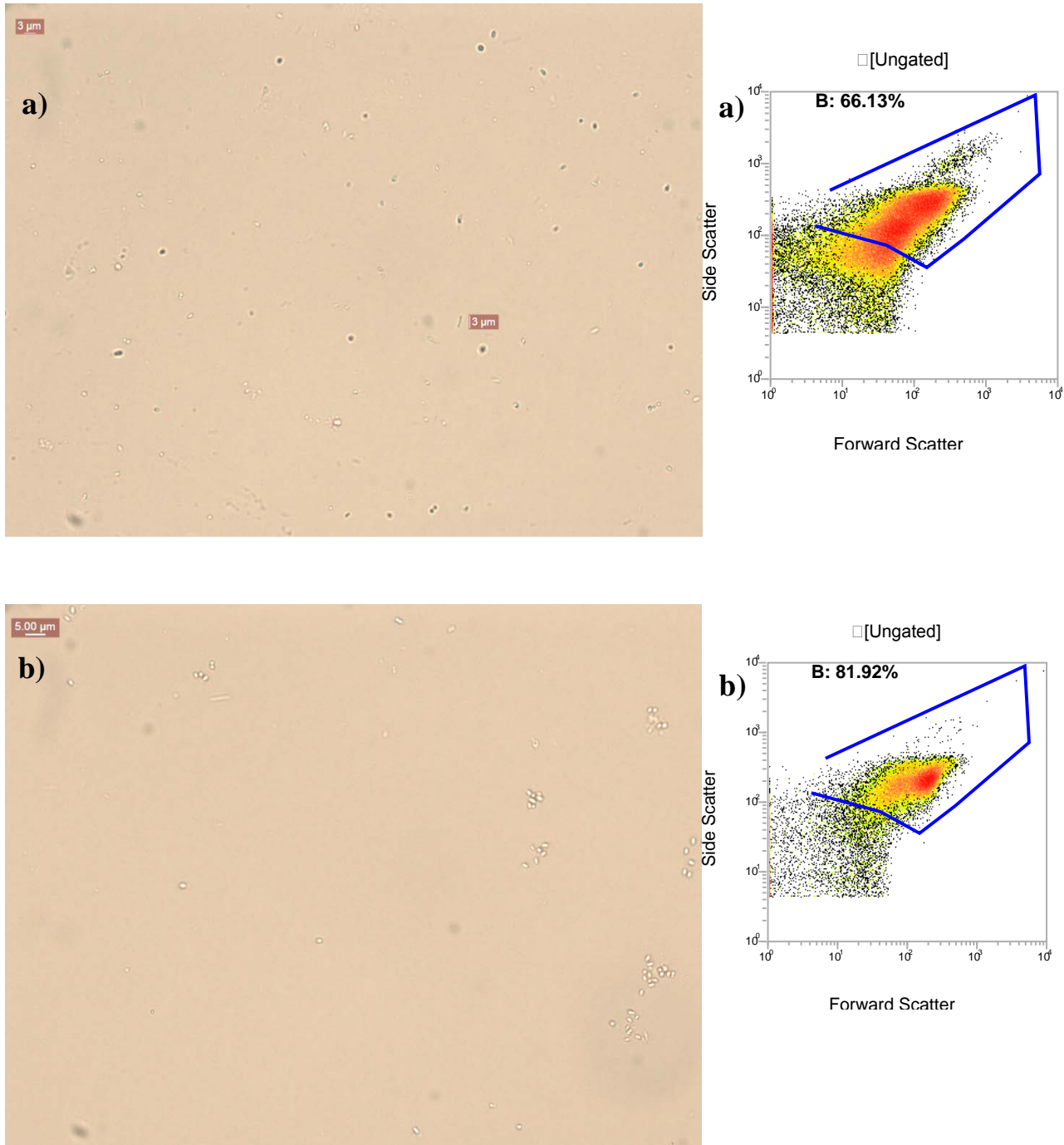


Figure 3.7 Fluorescent microscope output and FCM output of *B. subtilis* spore sample B, showing effect of filtering. a) Top row, left, DIC image using 63x objective before 0.2µm filter and right, FCM FSC vs SSC profile of the same sample, with Region B drawn around the cells and spore population. b) Bottom row, DIC image at 63x magnification post 0.2µm filter and right, FCM FSC vs SSC density profile, with Region B drawn around the cell and spore population for sample B.

In this example filtering definitely removes about 16% of the debris, where the initial percentage of events in region B was 66%, the filtering increases this to 82%. However, the spores are more sparsely distributed under the microscope, indicating a loss of cells and spores through the filtering process. The spores also appear to be forming aggregates. The same filtering process was carried out on the remaining samples (A, C-E) the FCM profiles and microscopic images are presented in Appendix 2, and the mean percentage of events in Region B is summarised below in Table 3.2.

Table 3.2 Average percentage of events in region B before and after 0.2µm filtering. Region B corresponding to that drawn in the FCM profiles in Figure 3.7. Mean values in bold.

Region B		
Sample	Before filter	After filter
A	70.12	59.44
B	66.13	81.92
C	66.29	73.67
D	62.14	68.2
E	57.99	61.51
Mean	64.53	68.95
SD	4.62	9.18

Whilst a clear improvement in the level of debris is observed following filtration in sample B and C, the results from sample A, D and E suggest filtering has not had any impact on the levels of debris present in the samples, with the percentage of events in region B (main cell and spore population) remaining close to 65%.

To conclude, despite the fact that filtering does sometimes reduce the amount of debris present in the samples, this is associated with a vast reduction in spore number and increased aggregation, thus it isn't suitable for mass production of dormant spore stocks.

Furthermore, this method is unsuitable for spore purification, as filtering cannot separate spores from cells.

3.3.3 Manganese supplementation

Accordingly, another strategy was employed in an attempt to increase spore stock purity, whilst also increasing the yield. Following a review of literature concerning spore purification strategies, a paper by Verma *et al.* (2013) exploring various media on *B. megatarium* sporulation used AK sporulating agar supplemented with MnSO₄. Manganese supplemented agar is also part of the SOP for the US Environmental Protection Agency Office of Pesticide Programs and the US army research facility for production of *B. subtilis* spores (Smith *et al.* 2011).

AK agar plates were made as described previously and supplemented with 200µl of 3.4mM MnSO₄ which was spread over the dried plate with a sterile bent glass rod. The spores were analysed by flow cytometry, shown below as Forward scatter vs side scatter density plots.

From the four example profiles illustrated in Figure 3.9, it is very clear that when no manganese is used it is difficult to determine the spore population due to debris signals overlapping with the spore region. However, manganese supplementation clearly reduces the level of debris present making FCM possible. Precision was addressed by recording the number of events in the debris region A and the number of events in Region B for ten samples (from three different preparations) each of manganese supplemented and non-manganese supplemented samples (Figure 3.9).

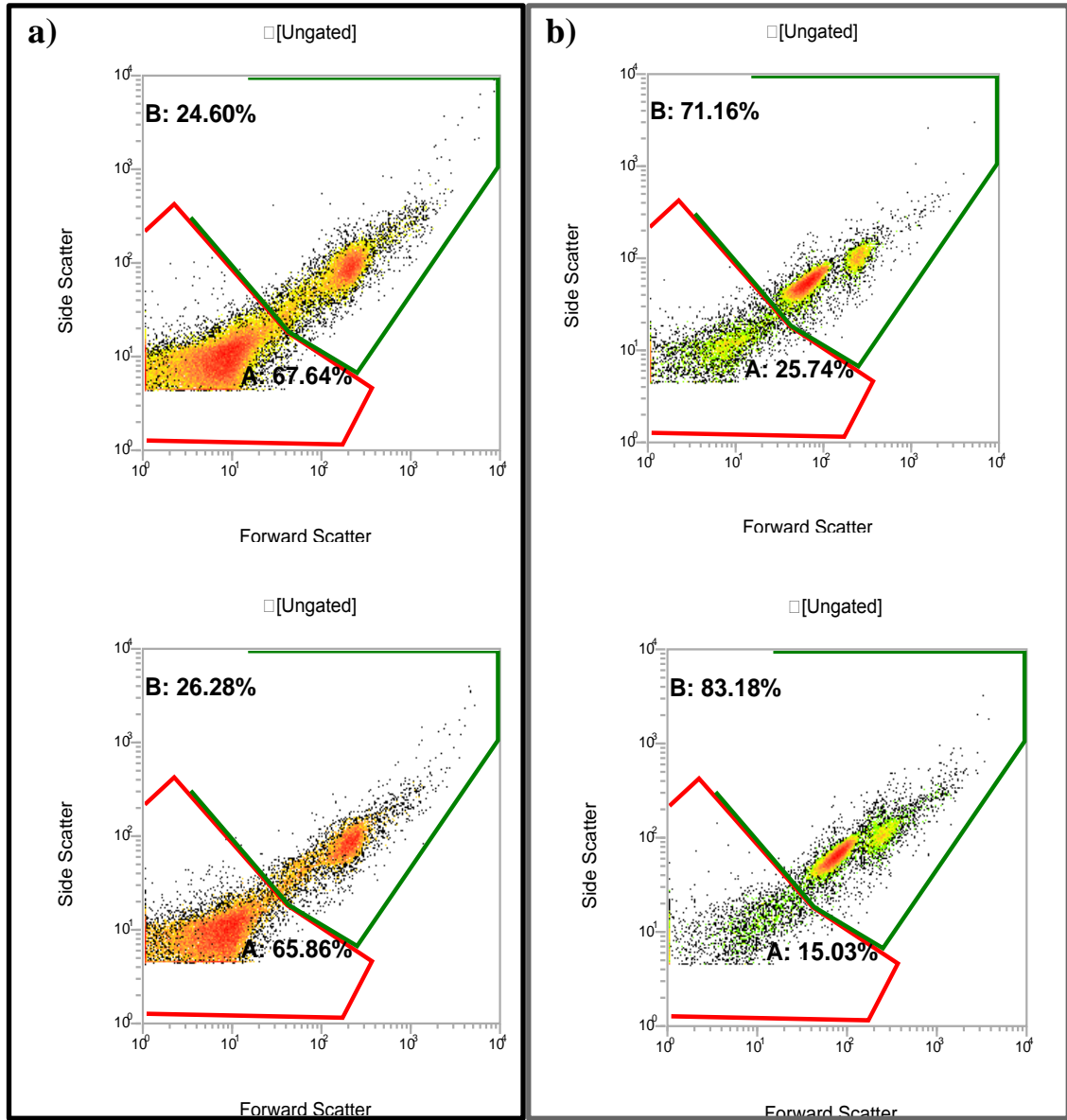


Figure 3.8 Examples of FCM density plot of FSC vs SSC, region A (red) corresponds to debris and region B (green) is the cell and spore location. Column a) *B. subtilis* spores harvested from a normal AK sporulating agar plate and column b) *B. subtilis* spores harvested from a $MnSO_4$ supplemented AK agar plate.

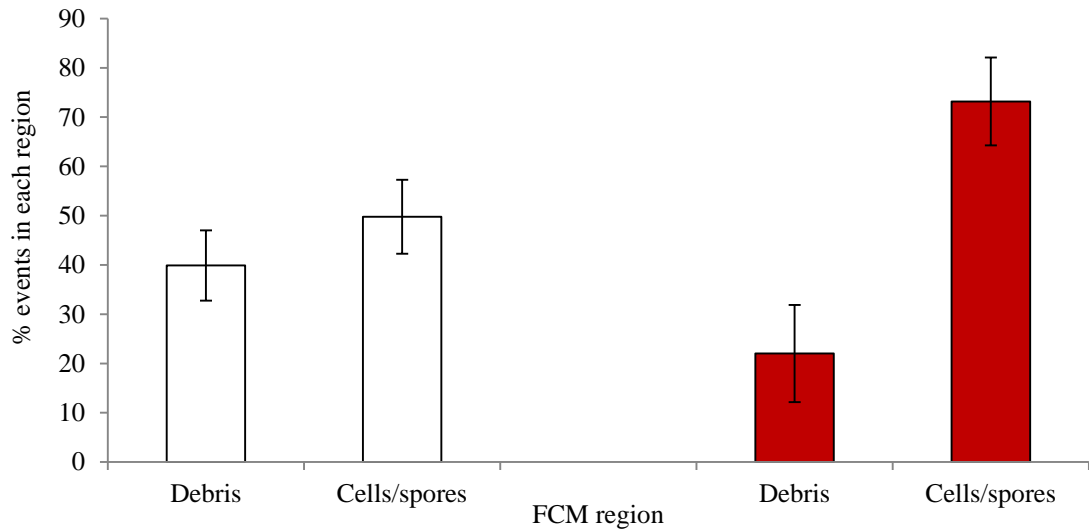


Figure 3.9 Effect of manganese supplementation on the amount of debris present in spore stocks. Debris corresponds to region A on the FCM FSC vs SSC plots and spores correspond to region B of Figure 3.8. White bars show spores grown on AK agar without additional manganese and shaded bars are spores grown on AK agar with 100µl 3.4mM MnSO₄. Error bars represent the 95% CI where n =10.

These results clearly indicate that the addition of manganese improves the quality of FCM profiles by reducing the amount of debris by 18% on average. By reducing the amount of debris present in the sample, the overlap between the ‘noise’ and the regions of interest is reduced, thus making FCM assignments of physiological state more reliable.

Following the results from the FCM analysis, a check was also made using the fluorescent microscope, to see if differences in spore purity could be noticed microscopically. The results are shown in Figure 3.10 and Figure 3.11 using the DIC light at 100x magnification.

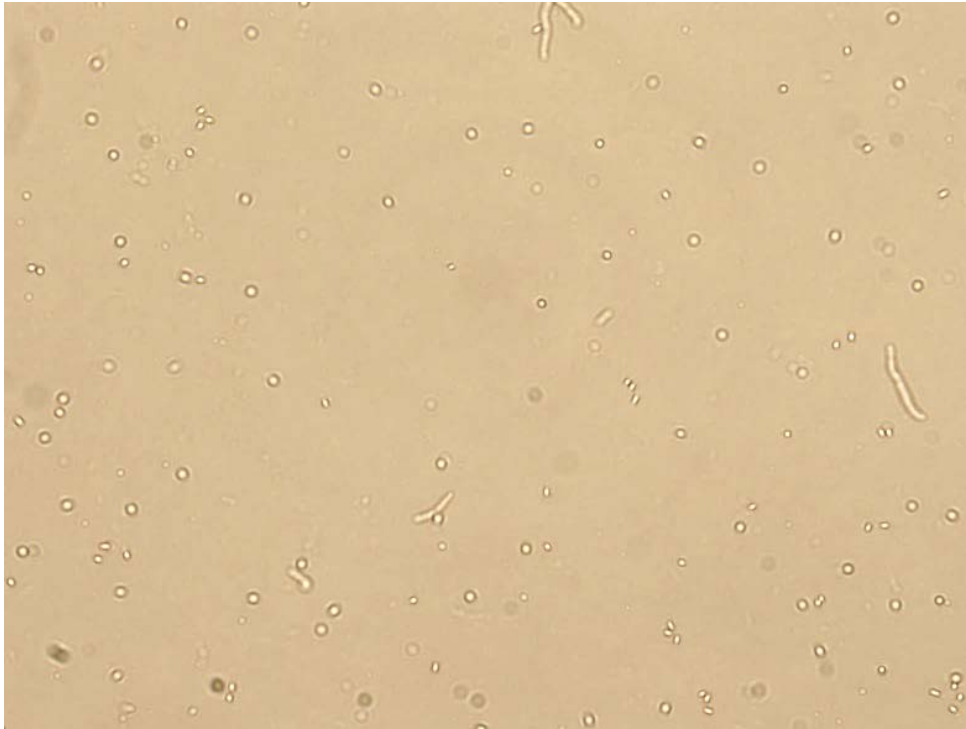


Figure 3.10 DIC image under 100x objective lens of *B. subtilis* spores grown on AK sporulating agar without additional Mn. Representative frame where n=10.

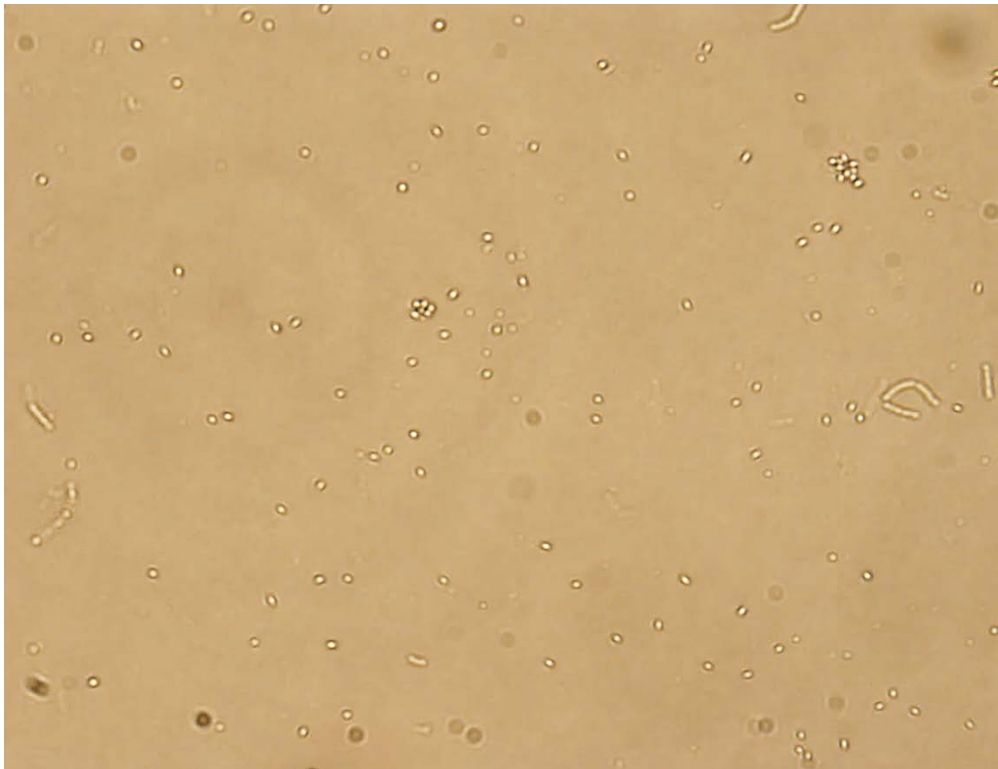


Figure 3.11 DIC image under 100x objective lens of *B. subtilis* spores grown on AK sporulating agar, supplemented with an additional 100 μ l 3.4mM MnSO₄. Representative frame where n=10.

When comparing the images in Figure 3.10 and Figure 3.11 there are no clear visible differences between the samples (five frames taken for each sample in total). Hence, the effect of manganese is only apparent by FCM analysis, and no clear distinction is seen even under the 100x objective lens.

3.3.4 Comparison between spore harvesting methods

Two methods of harvesting spores were used, either scraping the surface with a sterile loop before re-suspending, or flooding the plates with cold sterile water and gently agitating the spore layer. The effect these methods have on both manganese and non-manganese supplemented spores has been analysed by FCM. The assessment between each method was based on the levels of debris compared to the amount of events in the cell/spore region as shown in the representative FCM plot below (Figure 3.12).

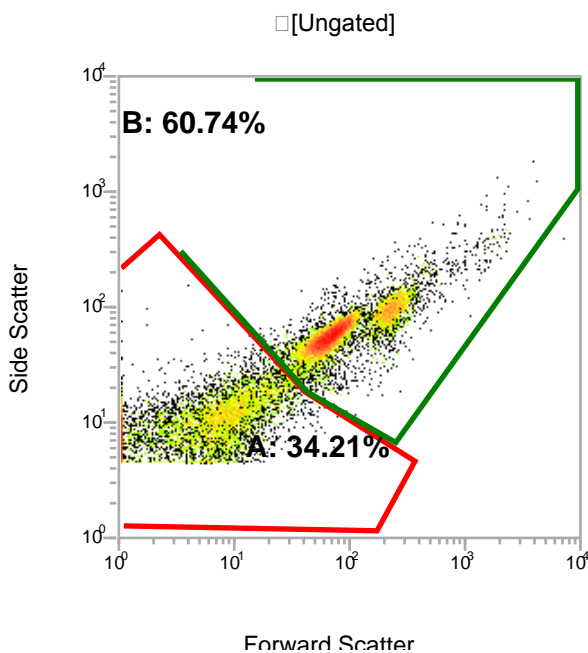


Figure 3.12 Representative FCM density output of manganese supplemented spores on a FSC vs SSC plot. Region A (red) is drawn around the debris or 'noise' population and region B (green) corresponds to the cell and spores area on the plot.

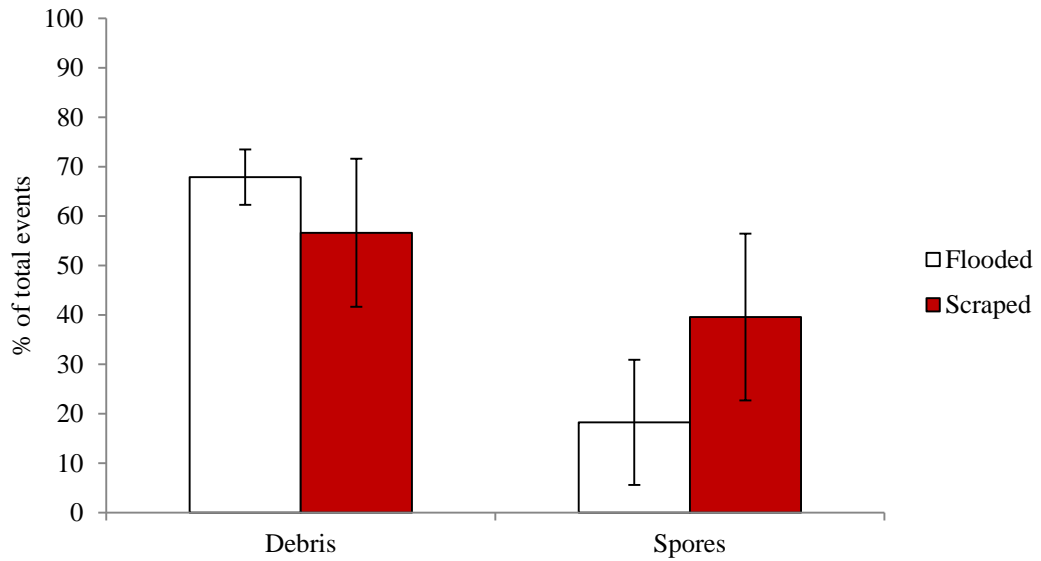


Figure 3.13 The percentage of events that correspond to either debris or spores as shown by FCM FSC vs SSC profiles for non-Mn supplemented samples. White bars indicate flooded samples and shaded bars are scraped plates. Error bars represent the 95% CI where n=4.

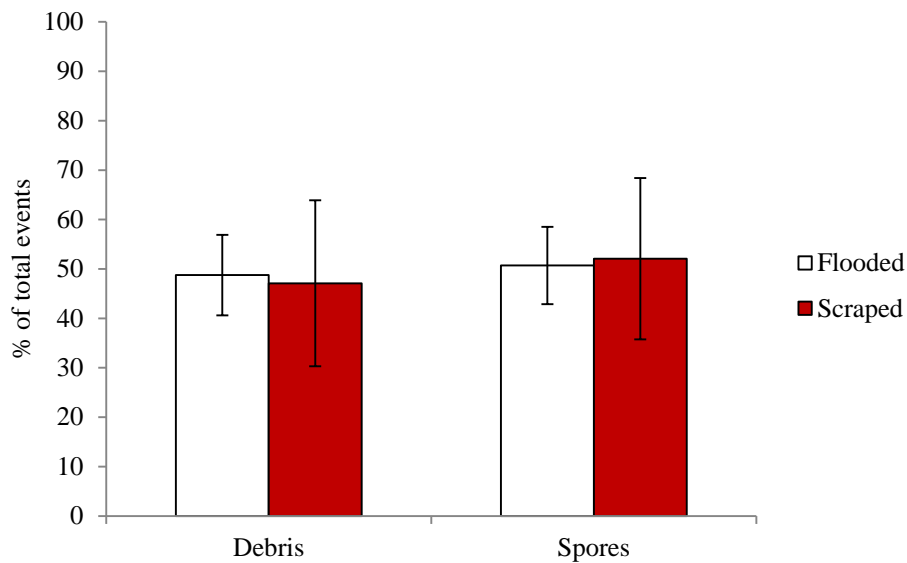


Figure 3.14 The percentage of events that correspond to either debris or spores as shown by FCM FSC vs SSC profiles for Mn supplemented samples. White bars indicate flooded samples and shaded bars are scraped plates. Error bars represent the 95% CI where n=7.

As is evident from the large 95% CI there is no significant difference between either harvesting method irrespective of culture medium (Figure 3.14). As such, the flooding

method was selected for further studies as this was a far more rapid method and eliminated the problem of puncturing the agar which would obviously lead to small amounts of the agar becoming deposited in the spore sample.

3.3.5 Alternative sporulation media

Finally, given that DSM culturing medium is frequently used by other researchers, a sample of spores prepared in this medium according to the method described by Nicholson and Setlow (1990) detailed in Appendi. These were analysed under a fluorescent microscope and *via* FCM following staining with 1.5uM Syto 16 and 48uM PI.

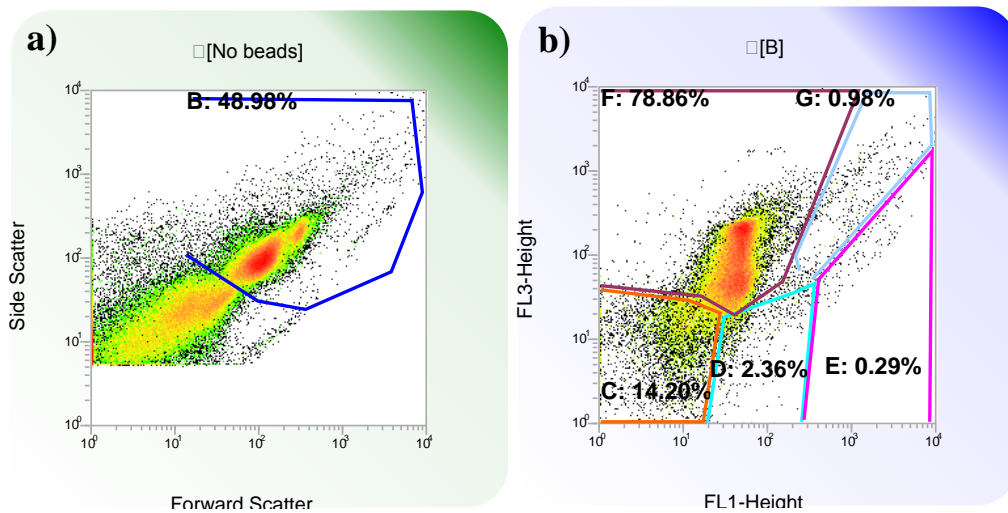


Figure 3.15 Typical example of FCM profiles for spores produced in DSM broth. a) shows density plots of FSC vs SSC where Region B (blue): cell and spores region b): Gated on Region B, region C (orange): dormant spores, region D (turquoise): germinating spores, region E (pink): Live cells, region F (burgundy): dead spores and cells, region G (light blue) cell doublets.

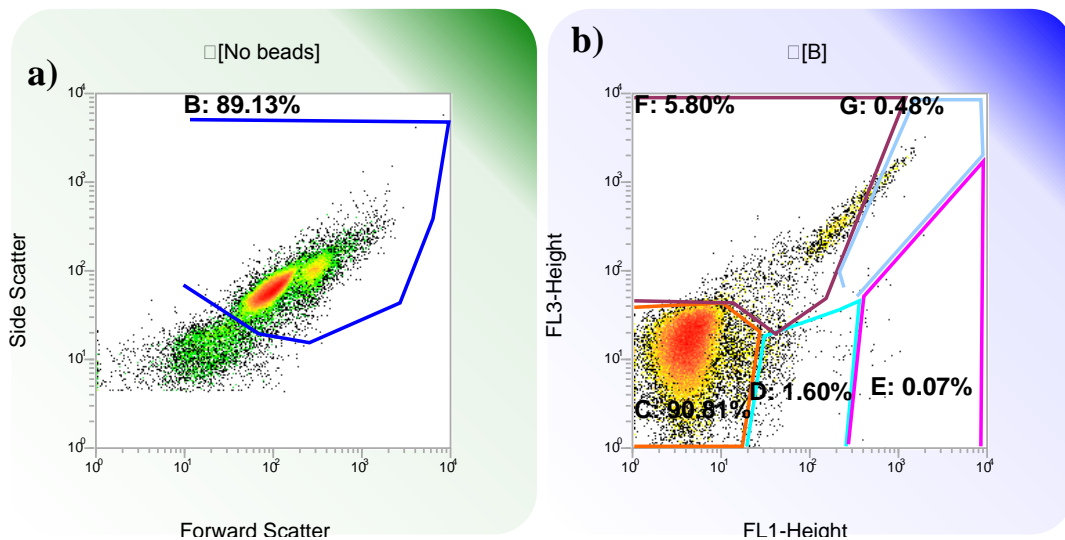


Figure 3.16 An example of typical FCM profiles for spores produced *via* AK sporulating agar. a) shows density plots of FSC vs SSC where Region B: cell and spores region, b) Gated on Region B, region C (orange): dormant spores, region D (turquoise): germinating spores, region E (pink): Live cells, region F (burgundy): dead spores and cells, region G (light blue) cell doublets.

As is clear from the FCM profiles, the spores produced in DSM, Figure 3.15 appear far less resistant to the EtOH washes than those from AK agar in Figure 3.16, meaning they have taken up a lot of the nucleic acid dye. The majority of these spores are either in the dead spore region, (which could also indicate immature spores, as there is little chance of dormant spores being killed during the sporulation process) or in the dead cell region, indicating remaining non-sporulated cells which are susceptible to the EtOH washes. A check was made on these spores under a fluorescent microscope (Figure 3.17) to further verify the physiology of the spores matched the FCM profile. The reasons for these differences in levels of susceptibility are currently not known

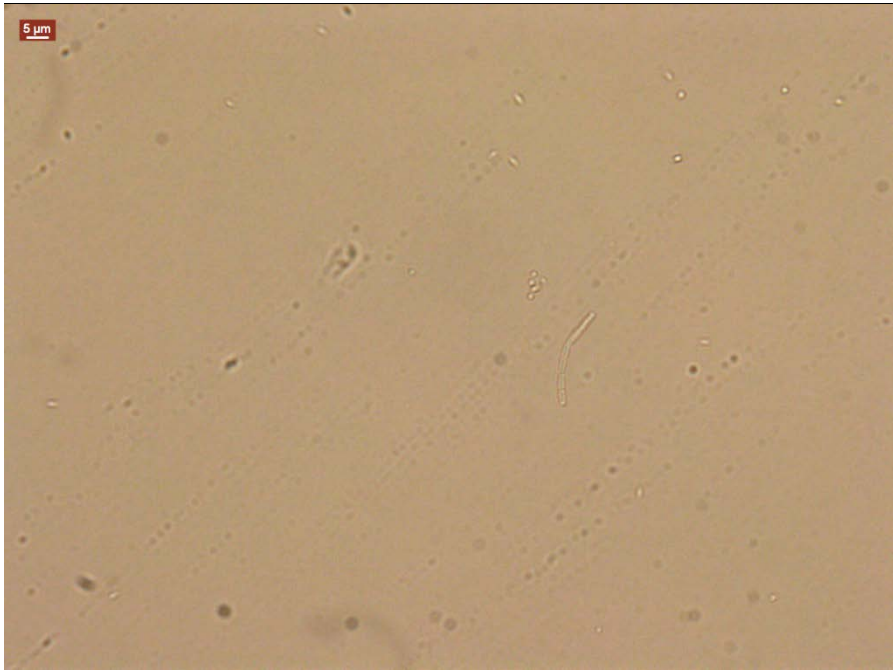


Figure 3.17 *B. subtilis* spores produced using DSM medium. DIC light under 63x objective lens.
Representative image where n=7.

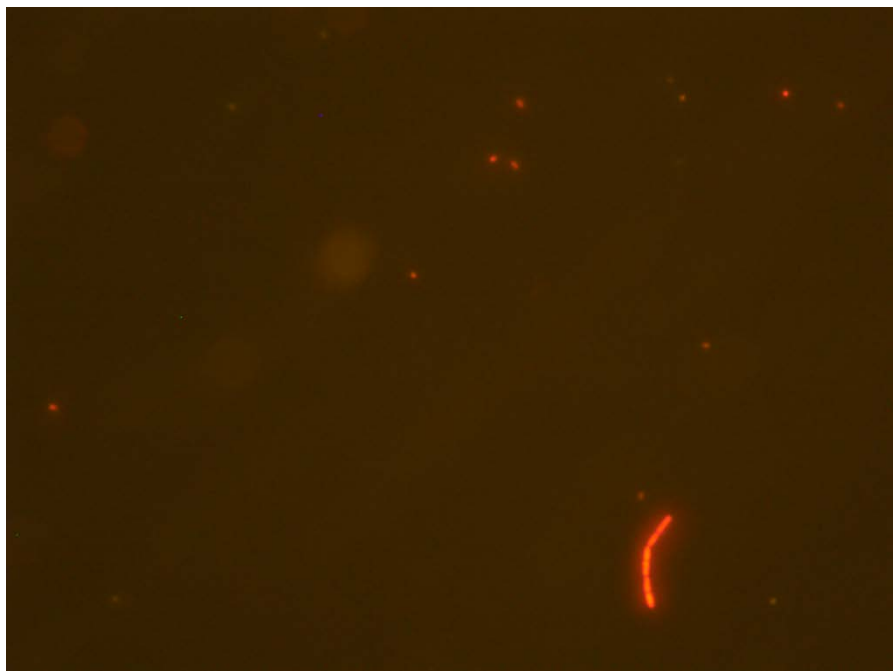


Figure 3.18 Double stained *B. subtilis* spores produced using DSM medium. I3 light under the 63x objective lens. Representative image where n=7.

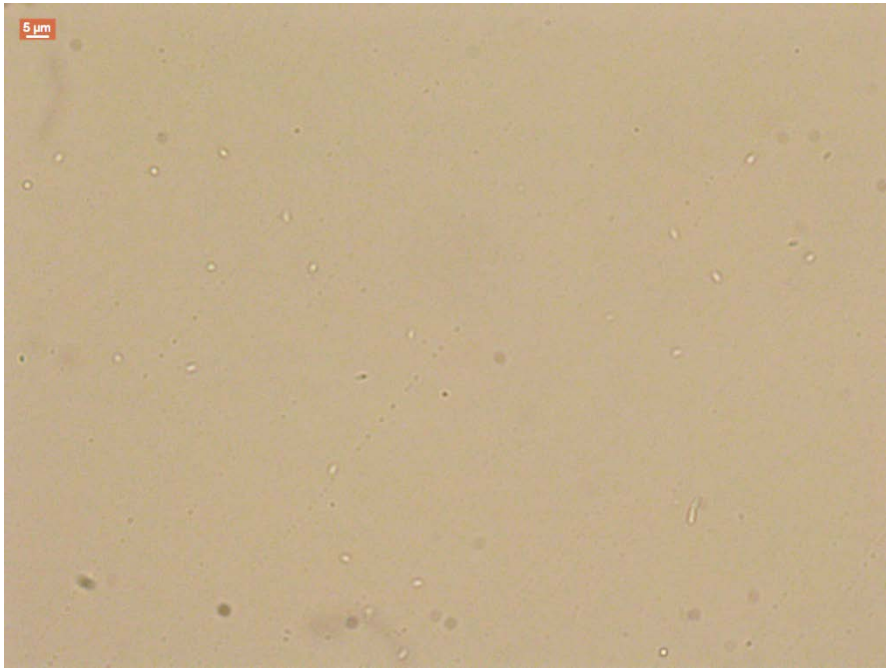


Figure 3.19 *B. subtilis* spores produced using DSM medium. DIC light under the 63x objective lens. Representative image where n=7.

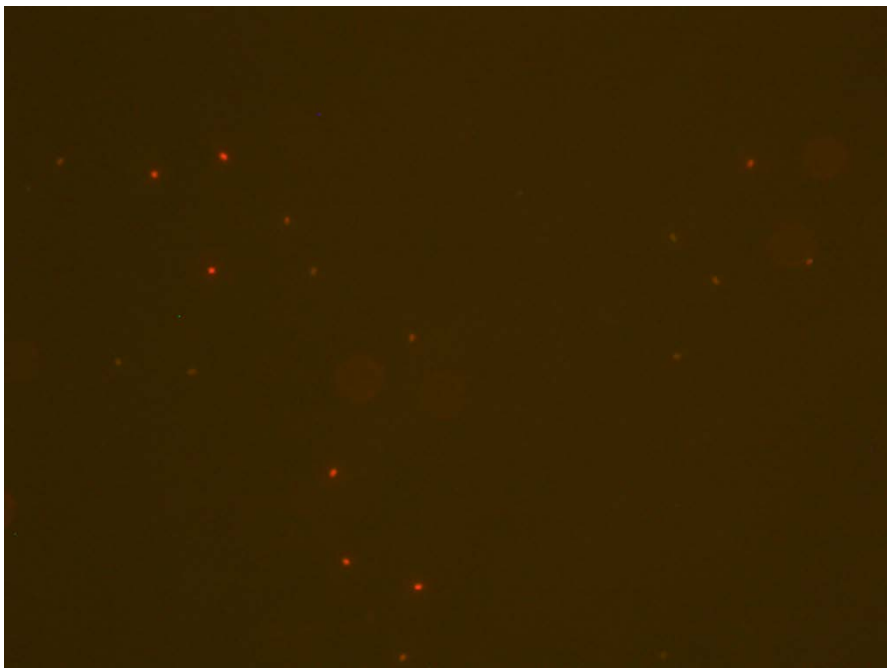


Figure 3.20 Double stained *B. subtilis* spores produced using DSM medium. I3 light under the 63x objective lens. Representative image where n=7.

As is clear from the image in Figure 3.20 many of the spores stained with PI, indicating they were no longer viable. In Chapter 5, cell sorting was done on PI stained cells and spores and yielded no growth on LB agar plates. Another key point with spores made using DSM broth

is that the yield produced in a large conical flask was very low in comparison with the number of spores produced *via* AK agar.

3.4 Conclusion

Given the five parameters investigated in this chapter, it was concluded that the optimum method for producing spores was to use AK agar, supplemented with 100µl 3.4mM MnSO₄. Harvesting using cold sterile and 0.2µm filtered water was the preferred method, and to purify, a 50% EtOH wash followed by at least three more washes in 0.2µm filtered H₂O. To gain spores of a high quality, spores were left refrigerated in sterile filtered H₂O for at least two more days before being used. This was thought to lyse any remaining vegetative cells. Prior to any experimentation, spores were centrifuged at 5,000 rpm for at least five minutes and re-suspended in cold sterile 0.2µm filtered PBS. This produced spores with a good quality (>90%) illustrated below in Figure 3.21.

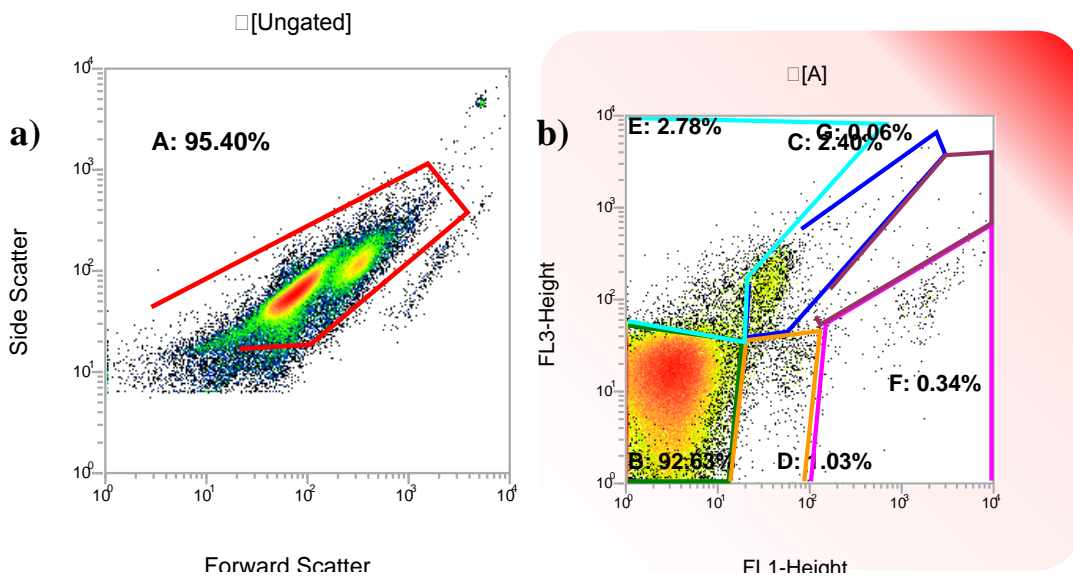


Figure 3.21 VenturiOne output for *B. subtilis* spores produced on manganese supplemented agar, following 50% EtOH treatment and multiple washes, a) density plot of FSC vs SSC, region A (red) drawn around the cell/spore area. b) density plot gated on region A of FL1 (Green) fluorescence vs FL3 (Red) fluorescence, Region A (red): cells and spores, region B (green): dormant spores, region C (blue): dead spores, region D (orange): germinating spores, region E (turquoise) dead cells, region F (pink): Live cells. Region G: double stained cells. Representative output where n=5.

3.4.1 Selection of sporulation medium

AK sporulating agar was preferable to DSM medium owing to the fact that many spores from DSM medium stained with PI, indicating the inner membrane has been damaged, likely causing these organisms to lose viability. Another reason AK agar was selected was that greater yields of spores could be produced. This corresponds with the study carried out by Smith *et al.* (2011) where agar was preferable to broth for all sporulation compositions studied.

3.4.2 Supplementation with Manganese

The significant difference in spore yield with the addition of MnSO_4 to the agar plates stems from the fact that without manganese, spores cannot be produced (Charney *et al.* 1951). Mn^{2+} acts as a cofactor with the enzyme phosphoglycerate phosphomutase. This glycolytic enzyme is needed for optimal spore production, as it ensures maximum use of carbohydrates. Without this enzyme, there is a build-up of 3-phosphoglyceric acid (3PGA) in the cell, which prevents carbohydrate uptake. This occurs before the first stage of sporulation, meaning the asymmetric septation does not occur in the cell (Oh and Freese 1976; Vasantha and Freese 1979). Whilst AK sporulating agar does contain manganese, the results from this study indicate that additional supplementation is necessary to ensure a suitable level of sporulation.

3.4.3 Assessment of spore purity

Harrold *et al.* (2011) point out that there are no standard procedures for assessing spore purity (i.e. dormancy, lack of debris) and yield, therefore many researchers do not have an accurate means to assess their spore stocks. Traditionally, spore purity has been checked using an optical microscope, and the number of phase bright spores counted until a suitably high level of spore purity is attained (usually >90%). Other researchers check spore yield by applying a heat treatment, and plating out the suspension before and after heat

treatment to estimate dormant spore numbers. This is a very lengthy procedure, thus in the research undertaken in this section, a far faster means of checking spore purity is to use FCM, and stain the samples with Syto 16 and PI. By performing this on a small sample, the purity can be assessed far more readily, and without the need for manual counts.

The approaches taken in the production of dormant spores are sound and thoroughly researched. One option to further purify the spore stocks would be to use Percoll gradients. This separates the cells from spores based on the different density of spores and cells. Unfortunately, Percoll gradients are not sensitive enough to resolve the tiny changes in density between spores and germinating spores so these physiological states cannot be separated using this method (Carrera *et al.* 2008). However this would be a good option to remove debris.

None-the-less, with these procedures in place to make good quality high purity spore stocks, work could progress to explore the impact of various different conditions on both spores and cells of *B. subtilis*.

4 Chapter Four: Assessment of the impact of antimicrobials and other microbiocidal treatments on *B. subtilis* cells and spores.

4.1 Introduction

With the ability to produce dormant spores with high purity (Chapter 3), and the FCM methodology in place (Chapter 2), the next stage was to explore how well the FCM could monitor the viability of *B. subtilis* cells and spores, following various different treatments.

4.1.1 Enumeration using counting beads

As stated previously, the use of flow cytometry as a quantitative tool remains an underused application. Uptake might be limited because viability estimations from FCM are often higher than plating results, meaning comparative studies may not show a strong agreement, and a higher bacterial recovery could mean there is a risk of over-prescribing antibiotics (Gunasekera *et al.* 2000; Keserue *et al.* 2012). However it could be argued that when assessing the effectiveness of an antimicrobial agent it may be better to overestimate cell survival in certain cases. Otherwise one would risk not sufficiently decontaminating a surface or wound and therefore potentially risk infection. For example Khan *et al.* (2010) used FCM to enumerate the numbers of theoretically living but non-culturable cells. Briefly, viable but non-culturable (VBNC) cells still exhibit metabolic activity, though they do not form colonies when plated (Ramamurthy *et al.* 2014). The advantage of using a method to analyse the staining properties of these cells is that they would still exhibit fluorescence when stained with Syto 16, assuming they still had an intact membrane to exclude PI as described in Table 1.1 in Chapter 1.

FCM-based quantitation is internally calibrated through the use of a known density of counting beads added to the sample, which allows cells to be enumerated ratiometrically. Whilst FCM enumeration has been used on cultures of *B. subtilis* before (Paulse *et al.* 2007;

Leser *et al.* 2008), the method has not been applied to the discrimination of specific sub populations/physiological states.

4.1.2 EtOH as a method of cell killing without activating spore germination

A key requirement for this study is a methodology that can be used to enumerate cells and spores of *B. subtilis* in complex mixtures. The established traditional methodology involves heating samples before plating (van Melis *et al.* 2011a). This treatment effectively kills vegetative cells but has a negligible effect upon spore viability, meaning only the spores will generate colonies on agar plates to be counted. On comparison with an identical but non-heated sample, the proportions of spore and cells in the *B. subtilis* suspension are revealed. However, it may be difficult to find a suitable temperature and treatment time that will effectively kill off all cells whilst leaving spores unaffected.

To confirm the results of such experiments there is a need to compare FCM with plating (the standard method in microbiological research) and direct counting using a Petroff Hausser haemocytometer.

A range of timings between 10 and 20 minutes have been reported for efficient cell killing at 80°C (Cronin and Wilkinson 2007; Mathys *et al.* 2007). The discrepancies between the heating conditions in the literature, suggest the need for experimentation prior to adopting a time and temperature protocol for effective cell killing, in the presence of spores.

To get the most accurate plate-counts possible for spores, it is necessary to completely prevent growth of vegetative cells present in the inoculum. However, temperatures around 80°C are close to levels that could damage or even kill spores; for instance, Jagannath *et al.* (2005) held spores at 89°C for 20 minutes causing a 0.5 log₁₀ reduction in spore number.

Furthermore, it is typical for spores of *B. subtilis* to be heat activated before germination. This heat activation is usually 70°C for 30 minutes which would kill off remaining vegetative cells and prematurely germinating spores (Yi and Setlow 2010; Zhang *et al.* 2011a). As the temperatures stated for killing cells exceeds this, it is very likely that

when spores are then returned to more favourable conditions, they may start to germinate and then subsequently be killed should the conditions become hostile.

As such, an alternative means of killing cells and leaving spores unharmed was investigated. Zhao *et al.* (2008) used 50% EtOH to purify spore populations by killing vegetative cells. It was thought a similar method to kill vegetative cells and leave the spores unaffected could be employed in this study.

4.1.3 Antimicrobials used and their effect on *Bacillus subtilis*

It is important that the methodology developed in these studies can be applied to the study of bacteria subject to a range of conditions. *B. subtilis* can be a safe model for the study of more dangerous organisms such as *B. cereus* and even *B. anthracis* (Harwood 2001). A highly relevant issue in bacterial spore research is that of industrial contamination. Food spoilage is a common issue affecting shelf life of processed foods. Antimicrobials offer a good solution and may help to increase the shelf life of foods. Common antimicrobials such as peracetic acid (PAA) and Chlorine are known to have strong bactericidal effects on *B. subtilis*, however, they can cause irritation to skin and eyes, and irritate the respiratory mucosae when inhaled (Herruzo *et al.* 2010). Natural antimicrobials such as green tea extract offer a safe alternative to this.

Industrially, one of the main problems with *Bacillus* biofilms is the fact that they are extraordinarily water-resistant, with a water repelling potential that exceeds Teflon. As such, it is very difficult for antimicrobials to be effective against biofilms as they cannot penetrate into the biofilm (Epstein *et al.* 2011).

Many industrial settings operate at low temperatures throughout the year (i.e. dairy, meat factories). This can be a problem as generally, antimicrobials are more effective at higher temperatures, largely due to increased movement of particles meaning the antimicrobial agents can come into contact with more bacteria (Huang *et al.* 1997). It is therefore important to find agents that can decontaminate surfaces at low temperatures.

4.1.3.1 Chlorine

Chlorine is a moderate oxidizing agent. It can penetrate the walls of bacteria causing the cytoplasmic membrane to be destroyed, meaning it is permeabilised (Virto *et al.* 2005). This leads to inhibition of bacterial respiration, mainly phosphotransferase is inactivated (Huang *et al.* 1997). The reaction that takes place is shown in Equation 4.1.

Equation 4.1 Action of sodium hypochlorite in water.

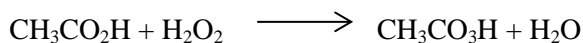


Chlorine is capable of oxidizing the peptide links of proteins and hence denatures them (Maris 1995). The microbial enzyme, glucose oxidase is destroyed by chlorine too, meaning its enzymatic activity is lost, so the glucose oxidation system is further impaired. As glucose breakdown is essential to all cells, the inhibition of glucose oxidation parallels the rate of cell death (Knox *et al.* 1948). It is worth noting that a lower pH will increase the antimicrobial activity of chlorine, and that a higher concentration of bacteria will require more chlorine to achieve effective killing (Knox *et al.* 1948; Huang *et al.* 1997).

4.1.3.2 Peracetic acid

Kitis (2004) describes PAA as an oxidizing agent with an oxidation potential higher than that of chlorine. It is the peroxide of acetic acid, and hence combines the active oxygen of the peroxide within the acetic acid molecule, demonstrated in Equation 4.2 below:

Equation 4.2 Quaternary equilibrium mixture of peracetic acid from Kitis (2004)



Where:

$\text{CH}_3\text{CO}_2\text{H}$ = acetic acid

$\text{CH}_3\text{CO}_3\text{H}$ = peracetic acid

H_2O_2 = hydrogen peroxide:

It releases active oxygen, which disrupts sulfhydryl and sulphur bonds in proteins, enzymes and other metabolites, meaning they are oxidized and double bonds reacted. This means important components in cells and membranes are broken by oxidative disruption (Block 2001). It is suggested that PAA disrupts the chemiosmotic function of the cytoplasmic membrane and transport through dislocation or rupture of cell walls. It acts on DNA, as well as intracellular enzymes, affecting biochemical pathways and active transport across membranes. Importantly, PAA is protein denaturing, therefore it can attack spore coats (Kitis 2004).

Industrially, PAA has been shown to be a better decontaminant than chlorine due to its environmental safety, as unlike bleach, PAA does not break down into harmful substances (Kunigk and Almeida 2001).

4.1.3.3 *Green Tea extract*

Green tea is believed to have antimicrobial effects due its tea polyphenols. In particular the flavonoid: epigallocatechin-3- gallate (EGCG), has been shown to have anti-tumour, antimicrobial, anti-inflammatory and anti-allergen properties and encourage the migration of smooth muscle progenitor cells to the cardiovascular system after injury (Gordon and Wareham 2010; Park *et al.* 2014b). It is particularly effective against Gram positive bacteria (such as *B. subtilis*) and has been shown to be effective against methicillin-resistant *Staphylococcus aureus* (MRSA), meaning it could be a novel disinfectant in a medical setting (Gordon and Wareham 2010). Its action is derived from the generation of hydrogen peroxide (H_2O_2) which inhibits the function of several membrane proteins in the cell envelope (Nakayama *et al.* 2015). The resulting irreversible damage to the bacterial cytoplasmic membrane means the bacteria no longer adhere to the cell membrane, effectively meaning the EGCG acts as an anti-adhesive agent (Lee *et al.* 2009; Sharma *et al.* 2012).

4.1.4 Aims and Objectives

For the present chapter, the following aims were proposed:

- Explore the effect of GTE, PAA and Chlorine on the viability of *B. subtilis* cells *via* plating and FCM
- Explore the impact of heat treatments and EtOH treatments on cell and spore mixtures and analyse *via* plating and FCM
- Compare the results of plating, FCM and PH

4.2 Materials and Methods

4.2.1 Antimicrobial treatments

Cells and spores were cultured as described in Chapter 3, Section 3.2 and 1 ml aliquots of cells were taken for each experiment. Treatment of cells with antimicrobials was carried out using 50ppm of PAA, 100ppm of Chlorine (Sodium hypochlorite from a household bleach), and 40ppm of Green Tea extract (GTE, green tea extract powder, Myprotein, UK) (a novel antimicrobial). Each sample was subject to a five minute treatment time with the antimicrobial in an ice box (<4°C) which was continuously shaken to mimic refrigerated conditions. Following this treatment, the samples were diluted 1 in 10 in sterile filtered PBS. It is important to note that centrifugation of the supernatant was not possible for these treatments as the particles of the green tea form pellets at the same force as the cells.

As well as the antimicrobial treatments, a heat activation was also carried out for 35 minutes at 85°C on a sample of dormant spores, a sample of vegetative cells and on a sample containing a 1:1 mixture of cells and spores. One sample of spores and cells were left on ice without any treatment, to act as a control.

4.2.2 Plating

LB agar plates (15g/L agar, 25g/L LB powder) were dried before use to prevent confluent growth in surface water. Samples of serial decimal dilutions (200µl) were spread using a sterile glass spreader onto the plates, which were then inverted and incubated at 37°C for 24 hours.

4.2.3 Petroff-Hausser counting chamber

A Petroff-Hausser counting chamber with improved Neubauer ruling (ProSource, Canada) was used for enumerating spores and cells of *B subtilis*. The Petroff-Hausser (PH) counting chamber is a specially designed shallow depth (0.01 mm) haemocytometer as opposed to the 0.1mm depth of a normal haemocytometer. A sample of 6µl was transferred onto the viewing plane and the cover slip was applied firmly. To minimise Brownian motion and prevent evaporation the cover slip was affixed with Vaseline.

4.2.4 FCM Enumeration

The following FCM settings were used for the trials under the cytometer 'low' flow rate setting: FSC: E01, SSC trigger 366; FL3 680 FL2: 665. Compensation: FL2 to FL1 50.2%; FL3 to FL2 14.5% FL1 to FL2 0.6%.

10µl of each sample was placed in 440µl of filtered PBS. 50µl of 6µm Countbright beads were added (0.47×10^5 beads per 50µl).

Enumeration was achieved by using 50µl of Countbright Beads in each sample. The counts/ml were then calculated using the following equation from Khan *et al.*, (2010):

Equation 4.3 Calculation of events obtained from FCM to cfu/ml using counting beads

$$\frac{\text{no. of events in cell region}}{\text{no. of events in bead region}} \times \frac{\text{no. of beads per test}}{\text{test volume}} \times \text{dilution factor}$$

FCM data were analysed first through FSC vs SSC plots to determine bead counts and total cell and spore counts. Corresponding data for the measured particles were used to create FL1 vs FL3 density plots to distinguish sub-populations. Counts of cells and spores in the dormant and viable regions were added together to get a total viable count. These were then compared with plate counts which can only show viable counts.

4.2.5 Effect of EtOH on cells and spores

Cells and spores were cultured as described in Chapter 3, Section 3.2. Before spores were used for analysis, aliquots of 1ml were centrifuged at 13,000 x g for two minutes and re-suspended in sterile filtered PBS (100mM, pH 5.5).

Cells and spores concentrations were estimated by measuring the OD₆₀₀ in PBS and diluting to 1.0, equivalent to 1.0 x 10⁸ cfu/ml as shown by Posada-Uribe *et al.* (2015). These concentrations were checked with PH counts. Two x1ml aliquots of 1:1 solutions of cells and spores in PBS were made. One sample was heated at 70°C for 17.5mins (originally suggested as 70°C for 15 minutes (van Melis *et al.* 2011b). However, the come up time was 2.5 minutes therefore time 0 was not started until then).

After heating, the sample was rapidly cooled in ice water. Following this, both samples were centrifuged at 13,000 x g for two minutes. They were then re-suspended in filtered EtOH and vortexed vigorously for 30 seconds. These were then kept overnight in a fridge at 6°C.

Each sample was re-suspended in filtered PBS for FCM analysis. 100µl of each sample was diluted with 84.5µl PBS and were stained with 2µM Syto 16 and 48µM of PI and then kept in an ice box (<4°C). Another set was stained with the same concentrations but kept in pre-warmed microtubes and then incubated at 28°C for 15mintues. After this incubation, the samples were removed and placed in the ice box. To ensure the effect of the EtOH treatment can be seen clearly, a sample of untreated dormant spores and a sample of only dead spores were also analysed.

4.2.6 Statistical analysis of the data collected

The enumeration data from FCM, plating and Petroff Hausser results were subjected to linear regression analysis. The goodness of Fit (R^2) and a and b coefficients of the linear equation were fitted to the data and calculated using Microsoft Excel.

For all data, experiments were run in triplicate (unless otherwise stated) and mean values, Standard deviation, % coefficient variation (%CV) and 95% confidence interval (95%CI) values were calculated using Excel for comparison of available data. Each point on a regression analysis shown represent mean values of triplicate samples.

4.3 Results

4.3.1 Antimicrobial assessment

The results of the antimicrobial treatments were gated on FSC vs SSC plots. This gating was required due to the potential interference of green tea particles, which have a slight orange auto-fluorescence and therefore show up on fluorescent profiles. Figure 4.1 illustrates the FL1 vs FL3 density plots of sample gated according to the cell FSC vs SSC profile. Regions were drawn around each sub-population showing dead cells (F, burgundy), damaged cells of unknown viability (Region G, light blue) and living cells in region E (pink). (No spores were present in this sample so the region assigned for dormant spores may contain unstained debris).

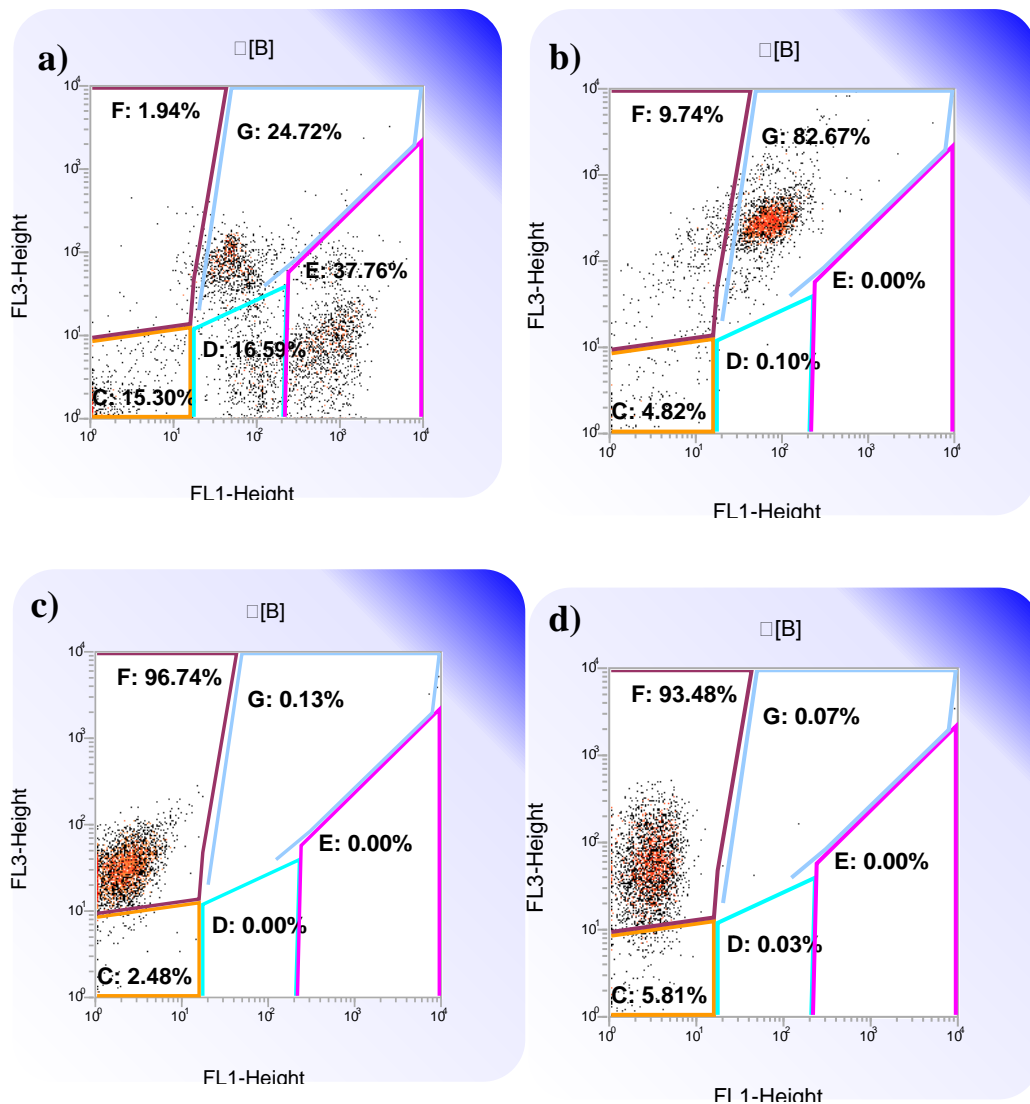


Figure 4.1 FCM density plots showing The FL1 – Height (green fluorescence) parameter against the FL3-Height (red fluorescence) parameter are shown as density plots of *B. subtilis* cells treated with a) untreated, b) Green Tea, c) PAA and d) chlorine. Regions assigned showing dead cells: Region F (burgundy), damaged cells: Region G (light blue), Living cells: Region E (pink), Germinating spores: Region D (turquoise) and Dormant spores (or unstained debris): Region C (orange). All plots gated using equation NOT A to remove beads followed by AND B to examine cells only and omit debris. Representative plots where n=3.

Figure 4.1 shows that chlorine and PAA induce high levels of cells death, with 97 to 98% cell death in each case. Green tea causes 92.18% of cell membranes to become compromised, whilst the untreated cells show 53% viability. The data collected from the density plots was then converted to counts/ml using the formula from Khan *et al.* (2010)

which ratiometrically works out the cell count. These results were then noted in Table 4.1 next to plate counts.

Table 4.1 Various treatments on cells and spores of *B. subtilis* and their viable counts.

Data set description	Enumeration Data			
	FCM		Plating	
	cfu/ml	%CV	cfu/ml	%CV
Spores no treatment (RUN 1)	4.08×10^7	4.2	4.70×10^7	14.0
Spores no treatment (RUN 2)	2.03×10^7	12.3	2.72×10^7	9.0
No treatment on cells grown for 24 hour in LB broth at 35°C	1.27×10^9	5.8	5.08×10^8	17.0
Peracetic acid 50 ppm contact with cells for 5 minutes at 4°C.	0.00	N/A	0.00	N/A
Chlorine 100 ppm contact with cells for 5 minutes at 4°C.	0.00	N/A	0.00	N/A
Cells heated for 85°C for 35 minutes	0.00	N/A	0.00	N/A
Cells and spores mix	2.32×10^8	17.7	1.61×10^8	8.0
Spores heated for 85°C for 35 minutes	2.67×10^8	5.5	1.67×10^8	6.0
Green tea extract 40 ppm for 5 minutes at 4°C	9.63×10^7	7.3	7.20×10^7	5.0
Cells and spores heated at 85°C for 20 minutes	1.01×10^8	0.6	1.61×10^8	8.0

n=3, %CV = Percentage coefficient variation

To better understand this relationship, log counts of the viable cells and spores were plotted to see the relationship between methods in Figure 4.2

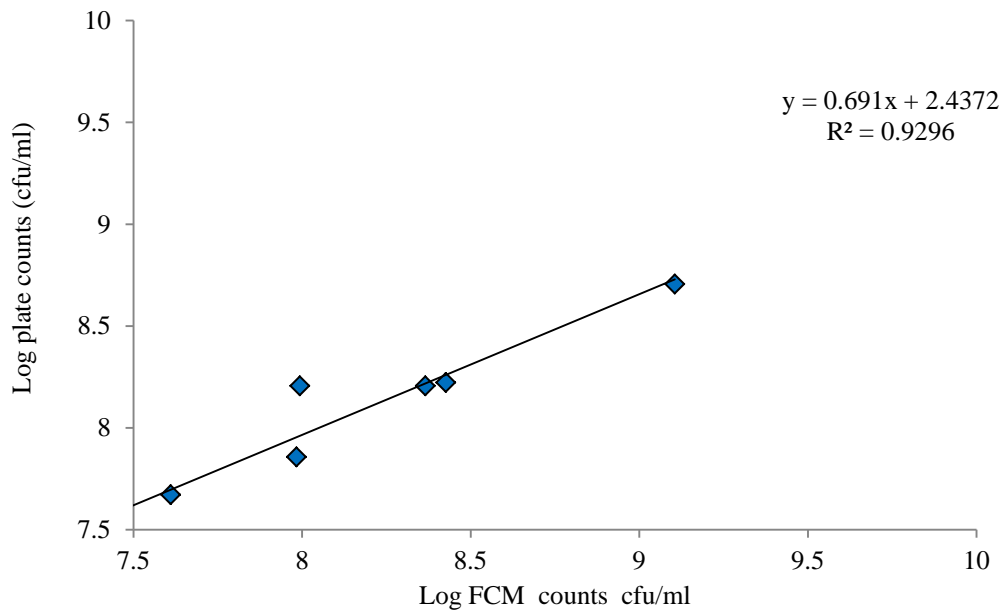


Figure 4.2 Log plate count and FCM count comparisons of various treatments shown in Table 4.1

A linear trend line was fitted to this data to obtain R^2 values, with no intercept set. Table 4.1 illustrates 100% cell death caused by the antimicrobials PAA and chlorine, similarly the heating for 35 minutes at 85°C meant no cell survived. The green tea treatment gave partial cell survival despite a 1.17×10^9 cell/ml drop in cell viability according to the FCM counts and a 4.36×10^8 cell/ml decrease in plate counts from the initial untreated cells grown in LB broth (Table 4.1). For the FCM counts this corresponded to 92.1% decline in viability, whereas for the plate counts this was an 85.5% decrease in viability. The R^2 value of 0.93 indicates a good correlation between the methods.

4.3.2 EtOH as method of cell killing without activating spore germination

The sub-population assignments were based on individual samples of pure populations shown below

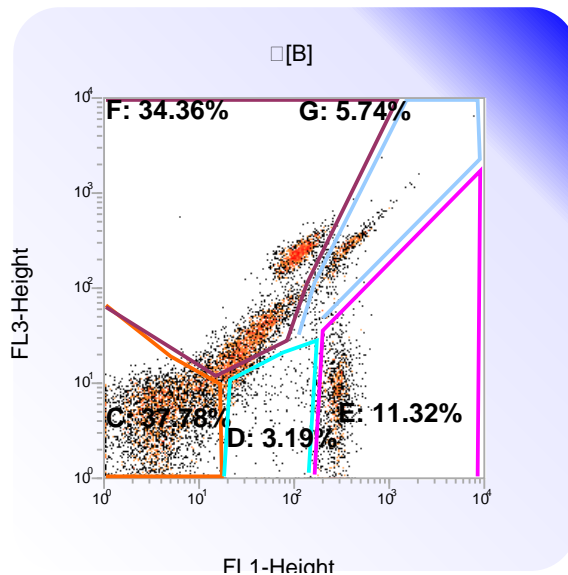


Figure 4.3 FCM density plot of Green fluorescence (FL1-Height) vs Red fluorescence (FL3-Height). Mixture of dormant spores, dead spores, live cells and dead cells. Gated on Region B (not shown, cell and spore region), region C (orange): dormant spores, region D (turquoise): germinating spores, region E (pink): Live cells, region F (burgundy): dead spores and cells, region G (light blue) cell doublets (one live and one dead cell joined together, Representative plot where $n=3$).

Region G in Figure 4.3 was assigned as cells doublets owing to the fact that there was a very high fluorescence on both channels, most likely meaning a dead and live cell were joined together and classed as one event. This may be caused by the presence of undivided growing cells. Though events in this could also indicate sub-lethally damaged cells, i.e. PI has been able to enter the cell but not in a high enough quantity to fully displace the Syto 16.

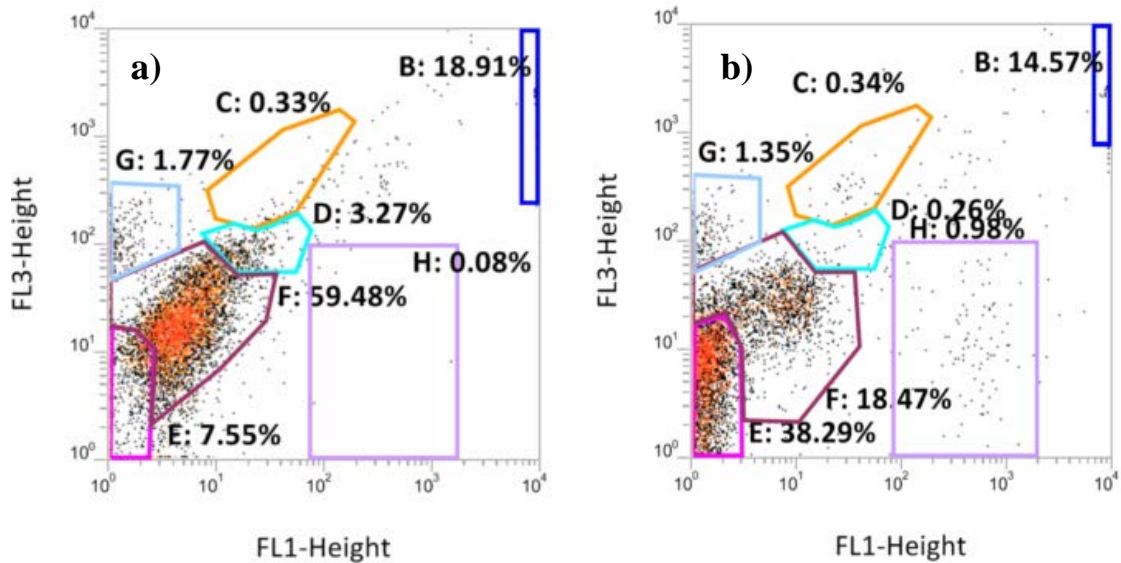


Figure 4.4 FCM density profiles of double stained *B. subtilis* spores. The FL1 – Height (green fluorescence) parameter against the FL3-Height (red fluorescence) parameter are shown as density plots of a) dead spores stained at 28°C and b) Dormant spores stained at 28°C, showing a smaller region of dead spores. Region H (lilac) indicates living cells, region C (orange) dead cells, (high PI staining indicating high DNA content) region D (turquoise) dead cells, region E (pink) Dormant spores, region F (burgundy) dead spores and region G (light blue) unknown sub-population. Representative plot where n=3.

In Figure 4.4 and Figure 4.5, an unknown sub-population was observed, shown as region G (light blue) on the density plots. As this population was only seen in the presence of dormant spores, it could be that these are dead spores.

The dormant spore samples (Figure 4.4) reveals a small population of living cells (region H) which constitutes 0.98% of the total events collected. There is also a small population of dead spores in our dormant spore sample, making up 18.5% of our total events. The dead spore sample (Figure 4.5) shows us a small amount of events in the ‘damaged’ region D. This may indicate cells which had been present in the original spores sample and then killed during autoclaving. In both cases the ‘unknown’ region G populated with 1-2% of events.

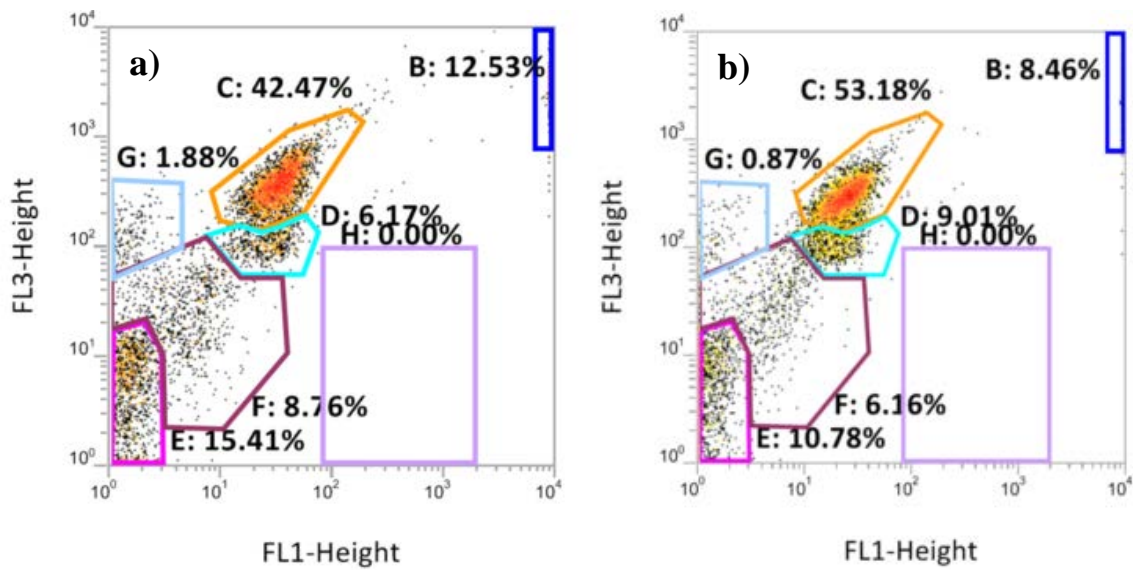


Figure 4.5 a) The FL1 – Height (green fluorescence) parameter against the FL3-Height (red fluorescence) parameter are shown as density plots of a) Heat activated EtOH treated cells and spores, and b) EtOH treated cells and spores (no heat activation). Region B: beads, Region C (orange): Dead cells (high DNA content), Region D (turquoise): Dead cells, Region E (pink): Dormant spores, Region F (burgundy): Dead spores, Region G (light blue): unknown sub-population. Region H (lilac): Live cells and germinating spores. Representative FCM plot where n=3.

In Figure 4.5, the high level of events in region C indicate a large proportion of dead cells, showing the EtOH has effectively killed cells, as there are no events stained with Syto 16 alone. To assess whether the unknown region was attributed to the cells or spores, the cell and spores mixtures were gated based on their FSC vs SSC plots (Figure 4.6). These regions were then used to gate FL1 vs FL3 density plots separately based on whether they were cells or spores (Figure 4.7). This means particles which do not fall into the region of interest are disregarded.

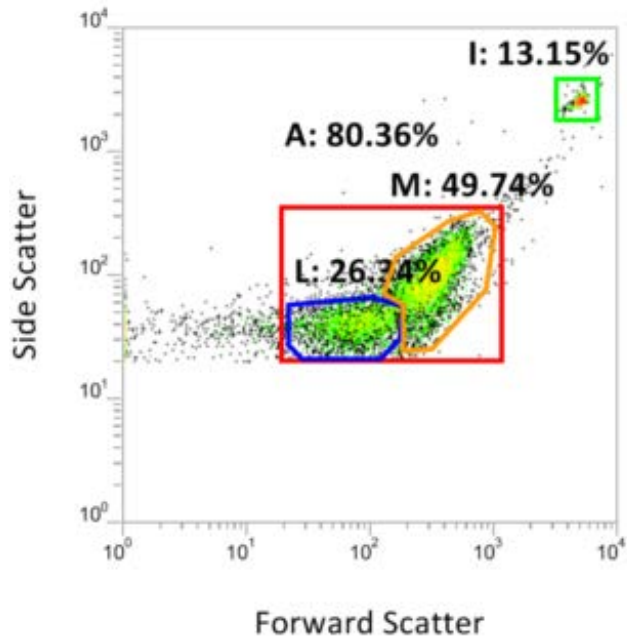


Figure 4.6 Representative forward scatter (FSC) versus side scatter (SSC) density plot of cells and spores heat activated and treated with EtOH. Region L (blue) corresponds to the spores region and region M (Orange) corresponds to the cell region. (Region I in green shows us the bead population) and region A encompasses the cell and spore population. Where n=3.

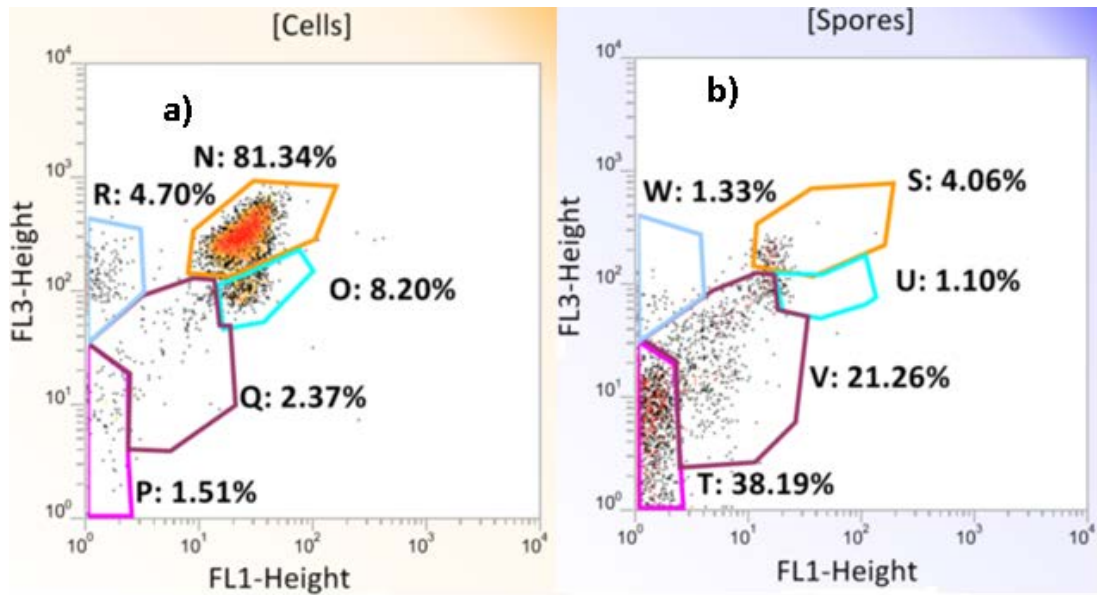


Figure 4.7 Heat activated EtOH treated cells and spores displayed on a) FL1 vs FL3 density plot of gated on the cell region M in Figure 4.6. Where Region N (orange): dead cells, Region O (turquoise) dead cells, Region P (pink): dormant spores, Region Q (burgundy): dead spores, Region R (light blue): Dead spores. b) FL1 vs FL3 density plots, gated on the spore region L from Figure 4.6. Where Region S (orange): dead cells, Region U (turquoise) dead cells, Region T (pink): dormant spores, Region V (burgundy): dead spores, Region W (light blue): Dead spores. Representative FCM profiles where n=3.

The results here illustrate that cells and spores can be at least partially identified based on their FSC and SSC profiles. As shown in the fluorescence plots in Figure 4.7, when considering region M in isolation, or just the cells, the fluorescence intensity clearly demonstrates that these are dead cells, stained with PI and therefore a high FL3 signal. Region L on the other hand is largely composed of unstained particles, correlating with dormant spores which do not stain with either Syto 16 or PI and therefore have little fluorescence.

To check the reliability of this method, plate counts and Petroff-Hausser (PH) Haemocytometer counts were carried out on all samples (Figure 4.4 - Figure 4.7) and results compared *via* linear regression analyses as described in Section 4.3.1.

Table 4.2 Viable counts of *B. subtilis* cells and spores following exposure to different treatments, and different staining conditions. n=3.

Sample	Plates	FCM 4°C	FCM 28°C	PH
EtOH	1.79×10^7	1.99×10^7	8.60×10^6	1.90×10^7
HA*EtOH	1.43×10^7	1.55×10^7	8.54×10^7	1.20×10^7
Spores	2.37×10^7	9.32×10^7	2.02×10^7	3.05×10^7

*HA = Heat activated

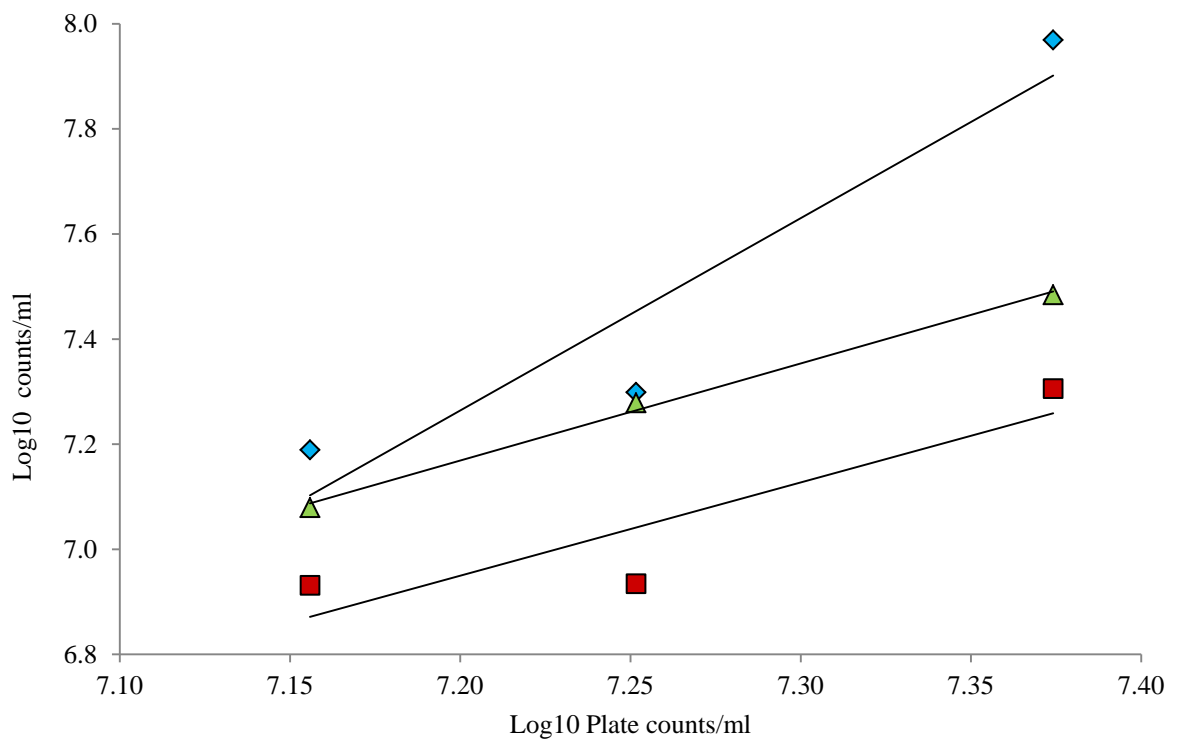


Figure 4.8 Correlation of viable counts shown in Table 4.2 via plating (x axis), Petroff-Hausser haemocytometer (▲) and FCM after staining at 4°C (◆) and 28°C (■). n=3.

Table 4.3 Linear regression analyses of bacterial enumeration methodologies vs culture on agar. equation and R² values for different methodologies against plating

Comparator Method	Equation	R² value
Petroff-Hausser	$y = 1.8477x - 6.1348$	0.9962
FCM at 4°C	$y = 3.6606x - 19.092$	0.8994
FCM at 28°C	$y = 1.7749x - 5.8292$	0.8139

The R² value for the Petroff-Hausser haemocytometer counts suggests a high level of correlation between plating counts and those from this method. The r² value of 0.8 and 0.9 for the FCM counts at 28 and 4°C respectively means there is a slightly lower level of correlation between these counts and plating, however since the trends in terms of increase in counts is still the same the two methods can complement each other.

4.4 Discussion

4.4.1 Antimicrobial investigations

The antimicrobials PAA (at 50ppm) and Chlorine (100ppm) both had a very efficient cell death rate, resulting in no plate counts, and no significant living counts for FCM (see Table 4.1 and Figure 4.1). This exceeds the standard 5 log reduction required for confirmation of activity of a product (Block 2001). Previous studies on the susceptibility of *Bacillus* cells to PAA revealed that 100µg/ml (100ppm) PAA was sufficient to cause almost a 3 log reduction in *B. cereus* cell count in just ten minutes (at 30°C) (Ceragioli *et al.* 2010) and a 40ppm treatment resulted in a 3.8 log reduction in *B. cereus* cell counts in five minutes at 22°C (Ryu and Beuchat 2005). Likewise, cells of *B. subtilis* treated for five minutes with peracetic acid/hydrogen peroxide lost 99.5% of viable numbers. The potency of PAA is such that even dormant spores of *B. subtilis* treated with 500ppm PAA suffered a 1.5 log reduction in counts in just five minutes, with visible destruction of the external spore coat layers shown by SEM (Park *et al.* 2014a). As stated in Section 4.2.1, PAA is thought to act by releasing active oxygen or producing oxidized sulfhydryl bonds. These disrupt bacterial cell walls and membranes, as well as targeting enzymes and the base of the bacterial DNA (Kitis 2004)

Similarly, the effects on *Bacillus* cells with chlorine are well characterised, a 50ppm treatment for five minutes at 22°C caused a 4.7 log reduction in *B. cereus* counts (Ryu and Beuchat 2005) showing good accordance with the results presented herein, where a 100ppm treatment caused greater than a five log reduction in count. As with PAA, chlorine is also sporicidal at relatively low concentrations, a 100µg/ml (100ppm) treatment with HCl-based ClO₂ (pH 3.8) reduced the population of *B. cereus* spores significantly ($p \leq 0.05$) within three minutes (Kim *et al.* 2008a). Destruction of bacteria is caused by chlorination of the lipid protein substance in the cell wall, forming toxic chloro-compounds. This results in macromolecular leakage from the bacterial cell (Kim *et al.* 2008b)

Green tea was less effective with a 92.4% death rate in five minutes with 40ppm GTE (Table 4.1). Sharma *et al.* (2012) reported that a minimum inhibitory concentration (MIC) for action against *B. subtilis* was 0.156mg/ml or 156ppm, and Daglia (2012) stated that 100ppm was sufficient to act against 90% of all bacteria. As GTE is not used industrially as an antimicrobial this is still a significant finding, and could be cause for further research to improve the decimal reduction (D) further, possibly by using the ECGC extract directly. However as Sharma *et al.* (2012) states, all the green tea catechins work synergistically, therefore the crude GTE has the strongest antimicrobial power. Indeed a very recent study by Park *et al.* (2014b) has shown that GTE improves skin wound healing and has the potential to prevent local skin infection. More interestingly still, the review by Daglia (2012) noted that GTE compounds were more active against *B. cereus* than vancomycin and tetracycline, and goes on to infer that such compounds could have a positive effect against GIIT diseases.

Another key finding in this research was that the FCM staining profiles indicate that whilst Chlorine and PAA cause cells to fluoresce only on the FL3 channel (indicating PI staining and no Syto 16 staining) the GTE treated cells have a small amount of green fluorescence also, indicating that they might be damaged rather than dead at the time of staining. This suggests that the cell membrane is compromised, however not to the same extent as the PAA and Chlorine treated cells. This is inferred due to the fact that PI displaces Syto 16 when in sufficient enough concentrations (Stocks 2004). If a cell was damaged but not greatly permeabilised, only a small amount of PI could pass into the cell, therefore this may not displace Syto 16. In cells which have severe membrane permeabilisation, the PI would completely displace the Syto 16.

An initial evaluation of the plating and FCM enumeration showed a tendency for FCM counts to be higher (Table 4.1). One could argue this type of result is to be expected as FCM will give counts for viable but non-culturable organism whereas plating will not. However, the r^2 value of 0.93 indicates a proportional relationship between results.

The Coefficient of Variation (%CV) values obtained during these experiments were occasionally above 10% however, Mathys *et al.* (2007) states that they found up to 15% variation in results so this is perhaps a common level of variation. As to truly assess the reliability of this method, more experiments involving different treatments and different mixtures of cells and spores are necessary.

Findings such as these highlight the significance of FCM as a descriptive tool, as plating or fluorescent microscopy would not give us information as to the numbers of damaged cells. It is also relevant when one considers the lack of FCM enumeration data available. To date, only Khan *et al.* (2010) and Leser *et al.* (2008) have used FCM to enumerate sub-populations. However, both these studies involved the use of just one dye, meaning a detailed sub-population enumeration was not possible. Whilst other studies, for example those by Mathys *et al.* (2007) and Black *et al.* (2005) using two stains have used FCM as qualitative tool and inferred results based on their staining profiles.

4.4.2 EtOH as a method of cell killing without activating spore germination

The region of 'unknown' sub-population 'G' is only stained with PI and no Syto 16 at all. As this region is populated in both the cell gated plot and the spore gated plot (Figure 4.7) there are a few possible explanations for this region. It could be that these are dead germinating spores, owing to the fact that the samples consist of mixtures of cells and spores which have been subject to harsh conditions. Alternatively, this region could be populated by cell debris caused by sporulating cells or germinating spores. Only with access to a cell sorter could these ideas be properly explored by examination under a fluorescent microscope. In Figure 4.5 a, the burgundy region 'F' denotes the region of dead spores. In this case, the region is moderately populated, with around 8-9% of total events. One may suggest that the heat activation could have caused early onset germination, followed by EtOH induced death. However Figure 4.5 b shows only EtOH treated cells and spores. As region F is also moderately populated in this profile with 6-7% of total events one can

assume that a moderate level of dead spores was already present in the spore mixture. This is also confirmed by the pure spore sample analysis (Figure 4.4 b)

The results shown in Table 4.2 and Figure 4.8 indicate a very strong correlation of PH and plating, with r^2 value of 0.99, a good level of correlation with 4°C stained samples (r^2 value 0.9) and a moderate correlation between 28°C stained samples (r^2 value 0.8).

4.5 Concluding Remarks

By studying a range of treatments of *B. subtilis*, the use of FCM as a quantitative and qualitative tool is emphasised. It is hoped that this will enable others to use FCM to gain a deeper understanding of the physiological states of bacteria under stressful conditions. Whilst many studies have investigated the effect of pressure on *B. subtilis* spores (Mathys *et al.* 2007; Shen *et al.* 2009), the application of FCM to assess damage to cells by antimicrobials, both novel and conventional, suggests this method could take a far more prominent role in bacterial research in the future.

5 Chapter Five: Assessing germination in *B. subtilis* spores

5.1 Introduction

FCM has the capacity to be an insightful tool for understanding the lethality inducing mechanisms of the GIT on *B. subtilis* spores. Since probiotics must reach the gut in a viable state to assert beneficial effects, information regarding their survival across the GIT is vitally important in the domain of probiotic research.

The gastrointestinal tract (GIT) has evolved to cause high levels of bacterial death during the process of digestion, which is a largely useful mechanism protecting animals and humans from countless potential pathogens consumed. Conversely, this hostile environment could become a hindrance when probiotics are administered, as these beneficial bacteria are also likely to be killed along the GIT. Whilst common probiotic products designed for human consumption attempt to circumvent the issue of low pH by using bacteria such as the acid resistant lactobacilli (Corcoran *et al.* 2005) there has been a shift in the agricultural sector to administer spores of probiotics rather than vegetative cells, since spores are highly resistant to lethality inducing conditions, and perhaps specifically adapted to life in the GIT (Tam *et al.* 2006). This means the spore should be resistant to both strong acids from the stomach and also the effects of bile in the duodenum. As the first major obstacle the spore faces is the stomach acid, this was investigated primarily in this study.

A decline of 75% of the initial probiotic counts administered has been observed in the stomach of pigs (Leser *et al.* 2008). There are a few factors that may be responsible for this (such as HCl, antimicrobial agents like pepsin), to determine the likely cause it was decided that HCl should be investigated first. Accordingly, loss of bacterial spore viability by HCl was proposed to be caused by two possible mechanisms, which might operate simultaneously. Death of individual bacterial spores could occur *via*

- a) the HCl ions exerting a direct sporicidal effect or

- b) The environment promotes germination, thus exposing less tolerant germinating bacteria to the HCl.

5.1.1 DPA release of acid treated spores

To test these hypotheses, germination was measured by monitoring release of DPA from the spore core. Complete release of DPA occurs in the very first stage of germination, meaning it is a good measure of commitment of spores to germination (Zhang *et al.* 2010a). However, there are still many unknown factors in the process of DPA release from the core, in particular, the mechanism for DPA release under wet-heat treatment is not yet understood (Zhang *et al.* 2011b; Setlow 2013). None-the-less, DPA release remains a far better method for detecting germination than measuring the OD₆₀₀ decrease, caused by the change from phase bright to phase dark due to the fact that DPA release occurs before the spore changes to phase bright (van Melis *et al.* 2011a) .

The experiments were therefore undertaken informed by the conventional wisdom that rapid DPA release is indicative of germination and can therefore be used as a criterion to assess this process (Kort *et al.* 2005; Zhang *et al.* 2010a). Under hostile conditions, i.e. in the gastric environment, it would be assumed that the spores which would germinate would suffer a loss of viability.

Recently, two modes of DPA release have been shown to occur:

- Physiologically induced DPA release: follows a sigmoid shape, with a very brief lag phase of under five minutes according to Setlow *et al.* (2013), characterised by bulk DPA release within 40 minutes.
- Damage induced DPA release, (e.g. by H₂O₂ and hypochlorite) follows a much slower and more linear trend.

According to Setlow *et al.* (2013), ca. 97% DPA release occurs within 60 minutes for spores germinated naturally compared with just 12% release for hypochlorite (Setlow *et al.* 2013). One could anticipate a similarity between the mode of action between hypochlorite and that of HCl since it is known that hypochlorite does not damage spore DNA and instead kills

spores by damage to the inner membrane, rendering the spores unable to germinate (Young and Setlow 2003), similarly it has been shown that spore rupture is the cause of spore death when treated with strong mineral acid (Setlow *et al.* 2002). By measuring the DPA released in an hour, this should mainly reflect the germination induced DPA release rather than the damage induced DPA release. Since germinated spores lose their resistance to stresses, it is reasonable to assume loss of viability soon after germination in the gastric environment, hence the link with plating to test the hypothesis. Irrespective of whether spore germination induced damage occurs, or direct spore death, neither spore will be able to form colonies.

To assess the effect of gastric conditions on spores, a range of *in vitro* experiments should be carried out. Ideally, these *in vitro* experiments should accurately reflect the true *in vivo* conditions. As such, the literature available on gastric conditions was explored to make an informed decision on the *in vitro* conditions required. One advantage of *in vitro* modelling is that spores can be sampled at any time point, permitting changes in spore physiology to be far more easily assessed. Given that the hypothesis, H₁, developed is that the germinants present in the stomach cause spores to germinate and then die due to the strong acid stress, it is necessary to individually assess the effect of strong acid and germinants.

HCl and pH of the porcine stomach

The conditions of the porcine stomach are discussed in detail in Chapter 1. Briefly, HCl is secreted and HCO₃ is released to neutralise this acid. As Chiang *et al.* (2008) mention, it is very difficult to simulate the constantly changing conditions of the pig stomach in a static model. For example, Babinszky *et al.* (1990) attempted to imitate gastric conditions of a pig but found that because they used a static model the hydrolysis of pepsin occurred at pH 1.0. (Chiang *et al.* 2008) further state ‘*In vivo*, gastric pH decreases from 4.8 to 2.1 and 1.7, after one and two hours, respectively, after ingestion of milk’ (Marteau *et al.* 1990). ‘The amount of digesta within the GI tract and digesta transit time significantly affects nutrient digestive capacity. None of these conditions can be properly simulated in a

batch, static model of *in vitro* digestibility.’ However a more sophisticated, dynamic model such as the TNO gastrointestinal tract simulator, could mimic conditions much more accurately since this model permits the incorporation of altered transit times and pH as well as other parameters (Déat *et al.* 2009). In the absence of such a highly sophisticated model in the department of Applied Sciences at Northumbria University, the investigations have instead focused on a wide range of conditions using simple batch *in-vitro* models.

Based on current literature, a bank of HCl concentrations and pH values from the pig stomach were collated, and a variety of experiments were set up to analyse the viability and germination of spores of *B. subtilis* under HCl/pH conditions which correlate with those found in the literature.

To cover a wide range of stomach conditions reported in the literature and at the same time to investigate the HCl effect on spore viability, the experiments detailed in this chapter focused on a range of HCl concentration and pH, in a buffered solution. Whilst pH has been studied separately by many researchers over the past 50 years, an interesting study by Gould and Sale (1970) explored the effects of pressure on germination in different *Bacillus* species and noted that when trying to initiate germination at 250 atm, only at a narrow pH range could any germination take place. Though pressure is not going to be explored in this research, it is important to note that germination may not take place at certain pH depending on pressure.

While other compounds such as enzymes will indeed have an impact on spore viability also, this was omitted for the first part of the experiment to focus on the effects of HCl only.

Table 5.1 illustrates the data from *in vivo* studies on HCl secretion and pH values (Cranwell *et al.* 1976; Barrow *et al.* 1977; Rislely *et al.* 1992; Mößeler *et al.* 2010). This is linked with piglet age.

Table 5.1 pH values and HCl concentrations of piglet stomach at different ages

Age (Days)	pH	HCl (mM)	Age (Days)	pH	HCl (mM)
1	4.7	44	7	5.2	78
	5	41		4.9	
2	4.1	67	8	4.1	51
	4.1	46		4	59
	3.5	76	10	4	51
	2.8	110		3.8	96
	6	40		4.7	
3	4.6	69		4.1	118
	3.8	58		4.4	66
4	5	56	11	4	120
	4.8	72		6	20
	4.3	49	13	2	120
5	74	6.5		20	
5	3.6	44	15	2	130
	3.5	120		6	42
	6	15	20	3	110
4	56	7		30	
6	4.3	45	20-24	4.4	67
	4	25		4.1	28
	5.5	60	19-33	4.1	144
	5.2	36		3.9	88
	4.5	48		3.8	118

A key point to acknowledge when looking at *in vivo* data is the effect that a meal will have on the pH and HCl concentration. Due to the increased volume of the stomach in its fed state, and the food composition, e.g. milk or pellet feed, the HCl concentration will undoubtedly drop at first due to the dilution caused by food. Similarly the pH will rise accordingly. Post-meal, a decrease in pH will be seen, due to gastric secretion. This will continue to fall until it reaches the ‘empty’ state as the food passes out the stomach (Wilfart *et al.* 2007).

Table 5.2 shows the values selected for testing in this study, compared to those reported in the literature. In these *in vitro* models which specifically mimic pig stomach conditions, HCl concentrations and pH values have been the main focus. The aim was to acquire a certain pH with a known amount of HCl, to mimic the gastric conditions reported in a pig stomach. It was found that it was not possible to match the correct pH with 100mM PBS, therefore the buffer was diluted to obtain the desired pH and HCl concentration.

Table 5.2 *In vitro* values used to mimic gastric secretion in pigs. NA= data not available.

Present study			Other <i>in-vitro</i> studies			
pH	HCl (mM)	Buffer (mM)	pH	HCl (mM)	Buffer (mM)	Source
0.8	100	0	1	NA	NA	(Letourneau-Montminy <i>et al.</i> 2011)
1.4	100	50	2	70	71	(Wilfart <i>et al.</i> 2007)
2.8	50	50	2	70	71	(Boisen and Fernández 1997)
3.6	45	50	2.5	100	NA	(Liu <i>et al.</i> 1997)
4.0	40	67				
4.8	0	50	2.5	180	NA	(Chiang <i>et al.</i> 2008)

Since HCl is likely to be the lethality inducing compound it is important to know the HCl concentration, interestingly this information was not always available in previous studies (Thacker and Baas 1996; Knarreborg *et al.* 2002; Letourneau-Montminy *et al.* 2011) .

Gastric residence time

Anderson *et al.* (2002) notes that the time taken for half clearance time of a liquid feed is 31 ± 4 min for non-nutrient and 30 ± 7 min for nutrient meal. For a solid meal, Gregory *et al.* (1987) noted that it took over an hour for 50% emptying.

Other factors affecting germination

A key factor in germination is the availability of nutrients. As detailed in Chapter 1, spores germinate upon exposure to L-alanine or AGFK. The concentrations needed to induce germination are reported to be 10mM L-alanine (Wuytack and Michiels 2001) or for the AGFK germination route, L-alanine (10mM), (D)- Glucose (5mM), (D) –Fructose (1mM) and KCl (24mM) (Wuytack *et al.* 2000).

5.1.2 FCM Cell sorting

The first experimental work undertaken on the flow cytometer was to analyse standards of all physiological states of *B. subtilis* and identify where and how these sub-populations would appear on the FCM profiles. Although it is not customary to verify regions by sorting (da Silva *et al.* 2005; Mathys *et al.* 2007; Cronin and Wilkinson 2008; Baier *et al.* 2010; Reineke *et al.* 2012; Zhang *et al.* 2012), meaning leading experts accept assignment of regions without further validation, and products have even been certified without the requirement for sorting, it would still be beneficial to verify the assumptions by using a cell sorter. Sorting of *B. subtilis* cells has been done previously into buffer solutions by Chung *et al.* (1995), and Davey and Kell (1996) note several studies where flow cytometric cell sorting of different species of bacteria has been successful. More recently, there has been successful sorting of *B. subtilis* into microtiter plate wells using PI and cFDA staining by Shen *et al.* (2009) and *B. cereus* using PI, RedoxSensor Green and DiOC₆ (Want

et al. 2011). However, to date and to the best of our knowledge this is the first time physiological states of *B. subtilis* have been sorted directly onto agar plates based on Syto 16 and PI staining. Furthermore, sorting has never been undertaken following acidic treatment of spores or cells.

5.1.3 Aims and Objectives

For this study, the following key aims and objectives were proposed:

- Explore the effect of different HCl concentrations on spore viability and germination *via* plate counts and DPA release respectively.
- Verify the FCM region assignments by cell sorting of cells and spore under different treatments

5.2 Materials and Methods

5.2.1 Spore production

Spores were prepared on AK sporulating agar (BD, UK), supplemented with 200µl MnSO₄ (3.4mM) spread onto the surface with a sterile glass rod to improve the rates of sporulation (Vasantha and Freese 1979). This was then allowed to be absorbed and the plates were inoculated with 200µl of an overnight culture of cells on each plate (grown in LB broth). Plates were left and additional 30 minutes, then inverted and incubated for seven days at 37°C. After this, the spores were harvested by flooding the plate with 0.2µm filtered cold (4°C) sterile deionised water and gently agitating the surface with a sterile glass spreader. The resulting spore suspension was poured into a sterile (15ml) falcon tube. Based on the method of Zhao *et al.* (2008) these suspensions were washed twice with sterile 0.2µm filtered H₂O at 10,000 x *g* at 4°C (Sorvall RC 5B plus centrifuge, Thermo Scientific, UK), and then re-suspended in 0.2µm filtered 50% EtOH (with H₂O). This mixture was left for 18 hours at 6°C, and then washed three times more in ddH₂O. This method was modified

slightly by leaving spores for two more days in pure water to lyse any remaining vegetative cells and washed again before being stored either at 6°C or -20°C (Kong *et al.* 2010).

Before spores were used for analysis, aliquots of 1ml were washed three times by centrifuging at 13,000 x *g* for two minutes. The top 995ul supernatant was removed and then the pellet was re-suspended in sterile 0.2µm filtered phosphate buffer (100mM, pH 7.4).

5.2.2 Analysis of DPA release from spores

The method for detecting DPA release is detailed in Chapter 2. Briefly, the total amount of DPA is calculated by boiling the spores for 90 minutes, to ensure the entire DPA deposit is released. The amount of DPA released from the samples which undergo treatment are therefore reported as percentages of the total (Setlow *et al.* 2003). Spores were at a density of between 5×10^8 and 1×10^9 cfu/ml (OD₆₀₀ between 1 and 2) to ensure a large enough pellet was formed to enable easier removal of the supernatant. The top 0.5ml of the supernatant was removed and pipetted into UV transparent plastic disposable cuvettes (Sarstedt, Germany). The optical density of the supernatant was then measured at 270nm (OD₂₇₀), the wavelength at which DPA absorbs, using a UV-Vis spectrophotometer Cary 50, (Varian Inc, USA) equipped with CaryWin UV Kinetics software to analyse the data. The alignment was checked prior to measuring to ensure the cuvette was correctly positioned. Absorbance was then measured every 0.5 seconds for 15 seconds.

The DPA release from spores was measured following immersion in water or PBS (50mM) at different HCl concentrations (see Table 5.2). The water simulated an extreme case where no food was present but some HCl secretion took place (this occurs due to stimulation of appetite). The variable concentration of HCl in PBS simulates the intake of feed, which causes a reduction in HCl concentration due to the increase in the volume of liquid in the stomach. The concentration of the PBS was altered to ensure the correct range of pH values and the corresponding HCl concentration was met. PBS also serves the purpose of mimicking the buffering capacity expected from food (Cranwell *et al.* 1976). The

experiments were carried out at 37°C in a rotating incubator set to 200rpm and treatment time was 1 hour.

Determining the magnitude of DPA release following an extreme acid treatment

The first experimental work into DPA release was designed to ensure that the DPA release seen was indeed due to the effect of the acid or the proton action on DPA release, rather than just the impact of the temperature (37°C). The aim was to find the maximum DPA release expected due to HCl only (i.e. an environment with little to no buffering capacity). To do this, a 1ml sample of spores (1×10^9 spores/ml) in pure water, kept at 37°C in a rotating incubator set to 200rpm was analysed. This was compared with spores subject to a harsh acid treatment (100mM) in water, where again, 1ml of a spore stock (1×10^9 spores/ml) was pipetted into 1.5ml sterile microtubes and were centrifuged at 14,000rpm for two minutes to pellet. The supernatant was removed and replaced with water then a second centrifugation step was undertaken, the top 600µl was removed and replaced with 500µl water and 100µl of 1M HCl (resulting pH0.8) and incubated for one hour at 37°C. Each treatment and control was performed in triplicate.

Following incubation, the samples were centrifuged again and the supernatants were retained in UV transparent cuvettes (Sarstedt, UK) for DPA release analysis by UV spectroscopy.

5.2.3 DPA release and viability of spores following different HCl treatments

The aim of the next set of experiments was to determine the levels of DPA following exposure to different concentrations of HCl. Again, all experiments were performed in triplicate and two runs were undertaken. A 1ml aliquot of spore stock (of $\sim 1 \times 10^9$ spores/ml) was pipetted into a 1.5ml sterile microtube. These were centrifuged at $10,000 \times g$ for two minutes to pellet, the supernatant was removed and replaced with 1ml PBS, then a second centrifugation step was undertaken, the top 800 μ l was removed and replaced with the following amounts of water, PBS and HCl to make up the treatments described in Table 5.2 shown below in Table 5.3

Table 5.3 Amount of PBS, water and HCl added to spores for each acid treatment

Sample code	PBS (μ l)	HCl (1M) μ l	Water (μ l)	pH
1	0	100	700	0.8
2	500	100	200	1.4
3	500	55	245	2.8
4	500	45	255	3.6
5	500 (pH4.8)	0	300	4.8
6	670	40	90	4.0

The samples were incubated at 37°C in a rotating incubator set to 200rpm for one hour to mimic the movement of fluids in the stomach. After this incubation period, the samples were removed from the incubator and 100 μ l was taken for plating viability assessment.

Samples were then centrifuged again and the supernatants were retained in UV transparent cuvettes (Sarstedt, UK) for DPA release analysis.

Germinant treatment

The following germinants were used in the study: L-alanine (10mM), D-Glucose (5mM), D-Fructose (1mM) and KCl (24mM) (GFK) (All Sigma-Aldrich, UK). These were

made up at 20x strength so they could be diluted to the correct level in the samples. Where germinants were added, the volume of supernatant removed was 850µl from each sample to ensure similarities between the samples without germinants. The amounts re-added are shown below in Table 5.4.

Table 5.4 Amount of PBS, water and HCl added to spores for each acid treatment

Sample code	PBS (µl)	HCl (1M) µl	Germinants mixture (µl)	Water (µl)	pH
7	500	100	50	200	1.4
8	500	55	50	245	2.8
9	500	45	50	255	3.6
10	500 (pH4.8)	0	50	300	4.8
11	670	40	50	90	4.0

Viability assessments

To assess the viability of the samples after treatment the Miles and Misra method for plating was undertaken (Miles *et al.* 1938). Plates of LB agar were used (12g/L agar with 25g/L LB broth). Briefly, the LB agar plates were dried thoroughly before plating, and then divided into six segments. Each segment was used for one serial dilution ranging from 10^1 to 10^6 . Following the one hour incubation period detailed in Section 5.2.3, the 100µl taken from each sample was pipetted into a sterile test tube containing 900µl PBS. Six serial dilutions were systematically carried out to a final 10^{-6} dilution. A 20µl droplet of each serial dilution was placed in each segment with the respective dilution and left for an hour to dry. Plates were inverted and incubated at 37°C for 24 hours and all samples were performed in triplicate.

Counts were taken from the segments which showed between 8 and 80 colonies. Segments with counts outside this range were designated either too numerous to count or too low to be significant.

Plating was implemented to provide an insight into the total lethal effect of the treatments. By using this information in combination with the DPA release, an equation was derived through which the lethality mechanism could be inferred. Hence, the data could be used to test the initial hypothesis of whether germination induced death takes place or a direct sporicidal impact is seen. The equation is presented below in Equation 5.1.

Equation 5.1 Lethality mechanism formula to determine lethality mechanism.

$$\% \text{ death attributed to germination} = \left(\frac{\text{Percentage DPArelease}}{\text{Percentage total lethal effect}} \right) \times 100$$

5.2.4 Cell Sorting

To verify the results obtained *via* FCM, cell sorting was deemed necessary to validate the denoted viability. Unfortunately, the FACSCalibur at Northumbria University was not equipped with this function; however an EPICS Coulter Elite cell sorter was available at Bedford Technology Park under the guidance of Dr. Gerhard Nebe-von-Caron. The cells and spores were sorted based on their forward scatter (FSC) and fluorescent staining properties, and the set up was as described by Nebe-von-Caron *et al.* (1998).

A sample of dormant spores was immersed in a variety of conditions that would trigger germination, or cause a decline in viability.

In a few cases, the raw data from the FCM, known as listmode files were corrupt and as such these could only be analysed using the WinMDI software as opposed to the VenturiOne software

To accurately see how well the culturability matched up with the region assignments, the following treatments were applied:

- Unstained cells (in PBS 100mM pH 7.4)
- Cells stained with Syto 16 only.

- Dormant spores immersed in LB (pH 6.5) for 30 minutes and double stained (three replicates)
- Spores immersed in LB broth for 30 minutes, then treated with 55mM HCl for 1 hour (pH 2.7)
- Spores immersed in LB broth to initiate germination, then shocked with 55mM HCl for 30 seconds (pH 2.7)

5.3 Results

5.3.1 Determining the magnitude of DPA release following an extreme acid treatment

To investigate the magnitude of DPA release as a result of the acid stimulus in the gastric environment an extreme acid treatment (100mM) was selected in pure water. As described in Section 5.2.2, to delineate the level of DPA release influenced by the acid treatment alone, a control sample of spores in pure water at 37°C for 60 minutes was included to determine the magnitude of DPA release due to exposure to this temperature. This was done because germination is known to occur at 37°C therefore it was necessary to ascertain that DPA release was linked to the gastric conditions and not just a product of the temperature. This is shown below in Figure 5.1. The OD₂₇₀ was measured in triplicate, and the results were pooled for each treatment to get the average OD values.

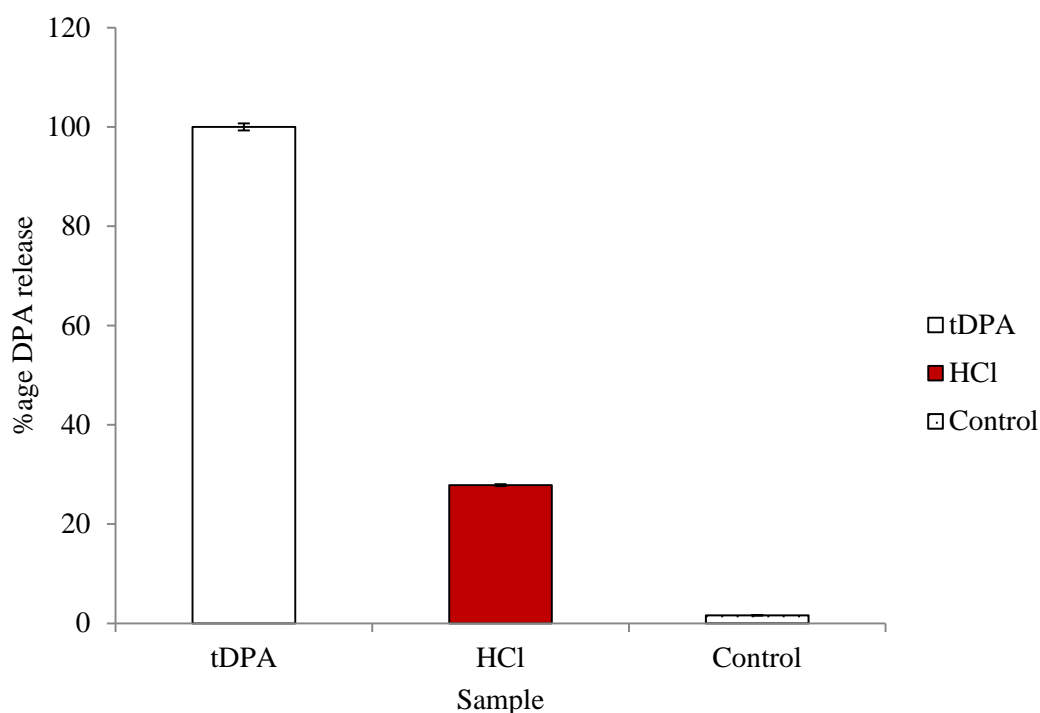


Figure 5.1 %DPA release of spore samples. Plain: showing the sample heated at 96°C for 90 minutes, Shaded: showing the sample treated with 0.1M HCl (pH 0.8) at 37°C for 1 hour in water, Dotted: Dashed: spores kept at 37°C in dd H₂O for one hour. Error bars showing the 95% CI where n=3.

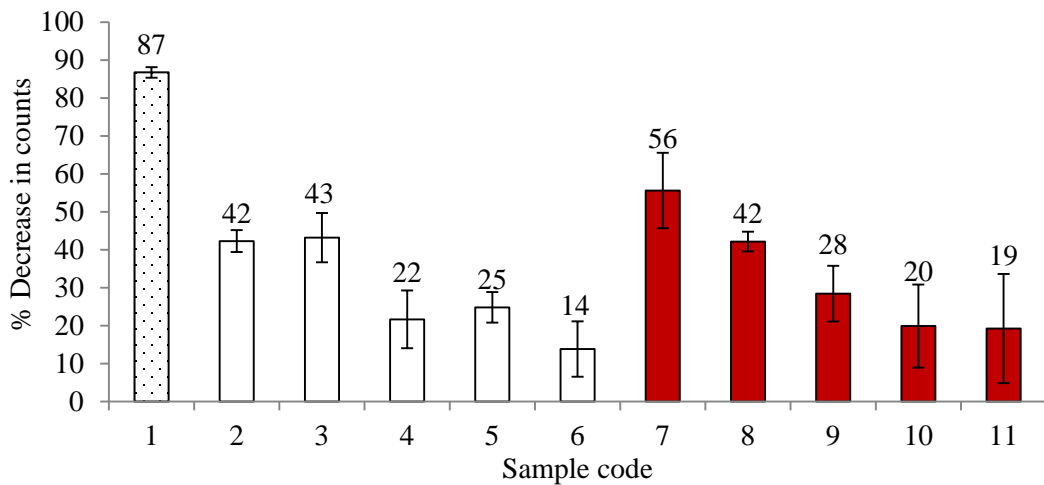
The control only released 2% of the total DPA possible, whereas the acid treatment caused significantly more germination to occur with 28% germination. By combining this information with the DPA release from the control, it emphasises that the temperature (37°C) was not a factor in the germination, suggesting that acid was responsible for 26% DPA loss. The results obtained were highly consistent as illustrated by the bars denoting the 95% confidence interval. Based on the analysis mentioned earlier in Section 5.1.1, given the 60 minutes duration and the fact that high hydrogen concentrations are known to induce germination it is reasonable to ascribe the observed DPA release to germination. Due to the severity of the conditions we could assume that all germinated spores will subsequently lose their viability.

It could be concluded that when germination is caused from a high proton concentration the germination induced mechanism could explain up to a maximum of 26%

reduction in ingested probiotic spores. This clear cut experiment suggests that even in the most hostile gastric conditions, 26% DPA release would be the maximum expected.

5.3.2 DPA release and viability of spores following different Hydrochloric acid treatment

To assess the viability of spores under different pH and HCl concentrations, plating was carried out on each sample and the percentage decline in viability was calculated. The results are illustrated in Figure 5.2.



1	2	3	4	5	6	7	8	9	10	11
pH 0.8 100mM HCl in water	pH 1.4 100mM HCl	pH 2.8 55mM HCl	pH 3.6 45mM HCl	pH 4.8 (PBS only)	pH 4.0 40mM HCl	pH 1.4 100mM HCl & AGFK	pH 2.8 55mM HCl & AGFK	pH 3.6 45 mM HCl & AGFK	pH 4.8 (PBS only) & AGFK	pH 4.0 40mM HCl & AGFK

Figure 5.2 shows the percentage decrease in viability of spores subject to the conditions described in the table below. Spotted bar  indicates spores in water, empty bars  indicate spores in PBS only and shaded bars  show spores in PBS with germinants. Error bars represent the 95% CI where n=6.

As would be expected, as the pH increases and the HCl content decreases, the perceived decline in viability is much reduced. For the HCl in water (sample 1), at pH 0.8 the large decline in viability (87%) is significantly higher than any other sample. This is particularly noticeable when comparing samples 1 and 2, which both contain the same amount of HCl (100mM), but the presence of a buffer in sample 2 means the decline in count is significantly lower at 42%. This signifies the impact of the buffering capacity since the lack of buffer in this sample means the spores are exposed to more H⁺ protons, so damage to the inner membrane is more likely. In sample 2, where the pH is 1.4, the decline is 42% which is statistically similar to the decline in counts seen in sample 3 at pH 2.3 where a 43% reduction in counts is observed. The decline in counts is significantly lower again in samples 4, 5 and 6 corresponding to pH 3.6, 4.8 and 4. It is interesting that even in sample 5 (pH 4.8 no HCl) the decline in counts is still 25%, since the environment is not as hostile in this case.

When germinants are used there are three levels of reduction in counts. At pH1.4 (sample 7) the decline in viability is 56%, when the pH increases to 2.8 the decrease is significantly lower at 42%. The decline in counts decrease significantly further in samples 9, 10 and 11, to 28, 20 and 19% respectively, with no statistically significant difference in the decrease of viability seen in these samples.

With the exception of samples 2 and 7, when looking at the comparable results for the samples without germinants compared to the samples with germinants, there was no statistically significant difference in spore count observed. Only at pH 1.4, (samples 2 and 7) did the addition of germinants cause a significant decline in counts by 14% more than the non-germinant sample as can be seen from the non-overlapping bars representing the 95% confidence interval.

Therefore, the addition of germinants does not tend to increase the death toll by a significant amount apart from at pH1.4, assuming that the plate counts are indicative of viability.

Based on the results from this experiment and the corresponding DPA release, the level of germination induced death was calculated. This was done using the lethality mechanism formula, presented in Equation 5.1.

Figure 5.3 shows the percentage of spore death attributed to the two postulated lethality inducing mechanisms i.e. direct sporicidal and germination induced mechanisms. The coding is the same as that used in the table in Figure 5.2

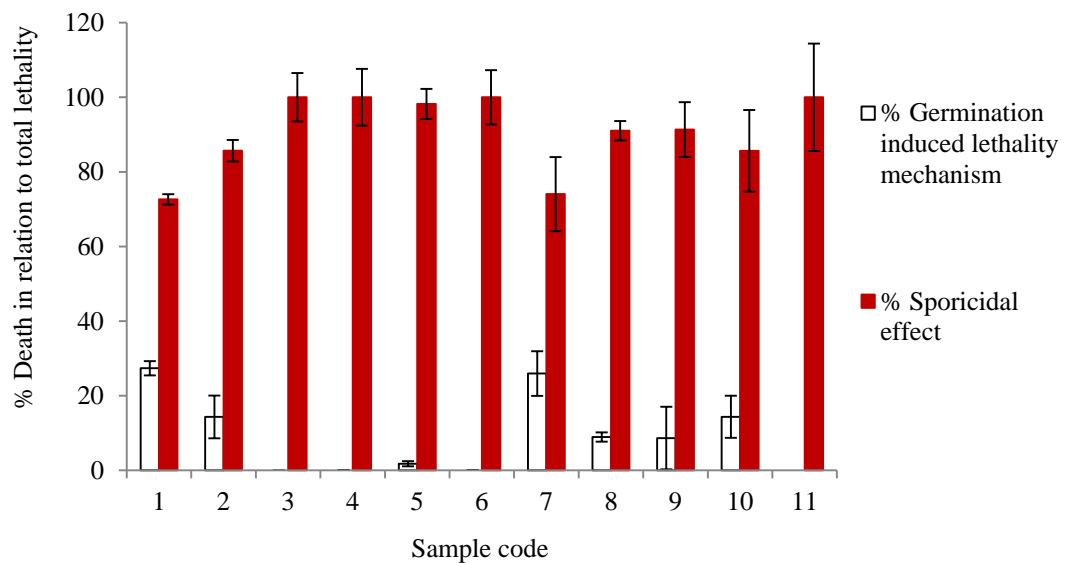


Figure 5.3 The percentage attributed to direct sporicidal effects is the total lethality minus the percent germination. Sporicidal effect implies the amount of death without release of DPA. Error bars represent the 95% CI where n=6. Sample codes as per Figure 5.2.

When no germinants are present there is no significant DPA release from pH 2.8 and above (samples 3-6) ($p > 0.05$). The only contribution can be seen at pH 0.8 and 1.4 where an increase of the sporicidal activity from pH 0.8 to 1.4 corresponds to a significant decrease in DPA release (from 24% to 8% actual DPA release).

In the presence of germinants, at pH 1.4 (sample 7) 26% of the total death toll is attributed to germination, and at pH 2.8, 3.6 and 4.8 the germination induced death is significantly less than at pH 1.4 but still contributes to 9, 10 and 14% of the total perceived decline in counts.

The addition of germinants caused an increased contribution ascribed to germination induced death at pH 2.8, 3.6 and 4.8 (samples 8, 9, and 10). From this perspective, inclusion of germinants increases germination induced death. It may not drive spore death but it is still a mechanism that may be notable. This means that the germinants do influence the levels of DPA release from the spores despite the presence of HCl. In particular, a statistically significant increase in DPA release was seen at pH 4.8 (noted when comparing sample 5 and 10) where the addition of germinants caused 12% more DPA release ($p < 0.05$), similarly at pH 1.4 (comparing samples 2 and 7) DPA release was 12% greater in the presence of germinants.

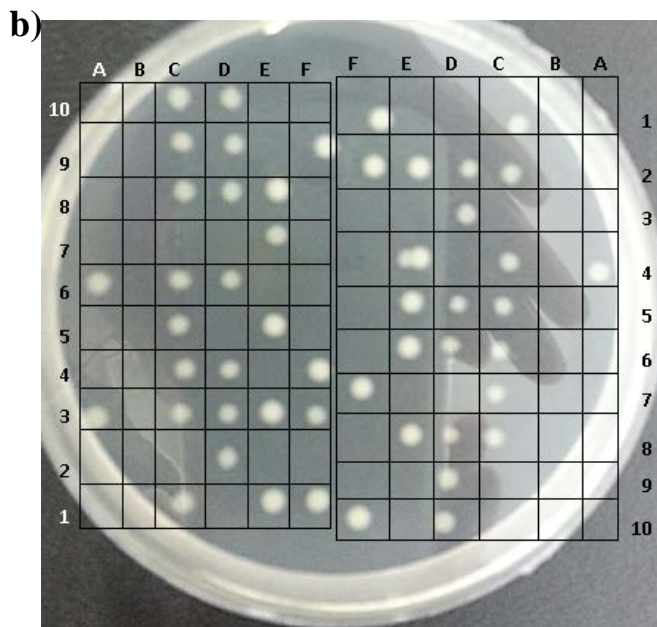
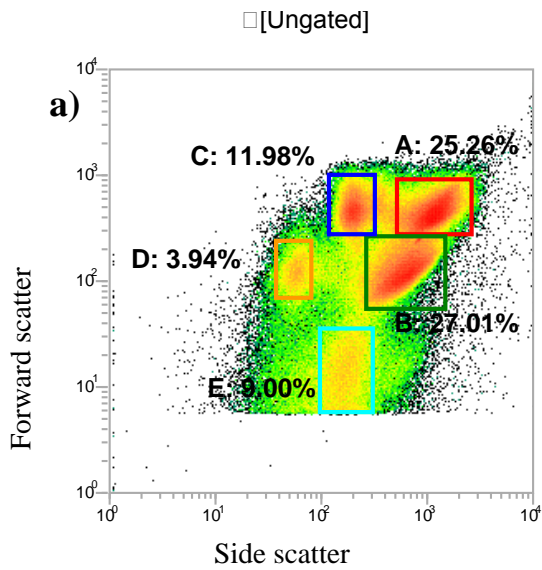
To explore the impact of HCl further, FCM analysis on HCl treated spores was carried out with cell sorting to look at the culturability in relation to the Syto 16 and PI staining properties.

5.3.3 Cell sorting

Cell sorting on B. subtilis cells grown in LB broth

A sort of cells grown overnight at 37°C in LB broth without being exposed to any lethality inducing acid treatments was undertaken, to check the recovery rate from the cell sorter. The cells were run through the FCM and then regions to be sorted were drawn and selected. Following region selection, the cells were sorted onto an LB agar plate. Sorting was organised so that there are columns from A to F and rows from 1 to 10 and each point (i.e. A2) is referred to as a well. The petri dish was separated into two halves and the sorting was mirrored on each side. For each well, the number of droplets could be altered so that recovery rates could be estimated. For regions where no anticipated cells were expected because they were branded debris a very high droplet number was used. In Figure 5.4 a) the strategy was to use a very high droplet number in column A and a varied droplet number in column B to determine whether any growth was likely in an area typically assigned as debris. In columns C to F the regions sorted were anticipated to have a high viability, therefore single droplets were sorted onto each well so an accurate recovery rate could be obtained. The results of this sorted plate are summarised in Table 5.5.

In Figure 5.4 a, the forward scatter (FSC) vs side scatter (SSC) profile of cells grown in LB broth overnight is displayed. In Figure 5.4 b the sorted plate of the same cells grown in LB broth is shown with a notional grid created showing the location of the columns and rows.



	A	B	C	D	E	F
1	0	3	1	1	1	1
2	50	3	1	1	1	1
3	50	30	1	1	1	1
4	50	10	1	1	1	1
5	50	3	1	1	1	1
6	50	1	1	1	1	1
7	50	30	1	1	1	1
8	50	10	1	1	1	1
9	50	3	1	1	1	1
10	0	1	1	1	1	1

Figure 5.4 Cells grown in LB broth, then re-suspended in PBS a) FCM profile of side scatter (SSC) vs forward scatter (FSC) where five sub-populations are apparent on the density plot. Region A (red): cell doublets in chains, Region B (green): single cells, Region C (blue): cell doublets (width ways), Region D (orange): single cells, width ways, Region E (turquoise): debris. b) FACS sorted LB agar plate, in columns A and B) Region E (turquoise) is sorted at rates of 1, 3, 10, 30 and 50 droplets per well. Cell regions (A-D) in columns C-F sorted at one drop per well. n=1

The percentage recovery rates have been tabulated and presented below in Table 5.5, which are based on the number of droplets sorted and the subsequent colony formed. Hence the viability is a function of the number of droplets per well.

Table 5.5 Estimated recovery from sorted plate. Parameter description according to sorted plate columns and FCM regions in Figure 5.4. Recovery rates are a function of number of drops per well.

Column	FCM Region	Physiology	Recovery (droplets)	% Recovery
A	E	Debris/ 'noise'	3/800	$\geq 0.4\%$
B	E	Debris/ 'noise'	0/194	0
C	B	Single cells	15/20	75%
D	D	Single cells, width ways	14/20	70%
E	A	Cells doublets/chains	11/20	55%
F	C	Cells doublets, width ways	8/20	40%

Primarily there was absolutely no growth in the column B since out of 194 droplets not a single colony was formed. When droplet numbers were increased to 800 (column A) three wells displayed colonies. Despite the fact that one cannot be certain whether the wells which displayed colony formation arose from just one bacteria, since we know that only three wells had growth and the 13 other wells (with 50 droplets) did not give rise to any colony formation, strongly implies that the recovery from this region was indeed close to just 0.4%. Based on this, one can assert the belief that region E does not hold any significant numbers of bacteria. As can be seen from Table 5.5 the first sorted plate illustrates that the maximum recovery of untreated cells from a cell sorter is around 75%. This can be stated with a good level of accuracy since single droplets were sorted for the viable regions.

Cell sorting on Syto 16 stained cells

In Figure 5.6, cells stained with Syto 16 alone were sorted. The aim of this was to see whether Syto 16 had any noticeable effect on the viability of the cell.

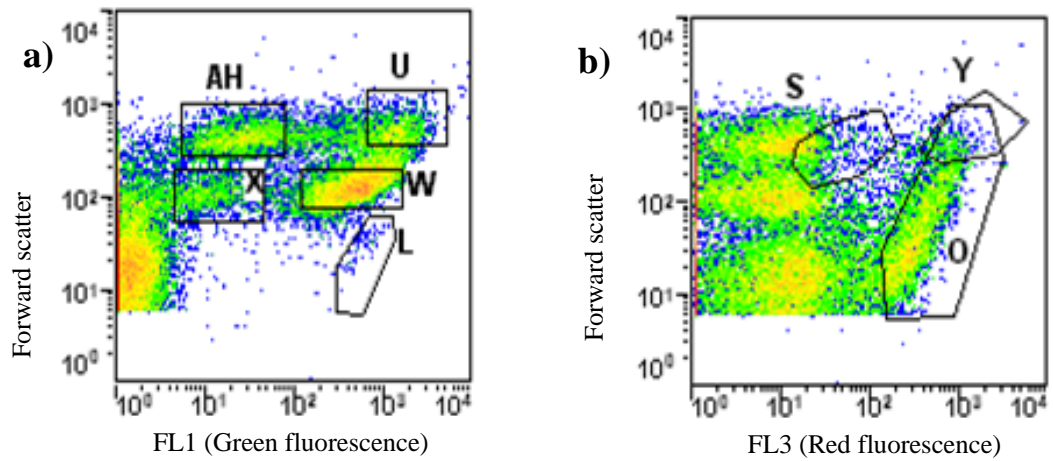
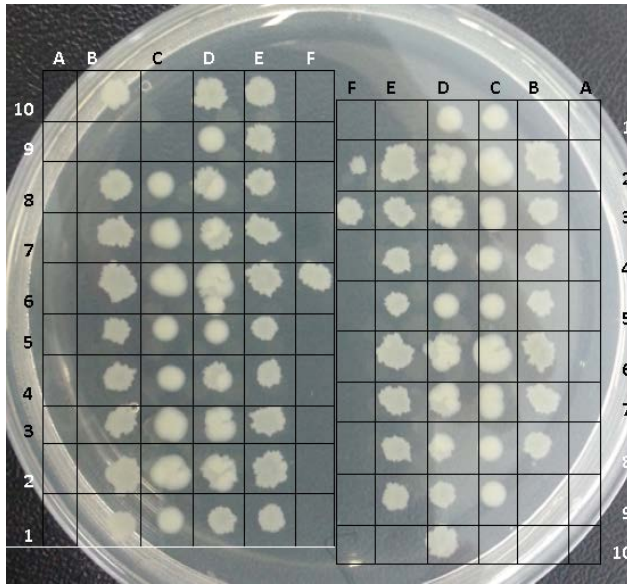


Figure 5.5 FCM profiles for live cells stained with, the Syto 16 only. Density plots created using WinMDI software. a) FL1 vs Forward scatter (FSC), Region L: small Syto positive particles, Region U: Outgrown spores, Region W: Germinating spores, Region X: Phase dark spores, or possibly spore aggregates, Region AH: dormant spores. b) FL3 vs FSC, region O: outgrown dead spores or dead cells, region S: germinating spores, Region Y: dead cells. n=1



	A	B	C	D	E	F
1	0	1	1	1	1	1
2	30	30	30	30	30	30
3	10	10	10	10	10	10
4	3	3	3	3	3	3
5	1	1	1	1	1	1
6	30	30	30	30	30	30
7	10	10	10	10	10	10
8	3	3	3	3	3	3
9	1	1	1	1	1	1
10	0	1	1	1	1	1

Figure 5.6 Sorted plate of cells grown in LB broth overnight and stained with Syto 16 (only)

The purpose of this sorted plate in Figure 5.6 was to check that the Syto 16 didn't cause any decline in the viable count itself. The recovery rates are described below in Table 5.6

Table 5.6 Estimated recovery from sorted plate. Parameter descriptions are based on the sorted plate columns and FCM regions. Recovery rates are a function of number of drops per well. n=1

Column	FCM Region	Physiology	Recovery	% Recovery
A	L	Stained debris	0/88 drops	0%
B	X	Single germinating spores	16/20 wells	≤80%
C	AH	Germinating spores (doublets)	17/20 wells	≤85%
D	U	Live cells (Strong green fluorescence indicating chains/doublets)	20/20 wells	≤100%
E	W	Single live cells	18/20 wells	≤90%
F	O	Dead cells (PI positive)	3/20 wells	≤3%

Given the recovery rates (maximum 80%) it can be agreed that the Syto 16 will not have an effect on the recovery of the cells as single sorted unstained cells showed a recovery of 55% to 70%. Interestingly there still appears to be some PI positive cells in this sample. This may be due to carry over from previous samples as this cell sort was performed last.

Cell sorting on germinated spores

A sort was performed on germinated spores, which were stained with both Syto 16 and PI. The aim of this was to check whether the staining procedure had any effect on viability and recovery from the cell sorter. In Figure 5.7 the FCM profile containing the sorted regions is presented and the sorted plate in. Figure 5.8 The further two sorted plates are displayed in Appendix 3.

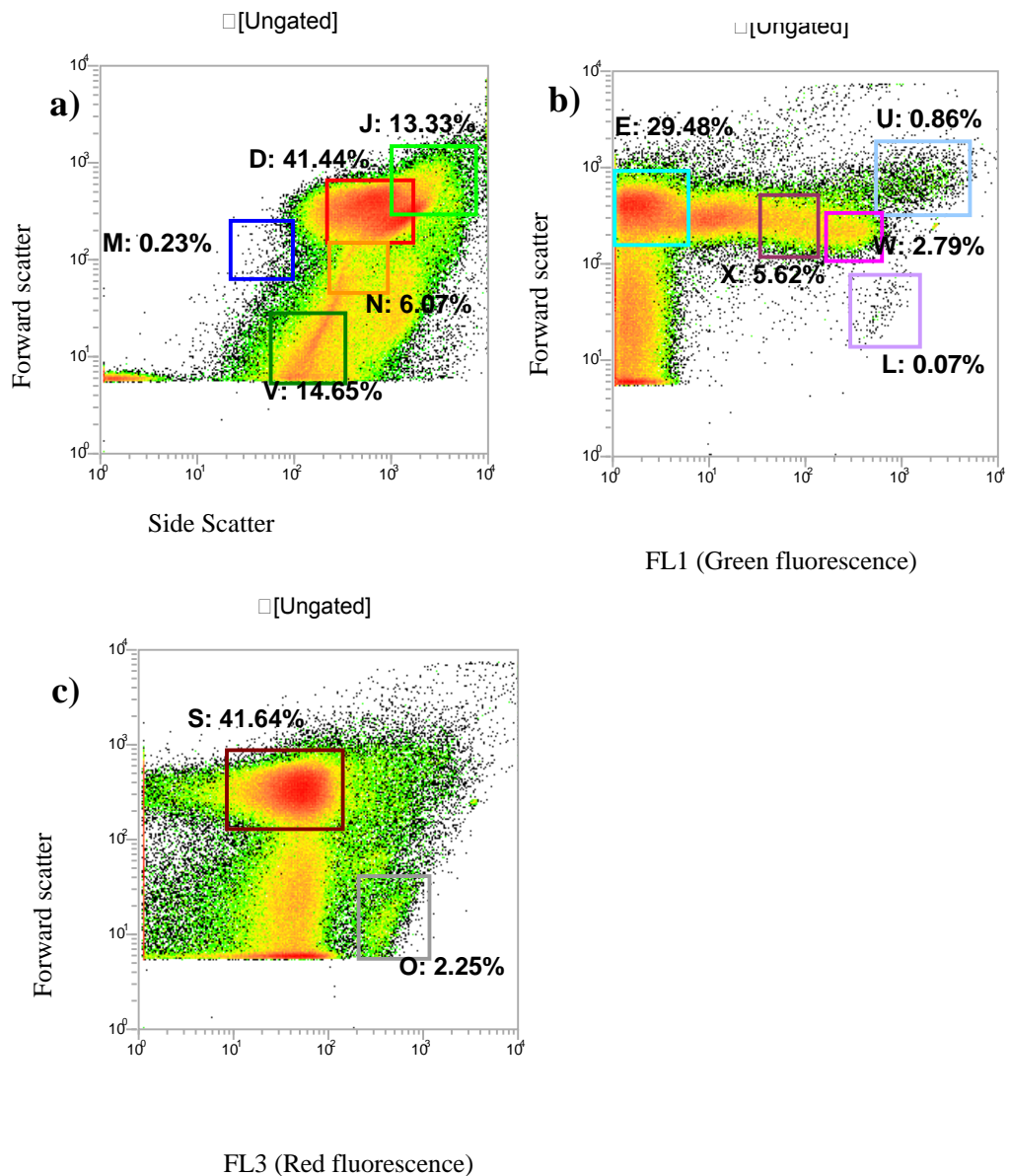


Figure 5.7 Representative FCM output on density plots created using VenturiOne software. a) FCM profiles for sorted plate 2 of side scatter SSC vs forward scatter FSC. Region D: all spores, Region J: Large particles (possibly germinating spores), Region N: small spores, Region M: small spores, region V: debris. b) FCM profiles for sorted plate 3. FL1 vs FSC, region L: small green particles, region E: Dormant spores, region U: large bright green particles, region W: germinating spores, Region X: germinating spores. c) FL3 vs FSC, region O: very small red particles, Region S: main cells/spores region. n=3.

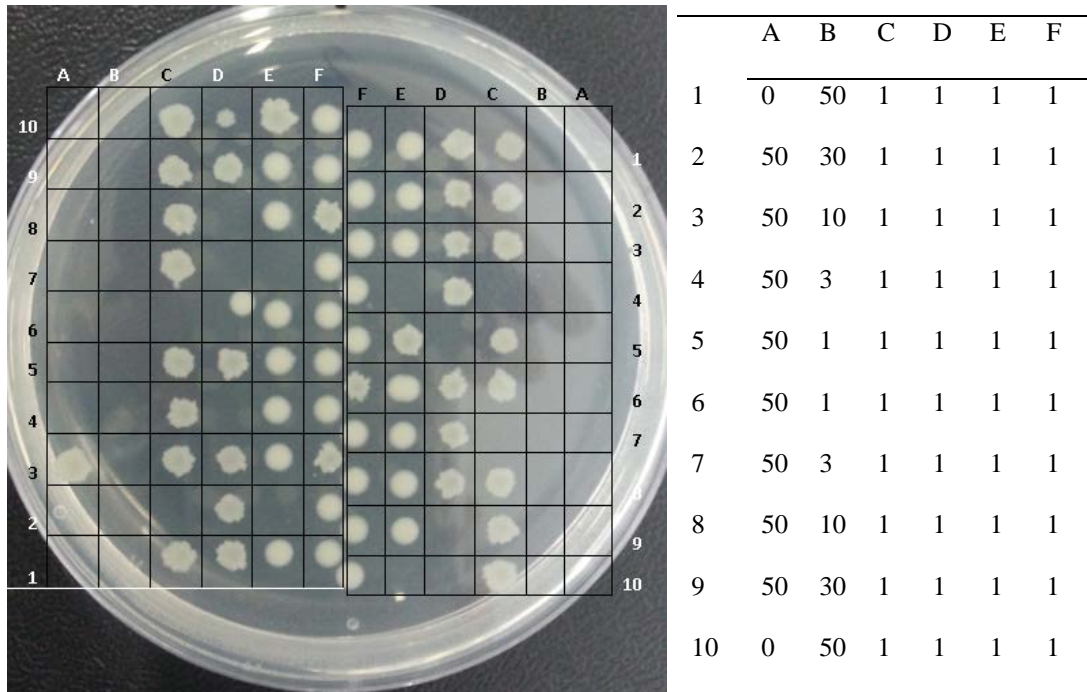


Figure 5.8 Representative sorted plate of spores immersed in LB broth, then re-suspended in PBS and stained with Syto 16 and PI. Region V (Figure 5.7a) in columns A and B: debris, sorted at rates of 1, 3, 10, 30 and 50 droplets per well shown in the grid. Cell and spore regions D, J, M, N from Figure 5.7a in columns C-F sorted at one drop per well. Representative sorted plate where $n=3$.

The cell sorting results were tabulated and presented below in Table 5.7. The remaining regions were sorted onto plates presented in Appendix 5. Percentage recovery rates are based on either the number of droplets sorted and the subsequent colonies formed, or the number of wells in which colonies are present.

Table 5.7 Estimated recovery from sorted plate. Parameter description according to sorted plate columns and FCM regions. Recovery rates are a function of number of drops per well. n=3.

Region	Physiology	Colony count	% age recovery	Mean	SD	%CV
N	Small single cells	16/20 drops	80%	N/A	N/A	N/A
M	Small particles	14/20 drops	60%	N/A	N/A	N/A
J	Large cells	16/20 drops	80%	N/A	N/A	N/A
V	Debris/ 'noise'	1/994 drops	0.1%	0.1	N/A	N/A
D	All cell/spores	51/52 wells	≤95%	98	2.89	2.94
O	Small red fluorescent particles	0/388 drops	0%	0	0.00	0.00
L	Small green fluorescent events	0/194 drops	0%	N/A	N/A	N/A
U	Live cells (Strong green fluorescence)	19/20 wells	≤95%	95	0.00	0.00
W	Germinating spores (Mid green fluorescence)	38/40 wells	≤100%	95	7.07	7.44
X	Germinating spores (phase dark) low green fluorescence	39/40 wells	≤95%	98	3.54	3.63
E	Dormant spores	17/20 wells	≤85%	N/A	N/A	N/A

In Figure 5.7 a, the regions were assigned so that a homogenous spore population could be observed which is incorporated in region D. The larger events in this region could be analysed by sorting the events in region J. The slight overlap between these regions was to highlight any culturability difference in the slightly higher FSC and SSC signals generated. Similarly, region N was sorted so that the events with lower SSC and FSC could be determined.

The sort of Region O and L (Figure 5.7 b and c) illustrates that the region with very low FSC i.e. very small particles but with high red and green staining, is not a viable organism based on the recovery rate of 0. This means that this region may be nucleic debris,

or it could possibly indicate that Syto 16 and PI have a slightly lipophilic nature, meaning they are binding to phospholipid membrane of the cells.

Figure 5.7 c illustrates the progression in Syto staining intensity as the stages of germination occur. As would be expected, the further the spores progress through the stages of germination, the more Syto 16 they take up. Another key aspect noted in the FCM profiles is that after the spores become phase dark (region X) their Forward scatter intensity decreases temporarily, followed by an increase in FSC signal once the cells are outgrown. This subtle difference in FSC signals are not apparent on the FACSCalibur due to the fact that the laser intensity cannot be altered on this machine, whereas with the EPICS Coulter Elite, the intensity of the laser can be adjusted so that more subtle changes can be detected.

Cell sorting on acid treated spores

Given that the recovery rates based on the staining profiles appeared to be in good accord with what was expected, a few HCl treatments were applied to the spores. In Figure 5.10 spores were in LB broth for 30 minutes, then in 55mM HCl for one hour (pH 2.6).

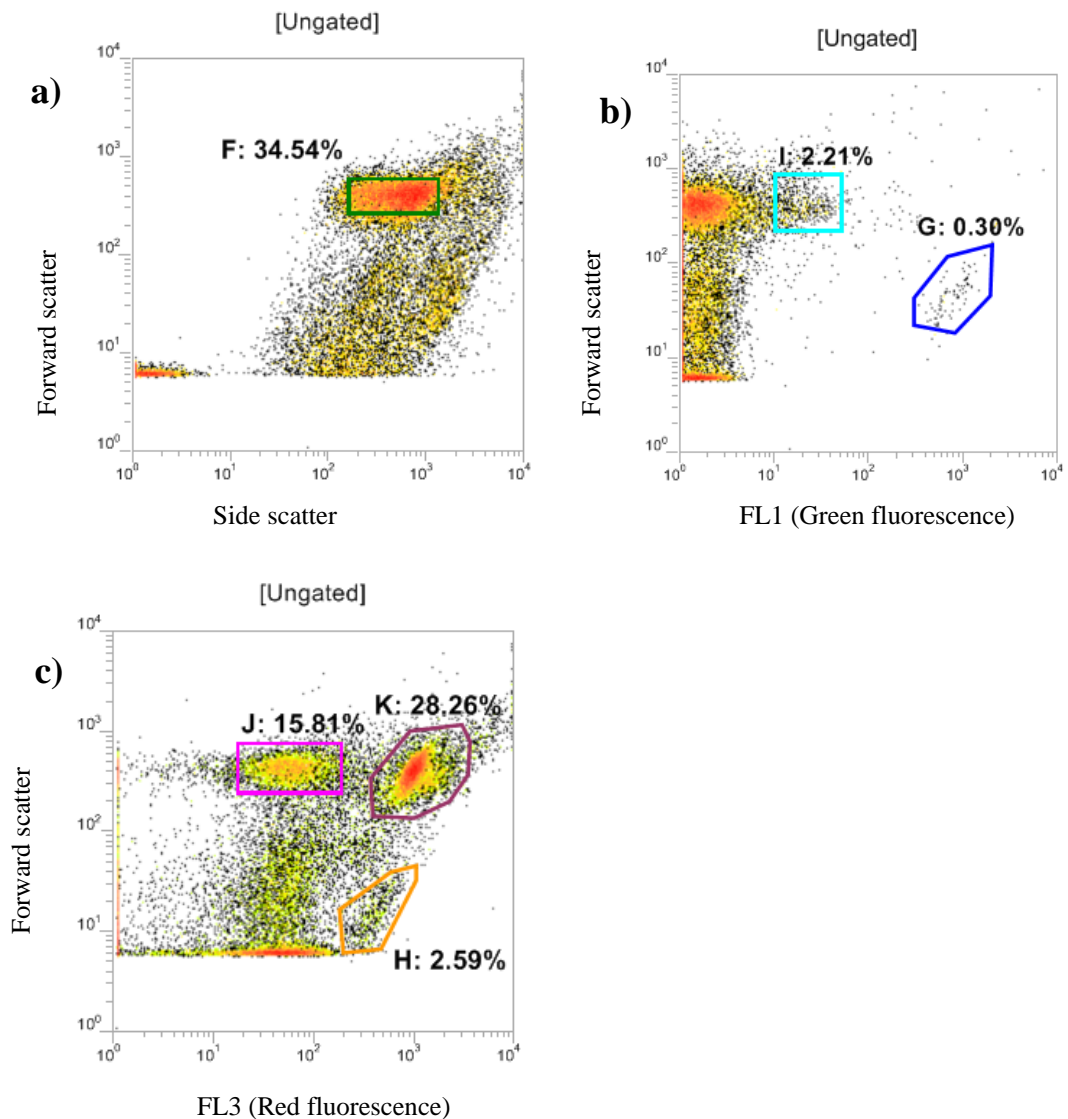
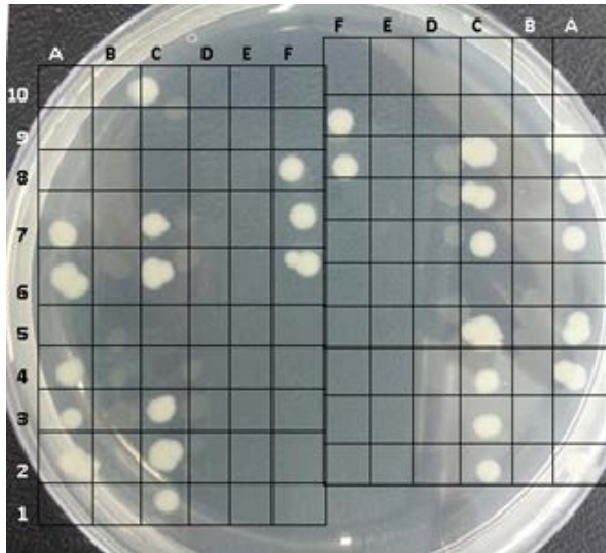


Figure 5.9 FCM profiles for spores immersed in LB broth for 30 minutes, then treated with 55mM HCl for one hour. Density plots created using VenturiOne software. a) Side scatter (SSC) vs forward scatter (FSC), Region F (green): all spores. b) FL1 vs FSC, region G (blule): small green particles, region I (turquoise): germinating spores. c) FL3 vs FSC, region H (orange): very small red particles, Region J (pink): main spore region, K (purple): germinated dead spores. n=1



	A	B	C	D	E	F
1	0	1	1	1	1	1
2	30	30	30	30	30	30
3	10	10	10	10	10	10
4	3	3	3	3	3	3
5	1	1	1	1	1	1
6	30	30	30	30	30	30
7	10	10	10	10	10	10
8	3	3	3	3	3	3
9	1	1	1	1	1	1
10	0	1	1	1	1	1

Figure 5.10 Spores immersed in LB broth for 30 minutes, than treated with 55mM HCl for 1 hour. Re-suspended in PBS and stained with Syto 16 and PI. All sorted at rates of 1, 3, 10, and 30 droplets per well. n=1.

The recovery rate appears far lower following the HCl treatment. The FCM profiles highlight that a large proportion (28%) of the population is now PI positive (region K in Figure 5.9 c). The recovery rates are presented below in Table 5.8.

Table 5.8 Estimated recovery from sorted plate. Parameter descriptions are based on the sorted plate columns and FCM regions. Recovery rates are a function of number of drops per well. n=1.

Column	FCM Region	Physiology	Recovery	% Recovery
A	F	All cell/spores	10/16 wells	≤63%
B	H	Very small red particles	0/194 drops	0%
C	J	Dormant spores	13/20 wells	≤65%
D	K	Dead germinating spores	0/90 drops	0%
E	G	Small green fluorescent particles	0/90 drops	0%
F	I	Germinating spores green fluorescence	5/20 wells	≤25%

Cell sorting on acid shocked spores

In the example shown below, dormant spores were placed in LB broth for 30 minutes at 37°C to initiate germination. Following this, 55mM HCl was added to the mixture and vortexed for 30 seconds. By performing this HCl ‘shock’ it was hoped that a sample containing dormant spores, germinating spores and dead germinated spores would be present. The results from this are presented below in Figure 5.11 and the sorted plate in Figure 5.12.

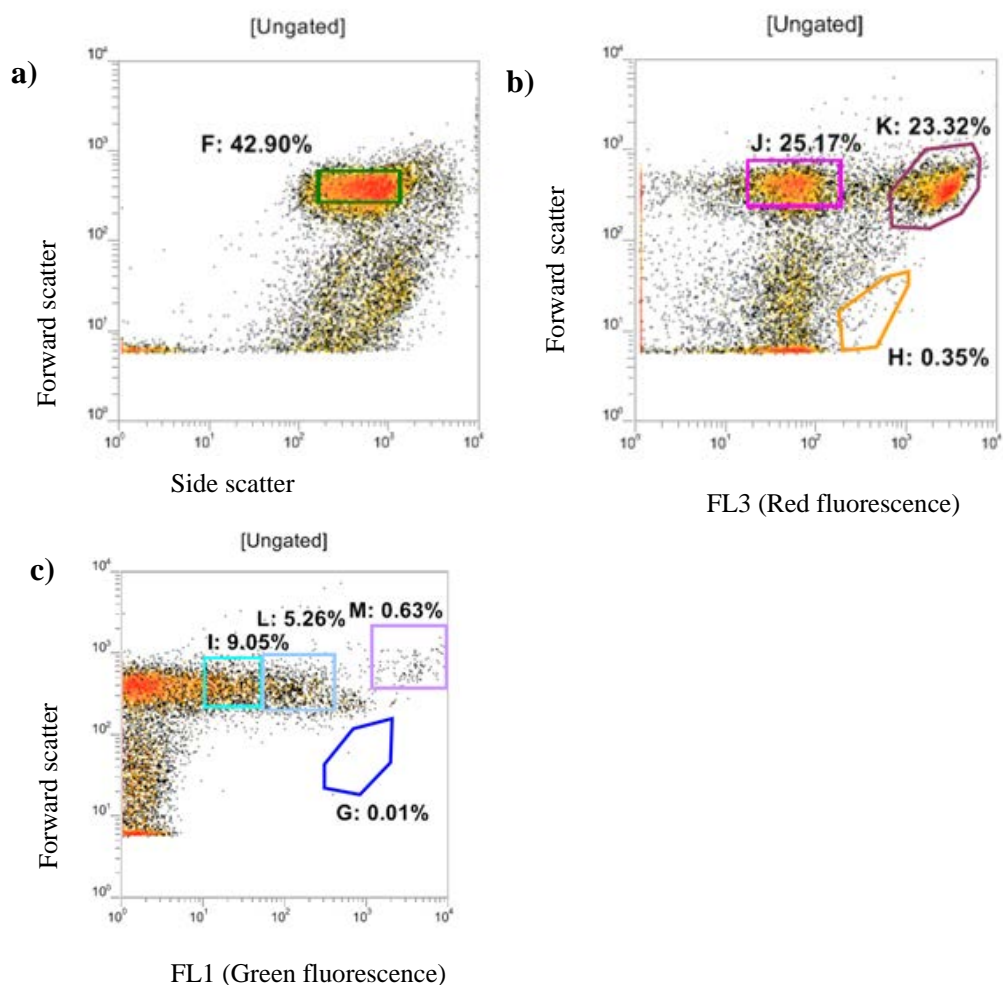
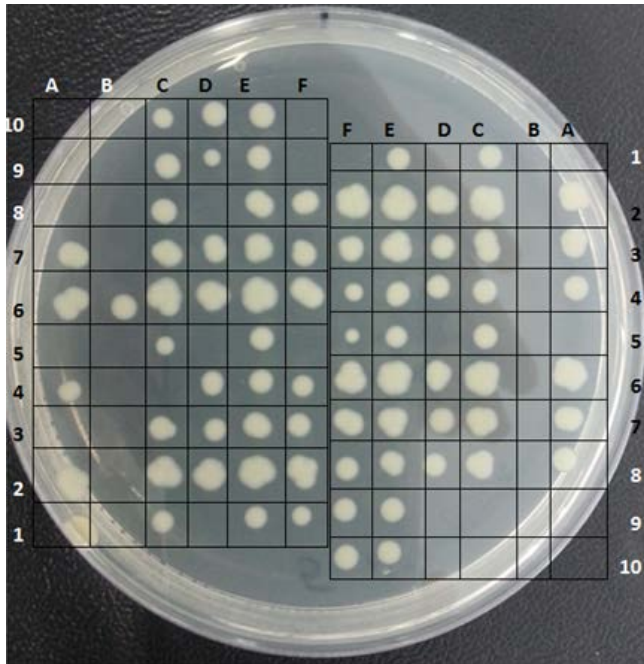


Figure 5.11 FCM profiles for sorted plate 4. Density plots created using VenturiOne software. a) Side scatter (SSC) vs forward scatter (FSC), Region F (green): all spores. b) FL3 vs FSC, region H (orange) very small red particles, Region J (pink): main spore region, K (purple): germinated dead spores. c) FL1 vs FSC, region G (blue): small green particles, region I (turquoise): germinating spores (phase dark). Region L (pale blue): germinating spores and Region M (lilac): outgrown spores and cells.



	A	B	C	D	E	F
1	0	1	1	1	1	1
2	30	30	30	30	30	30
3	10	10	10	10	10	10
4	3	3	3	3	3	3
5	1	1	1	1	1	1
6	30	30	30	30	30	30
7	10	10	10	10	10	10
8	3	3	3	3	3	3
9	1	1	1	1	1	1
10	0	1	1	1	1	1

Figure 5.12 Spores immersed in LB broth to initiate germination, then shocked with 55mM HCl. a) Plated double stained spores, germinated in LB broth then shocked with 55mM HCl for 30 seconds at room temperature (analysed in PBS). Sorted at rates of 1, 3, 10 and 30

To better understand how the FCM profiles link with the recovery rates, a description of the staining profiles and their likely viability and physiological characteristics are detailed in Table 5.9.

Table 5.9 Description of region assignments in relation to their staining profile.

Row	Region	Staining pattern and assigned state	Recovery
A	F	Region of cells and spores based on their FSC and SSC signals only. As no staining is visualised in this plot, the region will contain both living and dead organisms.	70%
B	K	High PI staining, indicating the spores in this region have a hydrated core, which the stain has been able to enter and bind with DNA to fluoresce. This is likely to represent the population that has been killed by the HCl 'shock' therefore most bacteria in this section will be non-viable.	1.6%
C	J	Dormant spores, based on their low PI staining and high FSC signal. A good recovery rate is anticipated in this region since the PI has not permeated the core.	85%
D	M	Very high Syto 16 staining but unknown PI levels. The high staining indicates these are outgrown spores.	65%
E	L	Medium Syto 16 staining likely show that these are germinating spores, e.g. spores which have had their core fully hydrated.	100%
F	I	Low Syto 16 staining indicates these are spores which have just recently underwent spore core hydration, meaning some Syto 16 has managed to penetrate the core, but not in large amounts. Spores at this stage in germination are most likely to be phase dark under a phase contrast microscope, though this hasn't been proven. Recovery for this region should be quite high	80%

The plating data clearly supports the assigned regions, where the area with high PI staining has less than 1.6% recovery and the regions which are stained with Syto 16 show >65 to 100% recovery.

Due to time limitations, it was not possible to perform more replicates or controls on these samples, however the sorted plates show that the regions assigned based on the staining properties correlate well with the culturability of the organisms. Following these trials, the next stage in the project was to assess the effect of simulated gastric conditions on spores.

5.4 Discussion

5.4.1 DPA release studies

In this chapter the experimental findings on DPA release show significant plate count decline but very little DPA release over the 60 minutes set time in some cases, while no DPA release is observed in others.

The percentage germination induced death for spores immersed in 100mM HCl in water for one hour was 27% (Figure 5.3). This corresponded to an 87% decline in count shown in sample 1 of Figure 5.2. Following the theory put forward, this would imply that 27% of spores are killed *via* germination induced death and their DPA is thus released. For the spores immersed in PBS with no germinants (samples 2-6 in Figure 5.2), at pH levels above 2.8 very little release of DPA was observed, characterised by an OD₂₇₀ as being the same as those in a control sample of dormant spores kept at 4°C. On the basis of these results, only at very low pH (<2.8) does DPA release occur in PBS.

In the presence of germinants (samples 7-11), the amount of DPA release reaches a maximum of 25%, however the total lethality in this sample is still far higher at 56%. This would imply that even in the presence of germinants, the majority of spores are killed without germinating or releasing any of their DPA.

When comparing the spores immersed in PBS and those immersed in PBS with germinants, the DPA release is higher in the presence of germinants. For example, since samples 2 (pH 1.4) and 7 are comparable, the DPA release is 12% higher in the sample with germinants present. Likewise, samples 3 (pH 2.8), 4 (pH 3.6) and 5 (pH 4.8) are comparable to 8, 9 and 10, which all have levels of germination above 9%, compared to <2% germination in the absence of germinants.

In general, the L-Alanine- GFK mixture appeared to be relatively ineffective at inducing germination, which was unusual given that Yi and Setlow (2010) reported high levels of germination (50% release of DPA) after 56 minutes in spores supplied with 10mM each of AGFK (L-asparagine and GFK). Though it was noted that this was far slower than when the spores were germinated with L-valine, which took only 14 minutes for spores to release their DPA depot. However this germination rate was reported in a medium without any acid content, thus it could be that the spores have a function whereby the acid in the environment is detected and therefore the spores do not commit to germination. Since it is widely acknowledged that spore germination occurs in favourable conditions, this theory could certainly be worthy of further investigation. Indeed it has been shown that pressure induced germination is inhibited at low pH (<5)(Wuytack and Michiels 2001), therefore it may be possible that nutrient germination is inhibited at low pH also.

The reduction of viable counts comes at conditions with unexpectedly low lethality power for bacterial spores, for example treatment 5 (pH 4.8) causes a reduction of 25% viability on dormant spores. This was unexpected as *B. cereus* spores immersed in a simulated gastric media at pH 5 for one hour have previously been shown to have no change in viable counts (Clavel *et al.* 2004). With regards to the effects of HCl, dormant spores have previously been shown to suffer a 90% loss in viability following 500mM HCl for 1 hour (at 24°C) (Setlow *et al.* 2002) likewise, a study where spores of *B. cereus* were subject to 0.2N (200mM) HCl indicated that after an hour less than 10% of high silicate spores remained viable, and only 1% of spores with a low silicon content remained viable, although silicon in

the *B. subtilis* spore coat is presumed absent (Hirota *et al.* 2010). This difference does draw attention to the impact that various compounds may have on spore resistance, or more specifically how certain compounds may confer greater acidic resistance to the spore. In the study by Hirota *et al.* (2010) it is noted that ‘strong mineral acids rupture *Bacillus* spores by breaking down spore permeability barriers’ hence anything that may improve the robustness of the spore layers would be likely to increase acid resistance.

In addition, one also observes conditions (sample 3 vs 8 at pH 2.8 with 55mM HCl in Figure 5.3) where the addition of germinants leads to an increased DPA release but the observed viable counts reduction is not altered (Figure 5.2). At this point, it is necessary to question if the reduction of counts illustrate genuine lethality or whether another mechanism exerts an influence on the outcome of viable plate counts.

For a number of conditions, for example the decline in plate counts for samples 3 (pH 2.8, 55mM HCl) and 4, (pH 3.6, 45mM HCl) of 43 and 22% respectively, occurred without any release of DPA for the first 60 minutes (Figure 5.2 and 5.3). This finding is in agreement with observations recently reported by Setlow *et al.* (2013) where plate count data indicated 93-97% spore death but very little DPA release was recorded in the first 60 minutes. Setlow *et al.* (2013) shows that damaged spores release their DPA in a linear fashion as opposed to when they are germinating, where an exponential release is observed. This means DPA release occurs very rapidly with germinating spores, but relatively slowly when spores are damaged. Indeed, when spores are germinated, close to 100% of their DPA is released within 45 minutes, whereas when spores are killed with H₂O₂, less than 10% of their total DPA is released in 45 minutes, and even after 150 minutes, only 60% of the total DPA was released (Setlow *et al.* 2013). This was postulated to be caused by damage to one or several spore germination proteins.

Tanghe *et al.* (2006) supports this theory, suggesting that damage to spore channel proteins involved in the bulk intake of water would inhibit the release of DPA. This influx of

water is essential as in the spore core, DPA (Figure 5.13) is chelated with Ca^{2+} sometimes in equal proportions forming Ca-DPA. This molecule forms 10% of the total spore dry weight (Leuschner and Lillford 1999). Huang *et al.* (2007) carefully studied the amount of Ca-DPA present in the spore core and found that the concentration of Ca-DPA in the core to be between 800mM to 1M. Since the solubility of DPA is far below this value, at 100mM, in the spore core the DPA will be insoluble, especially when one considers that the spore core is between 30 to 50% hydrated (De Vries 2004).

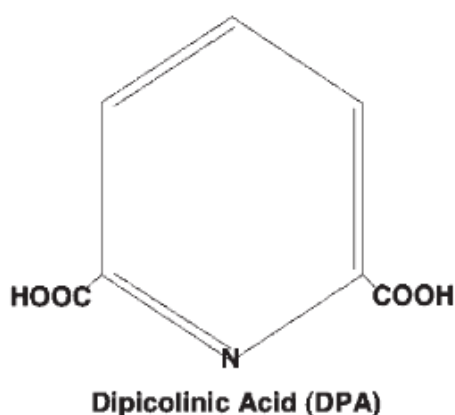


Figure 5.13 Structure of DPA from Yardimci and Setlow (2010)

This means that when DPA is released from the spore core, it needs to be extensively hydrated before it can exit. This hydration is largely accomplished by germinants binding to germinant receptors (Moir 2003), though such a rapid release of DPA, as seen in physiologically germinating spores, would require a very fast hydration. Such a rapid hydration would necessitate bulk water transport. This is only possible *via* the activation of aquaporins. These are known water channel forming proteins found in animals and more recently found in plant membranes. It has recently been suggested that *Bacillus* may have aquaporins, and indeed a possible sequence coding for an aquaporin related protein has recently been sequenced (Deng and Sun 2011). Whilst the existence of aquaporins remains under dispute, Setlow (2003) has shown that a CaDPA channel composed of SpoVA protein exists, supported by van Melis *et al.* (2011a) who have shown that sorbic acid can interfere

with the Ca-DPA channels. These are positioned in the spores inner membrane and outer membrane in numbers of 6000-8000 molecules per spore. It is known that these proteins are hydrophilic, though no detailed information on their mode of operation is known (Setlow 2013).

In summary, the data presented in Figure 5.2 and 5.3 could be ascribed to:

- a) a direct sporicidal impact of the conditions to which the spores are exposed
- b) a very slow release of DPA caused by damage to the inner spore membrane proteins
- c) the decline in counts is skewed by aggregation, and the actual decline in viability is much lower.

Given the fairly mild nature of treatments investigated in this chapter option a seems the least likely. Option b may have more weight, which would mean the DPA release percentage noted in Figure 5.3 only corresponded to the DPA release from the germinated spores as the limited 60 minute time frame would not provide enough time for the DPA to be released from the damaged spores. In short, the influence seen is down to the kinetics of DPA release from the spore and the data obtained in this experiment, could indicate that DPA release from the killed spores has not been completed.

Alternatively, option c also seems very plausible, that the perceived declines in plate counts are actually reflecting the increased levels of aggregation.

Importantly, the results shown do verify that germination induced death is a possibility in the gastric environment, and if aggregation is considered then the actual percentage of germination induced death could be far higher. Furthermore, the extent spore death in the gastric environment portrayed in the literature could be far less owing to the oversight of aggregation. In light of the aggregation phenomena there is more reason to believe that a germination induced mechanism is what causes the reduction in counts, rather than damage induced death. For example, if the actual reduction in viability was 50% less, it

would follow that the effect of germination induced mechanism was twice as high. This phenomenon is much more likely to have a profound impact when the pH is very low (<2.6).

From the experimental conditions investigated here, the data does not support the hypothesis that a significant loss of bacterial viability is caused by germination induced mechanisms. However, the data does clearly show that germination induced death mechanism does exist and would occur in the gastric environment. Such a mechanism could well contribute to the significant decreases in spore counts mentioned in the literature by Leser *et al.* (2008) though would not fully explain the extreme loss in viable counts.

5.4.2 Cell sorting

The cell sorting results are very promising, when comparing with the expected recovery rates of each region. Most prominently is the PI stained areas correlate with little to no recovery in any of the sorted plates. The maximum recovery is 3% (Figure 5.6) meaning that that PI can denote cell death with at least 97% accuracy. This result is similar to a study by Nebe-von-Caron *et al.* (1998) where PI positive stained *Salmonella typhimurium* were single sorted onto nutrient agar plates and showed no colony formation.

Another key outcome from the cell sorting is the fact that the regions denoted as 'noise' and debris, showed a maximum of 0.4% recovery (Figure 5.4). These results are very encouraging as it strongly suggests that the cell and spore regions are clearly defined based on their higher SSC and FSC signals, and smaller particles, even those which have stained, do not grow when sorted onto agar plates. This is shown by the sorting of region O, a PI positive region with a very low FSC signal, in Figure 9.11 c where no recovery was seen, and region G, a Syto 16 positive region with a very low FSC signal, in Figure 5.9 b. This indicates that FSC alone is a good detector of cells and spores.

Sorting of *Bacillus cereus* has been carried out by Want *et al.* (2011) using either a combination of DioC₆(3) and PI or RedoxSensor Green (an indicator of bacterial reductase activity) and PI, with successful results, however, this was performed on an asporulating

strain, therefore only vegetative cells were analysed in this work. This is the first time *B. subtilis* spores have been sorted based on their Syto 16 and PI staining profiles. As such, it appears that there is a good accordance between the staining profile region assignments and their recovery rates on agar.

6 Chapter Six: *In vitro* modelling of Pig stomach conditions

6.1 Introduction

Given that the region assignments were verified by cell sorting, the next stage in the research was to explore the effect of acid on spores in more depth. This was investigated as a basic means of determining spore behaviour in the gastric environment. It was hoped that through this experimental work, an understanding of the cause behind the reduction in spore count would be obtained.

6.1.1 *In vitro* conditions

Whilst studying the spores *in vivo* would be desirable, the use of an *in vitro* model, designed to mimic conditions seen in pigs is a clear alternative, without the need for killing or harming animals (Löwgren *et al.* 1989). In this study, spores of *B. subtilis* were subject to various acidic treatments designed as a simple means of mimicking the effects of the pig stomach (see Table 6.1). These treatments were derived from those reported in the literature (Cranwell *et al.* 1976; Löwgren *et al.* 1989; Ange *et al.* 2000; Mößeler *et al.* 2010).

Table 6.1 Composition of simulated gastric challenge to spores of *B. subtilis*

	Heat activation	pH	HCl (mM)	Medium	Temp	Time
Dormant	N	1.9	100	LB broth	37°C	60 and 120 minutes
	Y					
Pre-germinated	N					
	Y					
Dormant	N	2.6	55			
	Y					
Pre-germinated	N					
	Y					
Dormant	N	3.4	40			
	Y					
Pre-germinated	N					
	Y					

The reasoning behind assessing the impact of different acid concentrations and pH was due to the fact that pig gastric conditions will vary considerably as mentioned previously in Chapter 5.

By measuring the effect of these conditions on both dormant and pre-germinated spores the impact of different dosing methods could be predicted. Probiotic spores, whilst commercially available may be administered to pigs by mixing with pig feed and left throughout the day for pigs to be fed *ad libitum*. Problems arise from dosing the pigs in this manner, since the spores will inevitably be exposed to an uncontrolled environment. It is highly probable that the pigs themselves will transfer water from their water bottles to the feeding trough and the weather conditions (rain, humidity) could cause water to enter into the feeding area. Similarly during storage, it would be very difficult to keep the feed and spores dry, again due to the uncontrolled environment. An increase in the water activity (a_w) of the feed and spore mixture is therefore very likely. Since it has been previously shown that a_w as low as 0.5 can initiate germination of *B. subtilis* spores (depending on the environment) with typical a_w values around 0.7 to 0.8 causing germination (Marshall *et al.*

1963; Hagen *et al.* 1967) it would be very likely that at least part of the feed mix would contain areas with a_w at this level or higher. As such, by comparing the pre-germinated spores with the dormant spores, the impact of this pre-germination step could be explored. If this factor is shown to have a significant impact on viability, it could at least partially explain why probiotics do not always seem to have a beneficial effect on animals, as shown in a trial exploring the effect of Calsporin (a *B. subtilis* spore preparation), 3 out of 4 trials were shown to increase final body, daily weight gain and improve the feed to gain ratio, however in one trial consisting of 336 pigs, no significant effect was seen with the dosing of *B. subtilis* spores on any of these parameters (EFSA 2010b).

6.1.2 Heat activation

A common treatment administered to dormant spores noted in the literature is a wet heat activation to encourage germination. Optimal parameters for heat treatment will be both strain and medium dependent and for *B. subtilis* a range of treatments are reported. Yi and Setlow (2010) and Luu and Setlow (2014) report that a sample of spores with an OD₆₀₀ of 20 should be heat activated for 30 minutes at 75°C. Others have treated for 30 minutes at 70°C (Cowan *et al.* 2003; Zhang *et al.* 2011a) while Leuschner and Lillford (1999) employed a heat activation of 10 minutes at 65°C. Conversely, Paidhungat *et al.* (2002) noted that heat activation is not required for *B. subtilis* to achieve high levels of germination. In reality, an equivalent level of thermal energy may be delivered to the spores during spray drying, which is a key process for production of probiotics on an industrial scale.

As such, it was deemed necessary to explore the effect of heat activation, given that in Chapter 5 it became clear that germination induced lethality in the GIT could be significant. To investigate the effect of pre-germination, heat activation and HCl concentration on the viability and the physiology of probiotic spores, both conventional and novel methodologies were used. Culture of bacteria on solid media was undertaken since this is the gold-standard methodology commonly used to assess bacterial viability, but alongside this, FCM was also implemented. The benefit of using FCM analysis in this study

was that the physiological state of the spores could be analysed and equally importantly, the total counts (i.e. both viable and non-viable) of spores could be determined. This is of importance should one consider the possibility of aggregation within the system, as plating relies on the assumption that one bacterium will produce one colony, whereas in reality, this may not be the case.

6.1.3 Aims and objectives

- To explore the viability of both dormant and germinating spores subject to 40, 55 and 100mM HCl
- Keep track of total cell and spore numbers following exposure to each treatment condition *via* FCM

6.2 Materials and Methods

6.2.1 FCM settings

The FCM model used in these studies is the BD FACSCalibur, equipped with a 15 mW, 488 nm air-cooled argon ion laser. BD CellQuest Pro software was used for setting and acquiring data.

All sample analysis was collected using the cytometer 'low' setting, with data acquisition set to 20,000 events or 300 seconds. Two data acquisitions were performed, once using the FSC trigger with threshold set to 190 and a second acquisition using the Side Scatter (SSC 390). The E01 voltage setting was selected for the Forward Scatter (FSC) channel. The Photomultiplier detector (PMT) voltage settings for each of the three fluorescent detector channels used in the studies were: a.) Green Fluorescent channel 1 (FL1) 595, b.) Red Fluorescent channel 2 (FL2) 634 and c.) Far Red Fluorescent Channel 3 (FL3) 683. Under these settings, unstained cells were kept in the first decade of the FL1 versus FL3 density plots. Compensation settings were FL2 to FL1 30.6% and FL3-FL2 12.7%. These were checked monthly using single stained cells and spores. The 'low' flow rate setting was selected corresponding with a flow of 12 μ L/min (Picot *et al.* 2012).

6.2.2 FCM Enumeration

The FCM settings used for the trials were the same as those in 6.2.1

For each sample, 10 μ l of spore stock (spores generated according to Section 5.2.1) was placed in 440 μ l of filtered PBS containing 1.5 μ M Syto 16 and 48 μ M PI. 20 μ l of Spherotech beads were added (1x10⁷beads/ml).

Enumeration was achieved by using 20 μ l of Spherotech Beads in each sample. The counts/ml were then calculated using the following equation from Khan *et al.* (2010):

Equation 6.1 Conversion of FCM events into counts/ml using counting beads

$$\frac{\text{no. of events in cell region}}{\text{no. of events in bead region}} \times \frac{\text{no. of beads/test}}{\text{test volume}} \times \text{dilution factor}$$

Results from the FCM were analysed first through FSC vs SSC plots to give us bead counts and total cell and spore counts. These data were then transferred to FL1 vs FL3 density plots to see each sub-population. To compare the FCM with plating results the counts of cells and spores in the dormant and viable regions were added together to get a total viable count. These were then compared with plate counts which can only show viable counts.

Treatments with HCl were undertaken as described in Table 6.1, based on representative values reported across the literature. The samples were analysed 60 and 120 minutes after exposure to the LB/HCl mix. For each HCl concentration, a heat activated (HA) (70°C for 30 minutes) and a non-heat activated (NHA) sample were compared. For each concentration of HCl used, there were two experimental set-ups.

- a) Dormant spores: In the first set-up 200 μ l of dormant spore stock (ca. 2 x 10⁸ spores/ml) was added directly to 800 μ l of the HCl/LB mixture in a microtube. These were vortexed for 15s, 10 μ l removed and added to a microtube containing the FCM staining mixture (as described at the beginning of Section 6.2.2) and another 100 μ l was pipetted into a tube containing 900 μ l PBS for plating.

- b) Pre-germinated spores: The alternative experimental set-up involved a pre-germination step, where 200µl of dormant spore stock were placed in LB broth for 30 minutes at 37°C and following this, the appropriate amount of HCl was added to initiate the experiment (time 0), vortexed for 15s and then 10µl removed and added to a microtube containing the FCM staining mixture (see first paragraph Section 6.2.2) and another 100µl was pipetted into a tube containing 900µl PBS ready for plating.

As soon as the time 0 samples had been taken, the microtubes were placed in a beaker and into a rotating incubator set to 37°C at 200rpm. Further samples were taken at 60 and 120 minutes. The pre-germination step was designed to initiate a significant amount of germination without outgrowth. The previous work in Chapter 5 has revealed that spores very quickly germinate in LB broth, indicated by the Syto 16 uptake, whereas the outgrowth process is not initiated till much later (Pelczar *et al.* 2007; Pandey *et al.* 2013).

6.2.3 Plating

As described in Chapter 5, to assess the viability of the samples after treatment the Miles and Misra method for plating was undertaken (Miles *et al.* 1938). Plates of LB agar were used (12g/L agar with 25g/L LB broth) which were dried thoroughly before plating, and were divided into six segments. Each segment was used for one serial dilution ranging from 10^{-1} to 10^{-6} . A 20µl droplet was placed in each segment with the respective dilution and left for an hour to dry. Plates were inverted and incubated at 37°C for 24 hours.

Counts were taken from the segments which showed between 8 and 80 colonies. Segments with counts outside this range were deemed either too numerous to count or too low to be significant.

6.2.4 Viability of spores in simulated gastric conditions

For simplicity, LB broth was used to simulate a liquid meal (such as milk), due to its high nutrient content. This system was put in place since probiotics are mixed with feed

prior to be given to pigs. Briefly, the spores were immersed in LB broth with different amounts of HCl at 37°C and analysed after 60 minutes and 120 minutes. These time intervals were selected based on the fact that stomach half emptying time for a liquid meal is 30 minutes (Anderson *et al.* 2002). Spores were heat activated (HA) at 70°C for 30 minutes prior to experimentation, and compared with non-heat activated spores (NHA).

6.2.5 Statistics

The experiments were performed in triplicate, and the 95% confidence intervals (95% CI) were calculated in Excel, using an alpha of 0.05. Bacterial counts were converted *via* a log₁₀ transformation.

6.3 Results

6.3.1 FCM output from acid treated spores

To calculate the viability of spores based on their FCM profiles, it was necessary to determine the regions corresponding to viable spores and cells compared to the non-viable spores and cells. Since the cell sorting undertaken in Chapter 5 has shown that the staining profiles correspond well with recovery rates, the regions denoted as viable could be confidently denoted as presented below in Figure 6.1, which depicts a typical example.

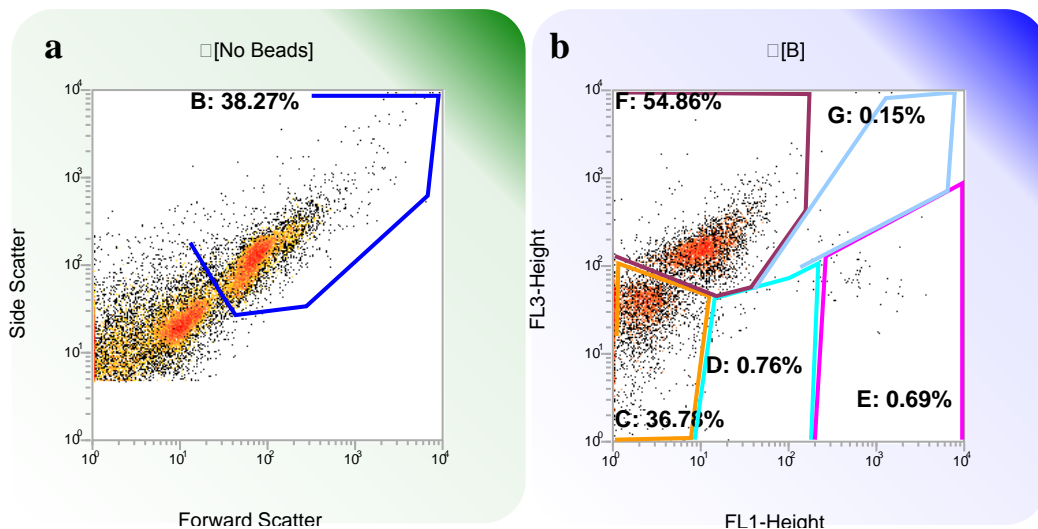


Figure 6.1 a) FSC vs SSC density plot of heat activated spores immersed in 55mM HCl for two hours, Region B denotes the cell and spore population. b) FL1 vs FL3 density plot gated on region B. Region C (orange) Dormant spores, Region D (turquoise) germinating spores, Region E (pink) outgrown spores/live cells, Region F (Burgundy) Dead cells and dead spores and Region G, double stained cells and/or cell doublets.

In the example given above, regions C, D and E would correspond to viable regions, and region B would yield the total counts. Since Region G would contain viable and non-viable events, 50% of the events in this region could be added to the other viable counts to obtain the total viable counts. Though in all samples, the events in this region were quite low so this will not have a drastic impact on viable counts.

6.3.2 Effect of 40mM HCl on spores in LB broth

Spores were immersed in LB broth with 40mM HCl for up to two hours, and analysed at 0, 60 and 120 minutes (Figure 6.2). Samples were analysed using FCM and plating. FCM viable counts were calculated by adding the events which did not stain, such as those seen in region C in Figure 6.1 b. (dormant spores) and events that stained with Syto 16 (germinating spores and cells) corresponding to region C and D in Figure 6.1 b. PI stained events were not classed as viable, since their recovery rates were shown to be very low. These were therefore not included in the viable count. In Figure 6.3, the spores were immersed in the same concentration of HCl (40mM) though for this experiment, the spores

were pre-germinated by immersion in LB broth at 37°C for 30 minutes prior to the addition of acid. The results for the plating and FCM counts are presented on the next page.

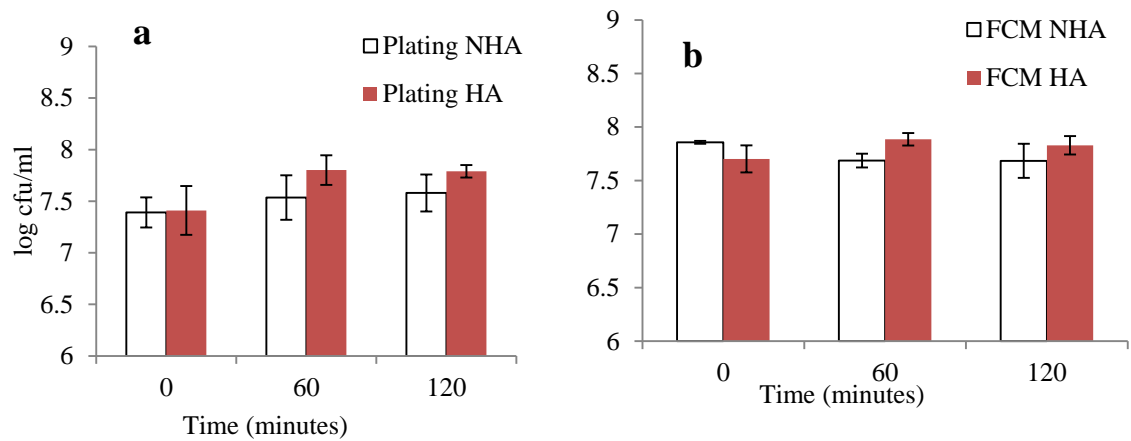


Figure 6.2 40mM HCl on dormant spores of *B. subtilis*, showing log (10) transformed data a) plating and b) viable FCM counts. Error bars represent the 95% CI where n=3. Shaded bars refer to heat activated (HA) spores and white bars denote the non-heat activated (NHA) spores.

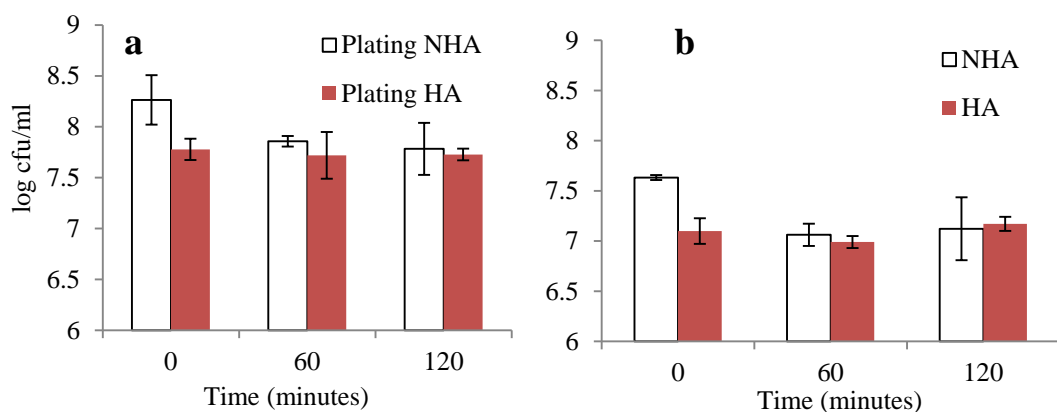


Figure 6.3 40mM HCl on pre-germinated spores, showing log 10 transformed a) plating counts and b) viable FCM counts. Error bars represent the 95% CI where n=3. Shaded bars refer to heat activated (HA) spores and white bars denote the non-heat activated (NHA) spores.

The plating results show that for the non-heat activated (NHA) samples, at 40mM HCl (pH3.4), there was no statistically significant decline ($p>0.05$) in viability seen for dormant spores (Figure 6.2 a) and for the HA spores, there was actually a statistically significant increase ($p<0.05$) in viable spore count after 120 minutes from time 0.

Similarly the FCM data indicates that the HA activated spores also increased in count, though this increase was within the statistical error ($p>0.05$). For the NHA spores in both intervals measured (60 and 120 minutes) a trend of reduction in viability, however only at 60 minutes is a statistically significant difference between the starting count observed ($p<0.05$).

It is unusual that in this experiment there was no impact seen on viability *via* plating, whereas in Chapter 5, where the impact of viability was assessed at pH 4 in PBS (50mM) (Figure 5.3) there was a 25% decline in viability. This would indicate that the different medium the spores are immersed in has a clear impact on viability, perhaps showing that the LB broth increases spore survival.

In Figure 6.3 b the FCM data shows there is a statistically significant decline seen in the NHA pre-germinated spores by FCM of 74 and 68% after one and two hours respectively ($p<0.05$). Similarly, a significant difference is seen in viability *via* plating Figure 6.3 a after two hours at 40mM HCl, illustrated by the non-overlapping 95% CI bars.

No statistically significant differences ($p<0.05$) were observed in the case of HA pre-germinated spore counts *via* either method.

6.3.3 Effect of 55mM HCl on spores in LB broth

Figure 6.4 shows spores exposed to 55mM HCl in LB broth (pH 2.7). The dormant spores were immersed in LB broth with the HCl already present and Figure 6.5 shows pre-germinated spores exposed to 55mM HCl in LB broth.

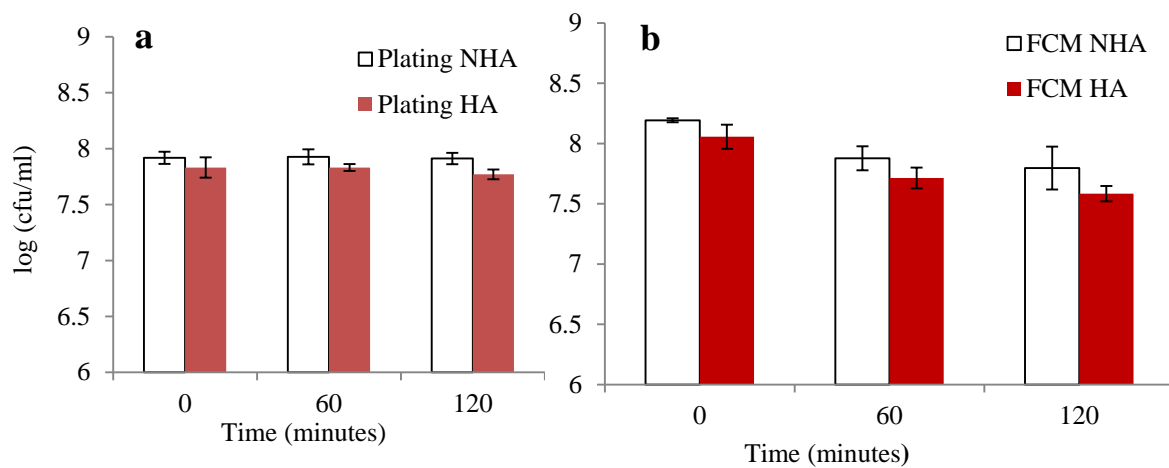


Figure 6.4 55mM HCl (pH 2.6) on dormant spores, showing log (10) transformed viable counts by plating (a) and by FCM (b). Error bars represent the 95% CI, where n=3. Shaded bars refer to heat activated (HA) spores and white bars denote the non-heat activated (NHA) spores.

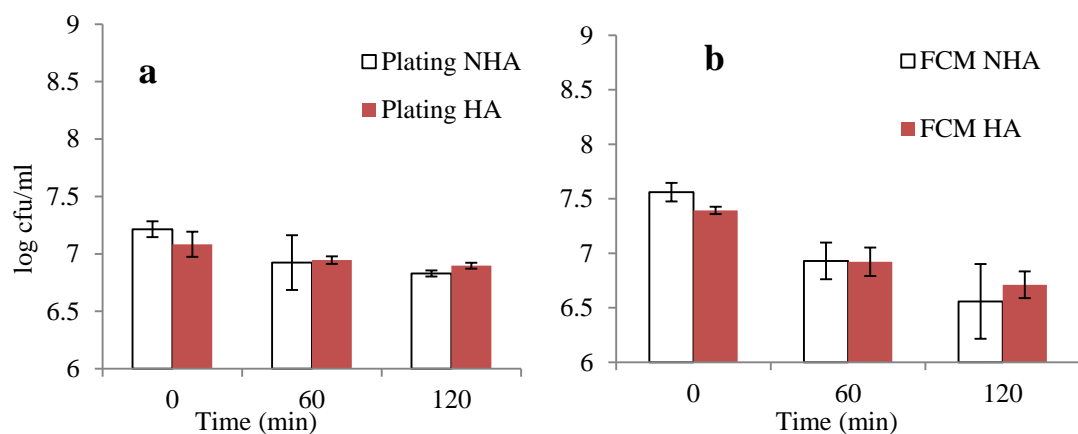


Figure 6.5 55mM HCl on pre-germinated spores, showing log (10) transformed viable counts by plating (a) and FCM (b). Error bars represent the 95% CI, where n=3. Shaded bars refer to heat activated (HA) spores and white bars denote the non-heat activated (NHA)

There is a statistically significant decline in counts seen for each treatment condition on dormant spores according to the FCM analysis (Figure 6.4 b). For the NHA samples this decline reaching a level between 52-60% over the duration of two hours. The decline in viability for the HA samples is slightly greater, from 67 to 75% over the two hours.

By contrast, the plating data (Figure 6.4.a) shows very little impact on dormant spore viable counts. There is a small decline in counts for the HA samples, however this decline does not fall outside the statistical error.

When the spores are pre-germinated, the effect of 55mM HCl is far more severe, with a statistically significant loss in viable counts seen in all cases *via* FCM reaching a 90% decline ($p<0.05$) after two hours for NHA spores and 86% decline ($p<0.05$) for the HA spores (Figure 6.5 b).

A significant decline of 51% ($p<0.05$) is seen *via* plate counts for the HA samples after two hours (Figure 6.5 a). The decline in plate counts is greater when there is no heat activation (NHA), where the average viable count decreases significantly by 59% ($p<0.05$) after two hours.

6.3.4 Effect of 100mM HCl on spores in LB broth

Figure 6.6 shows dormant spores exposed to 100mM HCl in acidified LB broth (pH 1.9) and

Figure 6.7 shows pre-germinated spores exposed to 100mM HCl in LB broth.

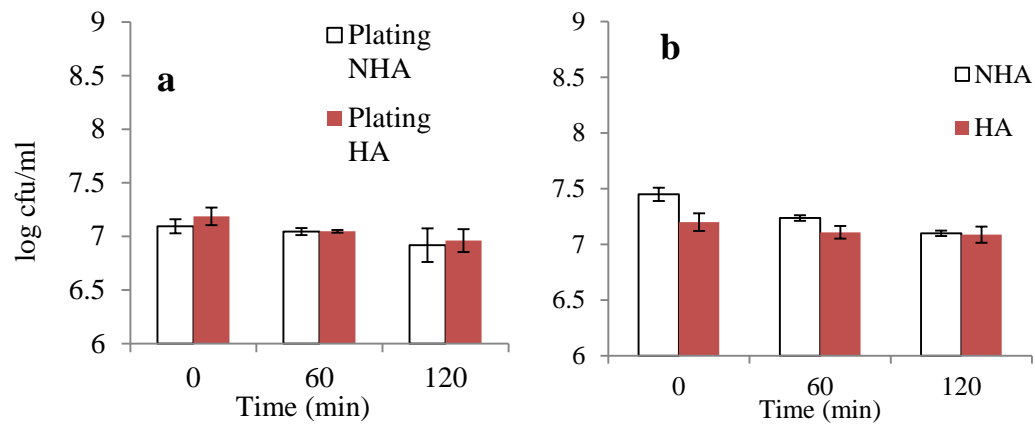


Figure 6.6 100mM HCl on dormant spores, showing log 10 transformed viable counts by plating (a) and FCM (b). Error bars represent the 95% CI, where n=3. Shaded bars refer to heat activated (HA) spores and white bars denote the non-heat activated (NHA) spores.

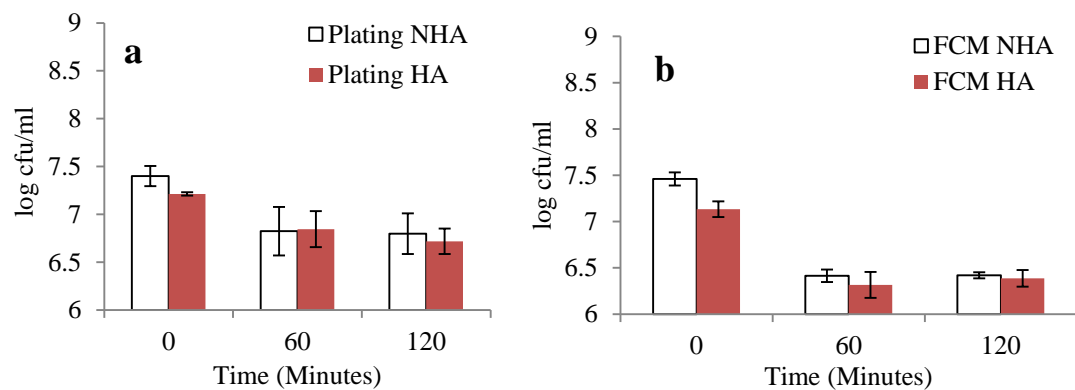


Figure 6.7 100mM HCl on pre-germinated spores, showing log 10 transformed viable counts by plating (a) and FCM (b). Error bars represent the 95% CI, where n=3. Shaded bars refer to heat activated (HA) spores and white bars denote the non-heat activated (NHA) spores

No statistically significant differences were revealed on viable plate counts for NHA dormant spores. Although a downwards trend was suggested from the corresponding plating data after two hours. FCM on the other hand, illustrates a significant decline ($p < 0.05$) for the NHA dormant spores of 39 to 55% loss in viable counts after one and two hours respectively (Figure 6.6. b).

The HA dormant spores do significantly decline in plate count by 40% ($p < 0.05$) after two hours (Figure 6.6.a). However, no statistically significant differences ($p > 0.05$) were revealed in the FCM obtained viable counts for HA dormant spores. HA dormant spore counts do still fall by 23% after two hours based on the FCM data (Figure 6.6 b).

For germinating spores (Figure 6.7), there is a clear significant decline ($p < 0.05$) in viability shown through both methods. For the FCM counts (Figure 6.7 b) this decline is greater than 90% reduction in all conditions. The plating data shows the decrease ($p < 0.05$) in viability ranges from 58% for HA germinated spores after one hour, up to 75% in NHA germinated spores after two hours.

6.3.5 Assessment of total counts

One main advantage of FCM analysis is that the entire population can be monitored and counted. Accordingly, the total counts in the system were checked, by using the number of events from Region A of the beads (Figure 6.8.a.) and the number of events found in the total population from region B in Figure 6.8.b. in the example given below. The numbers of events in each region were input into Equation 6.1 as described in Section 6.2.2 to generate the total counts/ml.

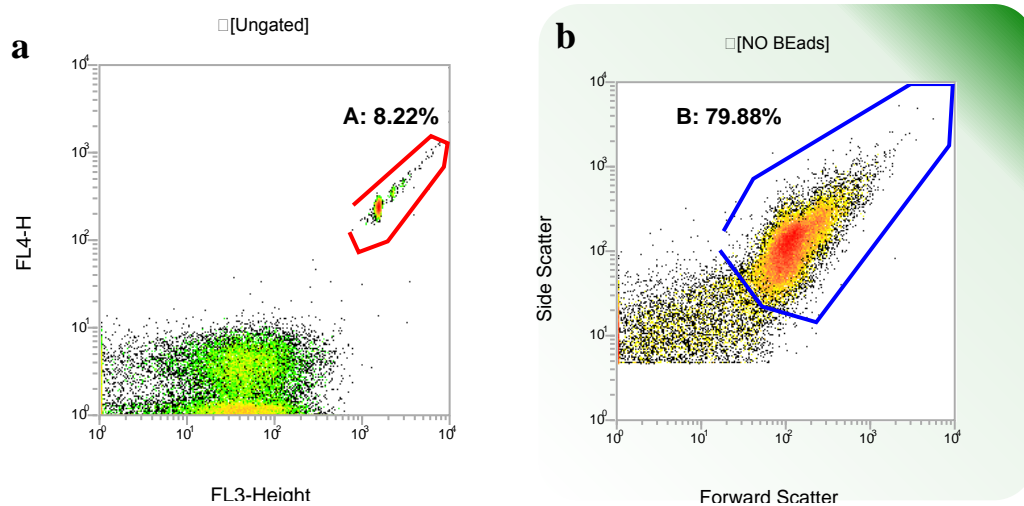


Figure 6.8 a) FL3 vs FL4 density plot for HA sample subject to 40mM HCl for 60 minutes, region A is drawn around the bead population b) Gated FSC vs SSC density plot using equation NOT A to remove beads. Region B denotes the cell and spore population.

These percentage reductions in total count are presented on the following page in Figure 6.9.

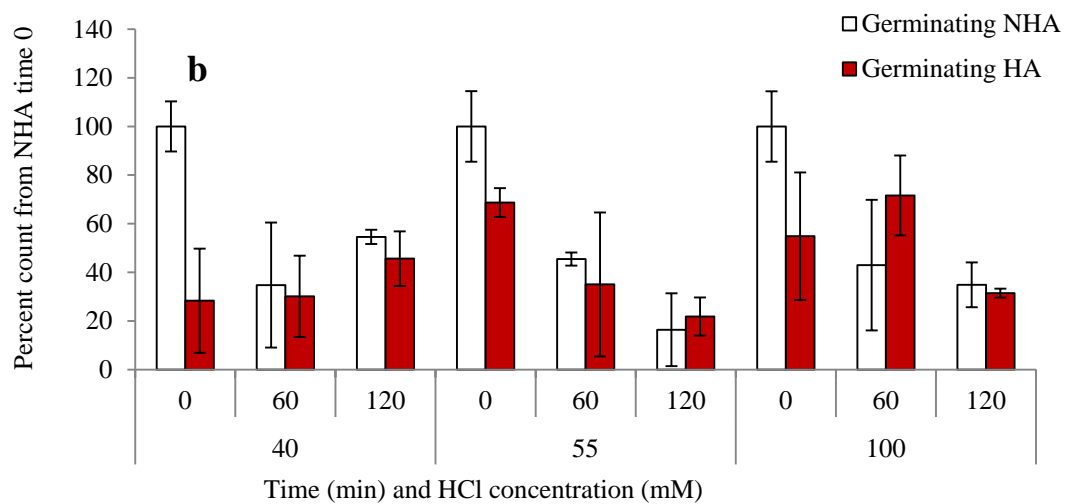
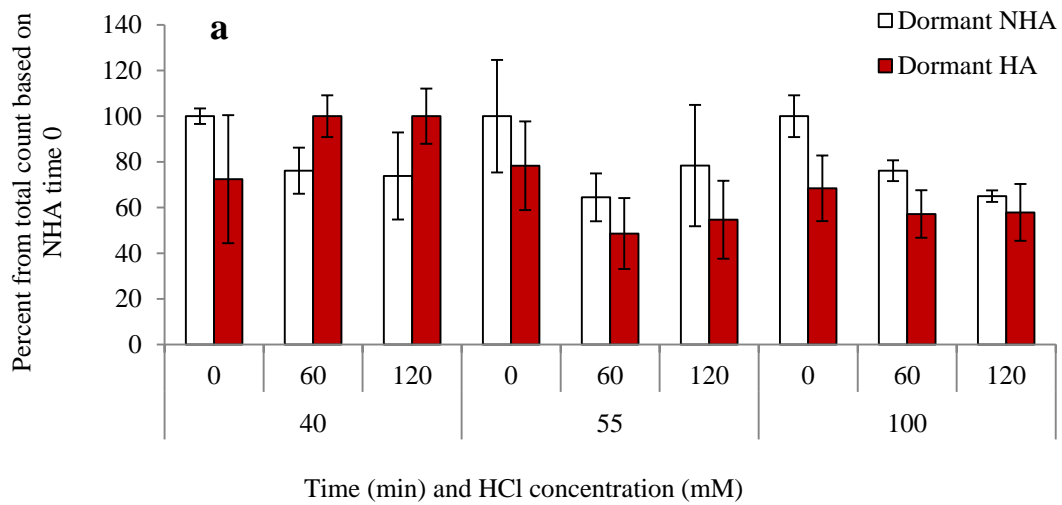


Figure 6.9 Percentage of total count for each sample in relation to the total count at time 0 for NHA spores. Error bars represent the 95% CI. a) Shows the dormant spores and b) the pre-germinated spores.

The total counts for the NHA dormant spores at time 0, were attributed to 100% of the total count, however it should be noted that this is an arbitrary denotation and it is very likely that this first count will also reflect a level of aggregation inherent in the samples. Therefore it is only possible to observe the relative decline from this point.

Comparing the total count values at time zero for NHA and HA for either dormant spores (Figure 6.9 a) or pre-germinated spores (Figure 6.9 b) it is evident that NHA counts are systematically higher than HA counts, thus it can be concluded that during heat activation the spore samples suffered aggregation. This is based on the fact that at time 0, there is no treatment given to the spores, other than the heat activation, which should not cause a decline in viability since spore purities are 95%, and all spores have been previously treated with 50% EtOH to kill off remaining vegetative cells. The data clearly show a significant decline ($p < 0.05$) for all the time 0 HA samples except the dormant 40 and 55mM treated samples where there is still a decline though it does not fall outside the statistical error ($p > 0.05$).

For all dormant samples (Figure 6.9 a), maximum total counts are achieved at time zero with total counts at 120 minutes to be the lowest or similar to the respective 60 minute counts within the statistical error. Interestingly FCM data reveals a similar pattern between the total count change (Figure 6.9 a) and the viability change (Figure 6.2 b, Figure 6.4 b, & Figure 6.6 b) suggesting a proportion of the perceived decline in total counts may be due to aggregation.

At 40mM HCl treatment, the NHA dormant spore total count undergoes a statistically significant reduction by 24 and 26% after 60 and 120 minutes ($p < 0.05$). The HA dormant spores subject to 40mM HCl do not suffer a statistically significant reduction in counts ($p > 0.05$) illustrated by the overlapping error bars in Figure 6.9 a.

For NHA dormant spores immersed in 55mM HCl the decline in total counts do not fall outside the statistical error ($p > 0.05$). For the HA dormant spores the decline in counts does fall by a statistically significant amount ($p < 0.05$) with a 51% decline in total count reached after 60 minutes (Figure 6.9 a).

The decline in total counts is statistically significant for NHA dormant spores at 100mM HCl treatment ($p < 0.05$). Interestingly the observed decline in viable counts (Figure

6.6 b) is only 10-20% lower than the percentage decline in total counts. It could be confirmed that the actual loss in viability is at least equal to the difference between the total count decline and the viable decline i.e the minimum decline in viability is 10 and 20% but could be as high as 39-55% (Figure 6.6 b).

Similar to the dormant spores, for all pre-germinated samples (Figure 6.9 b), maximum total counts are achieved at time zero with total counts at 120 minutes to be lowest or similar to the respective 60 minute counts within the statistical error. Interestingly again, a similar pattern between the total count change (Figure 6.9b) and the FCM viability change (Figure 6.3b, Figure 6.5b, & Figure 6.7 b) is becoming apparent, suggesting a proportion of the perceived decline in total counts may be due to aggregation. Comparing the total counts between dormant spores (Figure 6.9 a) and pre-germinated spores (Figure 6.9 b) at similar *in vitro* conditions a greater total count decline is evident for pre-germinated spores.

For the NHA pre-germinated spores at 40mM the decline in perceived viable counts closely matches the decline in total count, with a maximum difference of 21% for the sample after 120 minutes (Figure 6.3 b and Figure 6.9 b). The decline in HA pre-germinated total spore counts and total decline in viable counts are more similar, with a maximum difference in viable decline to total decline of 10% after 120 minutes.

Similarly, at 55mM HCl (Figure 6.5 b and Figure 6.9 b), the decline in total count corresponds closely with the decline in viability with a maximum of 22% difference between these counts after 120 minutes for the NHA pre-germinated samples but only 11% difference in the HA pre-germinated spores.

This trend continues to 100mM, where the decline in total counts was 28 to 69% but the decline in viability according to FCM was >90% (Figure 6.7 b and Figure 6.9 b). This may indicate that a minimum decline in viability was 23% (seen after two hours for the HA sample) by calculating the difference between the decline in total counts with the decline in

viable counts. Though the difference in total counts to viable was as much as 65% after one hour for the HA pre-germinated spores, indicating a much higher minimum death toll.

6.3.6 Assessing FCM sub-populations

Due to the phenomenon of aggregation, it is not possible to assess the decline in counts *via* cfu/ml alone as one cannot be sure about the absolute number of non-viable cells following exposure to each studied condition. The FCM event collection approach registers one aggregate as one event, despite this particle potentially containing hundreds of spores. The size of these aggregates can be estimated *via* FCM by using size calibration beads and their FSC signal, which is largely related to particle size. Size calibration beads are represented below in Figure 6.10.

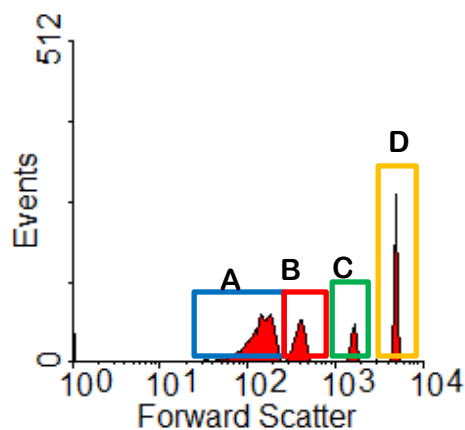


Figure 6.10 FCM output for size calibration beads on a single parameter histogram of Forward scatter (FSC) vs number of events. Region A: 1 μ m beads, Region B: 2 μ m beads, Region C: 4 μ m beads, and Region D 6 μ m beads. (Displayed using WinMDI software).

Using this example of size beads illustrates roughly where a particle of a particular size would lie on the FSC scale under the E01 setting. For example the beads of 4 μ m in diameter and greater fall beyond the 10³ point on the FSC scale, implying that particles of 4 μ m and above would have a signal in the 10³-10⁴ decade.

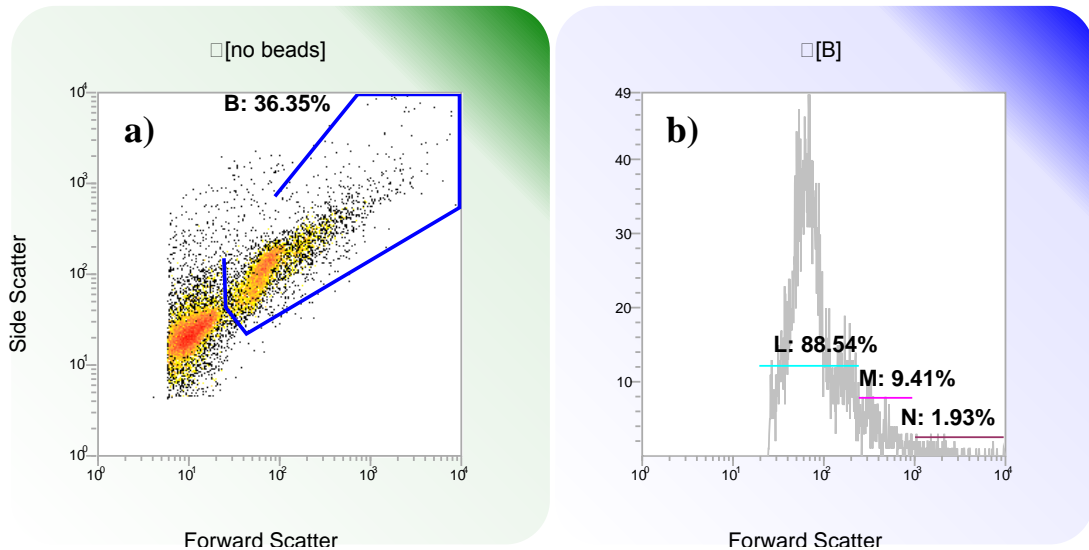


Figure 6.11 FCM analysis of a NHA sample of dormant spores subject to 55mM HCl for 120 minutes
 a) Gated FSC vs SSC density plot using equation NOT A to remove beads. Region B denotes the cell and spore population. b) Single parameter histogram of FSC vs number of events where Region L incorporates particles of $\leq 1 \mu\text{m}$, Region M approximately $2 \mu\text{m}$, and Region N particles greater than $4\mu\text{m}$.

On the forward scatter scale it appears that the impact of the larger particles is not always very profound, given the small percentage of events in this region. However the profound effect comes from the fact that depending on the aggregate size, one registered event could contain from a few tens up to a few hundred spores, therefore the effect of aggregation will have a minute effect on the viability profile in terms of percentages. To gain a rough idea of how many spores may be lost in these aggregates the assumption could be made that an aggregate has a spherical shape (this is only an approximation, aggregates will not be perfectly spherical) and then based on the volume of a sphere the number of spores in an aggregate of a particular diameter could be estimated using the volume of a sphere, i.e.

$$V = \frac{4}{3} \pi r^3$$

It is known that a spore has a diameter of ca. $0.5 \mu\text{m}$, therefore by calculating the volume of a spheroid aggregate and dividing this by the estimated volume of a spore, the number of spores per aggregate could be estimated. This is displayed below in Table 6.2. A spore will

have a more ellipsoid shape therefore the volume of a single spore would be better calculated using a cylindrical model:

$$V = \pi r^2 h$$

The spore dimensions could be approximated to 0.5 x 1µm therefore the volume of one spore would be 0.2µm³

Table 6.2 Particle volume analysis based on particle diameter

Particle size height (µm)	Particle size diameter (µm)	Volume (µm ³)	Estimated number of spores
1	0.5	0.2	1
	1	0.5	2-3
	2	4.2	21
	4	33.5	171
	6	113.1	576

As stated in Section 6.2.1, event collection was set to 10,000, which would mean that even if just 1% of the total events registered had a FSC signal greater than the 10³ mark, this would mean that 100 events were particles with a diameter greater than 4µm. Given that an aggregate of 4µm diameter would contain approximately 171 spores based on a spherical model (Table 6.2), it could be estimated that between 17,100 and 57,600 spores could be in this 1% of total events collected.

However, the death toll can still be quantified by assessing the FCM sub-populations, since PI has been shown to be a good indicator of loss of viability, and the aggregates themselves only form a small percentage of the total events collected. Thus the percentage change in PI positive events will mainly reflect the non-aggregating spores as the larger events constitute less than 5% of the total events (Figure 6.11 b) meaning the non-viable cells and spores could be denoted as a percent of the FCM events registered following

exposure to each studied condition. This information, although semi-quantitative still allows one to infer the level of lethality imparted on the cell population as a result of the investigated condition. Conditions that impart lethality should have a high percentage of events that take up PI. Therefore the difference between the % PI positive events between the starting time and the end time of a treatment could a reasonable, albeit semi-quantitative, measure of the lethality inducing potential of the treatment under the studied duration. An example of this PI uptake is shown on the FCM plots in Figure 6.12.

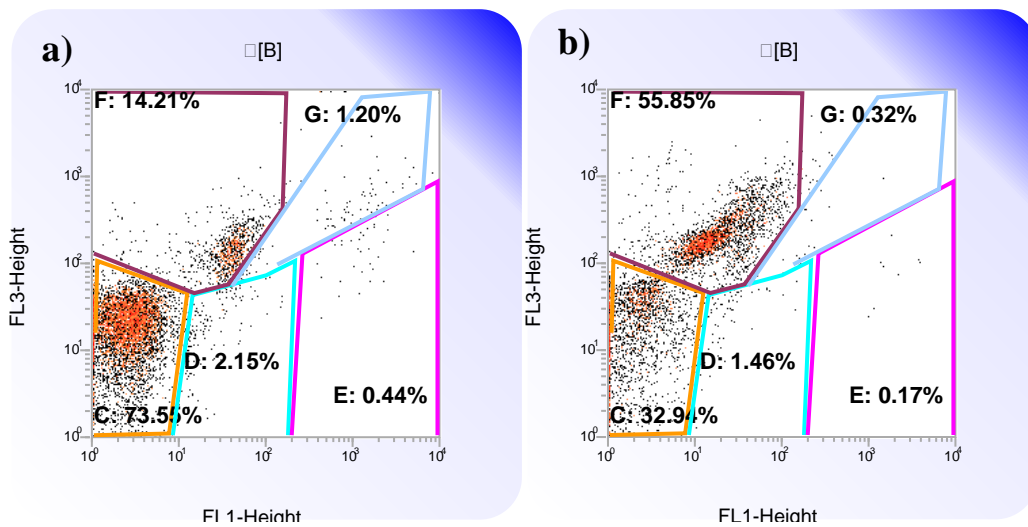


Figure 6.12 Representative FCM analysis of pre-germinated spores immersed in 55mM HCl in LB broth displayed on FL1 vs FL3 density plot at a) time 0 and b) 120 minutes. Region C: dormant spores, Region D: Germinating spores, Region E: Live cells and outgrown spores, Region F: Dead spores and cells, Region G: Cell doublets.

In this typical example, the change in profiles following the addition of HCl is demonstrated through the high percentage of events in the dormant spore region C at time 0 (74%) with only 14% of the events populating the ‘Dead’ region F. After 120 minutes, the percent events in this region reaches 56% and the percentage events in the dormant region is reduced to 33%. Using the percentage events from region F, Figure 6.13 was constructed to show the percentage increase of events in this region for all samples.

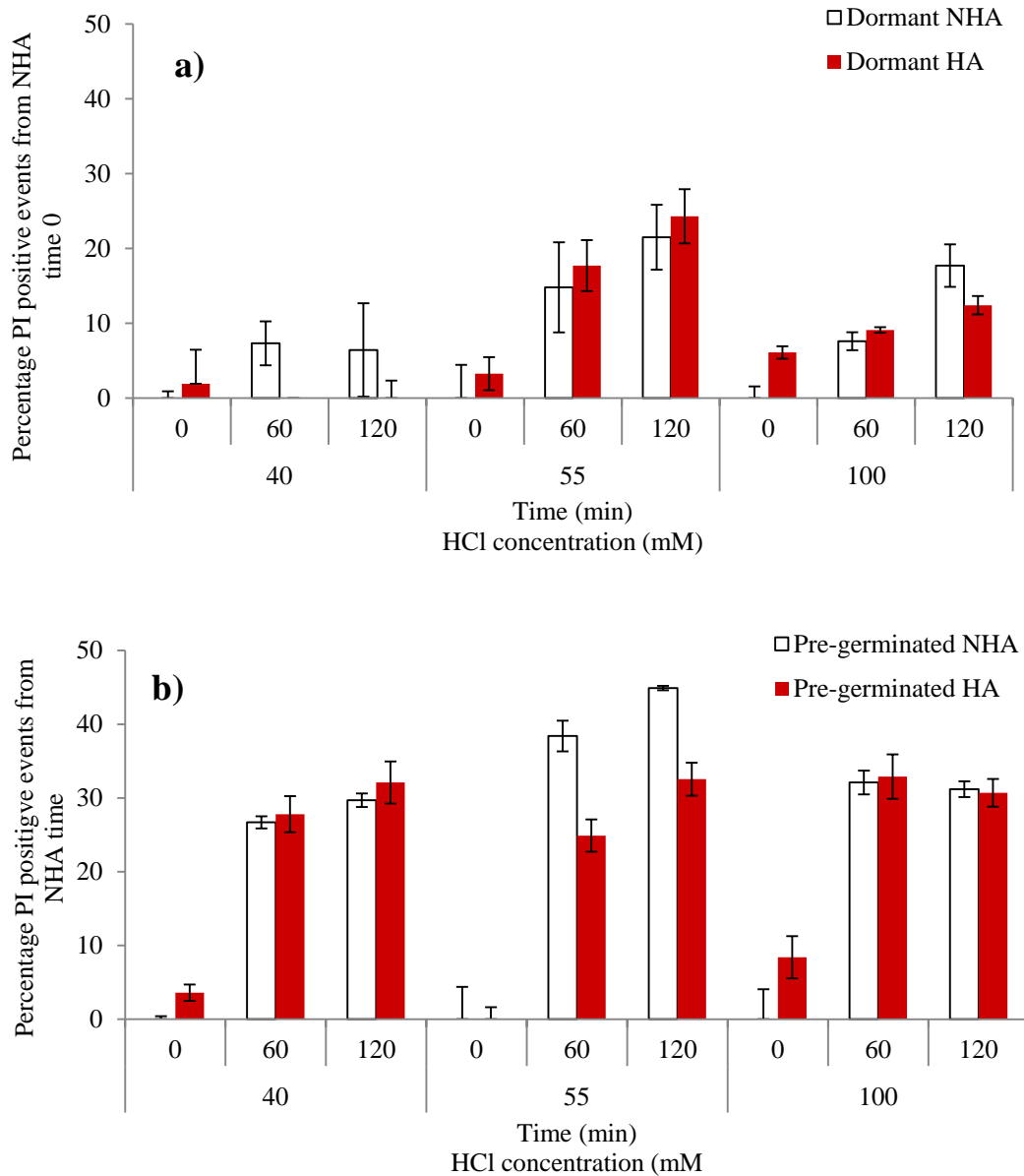


Figure 6.13 Percentage increase in PI positive events of a) dormant spores immersed in 40, 55 and 100mM HCl in LB broth and b) Pre-germinated spores immersed in 40, 55 and 100mM HCl. Error bars represent the 95% CI where n=3.

A comparison between the percentage increase in PI positive events between the dormant and pre-germinated spores shows a significantly higher lethality when spores are germinated in each case ($p < 0.05$). The effect of pre-germination is particularly relevant at 40mM HCl, which has little to no effect on the viability of HA dormant spores, but which causes a 28 and 32% increase in PI positive events on HA pre-germinating spores.

The NHA dormant spores subject to 40mM HCl increase in percentage of PI positive events after 60 minutes is statistically significant ($p < 0.05$) though after 120 minutes the percentage PI positive events do not fall outside the statistical norm ($p > 0.05$). The HA dormant spores show no statistically significant change in PI positive events ($p > 0.05$).

By contrast, the NHA pre-germinated spores show a 27 and 30% increase in PI positive events over 60 and 120 minutes and similarly the HA pre-germinated spores percent PI positive events increase by 24 and 28% over 60 and 120 minutes all of which are statistically significant ($p < 0.05$).

The NHA dormant spores subject to 55mM HCl undergo a statically significant increase in percentage PI positive events of 15 and 22% after 60 and 120 minutes respectively ($p < 0.05$). The HA dormant spores show a similar trend with a statistically significant increase in the percentage PI positive events of 18 and 24% after 60 and 120 minutes ($p < 0.05$).

The NHA pre-germinated spores subject to 55mM HCl show a 33 and 45% increase in PI positive events over 60 and 120 minutes and similarly the HA pre-germinated spores percent PI positive events increase by 25 and 33% over 60 and 120 minutes again these percentage increases are all statistically significant ($p < 0.05$).

NHA dormant spores subject to 100mM HCl undergo a statistically significant increase in the percentage PI positive events of 8 and 18% over 60 and 120 minutes ($p < 0.05$). The HA dormant spores show a similar trend with a statistically significant increase in the percentage PI positive events of 9 and 12% after 60 and 120 minutes ($p < 0.05$).

Whilst the NHA pre-germinated spores treated with 100mM HCl had a very high decline in viability according to FCM (>90%) PI positive percentages still significantly increase by 32% after 60 minutes ($p < 0.05$). Similarly, the HA pre-germinated spores

percentage PI positive events significantly increased by 22 and 24% over 60 and 120 minutes ($p < 0.05$).

6.4 Conclusion

6.4.1 Comparison of methodologies

Whilst plating has long been considered a suitable method for determining the levels of viability in different samples, it remains a very limited tool. This is due to the fact that only the reduction in colony forming ability can be quantified from the starting point. On the other hand, the insights possible through FCM can enable a much more detailed picture to be seen. For example, given the results from Section 6.3.2 to 6.3.4 the plating and FCM viability counts alone would imply large death tolls. However, by harnessing the potential of FCM to monitor the total counts in a given sample, the resulting decline in total numbers were noticed which then led to the deeper analysis of the data generated thus far. It was only by implementing the FCM methodology that this issue was highlighted, leading to an investigation into what other phenomena could be driving the total decline in count.

6.4.2 Effect of simulated feeding and gastric conditions on spores

The most significant effect seen throughout these studies is that of pre-germination. Where spores remain dormant, the impact on viability is systematically less than the equivalent conditions when spores are pre-germinated. Though the initial FCM viability analysis using counts/ml would indicate that spores which have been pre-germinated can suffer up to greater than a 1 log reduction in count following one hour exposure to 100mM HCl in LB broth (Figure 6.7 b) with the additional experimental insights generated in this research, it cannot be soundly concluded that the reduction in germinating spore counts it is more likely that a 45% reduction would be the largest decline seen (Figure 6.13 b). Interestingly the significant increase in PI positive events for pre-germinated spores exposed to 40mM HCl emphasises the fact that pre-germination can make spores susceptible to even

weakly acidic environments (Figure 6.13). This compliments previous studies on *B. cereus* where dormant spores remain fairly resistant to acidified media (J broth) at up to pH 1.5 for one hour, whereas cells of *B. cereus* can incur up to a 3 log reduction in counts at pH 3.5 in the same time (Clavel *et al.* 2004). With this data, it becomes apparent that ingested pre-germinating spores would be likely to suffer a significant death toll if consumed by a pig. For example, if spores are mixed with pig feed and left there during the day, any moisture that would enter this mixture would be very likely to initiate the germination process, as discussed in Section 6.1. Should the germinating spores then be ingested by the pig, the now susceptible germinating spores would likely be killed upon entry to the stomach. This is due to the fact that the spore will very quickly become hydrated in the first stages of germination, therefore losing most of its resistance to external stresses.

However the reduction in viable counts do not match the reduction in viable counts seen in Chapter 5 (Figure 5.2), where a much sharper decline in viable counts has been seen in all conditions, including conditions where lethality would not be anticipated. Previous studies have shown that 2.5% HCl (692mM) is sufficient to inactivate *B. anthracis* spores on hides and skins (Block 2001) whereas 500mM HCl treatment for 50 minutes (at 24°C) resulted in >90% *B. subtilis* spore killing according to Setlow *et al.* (2002). As mentioned in Chapter 5, an hours exposure to 0.2N HCl resulted in 90% death of *B. cereus* spores (with high silicon content) (Hirota *et al.* 2010). Interestingly there is little other data available on the effect of HCl on *B. subtilis* spores.

6.4.3 Assessment of total counts

It appears that the decline in viable counts is not solely related to the viability of the spores. *Via* the FCM total counts it was noted that the total counts were declining, as shown in Figure 6.9.

However, given that spores cannot escape from the FCM tubing, one of the most logical explanations for this would be that aggregation was occurring. It follows that the

perceived reduction in viable counts *via* plating or FCM is caused by not just genuine lethality mechanisms but is also driven by aggregation, as the decline in total counts frequently matches the decline in viable counts in measurements. Based on these findings, to assess the lethality inducing effect of GIT conditions it might be necessary to first disentangle the possible contribution of aggregation on skewing the viable counts of the samples analysed.

A simple means to determine the level of aggregation in these samples, is to add a surfactant to these mixtures prior to analysis. The results of such trials are detailed in Chapter 7.

6.4.4 FCM sub-population analysis

Although the presence of aggregates means assessing viability *via* cfu/ml is unreliable, the level of cell and spore death can still be inferred using FCM PI staining. The results from Figure 6.13 show there is a significantly higher level of PI positive events following acid treatment in all cases except 40mM HCl on dormant spores. This implies all other treatments cause a significant level of lethality. This analysis also highlights the statistically significant increase in dead spores and cells when spores are allowed to pre-germinate. The increase in PI positive events confirms that this is not just due to a decline in total counts, but is indeed a significant loss in viability.

7 Investigating the impact of aggregation on *B. subtilis* viability enumeration

7.1 Introduction

As has been heavily implied in the results seen in Chapter 6, total cell and spore numbers appear to fall in more acidic conditions. Aggregation often occurs in bacterial populations as a result of the physicochemical and biological parameters within the system. The bacteria can either be in the vegetative or spore form and it is important to note that in the dormant spore form the physicochemical aspects will be the dominating factor whereas for vegetative cells, the mechanisms behind adhesion will be different owing to the larger impact of the biological interactions.

7.1.1 Bacterial aggregation and intermolecular forces

Attachment of bacteria, either between themselves or to surfaces, irrespective of their physiological state, is considered to be a surface-driven phenomenon. Hence this is conventionally interpreted using the Derjaguin-Landau-Verwey-Overbeek (DLVO) theory. Bos *et al.* (1999) has claimed that the main forces at work causing aggregation are Lifshitz-van der Waals, acid-base (permanent dipole-permanent dipole) and electrostatic interactions. All other specific and localised molecular interactions are linked to one or more of these three forces. To a lesser extent, (and for non-motile bacteria) Brownian motion will also play a role in levels of adhesion and aggregation, however in microbial systems this is believed to have a small impact (Marshall *et al.* 1971; Bos *et al.* 1999) though in systems where profound environmental changes take place, such as strong thermal treatments e.g. pasteurization, sterilization or a drastic increase in pressure e.g. high pressure processing etc. Brownian motion could significantly contribute to aggregation.

To be able to predict the level of aggregation expected in a system one can follow a variety of different parameters. These are detailed in the paragraphs below.

7.1.1.1 *Electrostatic forces and Zeta potential*

Zeta potential, or electrokinetic potential, is the electric potential of the interfacial area between the bacterial surface and the aqueous environment. The electrostatic charge is a function of the total net charge across the bacterial cell or spore surface and is influenced primarily by the electrostatic forces and secondary by the ionic strength (Wilson *et al.* 2001). Spore charge is due to the fact that the spore coat surface is proteinaceous, and a protein will have an overall charge depending on the medium it is in, or more specifically, the spore coat protein structure is anticipated to have a charge as a function of the pH (McKenney *et al.* 2013). As a result of its proteinaceous nature, the spore coat will harbour polar and apolar regions. The polar (hydrophilic) protein regions consist of areas with amino acids that have positively charged side groups (e.g. lysine, histidine), negatively charged side groups (e.g. glutamate aspartate) and polar but uncharged side chains (e.g. serine, threonine). The latter will only contribute to permanent dipole-permanent dipole interactions due to their polar but uncharged nature. By contrast, amino acids with charged side chains will contribute directly to electrostatic interactions. The apolar (hydrophobic) protein regions consist of areas with amino acids that have nonpolar side chains (e.g. alanine, leucine). These nonpolar chains of these amino acids will contribute to the Lifshitz-van der Waals interactions (Gooding and Regnier 2002; Gitlin *et al.* 2006). Due to the 3D folding arrangement of the protein, polar areas as well as apolar regions will arise across the spore coat. Some of the positive and negative charges will cancel each other out whereas others will contribute to the net charge (Israelachvili 2011).

The electrostatic charges can be measured by passing an electrical current through a suspension of spores in an electrophoresis chamber. The direct movement of the spores and the velocity of this movement can be used to calculate the zeta potential, assuming the ionic strength, pH and temperature of the suspension is known (Wilson *et al.* 2001). Below in Table 7.1 are some reported zeta potential values for *Bacillus* species.

Table 7.1 Reported zeta potential values for a range of Bacillus species

Species	Medium	Zeta Potential (mV)	Author
<i>B. cereus</i> (NCTC 2599)		-14.1±1.5	
<i>B. cereus</i> (IAM 1110)		-15.5±1.2	
<i>B. mycoides</i> (ATCC 6462)		-23.9±0.8	
<i>B. polymyxa</i> (DSM 36)		-22.6±1.3	
<i>B. licheniformis</i> (DSM 13)	NaCl	-20.9±0.6	(Husmark 1993)
<i>B. megaterium</i> (DSM 32)	145mM	-33.7±2.6	
<i>B. megaterium</i> (ATCC 10778)		-35.1±1.4	
<i>B. brevis</i> (ATCC 8246)		-12.2±0.8	
<i>B. pumilus</i> (ATCC 14884)		-29.6±0.7	
<i>B. subtilis</i> (ATCC 6633)		-29.1±3.0	
<i>Bacillus</i> (various strains)	40mM PB	-23.74±3.97	(Parkar <i>et al.</i> 2001)
<i>B. subtilis</i> PY79		-30.7±0.9	
<i>B. subtilis</i> BZ213	Deionised water	-34.7±0.8	(Pesce <i>et al.</i> 2014)
<i>B. subtilis</i> ER220		-28.4±0.7	
<i>B. subtilis</i> S6633		-46.6±9.4	
<i>B. subtilis</i> F6633	(pH6.5)	-25.4±5.0	(Mamane-Gravetz and Linden 2005)
<i>B. subtilis</i> AY616160		-37.8 ± 4.5	

The results from Table 7.1 are not surprising since most microorganisms have a negative charge, and indeed *B. subtilis* spores have very recently been shown to have a negative surface charge by accurate measurement with optical tweezers (Pesce *et al.* 2014).

7.1.1.2 Hydrophobicity

Husmark (1993) places considerable emphasis on the hydrophobic nature of *B. cereus* spores and hence their propensity for adhesion to surfaces, though an important

distinction between spores of *B. cereus* and *B. subtilis* is that *B. cereus* spores have an exosporium with several filamentous appendages. *B. subtilis* spores do not possess an exosporium and therefore do not have these filamentous appendages. Previous studies have shown a variable correlation between hydrophobicity and adhesion levels. For example Kos *et al.* (2003) and Del Re *et al.* (2000) have shown a good correlation between hydrophobicity and adhesion, whereas the results seen by Seale *et al.* (2008) and Mamane-Gravetz and Linden (2005) do not support the theory that hydrophobicity is a good indicator of adhesion. It can be further deduced that depending on the physiological structure of the spore or bacteria, whilst hydrophobicity will always be a factor in adhesion or aggregation, it may not be the dominant mechanism in determining adhesion.

7.1.1.3 *Lifshitz-van der Waals forces*

Lifshitz van der Waals forces are a product of the apolar, therefore hydrophobic areas of the spore coat (Van Oss *et al.* 1988). They are caused by the occasional orientation of electrons in an apolar molecule causing instantaneous only dipoles (Burns and Dick 2002). When two particles get close enough the instantaneous dipole of one molecule can induce another instantaneous dipole moment in the other molecule. This induced weak polarity can cause the particles to reversibly adhere (Van Loosdrecht *et al.* 1990b). However, these forces are weaker than permanent dipole-permanent dipole interactions and consequently require close proximity to be effective, therefore cannot overcome the expected electrostatic repulsion between bacterial spore surfaces or more specifically, their respective spore coat layers, alone (Bos *et al.* 1999). In conclusion whilst Lifshitz-van-der Waals are active over several tens of nm (Busscher *et al.* 2008), they only have an effect at very short ranges of ~1nm (Mittal *et al.* 1998; Israelachvili 2011), and they become dominant in the vicinity of a surface (Hori and Matsumoto 2010).

7.1.1.4 *Acid- base (or permanent dipole-permanent dipole) forces*

Acid base (or permanent dipole-permanent dipole) forces, of which hydrogen bonding is the most common example, are always attractive and far more powerful than the ever

present Lifshitz-van der Waals forces, however they only have an impact over a short range, usually about 5nm (Bos *et al.* 1999). Permanent dipole-permanent dipole forces arise due to the existence of molecules with polar covalent bonds. This is a bond where either atom has electronegativity greater than 1.9 and the difference between the atoms is more than 0.5 but less than 2.1. In these conditions, the two shared electrons move closer to the more electronegative atom, such as the SH polar covalent bond in the side chain of cysteine. Hydrogen bonding is the most well-known permanent dipole-permanent dipole and exists in the case of water (the electrons move closer to the oxygen) forming polarised areas because they contain sites of electron poor and electron rich areas, i.e basic and acidic sites (Israelachvili 2011). This creates a permanent dipole. Amino acids with polar but uncharged side chains such as serine, threonine cysteine have exposed polarised side chains (e.g. hydroxyl groups) so permanent dipole-permanent dipole forces arise on the surface of spore coats due to their presence. Because these forces are only active over short range, the spores need to overcome the natural repulsion (or energy barrier) for this attractive force to have an effect.

7.1.1.5 *The energy barrier*

One important aspect of bacterial adhesion is the presence of an energy barrier that must be bridged in order for spores (or cells) to adhere. Since the spores are known to have a negative charge, the repulsive energy between each spore will be proportional to the reciprocal distance they are from each other (Van Loosdrecht *et al.* 1990b).

Protein net charge is known to be primarily governed by pH. In fact no protein charges occur at a pH equal to the isoelectric point of the protein, while a rise of the protein charge is observed as we move farther away from that point. The proteinaceous nature of spore coat is mainly responsible for the observed charges at the spore surface. A range of different spore coat proteins with individual isoelectric points should be acknowledged, nevertheless there is a pH point where a zero net charge will be shown (i.e. an overall isoelectric point) and will be characteristic for the spore coat proteins as a whole. It follows

that pH alterations in the environment where the spores are immersed could significantly influence the net charges on the spore surface in exactly the same pattern as with a single protein. When spores are exposed to a pH far away from the spore coat proteins' isoelectric point, maximum charges at the spore surface occur thus maximizing the repulsive forces amongst the neighbouring spores. This maximizes the energy barrier for aggregation to take place. When spores are exposed to a pH closer to the isoelectric point of the spore coat proteins, charges at the spore surface will be reduced, hence reducing the energy barrier to aggregation and increasing the spore propensity for aggregation.

Alongside the prime effect of pH on the development of net spore charges there will also be a secondary effect arising from the distribution of counter ions around these spores which will form an electric double layer (Hori and Matsumoto 2010). For a given pH and at very low ionic strengths, it is more difficult for spores to aggregate since additional energy is required to overcome the naturally repulsive forces exerted from the neighbouring spore due to the prevalence of a net negative spore coat charge. However, as the ionic strength increases, the ions will dampen this negative charge, by what is believed to be a compression of the electrical double layer around the spore. This leads to a reduction in the electrostatic interaction between two particles (spores) at a given distance of separation (Van Loosdrecht *et al.* 1990b). Hence, the spores can more easily overcome the energy barrier caused by the strength of the electrostatic repulsion and come into closer contact and are therefore more likely to aggregate. As soon as the ionic strength exceeds a level the energy barrier is negated, and spores will aggregate very readily. This is shown below in the diagram taken from Hori and Matsumoto (2010).

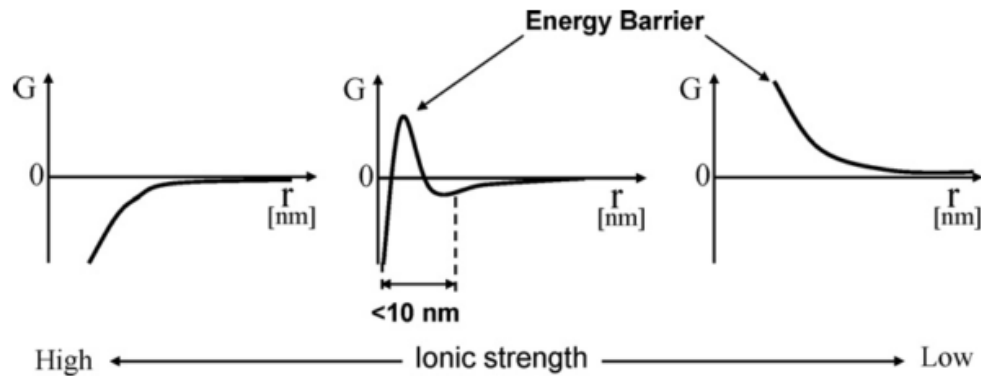


Figure 7.1 Total interaction between a bacterial cell and surface depending on ionic strength (Hori and Matsumoto 2010)

7.1.2 Models for determining adhesion

By obtaining an understanding of the forces at work within a bacterial system, it is possible to compose a model by which bacterial adhesion or aggregation could be evaluated. It was Zobell (1943) who first systematically investigated the effect of bacterial attachment to solid surfaces, but it wasn't until Marshall *et al.* (1971) used the DLVO theory of colloidal adhesion to interpret his work on bacterial to solid surface interaction that bacterial attachment to surfaces could be modelled.

The DLVO theory is based on three equations which can evaluate the likelihood of aggregation by assessing the electrostatic, the Lifshitz van der Waals forces and permanent dipole-permanent dipole forces as a function of their separation distance (Hori and Matsumoto 2010).

Van Loosdrecht *et al.* (1990a) have proposed a more appropriate notion on the DLVO theory including the addition of the Brownian motion. This is particularly significant for non-motile bacteria or spores. Harding and Johnson (1986) used the Stokes-Einstein equation to illustrate how a higher temperature increases the rates of diffusion/Brownian motion, but even at an ambient temperature of 25°C this movement is in the region 5×10^{-9} cm²/s which should not be disregarded.

Factors affecting the application of the DLVO theory

The DLVO theory is appropriate to most spore systems but when dealing with bacterial cells (and some spores such as *B. cereus*), there are uncertainties in the theory which are partially accounted for by the anatomical features of the spores and bacteria such as their pilli, flagella or other appendages (Husmark 1993). For *B. subtilis* spores, the outer crust recently reported by McKenney *et al.* (2013) will have an influence though it is not known what implications this will have on the applicability of the DLVO theory. In the case of bacteria these anatomical features could also be generated as a result of the environment they are subjected to, though in the case of spores, such a dynamic response element is lacking. In both cases, cells and particularly spores, the understanding of the outside layer is still not fully matured (McKenney *et al.* 2013). Inevitably, uncertainties will arise as a result of this lack in knowledge.

An example of how these unknown factors can have larger implications on adhesion behaviour is highlighted in a study on the probiotic *Lactobacillus rhamnosus* GG and its adhesive properties (Deepika *et al.* 2009). Specifically, the effects of different fermentation mechanisms on cell adhesion was investigated and it was found that cell adhesion to Caco 2 cells varied widely depending on the length of time the cells had been fermented. This emphasises the issue that even the same strain of bacteria may have different aggregation and adhesion properties depending on how they are cultured. This is thought to be the result of differences between components on the cell surfaces, such as (lipo-)teichoic acids, polysaccharides, covalently bound proteins and S-layer proteins. For spores, another uncertainty linked to anatomical features is that the outside layer is dictated by the preceding sporulation process and the harvesting processing. This is an additional source of complexity in the system and would therefore be a very appropriate area of further research.

On the basis of the DLVO theory, in the case of the vegetative form of bacteria the initial attachment could be either immediate, or, if they are in close proximity to a surface, a second step could aid the permanent attachment. The second step is facilitated by active

biological processes such as secretion of exopolysaccharides, or development of additional anatomical features that bridge the distance between the bacteria and the surface (Parker *et al.* 2001; Garrett *et al.* 2008). Since this is true for the interaction of bacteria to surfaces, this could also be true for bacteria to bacteria interactions.

7.1.3 The importance of aggregation in probiotics

In probiotic research, an organisms' ability to form aggregates is considered a favourable and possibly essential characteristic in order to be classed as a probiotic. Irrespective of whether spores or cells are investigated, adhesion to the GIT is a vital point in establishing whether or not an organism is able to exert a beneficial effect. Probiotic adhesion is frequently tested using Caco 2 cell lines, and sometimes mucus or extracellular matrix components (Deepika *et al.* 2012). For example, Castagliuolo *et al.* (2005) studied the adhesion of *Lactobacillus crispatus* to colonic mucosa and found that the auto-aggregating strain consistently adhered to the mucosa. However, when a mutant strain (MU5) which lacked the auto-aggregating properties of strain M247 was fed to mice, whilst the M247 strain was detected in high numbers in the faeces, the MU5 strain was not detected at all. This heavily implies that the lack of aggregating properties made this unsuitable as a probiotic.

For spore surface adhesion in particular, it has been previously shown that *B. subtilis* adhesion to Caco 2 cells varies depending on the physiological state, for example Tam *et al.* (2006) showed that while spores of strains HU58 and HU78, as well as the laboratory strain PY79, could adhere, the level of adhesion in the vegetative cells was much reduced. Strain to strain variation is also an important point to consider since it was found that the PY79 strain was not capable of forming biofilms, whereas as the HU58 and HU78 strains did have this capability (Branda *et al.* 2001). This emphasises the variability between not just species, but also strains of a bacterium and their tendency to form biofilms.

Seale *et al.* (2008) undertook an investigation into the adhesive properties of *Geobacillus* spores, in which adhesion, hydrophobicity and zeta potentials were measured. It was found that the spores were hydrophilic and had a negative zeta potential but would adhere to all surfaces tested. They concluded that whilst hydrophobicity definitely had an influence on adhesion, it was not consistently correlating with the adhesive ability of the spore. Another important point to note from this study was that the DLVO theory of adhesion was not applicable to this system, as spores were predicted to strongly adhere to a stainless steel surface, whereas in reality three out of the four isolates tested adhered less strongly to this surface in comparison to others. This study highlights the fact that there is no simple relationship between the individual physicochemical properties of a spore and its' ability to adhere to surfaces.

7.1.4 External factors inducing aggregation

Temperature, pH and pressure have all been shown to influence aggregation. For example Furukawa *et al.* (2005) found that a heat treatment of 85°C for 20 minutes (or more) caused an increase in spore clumps of spores of *B. licheniformis*, *B. cereus* and *B. coagulans*. They hypothesised that this increase in spore clumps was due to denaturation of the surface proteins of the spore coat, thereby increasing the hydrophobicity. Harding and Johnson (1986) have reported the diffusivity of *Bacillus* spores to be in the order of 5×10^{-9} cm²/s at 25°C. An increase in the temperature will inevitably cause an increase in the diffusion coefficient which will signify increased kinetic energy. This in turn will increase the collisions (in the unit of time) between spores thereby increasing the chances of aggregation to occur. As described above (Figure 7.1) when the energy barrier is bridged by bringing the spores in close enough proximity, the remaining forces e.g. permanent dipole-permanent dipole and Lifshitz van der Waals will be attractive and thus increasing the likelihood of aggregate formation.

In another study from Furukawa *et al.* (2006) the effects of high pressure CO₂ treatment on spore clumping was evaluated. Again, the treatment significantly increased the

percentage of *Bacillus* spore aggregates. The authors attribute these clumps to the denaturation of spore coat surface protein creating a more hydrophobic spore surface. In addition to their valid explanation, it is also possible that the reduction of net charges by the increased acidity has contributed significantly for bridging the energy barrier and allowing short range attractive intermolecular forces such as Lifshitz van der Waals and permanent dipole-permanent dipole to drive the reported spore clumping.

A lot of evidence suggests that bacterial aggregation occurs to a larger extent when exposed to different HCl concentrations, for example *Streptosporangium brasiliense* has been shown to aggregate at low pH and disaggregate at neutral and alkaline pH (Oh and Nash 1981). Similarly a study by Muda *et al.* (2014) has shown that 12 strains of bacteria would aggregate at acidic conditions and reduce the level of aggregation at higher pH.

During the course of the present project, a change in the FCM profiles has been continuously seen during studies after heating. Specifically, FCM analysis reveals that the cell and spores region gains a higher SSC and the samples appear 'cleaner' i.e. there's less debris. It is likely that this is because heating causes cells and spores to aggregate. It has previously been suggested that aggregation could partly be inhibited using a non-ionic surfactant such as Tween 80 (Furukawa *et al.* 2005).

7.1.5 Aims and objectives

To investigate the levels of aggregation in a system both microscopic and macroscopic approaches can be used. Given the available time for concluding the post graduate research degree, the expertise developed and the availability of experimental facilities, a macroscopic approach was favoured for investigating the extent that aggregation could have an influence across the experimental conditions used in the present study. The investigation involved a non-ionic surfactant for disaggregating the spores (Tween 20). The aggregation and disaggregation was explored in the relevant gastric conditions studied using

FCM and plate counts, aided with particle size distribution, and Zeta potential measurements.

7.2 Material and Methods

Spores were produced as described in Section 5.2.1 and the FCM settings were the same as those described in Section 6.2.1.

7.2.1 Effect of heating-induced aggregation on total counts

The effect of heating (70°C for 30 minutes) on total count in PBS (100mM, pH 7.4) with and without 1% Tween 20 was investigated. A 1ml aliquot of spore stock (~5 x 10⁸ spores/ml) was pipetted into a 1.5ml microtube and centrifuged at 10,000 x g for three minutes. The top 995µl supernatant was removed and replaced with the desired liquid.

7.2.2 Effect of surfactant on total spore counts exposed immersed in LB at different pH ranges

Assessment of aggregation *via* the addition of 1% Tween 20 was carried out in LB across different pH ranges (Preliminary experiments showed that higher concentrations of Tween 20 did not yield any higher counts). The pH was altered by adding either HCl or NaOH to the medium. Total counts were assessed using FCM, and the extent of aggregation in LB broth when following two different potential preparatory steps was evaluated. Two different approaches were followed in the Chapters 5 and 6, one method involved centrifuging the spores and then adding the desired liquid (owing to the fact that the supernatant was needed) whereas method 2, employed in Chapter 6, the spores were added directly to the *in vitro* media.

Method 1: simulated gastric media applied to directly centrifuged spores

Spores were centrifuged at 10,000 x g for three minutes and top 995µl supernatant was removed and replaced with the desired liquid. This was repeated twice more and the resulting suspension was vortexed vigorously until a homogenous liquid was observed.

Method 2: pre-dispersed spores added to simulated gastric media

This method was implemented in previous chapters (5 and 6), 800µl of the desired liquid was pipette into a microtube and 200µl of spores in sterile PBS were pipette into this. Tubes were vortexed vigorously before analysis.

It was anticipated that the execution of spore viability studies with samples prepared by Method 1 simulated gastric media applied to directly centrifuged spores should lead to higher spore aggregate formation. Spores which have been centrifuged will be mechanically compacted, and therefore in close proximity with each other. From a theoretical point of view (Section 7.1) when spores are compacted close enough together by the power of the centrifugal forces, the attractive short range intermolecular forces will exert a higher influence and thus increase the propensity of the compacted spores for clumping together.

7.2.3 Assessment of total counts in acidified PBS

Assessment of aggregation *via* the addition of 1% Tween 20 was carried out in PBS at pH 1, 3, 5 and 7. The pH was altered by adding HCl to the medium. Total counts were assessed using FCM and the samples were prepared as described by the method 2 procedure.

7.2.4 Assessment of viable spore counts in LB and PBS

Assessment of aggregation *via* the addition of 1% Tween 20 was carried out in acidified LB and PBS at pH 1, 3, 5, and 7. The pH was altered by adding HCl to the medium until the desired pH was obtained. Viable counts were assessed by plating and the samples were prepared as described by the method 2 procedure.

7.2.5 Assessment of spore counts in 100mM HCl acidified pig feed

Spore aggregation was also explored experimentally in a pig feed mixture designed to simulate a fed pig stomach. 125g of pig feed was mixed into 250ml water with 100mM HCl in a 500ml conical flask. Pre-dispersed spores were added (by experimental method 2) and sealed in sterile dialysis tubes (ServaPor MWCO 12-14kDa) and then immersed in this mixture, which was placed in a rotating incubator set to 200rpm at 37°C. Samples were recovered after two and four hours and analysed as described below.

7.2.6 Enumeration

FCM samples were stained with 48µM PI and 1.5µM Syto 16 to obtain viable counts. A microtube was filled with 540µl of this staining mixture and following the experimental 10µl of the relevant sample was added to this. Before FCM analysis, 490µl of this mixture was pipetted into an FCM tube and 10µl of Spherotech beads were added to enable conversion of events to counts/ml.

Plate counts were undertaken according to the Miles and Misra method (Miles *et al.* 1938). Briefly, serial dilutions (10^{-1} to 10^{-6}) were plated out on an LB agar plate by pipetting 20µl of the respective dilution onto the labelled segment of the plate. The dilutions were performed in triplicate. After allowing time to be absorbed, the plates were inverted and incubated at 37°C overnight. The drop method reduces the number of bacteria lost by spreading (Pope *et al.* 2008).

7.2.7 Particle size analysis

To gain a better understanding of the level of aggregation, the spores were also subject to particle size analysis using a Mastersizer 2000. Spores were analysed in PBS (100mM) at pH 1, 3, 5 and 7 or PBS (100mM) at pH 1, 3, 5 and 7 with 1 % Tween 20. The PBS (at the desired pH) was added to the dispersal chamber and the stirrer was set to 2000rpm. Spores were added to the PBS until they were in a detectable range for data analysis, and then data collection commenced.

7.2.8 Measuring zeta potential

Measurements were conducted in the National Centre for Macromolecular Hydrodynamics at Nottingham University led by Prof Harding. A Malvern zetasizer was used to assess the zeta potential of spores at 7×10^7 /ml ($OD_{580} = 0.45$) in accordance with the previous study by Harding and Johnson (1984) in 100mM PBS at pH 1, 3 5 and 7 with and without 1% Tween 20 according to method 2.

7.2.9 Statistical analysis

All bacterial counts were converted *via* a log₁₀ transformation. The data were processed in Excel and the 95% confidence intervals were calculated to check for statistical significance.

7.3 Results

7.3.1 Exploring the effect of heating on total counts using FCM

The aim of this first experiment was to check the levels of aggregation caused by heating at 70°C for 30 minutes in PBS (pH7.4 100mM), but also to ensure that the region assignment *via* the FCM didn't cause any distortion in the results. Samples were prepared according to Method 1 in Section 7.2 of the Materials and Methods section. Therefore Figure 7.2 shows the FCM region assignments and Figure 7.3 the corresponding counts for these different regions.

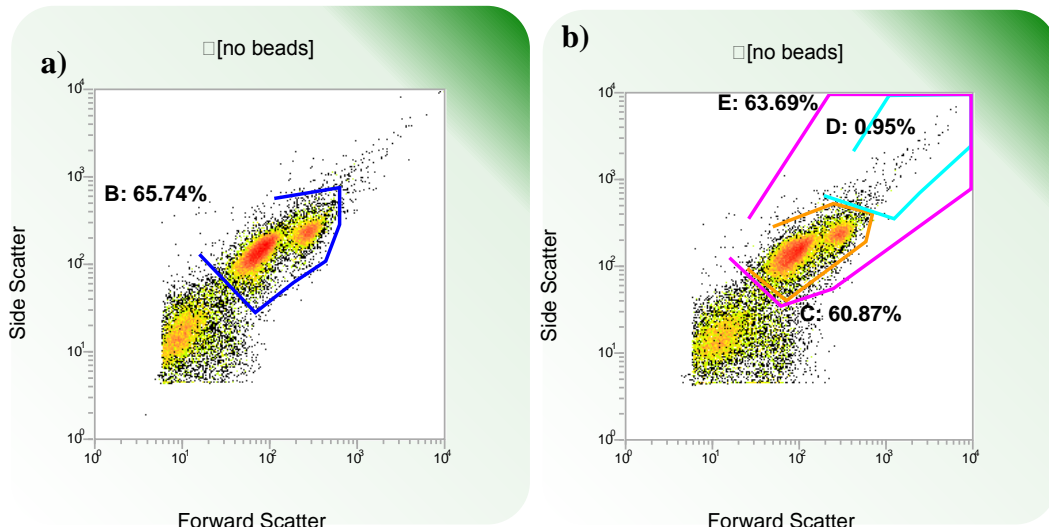


Figure 7.2 Representative FCM analysis of spores immersed in PBS with 1% Tween 20 displayed on a FSC vs SSC density plot. The plots have been gated to remove beads. I) Left, region B (blue) is drawn around the main cells and spore position. b) all high FSC and SSC events region E (pink) on the FCM profile. Other regions are C (pink)= dormant spores and cells, D (turquoise) = Large aggregates. n=3.

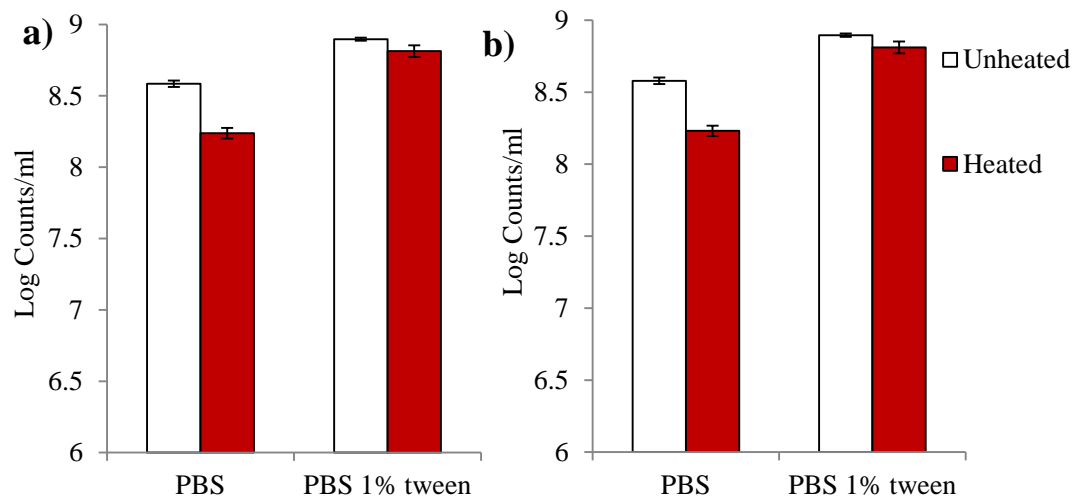


Figure 7.3 Total counts for heat activated and non-heat activated spores in different conditions, prepared according to method 1. a) the log counts/ml are from region B containing cells and spores, on the FCM profile above (Figure 7.2.). b) Counts for ‘large events’ shown as all high FSC and SSC events region E (pink) in Figure 7.2. Error bars represent the 95% CI where n=3.

It appears from this first trial that when spores are in PBS, the presence of Tween 20 causes a significantly greater number of events to be recorded ($p < 0.05$) and in fact this is over double the original count. As was expected, heating significantly reduced total counts ($p < 0.05$). For example the non-Tween unheated samples were 102% greater than the heated non Tween count. However when 1% Tween 20 was added to the heated sample, the counts increased almost 4 fold (to 275% of the heated count).

A check was made to see the effect of region assignments on the counts. Results from region B (Figure 7.2. a) mirror the trends seen in region E (Figure 7.2. b) indicating changes in total count are not linked to the region assignment.

7.3.2 Comparison of total numbers of spores in LB broth at different pH's with and without 1% Tween using two methods

For the next part of the investigation, dormant spores were placed in filtered (0.2µm) LB broth at different pHs, in conditions with 1% Tween 20 and without. Two different methods were employed, method 1, where spores were directly centrifuged Figure 7.4 a. and method 2, Figure 7.4 b. An example of the FCM output for these trials is presented in Figure 7.4 and the total counts obtained are presented below in Figure 7.5.

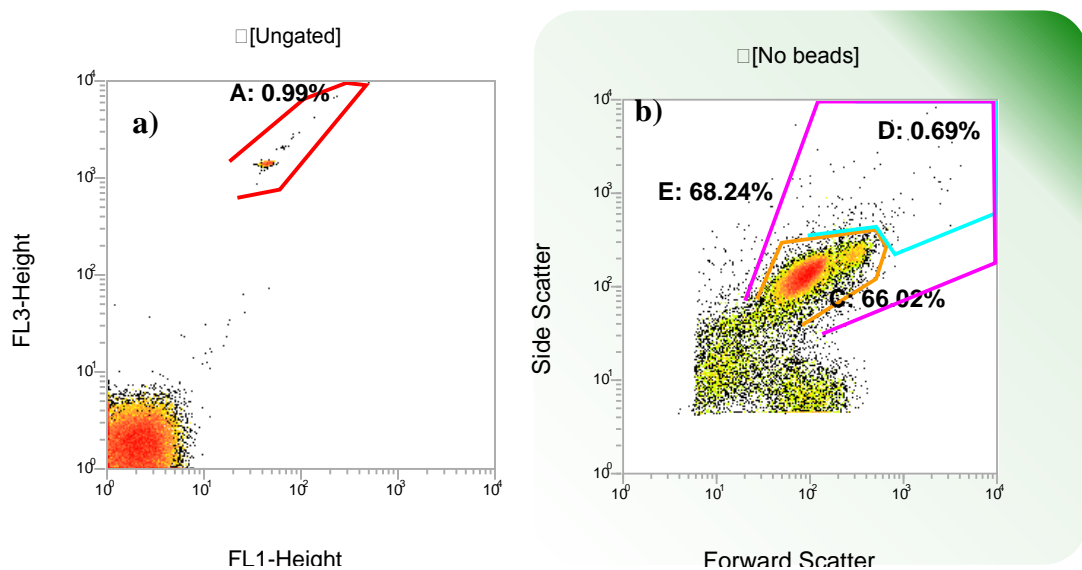


Figure 7.4 Representative FCM analysis of spores immersed in LB broth presented on a FL1 vs FL3 density plot (a) and region A (red) drawn around beads. b) regions drawn on a gated plot using equation NOT A to remove beads from the FSC vs SSC plot. Region E (pink): all spore events (including large aggregates), Other regions are C (orange)= dormant spores and cells, D (turquoise) = Large aggregates. n=3.

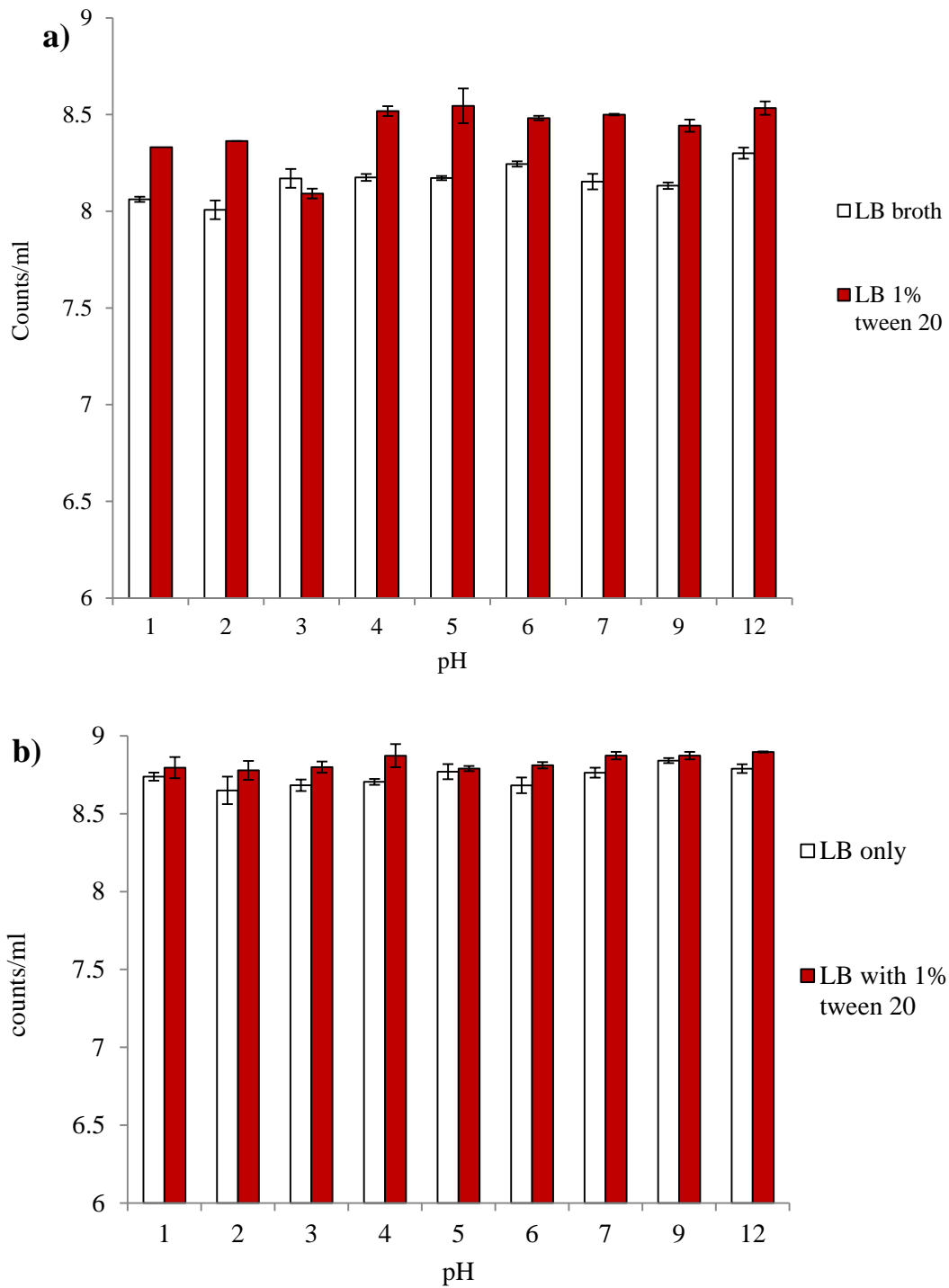


Figure 7.5 Comparison of log spore counts in LB over a range of pHs, showing a) run one according to method 1 (top) and b) run two according to method 2 (bottom). White bars indicate spores in LB broth only and red bars show spores in LB broth supplemented with 1% Tween. Values are based on the number of events in region E (burgundy). Error bars represent the 95% CI where $n=2$ in run one and $n=3$ in run two.

Similar trends are seen with both methods. For method 1, across all the pH ranges, except pH 3, there is a statistically significant increase when 1% Tween 20 is added, with a maximum increase of 136% seen at pH5 ($p < 0.05$)

At neutral pH (6 and 7), the addition of Tween causes a statistically significant increase in total counts in both runs ($p < 0.05$) where the Tween 20 samples were 73 and 122% higher than the non Tween samples.

At acidic pH (5 and below), in run one, whilst at pH 3 there is no statistically significant difference ($p > 0.05$) with the addition of 1% Tween 20, at all other acidic pH the addition of Tween increases the total counts ($p < 0.05$). In particular the counts for the 1% Tween samples at pH 2 reach 123% of the non Tween supplemented sample.

In run two, where method 2 was applied, (spores were added directly to the LB broth), whilst Tween was shown to increase the average counts in all cases, this increase was not always significant. For alkaline pH, the increase is statistically significant at pH12 ($p < 0.05$) of 28% but not at pH 9 ($p > 0.05$). At acidic pH a statistically significant increase in total counts is seen at pH 3 and 4 ($p < 0.05$) of 31 and 48% respectively.

A parameter that should not be overlooked is the spore concentration in both trials. For the first run, the average count was 2×10^8 spores/ml, whereas in run two, the spores concentration was higher, at 5×10^8 spores/ml. This difference may indicate that the spore tendency to aggregate changes depending on counts.

7.3.3 Comparison of total numbers of spores in PBS at different pH's with and without 1% Tween

To focus more on conditions of relevance to our studies the experiment was tapered to measure pH 1, 3, 5 and 7. This was first performed using PBS (100mM, pH 7.4) as the

medium in which spores were immersed. Furthermore, since the method 1, involving application of liquids directly to centrifuged spores seemed to be causing aggregates to form (Figure 7.3), only method 2 was employed from this point onwards.

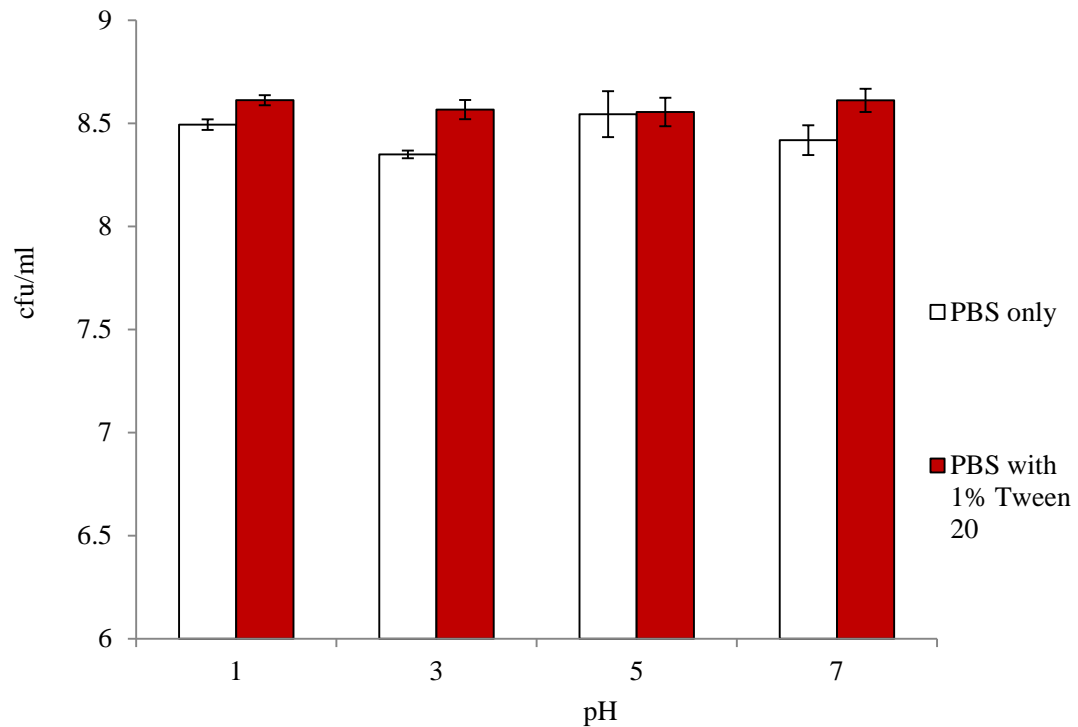


Figure 7.6 Comparison of total spore FCM counts in PBS over a range of pHs. White bars indicate spores in PBS only and red bars show spores in PBS supplemented with 1% Tween. Values are based on the total number of cells and spores according to FCM. Error bars represent the 95% CI where $n=3$.

At pH 1, 3 and 7, Tween significantly increases the total count by a statistically significant amount ($p<0.05$) of 31, 65 and 56% respectively. At pH 5 there was no statistically significant difference between the Tween and non Tween samples ($p>0.05$).

7.3.4 Exploring the effect of surfactant on plate count

Given that the results from FCM have been shown to highly suggest the presence of aggregates, an investigation into whether aggregation effected the plating data was also

undertaken. Plate counts from spores immersed in PBS and LB were investigated, owing to the fact that the work in previous chapters has largely focused on acidic conditions in these liquids.

7.3.4.1 *Plating counts of spores immersed in LB broth with and without 1% Tween 20*

The results from plating, investigating pH 1,3,5, and 7 were plotted for comparison against the Tween 20 supplemented and LB only samples shown below in Figure 7.7.

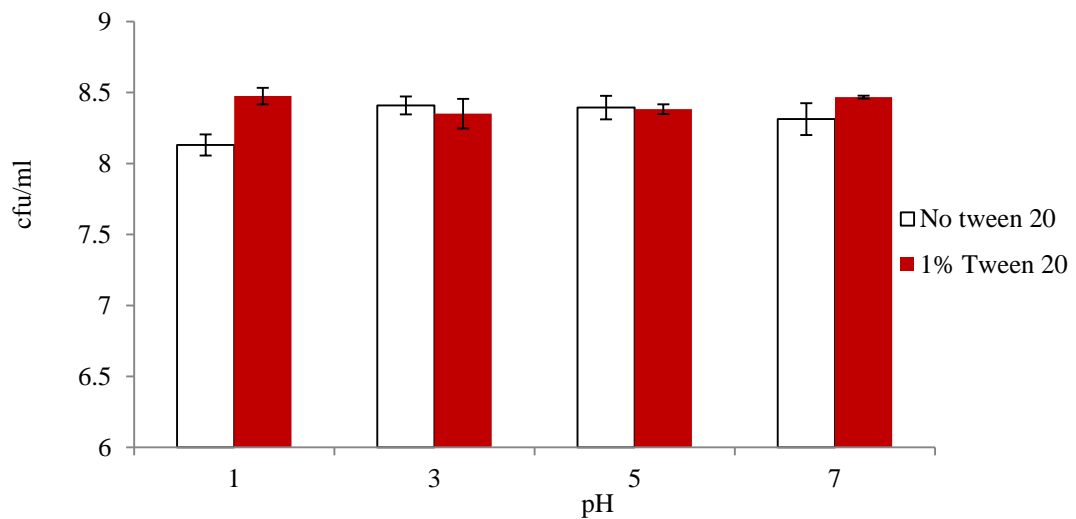


Figure 7.7 Plate counts of spores immersed in acidified LB broth. Error bars represent the 95% CI where n=3

It is clear that for the plate counts at pH 1 and 7 1% Tween 20 significantly increases the plate counts ($p < 0.05$) by 120 and 40% respectively. For pH 3 and 5, there is no statistically significant difference in the presence of Tween 20 ($p > 0.05$).

7.3.4.2 *Plating counts of spores immersed in PBS with and without 1% Tween 20*

The results from plating, investigating pH 1,3,5, and 7 were plotted for comparison against the Tween 20 supplemented and PBS only samples shown below in Figure 7.8.

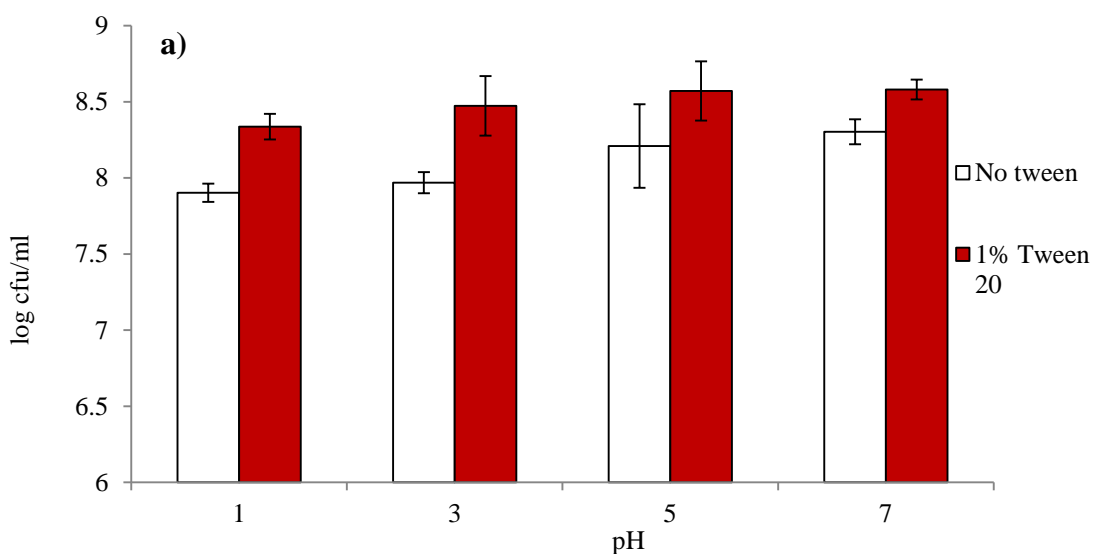


Figure 7.8 Comparison of plating counts for PBS alone and PBS with 1% Tween 20. White bars indicate spores immersed in PBS without Tween 20 and shaded bars represent spores immersed in PBS with 1% Tween 20. Error bars represent the 95% CI where n=3

The plating data show a significant increase in counts with the addition of Tween 20 at pH 1, 3, and 7 ($p < 0.05$) of 75, 101 and 51% respectively. At pH 5, there is greater variation in results, and thus no significant difference ($p > 0.05$), though the results with 1% Tween 20 are still higher on average by 60%.

7.3.5 Application of 1% Tween 20 to spores immersed in simulated fed stomach conditions

The spores were analysed in an acidified pig feed medium using dialysis tubing (MWCO 12-14kDa) that would prevent bacteria from escaping but would allow water and low molecular weight compounds to pass through. Viable FCM were taken using the total of events from the viable regions as shown in Figure 7.9

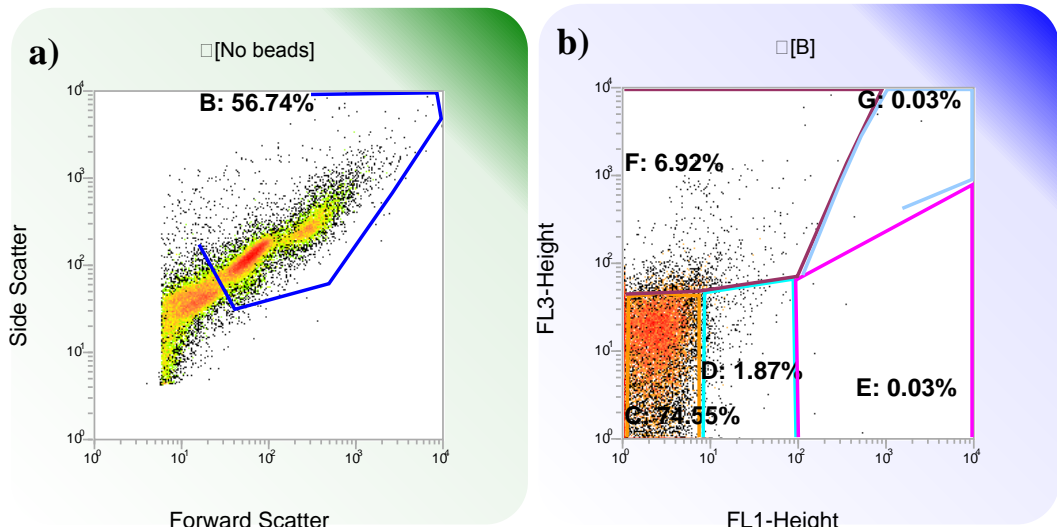


Figure 7.9 Spores immersed in 100mM PBS in Servapore dialysis tubing (time 0) displayed on a representative FCM density plot a) FSC vs SSC density plot gated to remove beads where region B (blue) is drawn around the total cell and spore region, b) FL1 vs FL3 fluorescent density plot gated on region B (blue), where region C (orange): dormant spores, Region D (turquoise): germinating spores, Region E (pink): Live cells and outgrown spores, Region F (burgundy): Dead spores and cells, and region G (light blue): double stained cells and spores. n=3.

Based on the FCM profiles in Figure 7.9 a, the total counts were assessed using the events from region B. This is presented in Figure 7.10.

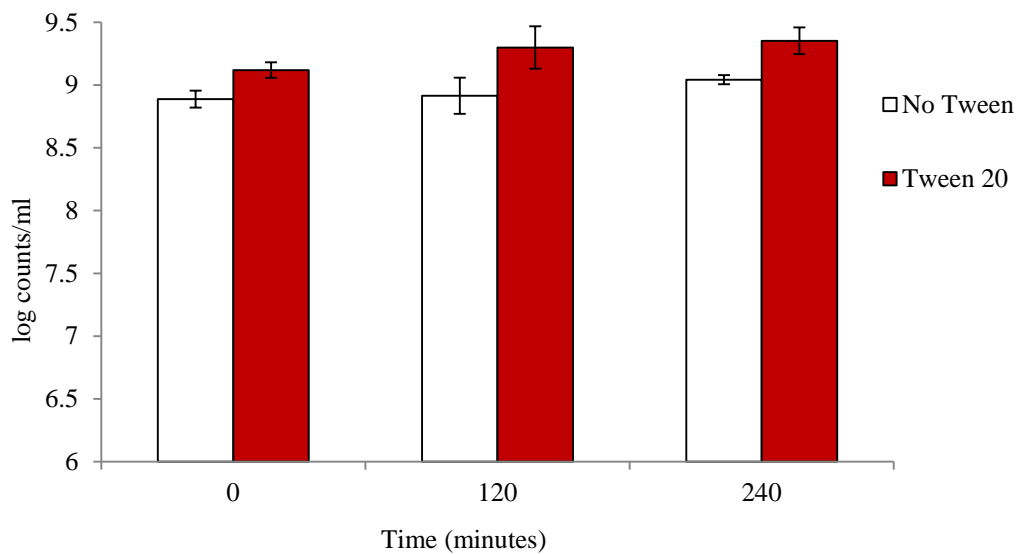


Figure 7.10 Total FCM counts of dormant spores immersed in 100mM HCl in pig pellet feed, based on Region B. Error bars denote the 95% CI where n=3.

A statistically significant increase in total counts is seen with the addition of 1% Tween at all the time points. At time 0 this increase is 70% and after two and four hours the increase reaches 146 and 107% of the respective non-Tween supplemented sample.

Based on the profile in Figure 7.9 b. the viable events were taken as the total from region C, D and E, and half the events from region G. The results from the plating and viable FCM analysis are shown in Figure 7.11.

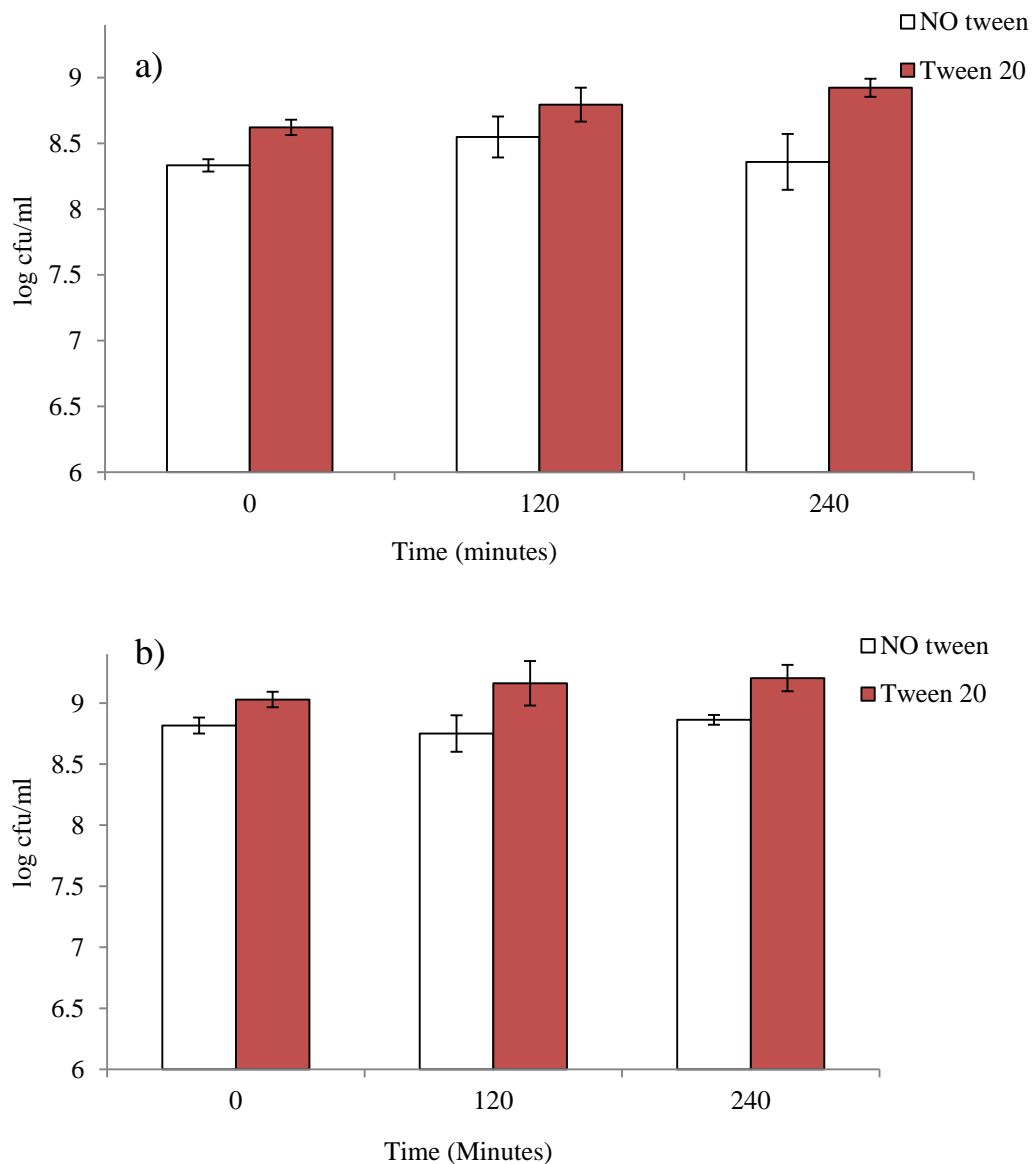


Figure 7.11 Dormant spores immersed in 100mM HCl in pellet pig feed. White bars denote samples analysed with no Tween and shaded bars with 1% Tween 20. a) Plating and b) viable FCM counts. Error bars denote the 95% CI where n=3.

For all cases the addition of 1% Tween 20 increases the counts, and this increase is statistically significant in all cases except the two hour plating data. There is no significant decline in viable counts seen during these trials, implying the spore viability remains unaffected by the presence of 100mM HCl in the pig pellet feed.

7.3.6 Spore particle size analysis

The data thus far provides strong evidence that aggregation is taking place in the samples. However to understand the processes taking place a little better, a particle size distribution analysis was performed using a Malvern Mastersizer.

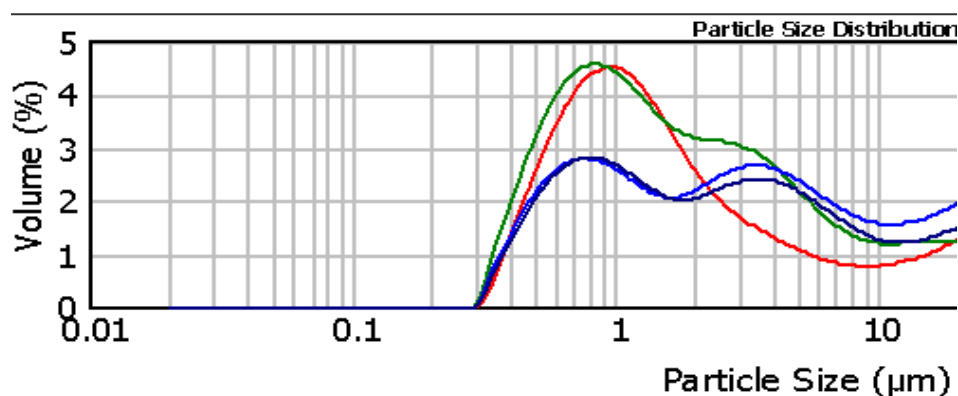


Figure 7.12 Particle size distribution of spores in PBS (100mM) at different pH levels. Values represent the average of three samples. Red line pH 7, green line pH 5, blue line pH 3, black line pH 1

The build-up of aggregates was evaluated up to a size of 20µm. This was based on previous optical microscopy observations where clumps of 20µm have never been noticed (see Appendix 2).

At pH 7 (red line in Figure 7.12) the distribution of spore sizes shows one clear peak and is more symmetrical, indicative of a more homogenous population with respect to particle size distribution. Whilst this single peak does not necessarily denote one population, the data from pH 5 (green line in Figure 7.12) show that the recorded distribution curve is becoming asymmetric indicating a spore sample with significant differences in the particle size. More specifically, this verifies that there are at least two populations with an average

particle size close to 1 and 2 μ m, respectively. The size distribution profile of the spores immersed in PBS at pH 3 and 1 clearly indicates the existence of at least two populations with distinctly different particle size averages; one at about 0.8 μ m and a second one at about 2.5 μ m. These observations suggest aggregation of spores in the investigated conditions and are verifying previously reported observations from this study.

Further to this, particle size analysis was also done on spore samples under pH 3 & 7, with 0, 0.05, 1% Tween 20 and the median particle size values were plotted on the figures below. Due to the possible reversible nature of aggregation a range of three different agitation levels in the stirring cell of the Malvern Mastersizer were investigated, namely 1000, 1500 and 2000 rpm.

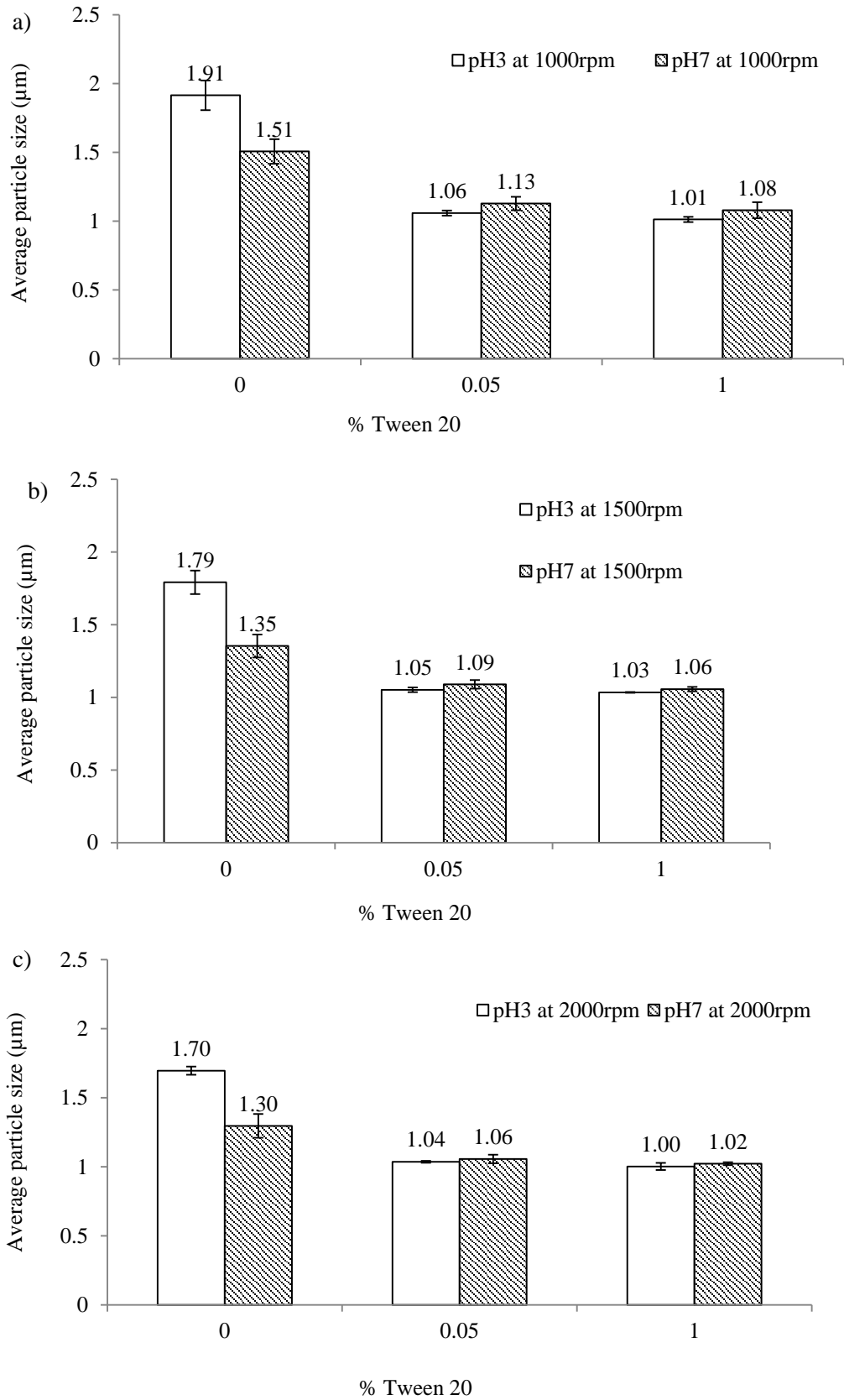


Figure 7.13 Analysis of average particle size of dormant spores immersed in PBS at pH 7 and 3, analysed at a) 1000rpm, b) 1500 rpm, and c) 2000 rpm. Error bars denote the 95% CI where n=3.

The average particle size was significantly higher when spores were exposed to pH 3, with the non Tween median value rising from 1.5 μ m at pH 7 to 1.9 μ m at pH 3. This higher average particle size indicates the presence of larger aggregates, further indicating aggregation increases at lower pHs. The data from Figure 7.13 also indicates that Tween significantly lowers the average particle size at both pH levels.

7.3.7 Zeta potential

As previously discussed in the introduction to this chapter, electrostatic repulsive forces amongst the negatively charged *B. subtilis* spores are expected to represent a significant barrier to be overcome for any aggregation to begin. Although the forces determining aggregation in our spore-medium system will interact in a complex way, it is still valid to assess the zeta potential of the spores to indicate the level of electrostatic repulsion likely in different conditions. Figure 7.14 below shows the zeta potential measurement for spores immersed in PBS at different pH.

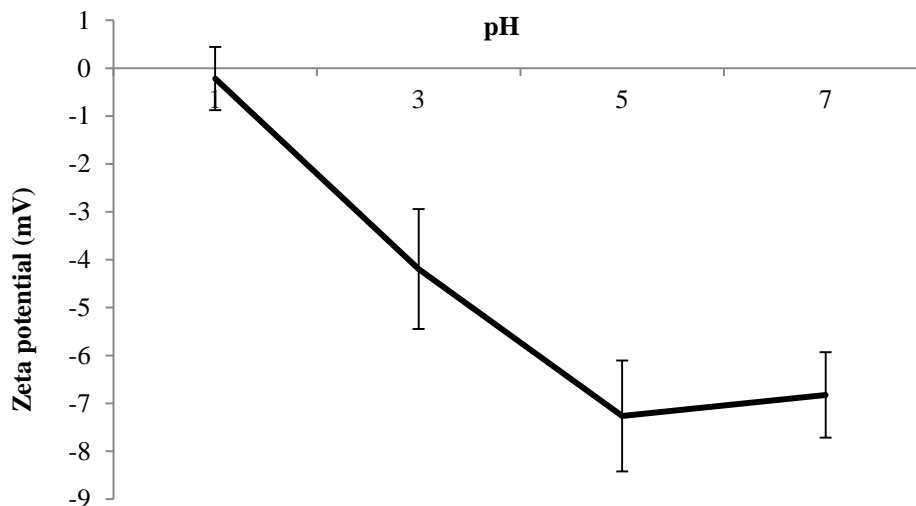


Figure 7.14 Zeta potential for spores immersed in PBS at pH 1, 3, 5 and 7. Data represent the average of 9 measurements and error bars represent the 95% CI.

The zeta potential measurements clearly demonstrate that between pH 5 and 7 there is no statistically significant decline in spore charge, however at pH 3, there is a statistically

significant reduction in the charge, and this drops significantly again at pH 1 where the zeta potential is close to 0.

7.4 Conclusion

7.4.1 Conclusions relating to the addition of 1% Tween 20

7.4.1.1 Effect of heat activation on total spore count

As seen from the results in Figure 7.3, heating causes aggregation, denoted by the decline in counts. As anticipated by Furukawa *et al.* (2005), this is believed to be due to an increase in spore hydrophobicity caused by spore coat surface proteins being denatured. However as postulated in 7.1.4 the increased kinetic energy will also promote aggregation by increasing the number of spore collisions, enabling the attractive forces to act between spores.

7.4.1.2 Comparison of total numbers of spores in LB broth at different pH's with and without 1% Tween using two methods

In general, the results so far have shown that the addition of 1% Tween 20 to LB broth will significantly increase counts for all pH values in run 1, with the exception of pH 3 (Figure 7.4 a) and in run 2 (Figure 7.4 b) the increase in counts is apparent but is only significant at pH 3, 4, 6, 7 and 12. The reason for this variable effect of Tween 20 is not clear, though it may be that spores are less aggregated in some cases.

7.4.1.3 Effect of preparation method on levels of aggregation

As expected, spores prepared *via* method 1, which were pelleted before analysis, displayed far higher levels of aggregation than those which were immersed in the media. This perceived decline in counts was attributed to the compacting of the spores caused by centrifugation, meaning spores were mechanically brought into close contact, allowing the

attractive forces to become dominant and therefore cause aggregate formation. This could have serious implications for general bacterial cell counts, as bacterial cells are usually washed using a centrifugation step, however this could mean counts from spore stocks are actually higher than perceived, owing to the impact of this induced aggregation.

7.4.1.4 Effect of surfactant on total spore counts in PBS

At pH 1, 3 and 7 the addition of 1% Tween 20 to the spores was shown to significantly increase the total counts. Whereas at pH 5 there was no significant effect seen. This implies that at acidic pH, there is a tendency for spores to aggregate more.

7.4.1.5 Effect of surfactant on plate counts

Plate count results for spores immersed in acidified LB broth indicated a variable contribution from the addition of Tween, where at pH 1 and 7, the counts significantly increased but at pH 3 and 5 there was no impact seen. This is similar to the impact of Tween on total *via* FCM where a variable impact of total count was found. This also ties in with the previous results seen in Chapter 6, where the total counts of dormant spores were highly variable. For example no significant change in total count was seen at pH 2.7 (55mM HCl) but there was a significant decline in total count at pH 1.9. (100mM HCl) and 3.4 (40mM HCl).

The effect of 1% Tween 20 on PBS at acidified pH was statistically significant at pH 1, 3, and 7, but again, as seen with the total counts in PBS by FCM, at pH 5 there was no difference seen in the counts.

It is also worthy to note that aggregation causes not just FCM counts to decline, but also plate counts. This implies that one aggregate may only form one visible colony, which can lead to confusing results given that a colony forming unit could either be one cell or an aggregate of an unknown number of cells (Shapiro 2005). This can lead to complications when researchers use plating to assess viability, for example in a study on spore germination in the murine GIT, plate counts were used to assess spore counts in mice feces. The problem

with such an approach being that the conditions encountered by the spores will be extremely varied, thus there is no clear way to determine what levels of aggregation may have occurred (Casula and Cutting 2002). Likewise, in studies exploring the effect of acid treatment on other species of bacteria, the issue of aggregation is still likely to persist (Ampatzoglou *et al.* 2010)

7.4.1.6 *Application of 1% Tween 20 to spores immersed in simulated fed stomach conditions*

The results from the spores immersed in pig pellet feed again imply that significant levels of aggregation are occurring, where 1% Tween 20 significantly increases counts in all but one sample point. Again, the effects of aggregation are shown through both FCM and plating. It is known that buffering capacity of the feed is quite strong given the fact that 100mM HCl does not impact viability at up to four hours (Lawlor *et al.* 2005).

The impact of Tween 80 on disaggregating *B. subtilis* spore clumps has been well established (Rao *et al.* 2015), it is notable that the Tween 80 does not have any significant impact on germination, hence it can be assumed that the presence of Tween in the samples will act to disaggregate the spores but should not affect their physiology in any other significant manner (Blank *et al.* 1987).

7.4.2 Particle size distribution and zeta potential

Data from the Malvern mastersizer strongly support the theory that the average particle size increases as the pH lowers. Since the zeta potential data show that the charge moves closer to 0 as the pH lowers, this could imply that the electrostatic repulsive forces that would stop the spores from aggregating become less powerful at lower pHs and almost zero at pH 1. This will likely be due to the primary composition of the proteinic spore coat as a result of the different amino acid side chains. As discussed in 7.1.1 this leads to an uneven distribution of charges across the spore coat giving both positive and negative areas. The zeta potential will only give a net charge, and will not factor in the spatial distribution of

charges across a proteinic molecule. This effect is only extenuated in the case of the spore surface, which consists of a number of proteinic layers of different proteins (Wilson *et al.* 2001; McKenney and Eichenberger 2012). Never-the-less, since proteins have a different charge depending on the pH they are in, a protein in an environment above its isoelectric point will be negative, whereas below its isoelectric point its' net charge will be positive. This means that at a certain pH the overall net charge of the spore surface will be 0, and will therefore lack the repulsive force to prevent aggregation. The zeta potential data indicates that this is around pH 1 for the system studied herein. This would fit with the results seen throughout this chapter, as consistently at pH 1 there has been an increase in total and viable counts when 1% Tween 20 is added.

Whilst the charges shown in this study are less negative than previous studies (see Table 7.1) (Mamane-Gravetz and Linden 2005; Pesce *et al.* 2014) it is important to remember that in this experiment, the zeta potential was measured in 100mM PBS of which the actual ionic strength is much higher. In the previous studies, the zeta potential is measured in deionised water, 145mM NaCl or 40mM PBS. Since the ionic strength is much lower in these cases, the negative charge of the spores is not dampened to the extent shown in these trials.

7.4.3 Concluding remarks

There appears to be a good correlation with the reduction of counts seen at very acidic pH, where a significant reduction in total counts was seen in Chapters 5,6 and 7 for dormant spores subject to 100mM HCl, whilst at pH 5 the decline in total count was not seen when method 2 was employed. This corresponds with the particle size distribution data (Figure 7.12), where at pH 3; the average particle size was significantly greater than the average particle size at pH 5.

The studies detailed in this chapter highlight the fact that aggregation occurs in different media, and that the level of aggregation increases at lower pHs. The zeta potential

data would suggest that at least part of the reason for this trend may be that the repulsive negative charge of the spore coat surface becomes less negatively charged as it reaches pH 1, therefore as a result of the absence of the electrostatic repulsion barrier the spores are more likely to stick together.

Fluctuating counts have been reported previously in studies by Leser *et al.* (2008) and Hoa *et al.* (2001). Conclusions based on these previous studies on the enumeration of spores (and cells) across the GIT should be treated with caution, as without the presence of a non-ionic surfactant or another agent to break apart aggregates, it is likely that the resulting counts could reflect changes in the levels of aggregation, rather than a perceived decline in viability (or even growth), depending on the conditions the spores are exposed to.

On a wider perspective, the complexity of physicochemical interactions between spores and their significance for the perceived spore viability under the GIT conditions appear to be underestimated and further studies delineating these interactions would be worth pursuing.

8 Chapter Eight: Discussion and Conclusion

The following chapter summarises the main conclusions from the research presented throughout the thesis, in order to meet the primary objective: to investigate the fate of ingested spores in *in vitro* simulated pig gastric conditions as a means of delineating the phenomena involved with the reported loss of viability of probiotic spores. The project focused on why such large declines in viable counts had been reported in gastric conditions followed by a rapid recovery of cell and spore numbers in further parts of the GIT (Casula and Cutting 2002; Cartman *et al.* 2008; Leser *et al.* 2008). To do this, experiments were undertaken to determine what factors were responsible for the decline in counts, or more specifically, what phenomena influence the standard perception of spore viability in the gastric step of the GIT. The resulting insights and novel information derived from these experiments are highlighted in this chapter.

8.1 Selection and optimisation of FCM settings

It was deemed essential to develop a methodology that could accurately assess and enumerate the sub-populations of *B. subtilis* in order to fulfil the primary objective of the project, that of investigating the fate of spores in *in vitro* pig gastric conditions. This was needed so that the phenomena that influenced the spore and cell counts could be better investigated. The steps undertaken throughout Chapter 2, illustrate how a full analysis of all FCM parameters and settings was required in order to achieve this aim.

8.1.1 Setting FCM acquisition

The results from Figure 2.5 suggest that for bacterial analysis, the SSC trigger is preferential as it provides a better signal since the SSC trigger is a photomultiplier (PMT) channel, whereas the FSC channel is a photodiode detector. As mentioned in Chapter 2, the photomultiplier channels have significantly lower light levels, but have high gain, meaning even the unstained cell and spores can be differentiated from the noise, thus meaning the

signal to noise resolution is much clearer (BDBiosciences 2005; Díaz *et al.* 2010). However there is a recent consensus that both the FSC and a PMT channel should be used as dual trigger signals, mainly as a fluorescent channel will aid to distinguish between actual cell and debris (Ambriz-Avina *et al.* 2014). As illustrated in the FCM output when the EPICS Coulter Elite FCM was used (Figure 5.4, Figure 5.5, Figure 5.7, Figure 5.9 and Figure 5.11), the FSC trigger could actually identify more sub-populations. This was related to the instrument capabilities, as the strength of the laser could be altered on this machine but this function was not available on the FACSCalibur. As a general rule, for the FACSCalibur used throughout this research, it appears the SSC trigger channel is preferential for bacterial or small particle (<0.6µm) analysis, though the trigger channel did not appear to affect the data following the laser realignment in Section 2.3.7.

8.1.2 Staining procedure

The investigations undertaken throughout Chapter 2 highlight the importance of adopting a staining procedure that will enable the highest number of physiological states to be identified. Dye concentration, temperature and cell concentration have all been shown to have an impact on the staining intensities (Section 2.3.3) and whilst this was anticipated (Stocks 2004), the results show that by manipulating these parameters, greater insights can be gained. This is highlighted in Figure 2.21, where the dead spores are only separated from the dormant *via* an elevated staining temperature.

Further key information from these trials for other researchers is that compensation should be set using singly stained samples with the dyes that will be implemented in the experiments, rather than using universal fluorescent beads (Nebe-von-Caron 2012). Upon advice from Nebe-von-Caron (2012) the Calibrite beads that were previously used to set the compensation levels were discontinued owing to the fact that the fluorescence spectrum is different for these beads compared to the stains used in the study. This realisation was

essential in setting the FCM protocol, and again, is vital information for others who wish to design a new FCM methodology.

8.1.3 OD₂₇₀ measurements

Implementing an amended version of the OD₂₇₀ measurements of DPA release was necessary to check levels of germination (Setlow *et al.* 2013). By using a sensitive method to check the onset of germination it can be soundly concluded that the changes observed in the FCM profiles when elevating the staining protocol temperature from 4°C to 28°C were not due to temperature induced germination. Hence, the sub-population assignments should accurately reflect the true nature of the samples. Based on the information from Figure 2.26, it was evident that the staining protocol could be amended to up to 28°C incubation time at 60 minutes, or 30 minutes incubation at 37°C. The implications for this are that spores kept at this temperature in PBS (or water) should undergo no germination.

8.2 Spore generation and purification

The thorough investigations undertaken to produce high purity dormant spores has highlighted several current issues in relation to spore production. One key issue, is that there is no standard method for determining spore purity (Harrold *et al.* 2011), this means that whilst many researchers may assess spore purity based on microscopic examinations (Carrera *et al.* 2008; Carroll *et al.* 2008; Chen *et al.* 2010; Yi and Setlow 2010; Zhang *et al.* 2014), others may plate out heat activated samples to assess the levels of spore dormancy (Dragon and Rennie 2001). What is very notable is that both these methods are laborious and take considerable time to implement. The FCM assessment of spores detailed in Chapter 3 provides good evidence that FCM could be an excellent alternative to assess spore purity in the future due to its speed and accuracy.

8.2.1 The impact of manganese on sporulation

The influence of manganese on spore production has been shown to be a vital element in creating spores with a high enough purity to be used. Importantly, it is clear that the amount of manganese present in AK sporulating agar does not seem to be sufficient to produce spore stocks of high enough purity. Whilst it is likely that each strain of *B. subtilis* will vary in its sporulating ability, the addition of MnSO_4 would be a sensible course of action for any researchers wishing to produce large amounts of high purity spores as it significantly lowers the amount of debris present in samples as illustrated in Figure 3.9. As detailed in Chapter 3, manganese is essential to the sporulating process owing to its use as a cofactor to the enzyme phosphoglycerate phosphomutase (Oh and Freese 1976). As Vasantha and Freese (1979) state, sporulation is dependent on establishing the correct balance of intracellular metabolites. If these are disturbed in any way, sporulation is arrested. This may lead to a build-up of dead cells, which will eventually be broken down resulting in far greater amounts of cellular debris as demonstrated in Figure 3.12. Such sensitivity may explain the variation in levels of spore purity seen throughout this project, accordingly, the sporulation processes detailed in Chapter 3 should be followed diligently when a high spore purity stock is required.

8.3 FCM assessment of antimicrobials on cells of *B. subtilis*

As stated in Chapter 1, one of the key objectives required to establish the validity of the FCM methodology was to assess the effect of different treatments on *B. subtilis* cells and spores *via* FCM and plating. The assessment of different antimicrobial compounds on cells of *B. subtilis* have shown that FCM can accurately determine the lethality of certain treatments (Figures 4.3 and 4.9) though there are differences in count between FCM and plating. These differences are related to the contrast between viability (measured by FCM) to culturability (measured by plating). Whilst these two parameters are often considered to be synonymous, it remains that culturability only measures an organisms' ability to form

colonies on a given medium, whereas viability could refer to any number of parameters. In the case of the research presented herein, the integrity of cell membranes, metabolic activity or membrane potential could also be used to assess viability (Nebe-von-Caron *et al.* 1998; Lehtinen 2007).

Whilst the reported values are generally higher for FCM than plating, this can actually be an advantageous trait, owing to the fact that FCM will not underestimate viable counts of cells. This is particularly relevant when screening for new bactericidal agents, where an overestimate of the efficacy of a novel antimicrobial could have potentially fatal consequences. Given the success with which the GTE has been evaluated (Figure 4.1, Table 4.1) it would seem that FCM could well be implemented in the ongoing quest for other novel antimicrobial agents, where high numbers of potential candidates will need to be screened quickly and efficiently, often in a limited time period (Ambriz-Avina *et al.* 2014).

8.4 FCM assessment of germination and cell sorting

Based on the initial literature search, it had been hypothesised that spore death in the gastric compartment would either be due to germination induced death or a direct sporicidal affect. To analyse whether this was case, the OD₂₇₀ method to monitor DPA release was employed to determine the extent of germination in *in vitro* GIT conditions

8.4.1 Monitoring the release of DPA via UV spectroscopy

The low levels of DPA release, in combination with high death tolls, indicated a possible scenario where spores were killed and the receptors that mediate the release of DPA were also destroyed or damaged (Figure 5.3). There is some current evidence that may point to the existence of aquaporin like structures on the spore coat. For example a gene has been sequenced that could be an aquaporin related protein [L8AJL5_BACIU (UniProt 2014)]. The existence of these structures in cells may indicate there are similar structures in the spore coat which could point to one possible reason why spores may lose their viability but

retain their DPA depot, at least within the time frame stipulated in the experiments undertaken in Chapter 5 (i.e. 60 minutes). However, as mentioned in Section 5.4.1, it is more likely that aggregation drives the decline in plate counts noted, hence, it is very probable that the combination of slow DPA release coupled with the potential formation of aggregates would mean that the actual death tolls were linked to a germination induced method, rather than the direct sporicidal effect.

8.4.2 FCM analysis of spore germination

It has been proven that FCM can monitor the germination process, i.e. Syto 16 uptake occurs very rapidly once the spores have been exposed to a nutritionally rich environment, demonstrated by an increase in the intensity on the FL1 (green) fluorescence axis displayed in Figure 5.7. This method could be used in conjunction with others as a means to assess the physiological states of *B. subtilis* spores in close to real time scenarios.

Cell sorting (Figure 5.4, to Figure 5.12) verifies the physiological assignment based on FCM analysis, and furthermore confirms that the areas labelled as ‘debris’ do not harbour any culturable bacteria either. Thus it can be affirmed that the Syto 16 and PI staining are an accurate and rapid means to assess the physiological states of *B. subtilis*.

Whilst it would be advantageous to assess the sorted sub-populations in further downstream analysis, it remains that the technology required to cell sort is only capable of sorting up to a certain speed (estimated 40,000 events/second maximum (Ambriz-Avina *et al.* 2014)). It can therefore take a considerable amount of time to collect a statistically sufficient number of cells or spores for microscopic analysis or PCR, particularly if the sub-population is a low percentage of the total events. Hence, the advantage of sorting onto plates is that only a small number of droplets are required to elicit colony growth, and should DNA analysis be desired, this can be done following colony formation (Hernlem and Ravva 2007). The limitation of this process is that transient sub-populations cannot be analysed owing to the length of time such analysis would need. However, FACS remains very

important in the verification of any new FCM methodology, and would be particularly important when implementing novel viable stains (Nebe-von-Caron *et al.* 1998).

8.5 *In vitro* porcine gastric conditions

The experimental findings from the present study have shown that heat activation does not significantly alter the susceptibility of spores to acid stress. This has been also reported by Leuschner and Lillford (1999) where a 65°C heat activation for 10 minutes only increased the homogeneity of germination, as the times taken for spores to turn from phase bright to phase dark were highly consistent, though the average time taken for germination did not differ from the non-heat activated spores.

Based upon the knowledge that spores will germinate in the presence of nutrients and moisture, hence losing their resistance to harsh conditions, the comparison between dormant and pre-germinated spores detailed in Chapter 6 was considered particularly important from an animal husbandry stand point. As was hypothesised, pre-germination does significantly decrease viability when looking at comparable conditions (Figure 6.13 b). Even at relatively low HCl concentrations (40mM) there is up to a 32% decline in viability of the pre-germinated spores, whereas the dormant spores exposed to the same conditions do not undergo any significant change in viability. As such it is essential that farmers and others involved in pig husbandry are alerted to the fact that if the probiotics are not kept in sealed, dry conditions they risk losing a high proportion of the spore stock. With this in mind, it is also essential to dose the pigs with the probiotic either in water or as a dose with a restricted feed. If spores are left in a pig feed where pigs are fed *ad lib*, it is highly probable that the spores will begin to germinate in this feed and therefore lose their dormancy. As highlighted by the pre-germinated spores in Chapter 6, this would have a significant effect on probiotic survival, with up to 45% reduction in viability (Figure 6.13 b). Hence, in order to gain the maximum benefit from the spores and to minimise profit loss, farmers should adhere to these guidelines.

The variability reported by previous researchers into the effectiveness of probiotics may well be linked to the variability of individual pigs. For pigs who are not secreting high HCl it could be that this low acid concentration has minimal impact on spore (or indeed cell) viability, whereas high HCl concentrations do have a significant impact on germinated spores and therefore cells. This could be a contributing factor in explaining why the effect of probiotics varies from pig to pig, as each pig will have a different amount of acid secretion in the stomach.

8.6 Bacterial spore aggregation

The experimental findings from Chapters 5 and 6 heavily implied that aggregate formation was a driving factor behind the declining counts seen in *in vitro* gastric conditions. In Chapter 7, these assumptions were validated as *B. subtilis* spores were clearly indicated to aggregate in a variety of *in vitro* conditions studied in LB and PBS as can be seen by FCM and plating count evidence. Though aggregation and adhesion are considered important points for probiotics this can also mean enumeration can be difficult, thus requiring additional and complementary enumeration techniques to be used in conjunction with plating. Whilst it is acknowledged that traditional plating has the disadvantage of underestimating counts due to aggregation there are few researchers who have tried to circumvent this issue (Reimann *et al.* 2010). The effect of aggregation on probiotic enumeration is not a widely reported phenomenon but it offers a perfectly plausible explanation as to why previous spore counts have been drastically reduced in the stomach only to rapidly recover again in the duodenum (Leser *et al.* 2008). This could reflect the fact that acid causes the spores to aggregate, whereas the bile from the gall bladder released emulsifies the digesta, thus causing the spore aggregates to break apart. Although aggregation would be expected to occur at least during the gastric phase, the extent of aggregation might be dependent on the wider digesta composition, as can be inferred from the differing results in terms of percentage decline in total counts between spores in PBS (Figure 7.6) and LB (Figure 7.5 b). For example, when dormant spores are immersed in

acidified PBS or LB (using the same concentration of HCl), there is a greater loss in number when the spores were immersed in PBS. The effect of the digesta is further emphasised when one considers the results from Figure 7.10, where the addition of 1% Tween 20 was shown to significantly increase both viable (FCM and plating) and total counts (FCM) over each time point analysed.

For PBS, investigation of aggregation phenomena involved also the use of particle size analysis and Zeta-potential measurement. These additional methods have created a range of compelling evidence pointing towards the existence of spore aggregation at least under the investigated conditions. Indeed the Zeta-potential measurements (Figure 7.14) revealed that the electrostatic repulsion force is reduced. In particular a low negative charge of 7.26mV at pH 5 was observed, which was further reduced to -4.20mV at pH 3 and reached practically a zero charge at pH 1. In line with the DLVO theory, the reduced Zeta-potential value could explain a high propensity for spore aggregation.

This indicates aggregation is very likely and accordingly it is most likely that the effects of aggregation will have influenced the results of previous researchers of spore viability in the gastric environment (Hoa *et al.* 2000; Casula and Cutting 2002; Tam *et al.* 2006; Leser *et al.* 2008) Where a vast decline in counts are observed and then an unusually high increase in counts as the spore move further across the GIT are seen. This would support the idea that bile acts as a surfactant on the counts.

8.7 Conclusion

Whilst flow cytometry has been used frequently in literature since the 1980's (Shapiro and Nebe-von-Caron 2004) there has been little effort to extend this tool to enumerate sub-populations of cells and spores. The reasons for this may be due to the high risk of contamination when dealing with axenic cultures, i.e. cells which have been exposed to environmental conditions will be contaminated with other species of bacteria. It may be that FCM is not used as readily as other methods due to the fact that determining different

species of bacteria is not yet possible. Though older studies attempted to group bacteria based on the staining profiles with PI and FITC, out of 19 bacteria, these could only be sorted into three related groups, and differentiating bacteria in the same genus was only possible in a few instances (Miller and Quarles 1990). This may have given rise to the precedence of molecular methods in microbial research (Thanantong *et al.* 2006; Degnan and Ochman 2012).

However, the results generated from this study show that FCM is a potentially valuable tool for the assessment of the impact of treatments upon cells and spores of *B. subtilis*. As stated by Abee *et al.* (2011) the ability to analyse bacteria at the single cell level is highly desirable. Although time lapse microscopy can provide information on specific individual cell behaviour, it is highly time consuming and is not adaptable to assess very high numbers of cells. In these ways FCM really does provide insights not possible by other methods. What is noteworthy is that the results from this study were only possible upon examining all FCM parameters (Cronin 2012).

The specific alterations to the staining protocols were based on key insights highlighted through collaborations with Cronin (2012). The basis of this was a study by Cronin and Wilkinson (2007) where it was first noticed an elevated staining temperature was used. This led to the survey of staining protocols in current available literature. The source of the variation observed in the staining protocols was not apparent in the literature as the selection criteria for each method was not detailed. Furthermore, the underpinning assumptions relating to staining temperature and time, and the behaviour of the micro-organisms were not mentioned. In this research, the steps leading to the selection of the current staining regime, are clearly outlined. It is also clear that informed steps have been made in order to select the optimum FCM settings. The findings from these studies are therefore highly important.

By studying a range of treatments upon *B. subtilis*, the use of FCM as a quantitative and qualitative tool is emphasised. It is hoped that this will enable others to use FCM to gain a deeper understanding of the physiological states of bacteria under stressful conditions.

Whilst many studies have investigated the effect of pressure on *B. subtilis* spores (Mathys *et al.* 2007; Shen *et al.* 2009); the application of FCM to assess damage to cells by antimicrobials, both novel and conventional, suggests this method could take a far more prominent role in bacterial research in the future.

It has been suggested by this research that spore DPA release may be inhibited by certain conditions, for example, the presence of HCl in PBS with no germinants caused spore death yet no significant DPA release. As discussed in Section 8.4, this may be due to the damaging of DPA release channel proteins, or a similar structure.

Aggregation is a key parameter that has been overlooked in probiotic assessments to date. This could at least be a contributing factor if not completely explain why counts of viable probiotic have varied so widely. Indeed the nature of aggregation is complex and difficult to predict across a variety of gastric conditions, therefore it might be argued that is unreasonable to expect that probiotic assessment would follow a strict trend. However for future research, it is essential to keep this in mind as it has the potential to severely distort the accuracy of results obtained.

To the best of our knowledge this is the first example of FCM enumeration and cell sorting used to assess the physiological states in mixtures of *B. subtilis* cells and spores. By combining the FCM results with other methods, i.e. plating and Petroff-Hausser haemocytometry, it can be agreed that the results obtained are an accurate reflection of the effects of various treatments upon this organism. The key insights generated throughout this research are that FCM can be used as a tool to assess spore purity much faster than current microbiological methods. Furthermore, it can be used to keep track of mass balances across experiments, as a result of its ability to count not just viable cells and spores, but also dead and damaged organisms.

8.7.1 Future Work

With respect to the FCM methodology developed, the most current developments in this field involve the replacement of the analogue technology (developed 20 to 30 years ago) with modern, solid state opto-electronics. This, combined with micro-fabrication and digital signal processing technology would increase the resolution of FCM outputs, meaning more subtle changes in physiology could be detected with the intent that this should lead to more user-friendly and robust technology, better suited for microbial analysis (Veal *et al.* 2000; Ambriz-Avina *et al.* 2014).

The most imminent further work to be carried out will involve direct high resolution microscopic analysis of spores in media at different pH to confirm the presence and size of the aggregates formed. This will be coupled with further investigations into flow cytometric analysis of spore behaviour in further parts of the GIT, i.e. the addition of bile salts to the *in vitro* simulated GIT conditions, thus extending the insights gained in this research to more thoroughly examine spore behaviour in other conditions.

It is envisaged that the methodologies and insights generated will be applied to other species of bacteria, for example *Alicyclobacillus spp.* or *B. cereus*, in the fields of food spoilage to better enumerate bacterial concentrations and assess food preservation methods with greater accuracy. This will continue to explore the link between acidity and aggregation phenomena, as well as furthering the applications of these findings potentially into industrial fields. There is also scope to extend the FCM methodology into further antimicrobial assessments, particularly sporicidal agents and treatments. Such research could be of value not only in food science, but also medical fields, anti-bioterrorism (Oie *et al.* 2011; Xing *et al.* 2014), and even astrobiological spore behaviour (Hagen *et al.* 1967; La Duc *et al.* 2003).

9 Appendices

Appendix 1

BBL™ AK Agar #2

Per litre

Pancreatic Digest of Gelatin	6.0 g
Pancreatic Digest of Casein	4.0 g
Yeast Extract	3.0 g
Beef Extract	1.5 g
Dextrose	1.0 g
Agar	15.0 g
MnSO ₄	0.3 g

Suspend 30.8 g of the powder in 1L of purified water. Mix thoroughly and heat with frequent agitation and boil for 1 minute to completely dissolve the powder.

Difco Sporulation Medium (DSM)

Per litre

Bacto nutrient broth (Difco)	8 g
10% (w/v) KCl	10 ml
1.2% (w/v) MgSO ₄ ·7H ₂ O	10 ml
1 M NaOH	~1.5 ml (pH to 7.6)

Adjust volume to 1 litre with dd H₂O pH 7.6. Autoclave and allow to cool to 50°C. Just before use, add the following sterile solutions:

1M Ca(NO ₃)	1ml
0.01M MnCl ₂	1ml
1mM FeSO ₄	1ml

Step Gradients of Renografin (Nicholson and Setlow 1990)

Gradient Solutions:

A. For 20% Renografin for 10ml

Reno-60	3.33ml
dd H ₂ O	6.66ml

B. For 50% Renografin for 30ml

Reno-60	25ml
dd H ₂ O	5ml

1. Inoculate colony into 25ml DSM and grow to mid log phase $0.45 < A_{600} < 0.6$ (~2 hours)
2. Dilute by 1 to 10 into 250ml pre-warmed (37°C) DSM in 2L flask. Incubate a further 48 hours at 37°C at 150rpm.
3. Observe culture occasionally during growth & continue to next step when >90% culture are free spores
4. Centrifuge culture for 10min at 10G & discard supernatant
5. Wash pellet with 200ml cold sterile ddH₂O.
6. Centrifuge for 10min at 10G again and discard supernatant
7. Re-suspend the pellet in 200ml cold distilled water and leave at 4°C overnight.
8. Repeat steps 4-7 and then check pure spore suspension under phase contrast microscopy – when >90% are phase bright, the Renografin purification to eliminate vegetative cells can be carried out.
9. Collect spores by centrifugation and suspend in 2-3ml 20% Renografin soln.
10. Layer the suspension over 15ml 50% Renografin in a glass Corex tube and centrifuge for 30 mins at 10G.
11. Use a pipette connected to a vacuum line to remove all layers of the gradient except the pellet which contains free spores

12. Suspend the pellet in 10ml cold sterile water, then transfer to a falcon tube and centrifuge at 7G for 10 minutes
13. Repeat the above step 3 more times to remove all Renografin as tract amounts may induce germination
14. Re-suspend the pellet in 2ml sterile ddH₂O and count 1:100 dilution using a Petroff Hauser haemocytometer
15. Keep the spores at 4°C and every 2-4 weeks re-pellet and decant the water and replace with fresh cold ddH₂O to prevent germination.

Available online at:

<http://docs.google.com/viewer?a=v&q=cache:MxyoR0kETJYJ:www.uab.edu/luckielab/protocols/sporeprep.doc+purification+of+spores&hl=en&gl=uk&pid=bl&srcid=ADGEESjIS9x5IrWMBkHibNg84XACvFTaLHUvFbGv6atacBeKuF2aDCF1TIY17qCzQNkgYsSbXPL5HIWjON5yuef5mxkWjX6VKK6TXltVYyrayUqxch2EldAWhD866sspN1j3&sig=AHIEtbRU4JY5S9AVwpj8vblwtM0YumSHw> (Accessed 17 October 2011)

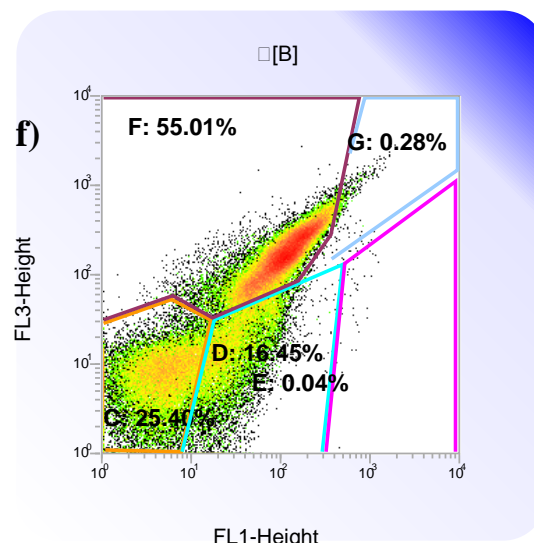
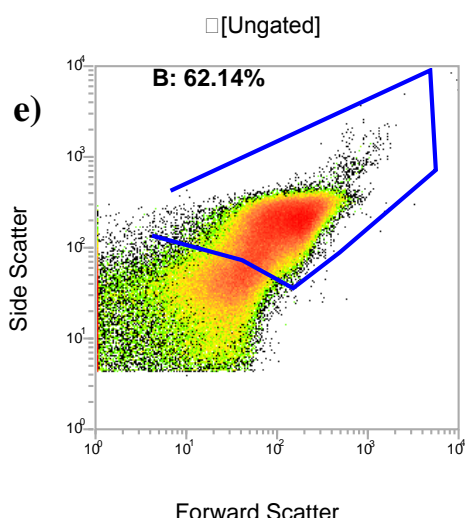
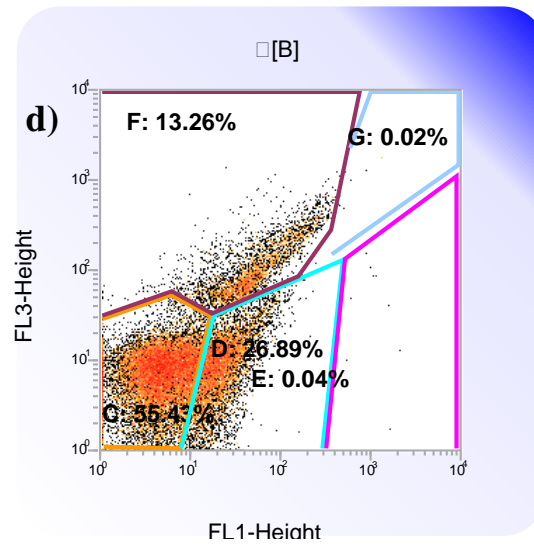
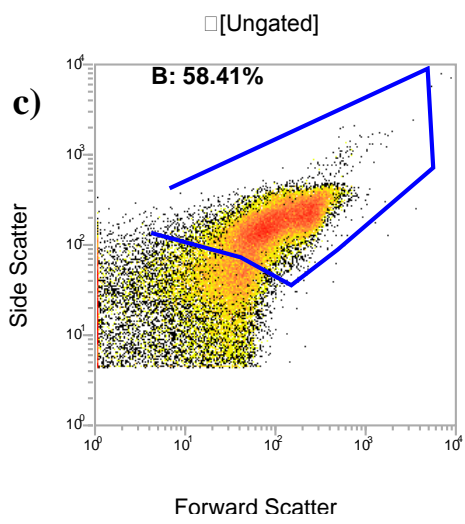
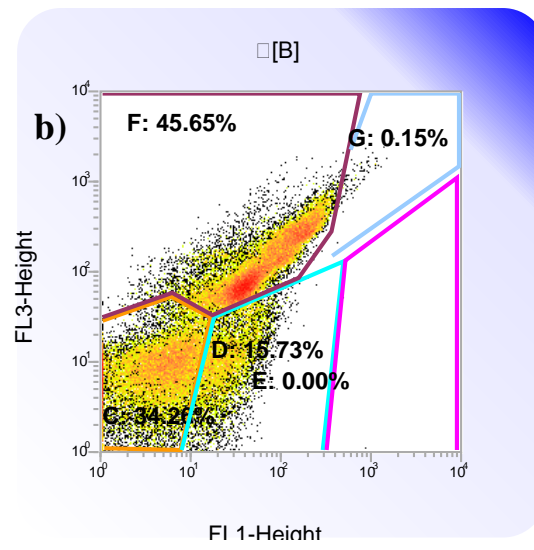
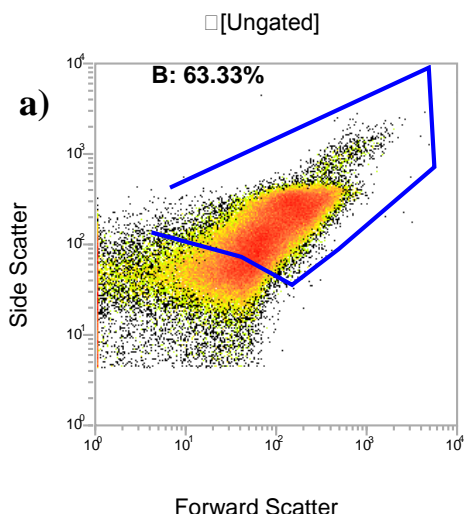
Ethanol treatment (Zhao *et al.*, 2008):

- Add 0.1mM MnSO₄ (or MnCl₂) to the growth medium to maximise spore efficiency and stability.
- Harvest a suspension of spores and vegetative cells by taking 70ml culture and transferring to an 85ml centrifuge tube
- Centrifuge at 10,000×g for 10 min at 4°C
- Decant supernatant and wash pellet with 20ml sterile deionized water by vortexing for 20s.
- Centrifuge at 10,000xg for 10 min at 4°C
- Resuspend the pellet in 20ml of 1:1 sterile deionized water and ethanol (200 proof;

99.5%).

- Cap centrifuge tube and incubate at 22°C for 12 h on an orbital shaker (Lab Line) at 100 rev/min (3-day culture) or for 2 h at 200 rev/min (10-day culture).
- Centrifuge again and wash suspension twice with sterile deionized water.

Appendix 2



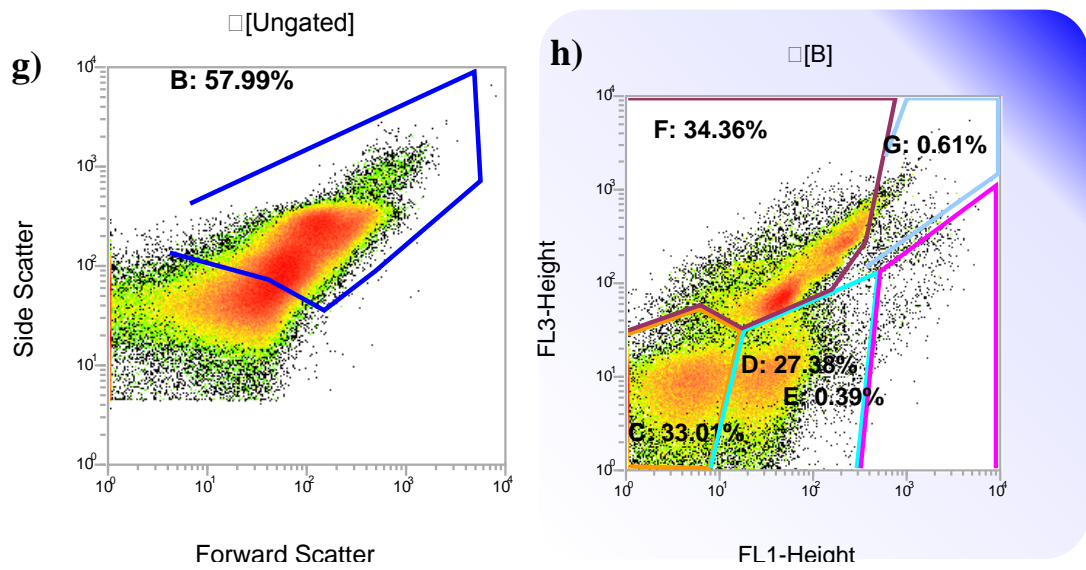


Figure 9.1 FCM output for spore samples B, C and D and E following multiple washing steps. Left column) density plot of FSC vs SSC, region A (red) drawn around the cell/spore area of a) sample B, c) Sample C, e) Sample D and g) Sample E. Region B (blue): cells and spores. Right column) density plot gated on region B of FL1 (Green) fluorescence vs FL3 (Red) fluorescence, region C (orange): dormant spores, region D (turquoise): germinating spores, region E (pink): live cells, region F (burgundy): dead spores and cells, region G (light blue): double stained cells. b) Sample B, d) Sample C, f) Sample D and h) Sample E.

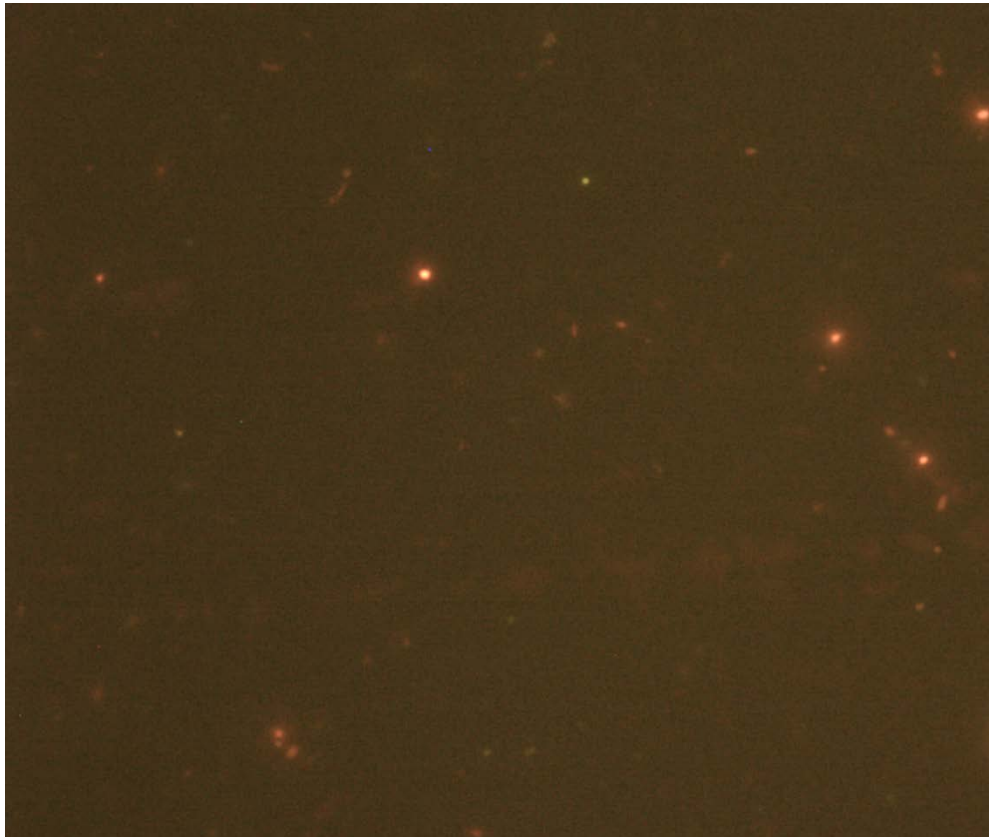
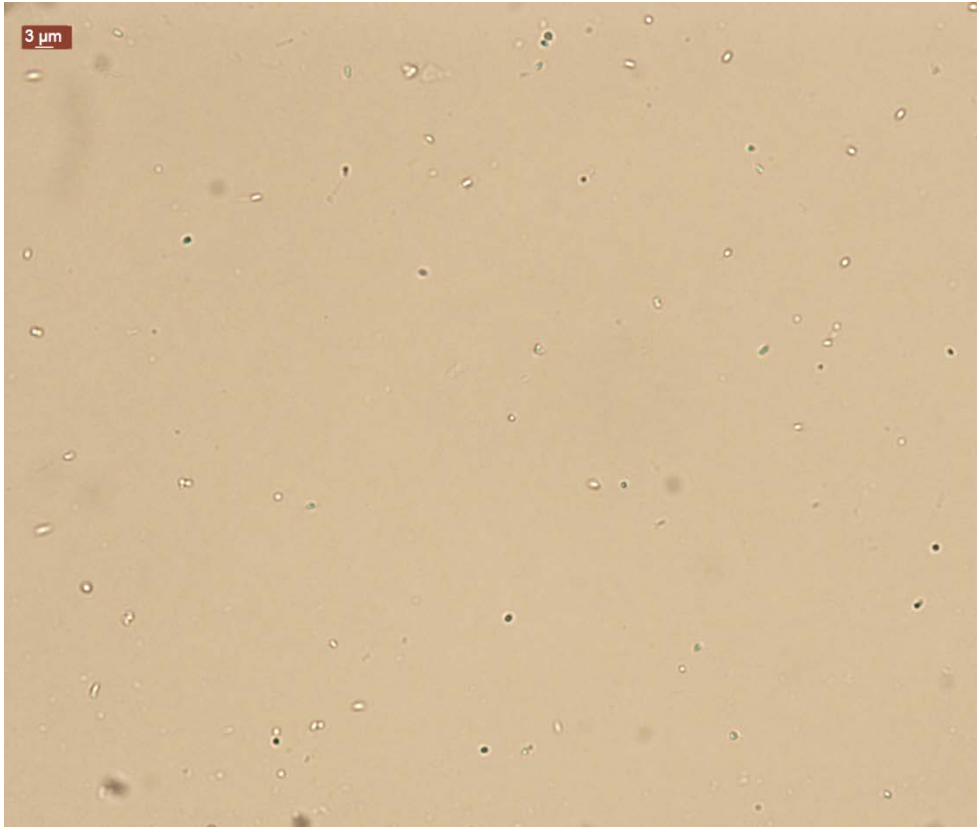


Figure 9.2 Fluorescent microscopy image of *B. subtilis* spore sample B, taken using the 63x objective lens. Stained with Syto 16 and PI under a) DIC light and b) I3 (blue) light

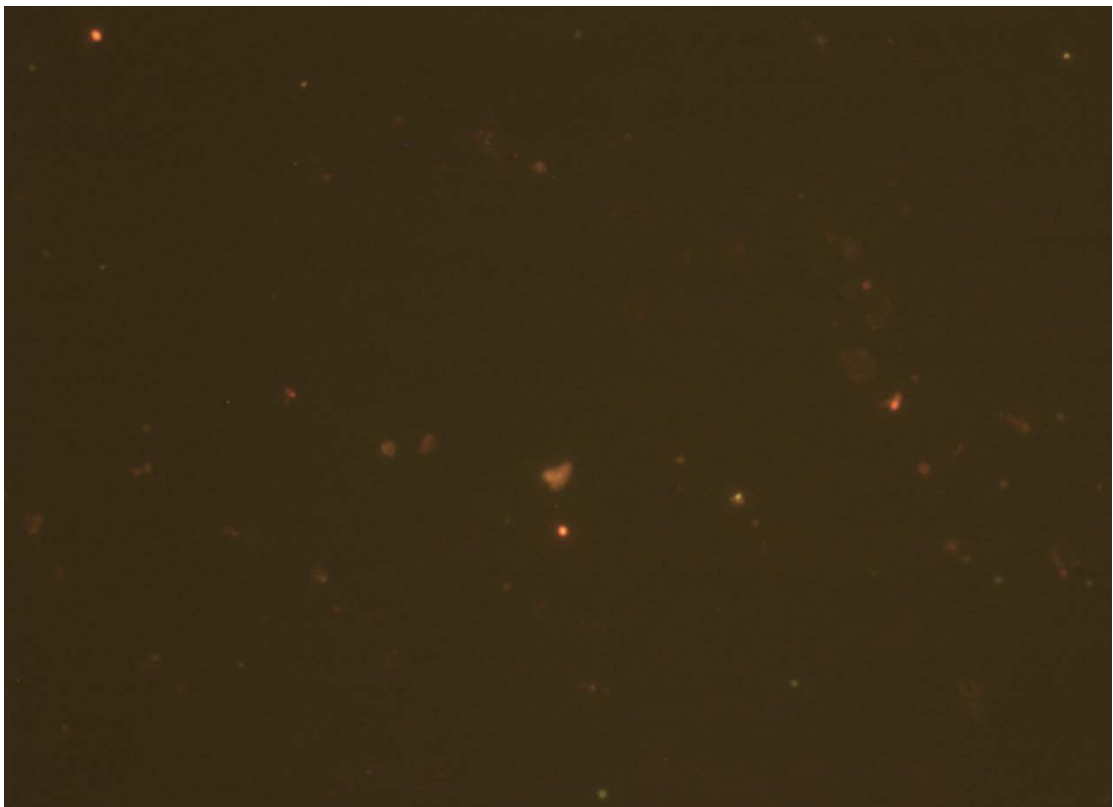
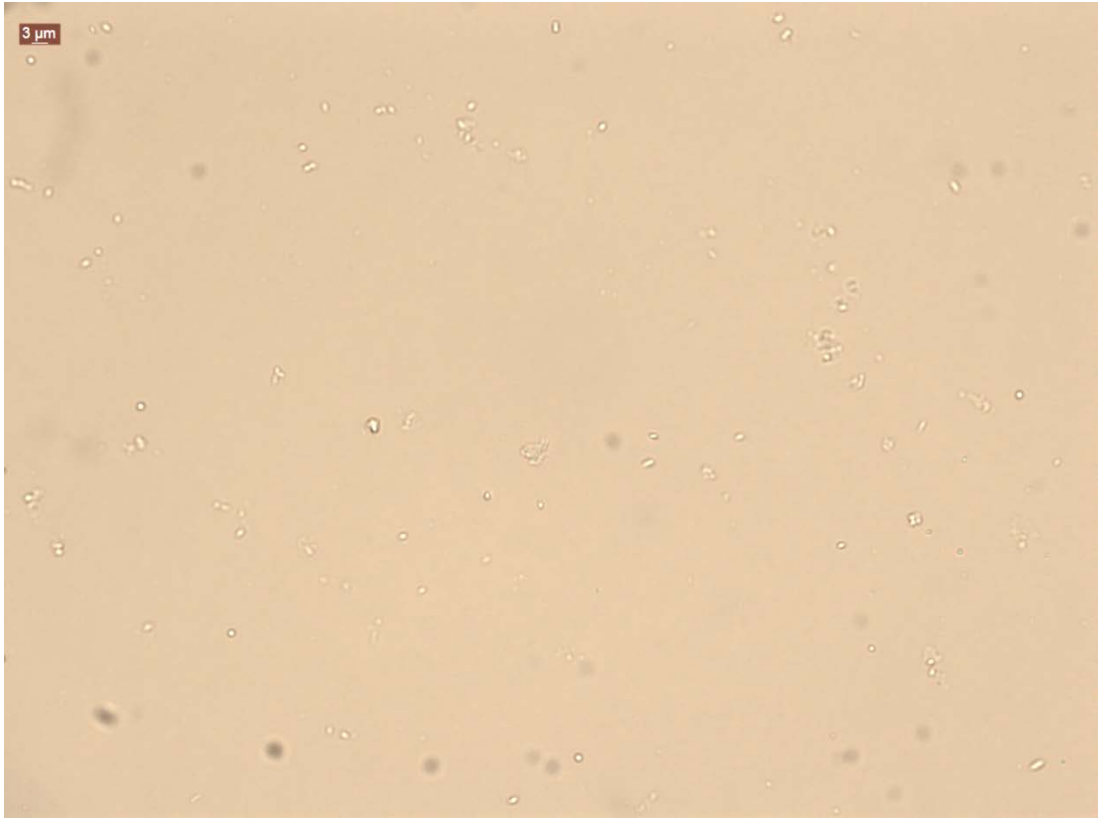


Figure 9.3 Fluorescent microscopy image of *B. subtilis* spore sample C, taken using the 63x objective lens. Stained with Syto 16 and PI under a) DIC light and b) I3 (blue) light

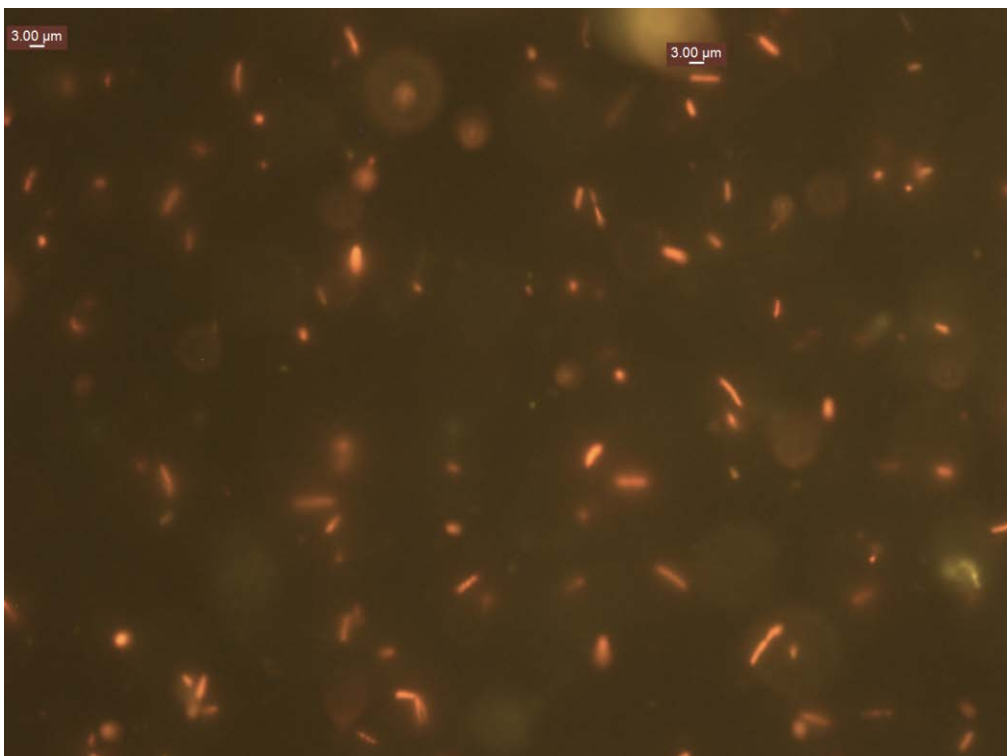
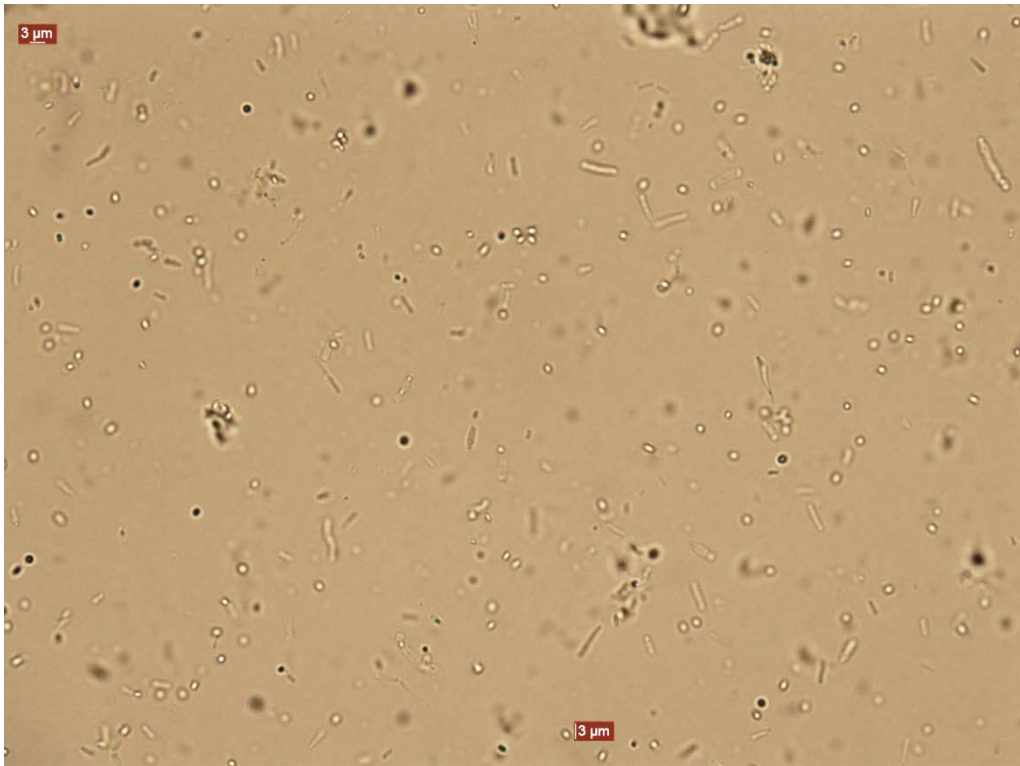


Figure 9.4 Fluorescent microscopy image of *B. subtilis* spore sample D, taken using the 63x objective lens. Stained with Syto 16 and PI under a) DIC light and b) I3 (blue) light

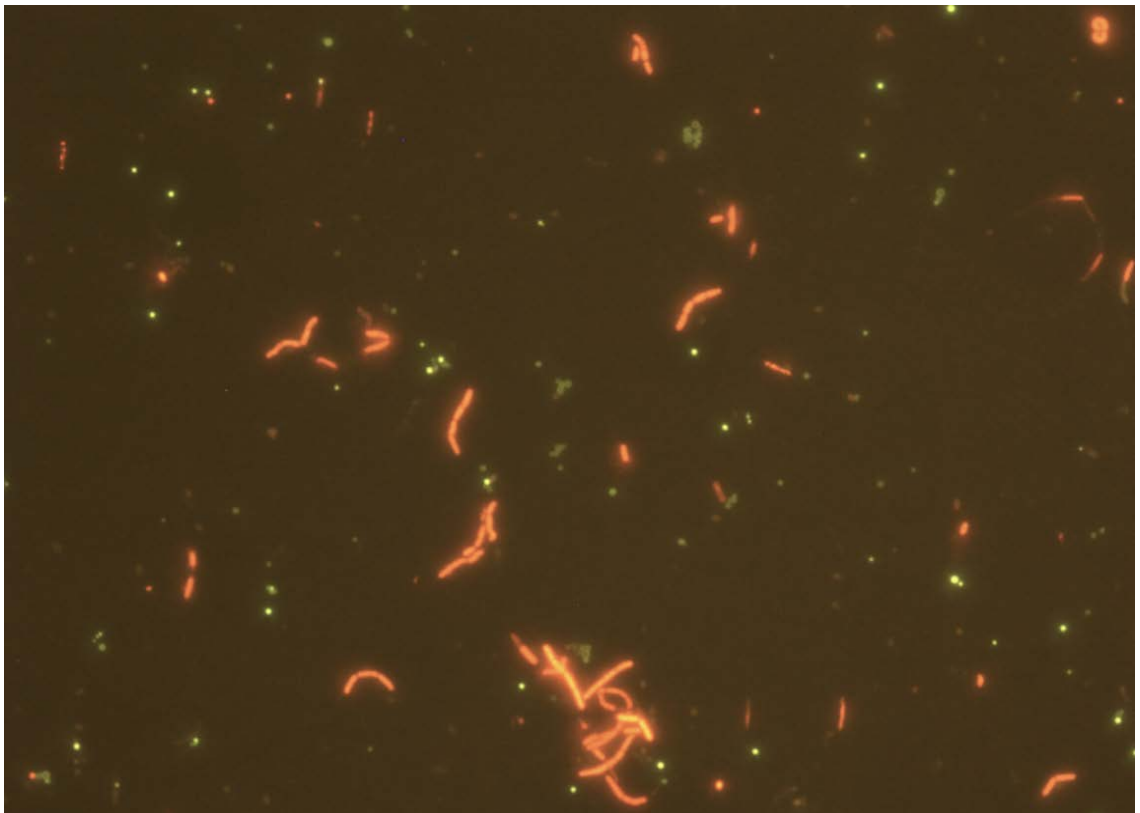
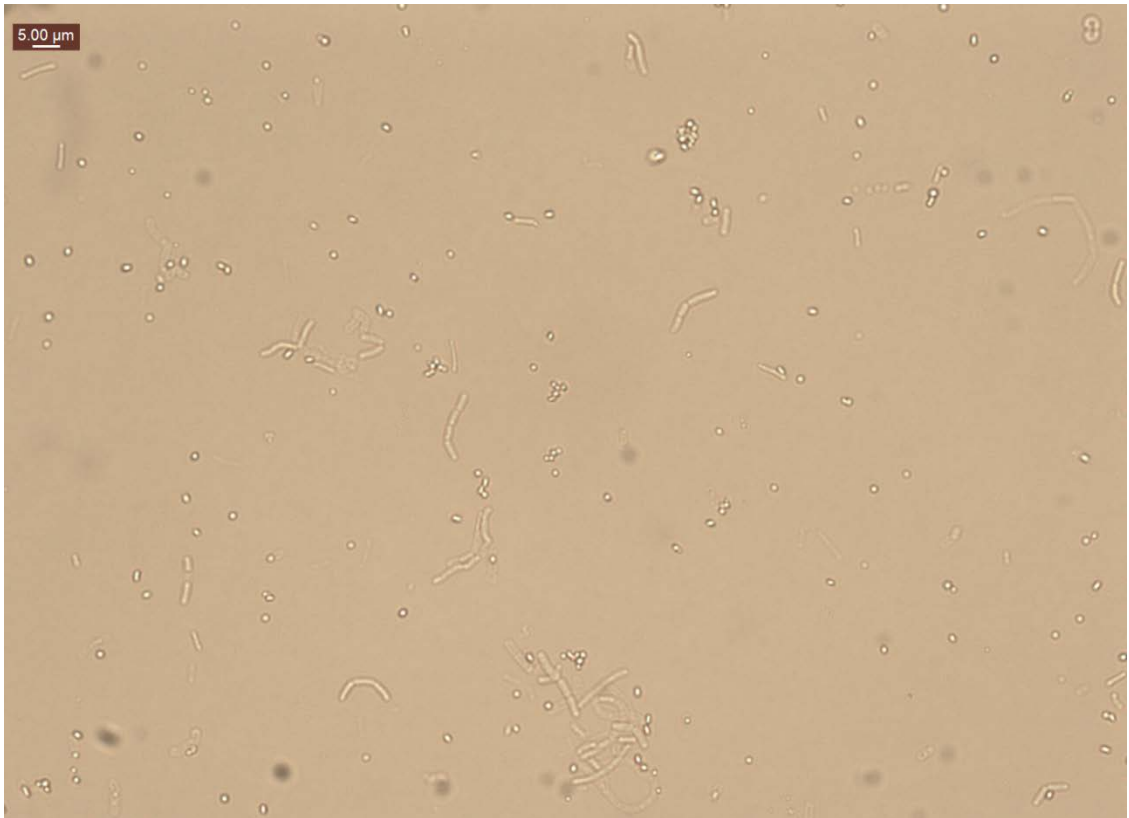


Figure 9.5 Double stained *B. subtilis* spores sample E under the 63x objective lens a) DIC light image
b) I3 light image.

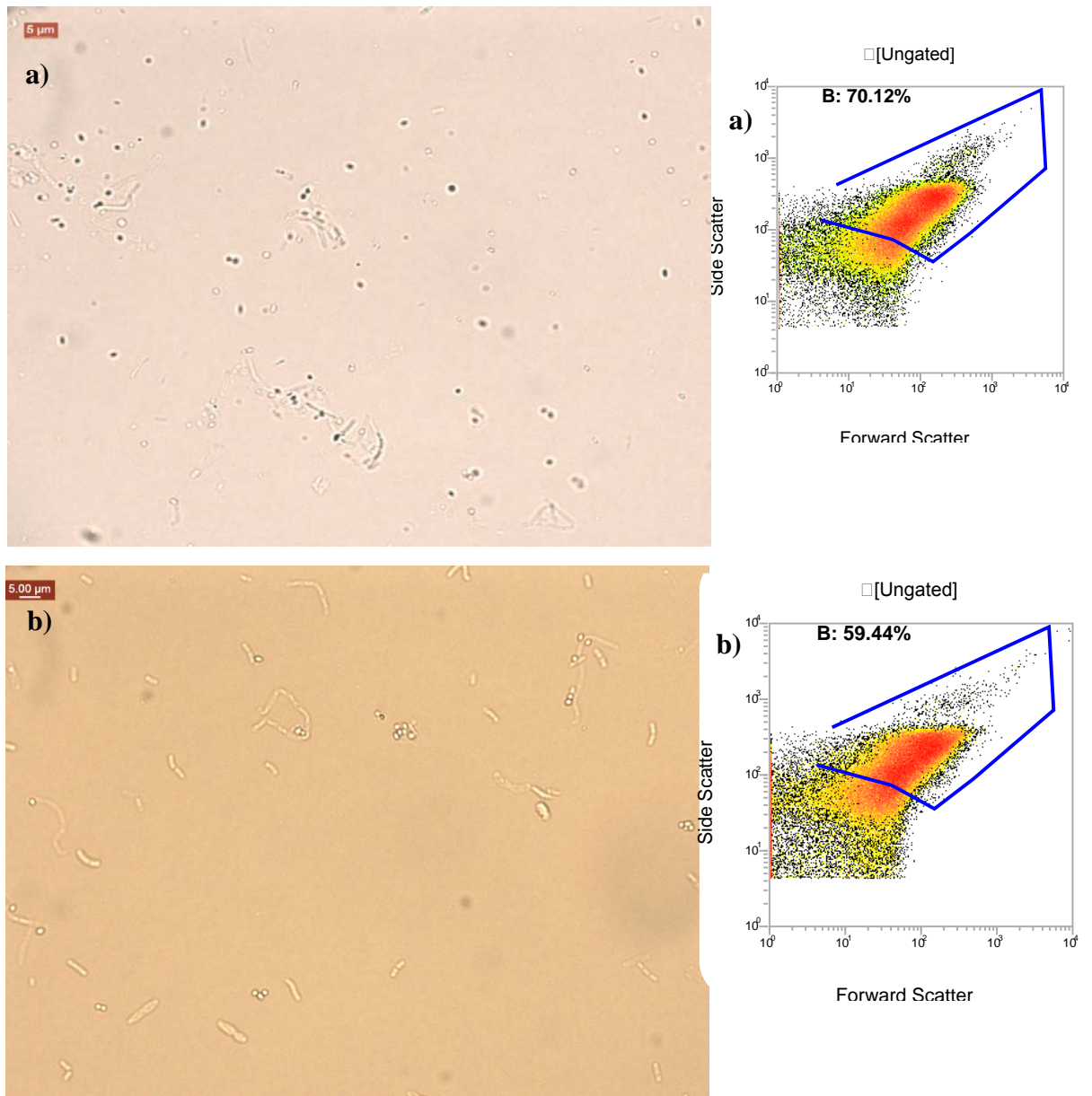


Figure 9.6 Sample A of *B. subtilis* spores. a) Top row, left, DIC image using the 63x objective lens before 0.2µm filter and right, FCM FSC vs SSC profile of the same sample with Region B drawn around the cell and spore population. b) Bottom row, DIC image at 63x magnification post 0.2µm filter and right, FCM FSC vs SSC density profile with Region B drawn around the cell and spore population.

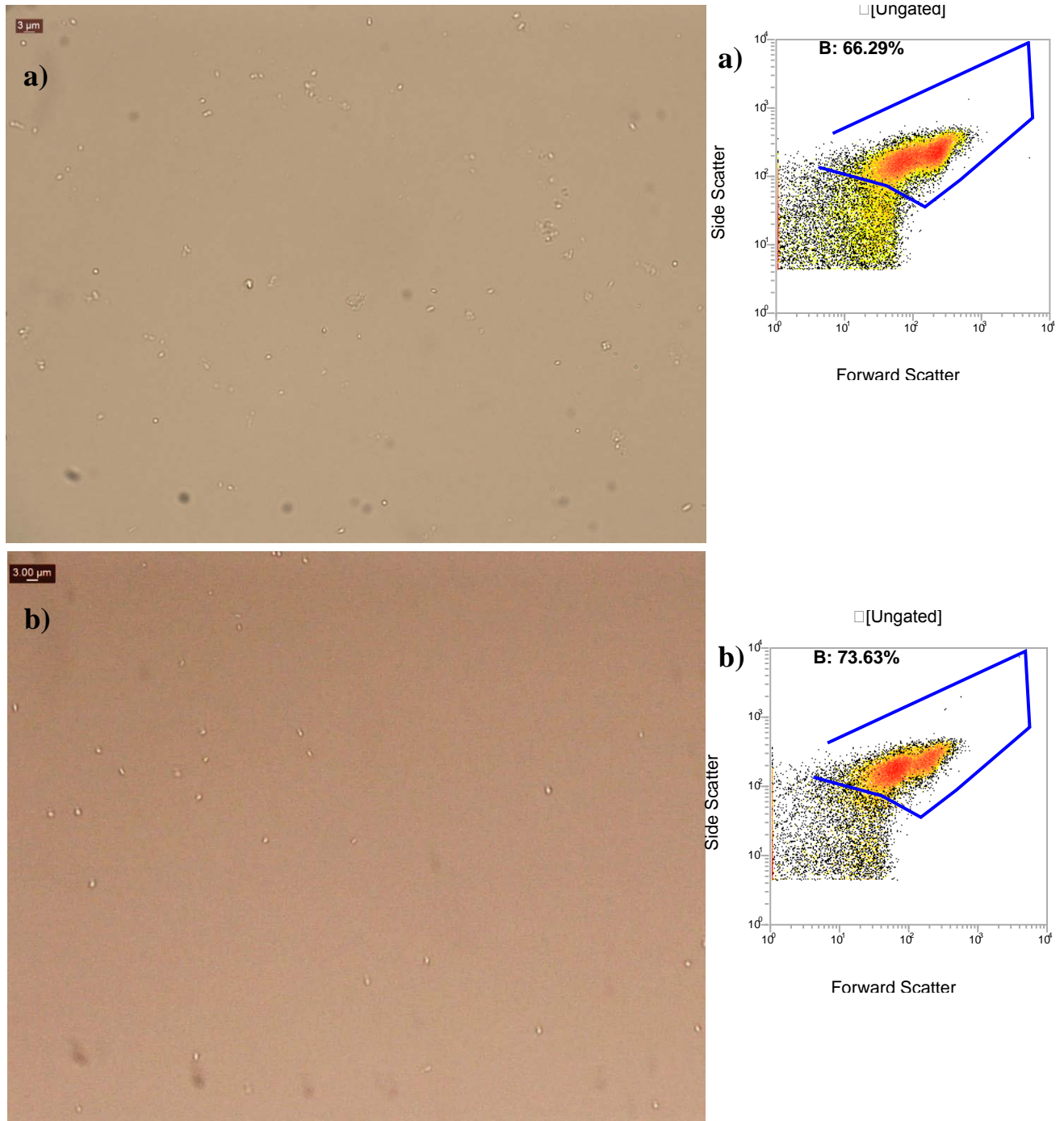


Figure 9.7 Sample C of *B. subtilis* spores. a) Top row, left, DIC image at 63x magnification before 0.2µm filter and right, FCM FSC vs SSC profile of the same sample with Region B drawn around the cell and spore population. b) Bottom row, DIC image at 63x magnification post 0.2µm filter and right, FCM FSC vs SSC density profile with Region B drawn around the cell and spore population.

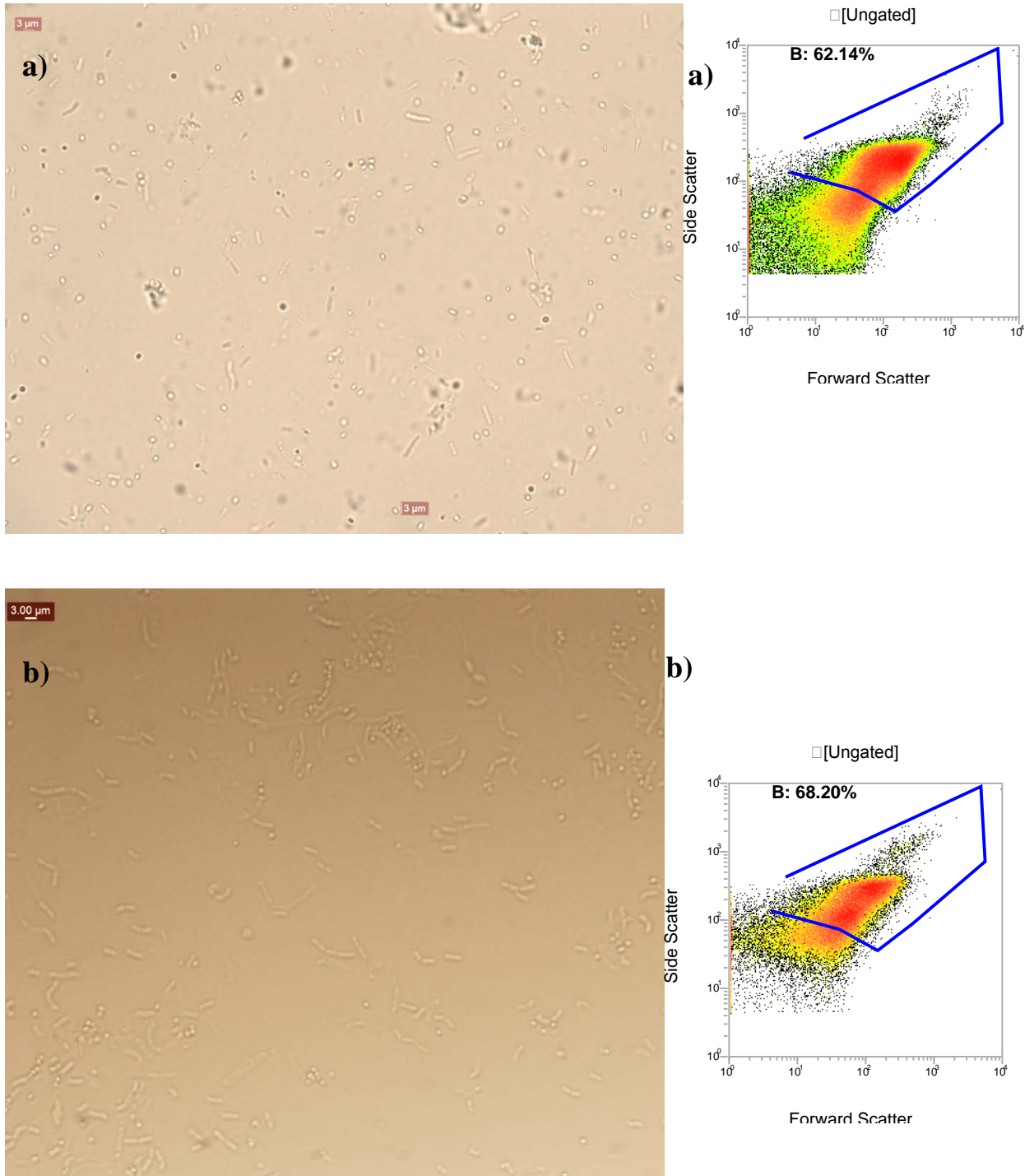


Figure 9.8. Sample D of *B. subtilis* spores. a) Top row, left, DIC image using 63x objective lens before 0.2µm filter and right, FCM FSC vs SSC profile of the same sample with Region B drawn around the cell and spore population. b) Bottom row, DIC image at 63x magnification post 0.2µm filter and right, FCM FSC vs SSC density profile with Region B drawn around the cell and spore population.

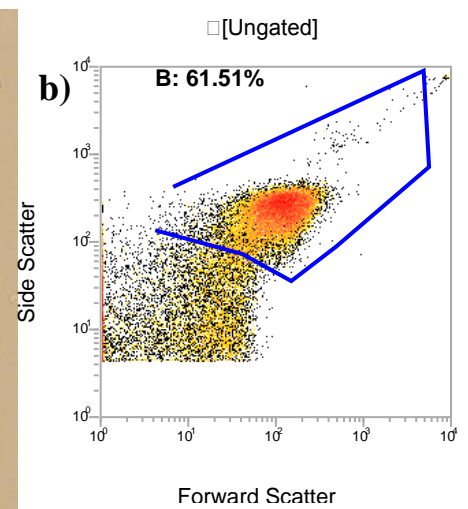
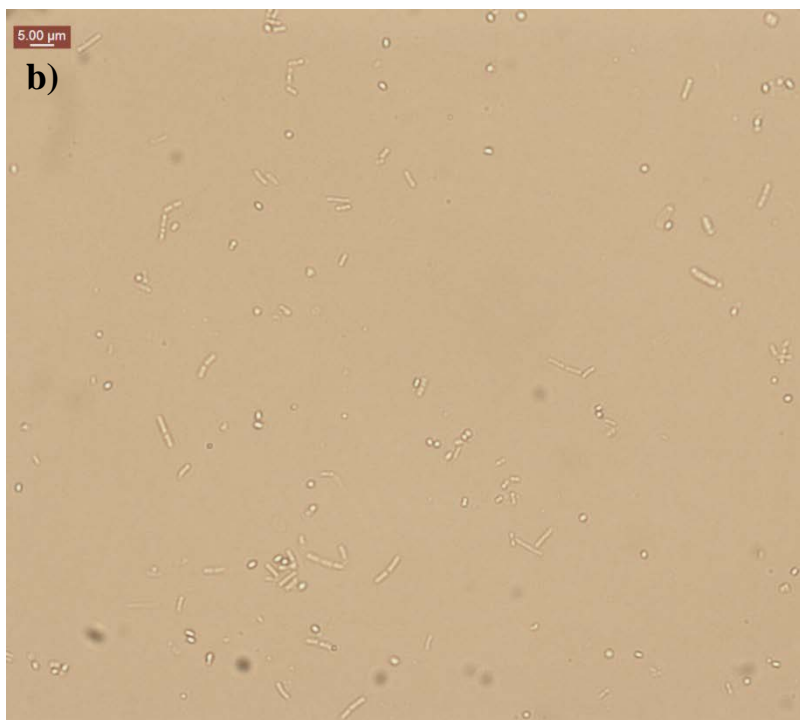
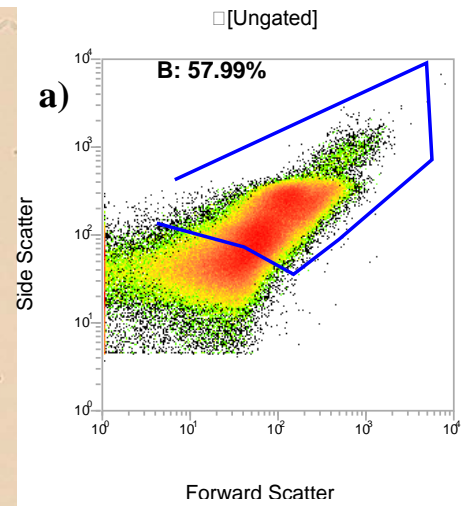
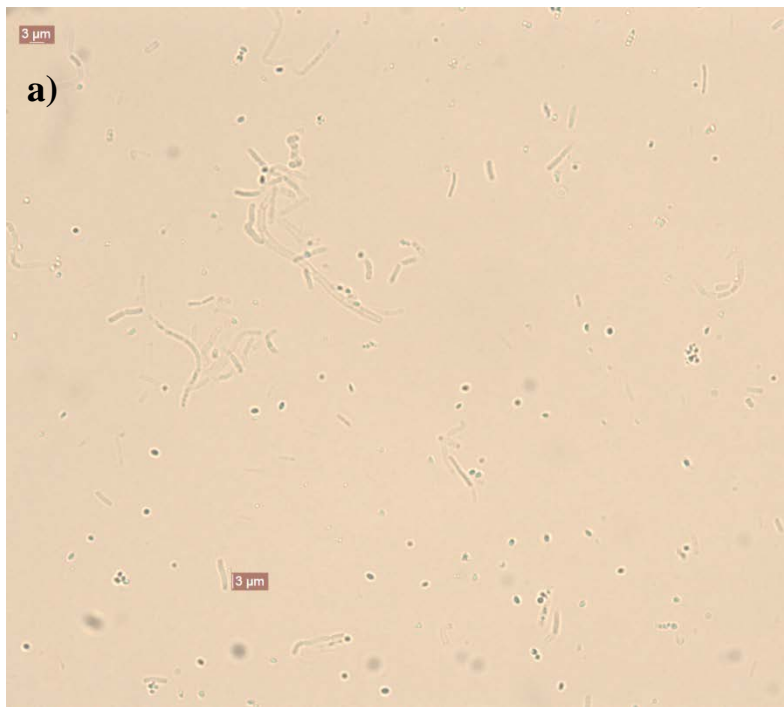
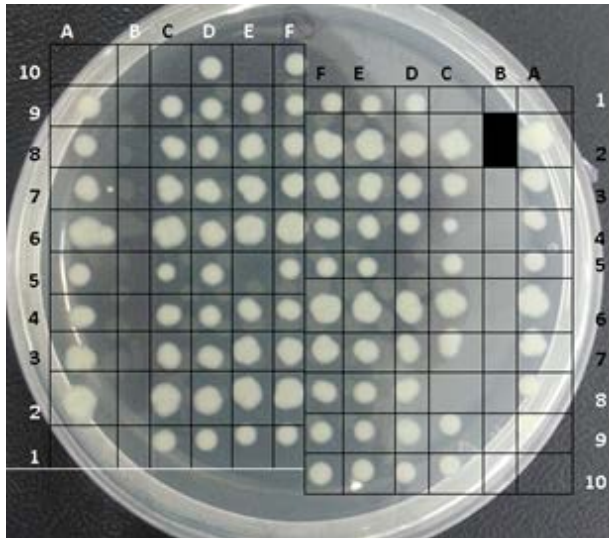


Figure 9.9 Sample E of *B. subtilis* spores. a) Previous page, left, DIC image under the 63x objective lens before 0.2 μ m filter and right, FCM FSC vs SSC profile with Region B drawn around the cell and spore population. b) DIC image under the 63x objective lens post 0.2 μ m filter and right, FCM FSC vs SSC density profile with Region B drawn around the cell and spore population.

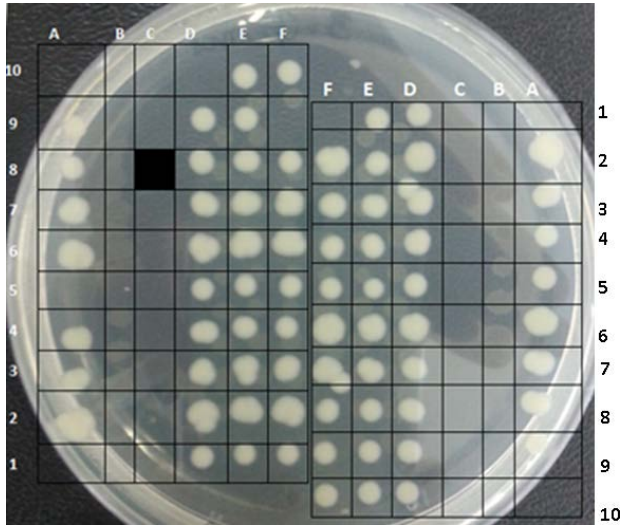
Appendix 3

Cell sorting on germinated spores (repeat)



	A	B	C	D	E	F
1	0	1	1	1	1	1
2	30	30	30	30	30	30
3	10	10	10	10	10	10
4	3	3	3	3	3	3
5	1	1	1	1	1	1
6	30	30	30	30	30	30
7	10	10	10	10	10	10
8	3	3	3	3	3	3
9	1	1	1	1	1	1
10	0	1	1	1	1	1

Figure 9.10 Spores immersed in LB broth for 30 minutes, then re-suspended in PBS and stained with Syto 16 and PI. All sorted at rates of 1, 3, 10, and 30 droplets per well as shown in the grid on the right.



	A	B	C	D	E	F
1	0	1	1	1	1	1
2	30	30	30	30	30	30
3	10	10	10	10	10	10
4	3	3	3	3	3	3
5	1	1	1	1	1	1
6	30	30	30	30	30	30
7	10	10	10	10	10	10
8	3	3	3	3	3	3
9	1	1	1	1	1	1
10	0	1	1	1	1	1

Figure 9.11 Spores immersed in LB broth for 30 minutes, then re-suspended in PBS and stained with Syto 16 and PI. All sorted at rates of 1, 3, 10, and 30 droplets per well as shown in the grid on the right.

References

Abee, T., Groot, M. N., Tempelaars, M., Zwietering, M., Moezelaar, R. and van der Voort, M. (2011). "Germination and outgrowth of spores of *Bacillus cereus* group members: diversity and role of germinant receptors." Food Microbiology **28**(2): 199-208.

Alander, M., Satokari, R., Korpela, R., Saxelin, M., Vilpponen-Salmela, T., Mattila-Sandholm, T. and von Wright, A. (1999). "Persistence of colonization of human colonic mucosa by a probiotic strain, *Lactobacillus rhamnosus* GG, after oral consumption." Applied and Environmental Microbiology **65**(1): 351-354.

Alexopoulos, C., Georgoulakis, I. E., Tzivara, A., Kyriakis, C. S., Govaris, A. and Kyriakis, S. C. (2004). "Field evaluation of the effect of a probiotic-containing *Bacillus licheniformis* and *Bacillus subtilis* spores on the health status, performance, and carcass quality of grower and finisher pigs." Journal of veterinary medicine. A, Physiology, pathology, clinical medicine **51**(6): 306-312.

Allen, A. and Garner, A. (1980). "Mucus and bicarbonate secretion in the stomach and their possible role in mucosal protection." Gut **21**(3): 249-262.

Ambriz-Avina, V., Contreras-Garduno, J. A. and Pedraza-Reyes, M. (2014). "Applications of flow cytometry to characterize bacterial physiological responses." BioMed Research International **2014**: 14.

Ampatzoglou, A., Schurr, B., Deepika, G., Baipong, S. and Charalampopoulos, D. (2010). "Influence of fermentation on the acid tolerance and freeze drying survival of *Lactobacillus rhamnosus* GG." Biochemical Engineering Journal **52**(1): 65-70.

Ananta, E., Voigt, D., Zenker, M., Heinz, V. and Knorr, D. (2005). "Cellular injuries upon exposure of *Escherichia coli* and *Lactobacillus rhamnosus* to high-intensity ultrasound." Journal of Applied Microbiology **99**(2): 271-278.

Anderson, D. L., Bartholomeusz, F. D., Kirkwood, I. D., Chatterton, B. E., Summersides, G., Penglis, S., Kuchel, T. and Sansom, L. (2002). "Liquid gastric emptying in the pig: effect of concentration of inhaled isoflurane." Journal of Nuclear Medicine **43**(7): 968-971.

Ange, K. D., Eisemann, J. H., Argenzio, R. A., Almond, G. W. and Blikslager, A. T. (2000). "Effects of feed physical form and buffering solutes on water disappearance and proximal stomach pH in swine." Journal of Animal Science **78**(9): 2344-2352.

Anukam, K. C. and Reid, G. (2007). "Probiotics: 100 years (1907-2007) after Elie Metchnikoff's Observation." Communicating current research and educational topics and trends in applied microbiology **1**: 466-474.

Arret, B. and Kirshbaum, A. (1959). "A rapid disc assay method for detecting penicillin in milk." Journal of Milk and Food Technology **22**: 329-331.

Atluri, S., Ragkousi, K., Cortezzo, D. E. and Setlow, P. (2006). "Cooperativity between different nutrient receptors in germination of spores of *Bacillus subtilis* and reduction of this cooperativity by alterations in the GerB receptor." Journal of Bacteriology **188**(1): 28-36.

Atrih, A., Zöllner, P., Allmaier, G. and Foster, S. J. (1996). "Structural analysis of *Bacillus subtilis* 168 endospore peptidoglycan and its role during differentiation." Journal of Bacteriology **178**(21): 6173-6183.

Babinszky, L., Van Der Meer, J. M., Boer, H. and Den Hartog, L. A. (1990). "An in-vitro method for prediction of the digestible crude protein content in pig feeds." Journal of the Science of Food and Agriculture **50**(2): 173-178.

Bagwell, C. B. and Adams, E. G. (1993). "Fluorescence spectral overlap compensation for any number of flow cytometer parameters." Annals of the New York Academy of Science **677**: 167-184.

Baier, D., Mathys, A. and Knorr, D. (2010). "Identification of different physiological states of bacterial spores and distinction from vegetative cells after high pressure treatments via flow cytometry."

Bakker, R. G., Li, C., Miller, M. R., Cunningham, C. and Charon, N. W. (2007). "Identification of specific chemoattractants and genetic complementation of a *Borrelia burgdorferi* chemotaxis mutant: flow cytometry-based capillary tube chemotaxis assay." Applied and Environmental Microbiology **73**(4): 1180-1188.

Barrow, P. A., Fuller, R. and Newport, M. J. (1977). "Changes in the microflora and physiology of the anterior intestinal tract of pigs weaned at 2 days, with special reference to the pathogenesis of diarrhea." Infection and Immunity **18**(3): 586-595.

Baxter, J. and Cummings, S. P. (2008). "The degradation of the herbicide bromoxynil and its impact on bacterial diversity in a top soil." Journal of Applied Microbiology **104**(6): 1605-1616.

BDBiosciences (2005). Establishing Optimum Baseline PMT Gains to Maximize Resolution on BD Biosciences Digital Flow Cytometers. BD™ Digital Flow Cytometers: 1-8.

Binnendijk, K. H. and Rijkers, G. T. (2013). "What is a health benefit? An evaluation of EFSA opinions on health benefits with reference to probiotics." Beneficial Microbes **4**(3): 223-230. doi: 210.3920/BM2013.0019.

Black, E. P., Koziol-Dube, K., Guan, D., Wei, J., Setlow, B., Cortezzo, D. E., Hoover, D. G. and Setlow, P. (2005). "Factors influencing germination of *Bacillus subtilis* spores via activation of nutrient receptors by high pressure." Applied and Environmental Microbiology **71**(10): 5879-5887.

Black, E. P., Wei, J., Atluri, S., Cortezzo, D. E., Koziol -Dube, K., Hoover, D. G. and Setlow, P. (2007). "Analysis of factors influencing the rate of germination of spores of *Bacillus subtilis* by very high pressure." Journal of Applied Microbiology **102**: 65-76.

Blank, G., Al-Khayat, M. and Ismond, M. A. H. (1987). "Germination and heat resistance of *Bacillus subtilis* spores produced on clove and eugenol based media." Food Microbiology **4**(1): 35-42.

Block, S. S. (2001). Disinfection, sterilization, and preservation, Lippincott Williams & Wilkins.

Bogovič-Matijašić, B. and Rogelj, I. (2011). Bacteriocins of Probiotics and Enteric Cytoprotection. Probiotic Bacteria and Enteric Infections. J. J. Malago, J. F. J. G. Koninkx and R. Marinsek-Logar, Springer Netherlands: 313-354.

Boisen, S. and Fernández, J. A. (1997). "Prediction of the total tract digestibility of energy in feedstuffs and pig diets by in vitro analyses." Animal Feed Science and Technology **68**(3-4): 277-286.

Bos, R., van der Mei, H. C. and Busscher, H. J. (1999). "Physico-chemistry of initial microbial adhesive interactions-its mechanisms and methods for study." FEMS Microbiol Rev. **23**(2): 179-230.

Branda, S. S., González-Pastor, J. E., Ben-Yehuda, S., Losick, R. and Kolter, R. (2001). "Fruiting body formation by *Bacillus subtilis*." Proceedings of the National Academy of Sciences **98**(20): 11621-11626.

Bunthof, C. J. and Abee, T. (2002). "Development of a Flow Cytometric Method to Analyse Subpopulations of Bacteria in Probiotic Products and Dairy Starters." Applied and Environmental Microbiology **68**(6): 2934-2942.

Burns, R. G. and Dick, R. P. (2002). Enzymes in the Environment: Activity, Ecology, and Applications, Taylor & Francis.

Busscher, H. J., Norde, W. and van der Mei, H. C. (2008). "Specific molecular recognition and nonspecific contributions to bacterial interaction forces." Applied and Environmental Microbiology **74**(9): 2559-2564.

Canibe, N., Højberg, O., Højsgaard, S. and Jensen, B. B. (2005). "Feed physical form and formic acid addition to the feed affect the gastrointestinal ecology and growth performance of growing pigs." Journal of Animal Science **83**: 1287-1302.

Canibe, N. and Jensen, B. B. (2003). "Fermented and nonfermented liquid feed to growing pigs: Effect on aspects of gastrointestinal ecology and growth performance." Journal of Animal Science **81**: 2019-2031.

Capcarová, M., Weis, J., Hrncar, C., Kolesarova, A., Pertruska, P., Kalafova, A. and Pal, G. (2011). "Effect of Probiotic Supplementation on Selected Indices of Energy Profile and Antioxidant Status of Chickens." Journal of Microbiology, Biotechnology and Food Sciences **1**(2): 225-235.

Carlberg, D. M. (1995). Cleanroom Microbiology for the Non-Microbiologist, Taylor & Francis.

Carrera, M., Zandomeni, R. O. and Sagripanti, J. L. (2008). "Wet and dry density of *Bacillus anthracis* and other *Bacillus* species." Journal of Applied Microbiology **105**(1): 68-77. doi: 10.1111/j.1365-2672.2008.03758.x. Epub 02008 Feb 03720.

Carroll, A. M., Plomp, M., Malkin, A. J. and Setlow, P. (2008). "Protozoal digestion of coat-defective *Bacillus subtilis* spores produces "rinds" composed of insoluble coat protein." Applied and Environmental Microbiology **74**(19): 5875-5881. doi: 5810.1128/AEM.01228-01208. Epub 02008 Aug 01228.

Cartman, S. T., La Ragione, R. M. and Woodward, M. J. (2008). "*Bacillus subtilis* spores germinate in the chicken gastrointestinal tract." Applied and Environmental Microbiology **74**(16): 5254-5258.

Carvalho, A. L. U. d., Oliveira, F. H. P. C. d., Mariano, R. d. L. R., Gouveia, E. R. and Souto-Maior, A. M. (2010). "Growth, sporulation and production of bioactive compounds by *Bacillus subtilis* R14." Brazilian Archives of Biology and Technology **53**(3): 643-652.

Castagliuolo, I., Galeazzi, F., Ferrari, S., Elli, M., Brun, P., Cavaggioni, A., Tormen, D., Sturniolo, G. C., Morelli, L. and Palù, G. (2005). "Beneficial effect of auto-aggregating *Lactobacillus crispatus* on experimentally induced colitis in mice." FEMS Immunology & Medical Microbiology **43**(2): 197-204.

Casula, G. and Cutting, S. M. (2002). "*Bacillus* probiotics: spore Germination in the gastrointestinal tract." Applied and Environmental Microbiology **68**(5): 2344-2352.

Catalano, F. A., Meador-Parton, J., Popham, D. L. and Driks, A. (2001). "Amino acids in the *Bacillus subtilis* morphogenetic protein SpoIVA with roles in spore coat and cortex formation." Journal of Bacteriology **183**(5): 1645-1654.

Ceragioli, M., Mols, M., Moezelaar, R., Ghelardi, E., Senesi, S. and Abee, T. (2010). "Comparative transcriptomic and phenotypic analysis of the responses of *Bacillus cereus* to various disinfectant treatments." Applied and Environmental Microbiology **76**(10): 3352-3360.

Ceuppens, S., Boon, N., Rajkovic, A., Heyndrickx, M., Van de Wiele, T. and Uyttendaele, M. (2010). "Quantification methods for *Bacillus cereus* vegetative cells and spores in the gastrointestinal environment." Journal of Microbiological Methods **83**(2): 202-210.

Ceuppens, S., Uyttendaele, M., Hamelink, S., Boon, N. and Van de Wiele, T. (2012). "Inactivation of *Bacillus cereus* vegetative cells by gastric acid and bile during *in vitro* gastrointestinal transit." Gut Pathogens **4**(1): 11. doi: 10.1186/1757-4749-1184-1111.

Charney, J., Fisher, W. P. and Hegarty, C. P. (1951). "Manganese as an essential element for sporulation in the genus *Bacillus*." Journal of Bacteriology **62**(2): 145-148.

Chen, Z. M., Li, Q., Liu, H. M., Yu, N., Xie, T. J., Yang, M. Y., Shen, P. and Chen, X. D. (2010). "Greater enhancement of *Bacillus subtilis* spore yields in submerged cultures by

optimization of medium composition through statistical experimental designs." Applied Microbiology and Biotechnology **85**(5): 1353-1360.

Chesnokova, O. N., McPherson, S. A., Steichen, C. T. and Turnbough, C. L. (2009). "The spore-specific alanine racemase of *Bacillus anthracis* and its role in suppressing germination during spore development." Journal of Bacteriology **191**(4): 1303-1310.

Chiang, C. C., Croom, J., Chuang, S. T., Chiou, P. W. S. and Yu, B. (2008). "Development of a dynamic system simulating pig gastric digestion." Asian-Australasian journal of animal sciences **21**(10): 1522-1528.

Chiquette, J. (2009). "Evaluation of the protective effect of probiotics fed to dairy cow during a subacute ruminal acidosis challenge." Animal Feed Science and Technology **153**(3-4): 278-291.

Chubukov, V. and Sauer, U. (2014). "Environmental dependence of stationary-phase metabolism in *Bacillus subtilis* and *Escherichia coli*." Applied and Environmental Microbiology **80**(9): 2901-2909.

Chung, J. D., Conner, S. and Stephanopoulos, G. (1995). "Flow cytometric study of differentiating cultures of *Bacillus subtilis*." Cytometry **20**(4): 324-333.

Clavel, T., Carlin, F., Lairon, D., Nguyen-The, C. and Schmitt, P. (2004). "Survival of *Bacillus cereus* spores and vegetative cells in acid media simulating human stomach." Journal of Applied Microbiology **97**(1): 214-219.

Coleman, W. H., Chen, D., Li, Y., Cowan, A. E. and Setlow, P. (2007). "How Moist Heat Kills Spores of *Bacillus subtilis*." Journal of Bacteriology **189**(23): 8458-8466.

Comas-Riu, J. and Vives-Rego, J. (1999). "Use of calcein and SYTO-13 to assess cell cycle phases and osmotic shock effects on *E. coli* and *Staphylococcus aureus* by flow cytometry." Journal of Microbiological Methods **34**(3): 215-221.

Comas-Riu, J. and Vives-Rego, J. (2002). "Cytometric monitoring of growth, sporogenesis and spore cell sorting in *Paenibacillus polymyxa* (formerly *Bacillus polymyxa*)." Journal of Applied Microbiology **92**: 475-481.

Commission, E. (2000). Report of the Scientific Committee on Animal Nutrition on Product BioPlus 2B for use as Feed Additive. Scientific Health Opinions. H. C. P. Directorate-General: 1-8.

Corcoran, B. M., Stanton, C., Fitzgerald, G. F. and Ross, R. P. (2005). "Survival of probiotic lactobacilli in acidic environments is enhanced in the presence of metabolizable sugars." Appl Environ Microbiol. **71**(6): 3060-3067.

Cowan, A. E., Koppel, D. E., Setlow, B. and Setlow, P. (2003). "A soluble protein is immobile in dormant spores of *Bacillus subtilis* but is mobile in germinated spores: implications for spore dormancy." Proceedings of the National Academy of Sciences **100**(7): 4209-4214.

Cranwell, P. D., Noakes, D. E. and Hill, K. J. (1976). "Gastric secretion and fermentation in the suckling pig." British Journal of Nutrition **36**(1): 71-86.

Cronin, U. P. (2012). FCM work on *Bacillus subtilis* cells and spores. Madrid.

Cronin, U. P. and Wilkinson, M. G. (2007). "The use of flow cytometry to study the germination of *Bacillus cereus* endospores." Cytometry A **71**(3): 143-153.

Cronin, U. P. and Wilkinson, M. G. (2008). "*Bacillus cereus* endospores exhibit a heterogeneous response to heat treatment and low-temperature storage." Food Microbiology **25**(2): 235-243.

Cutting, S. M. (2011). "*Bacillus* probiotics." Food Microbiology **28**(2): 214-220.

da Silva, T. L., Reis, A., Kent, C. A., Roseiro, J. C. and Hewitt, C. J. (2005). "The use of multi-parameter flow cytometry to study the impact of limiting substrate, agitation intensity, and dilution rate on cell aggregation during *Bacillus licheniformis* CCM1 1034 aerobic continuous culture fermentations." Biotechnol Bioeng **92**(5): 568-578.

Daglia, M. (2012). "Polyphenols as antimicrobial agents." Current Opinion in Biotechnology **23**(2): 174-181.

Davey, H. M. and Kell, D. B. (1996). "Flow cytometry and cell sorting of heterogeneous microbial populations: the importance of single-cell analyses." Microbiol Rev. **60**(4): 641-696.

Davies, D., Grenfell, R., Walker, R. and Titley, I. (2006, 2014). "Flow Cytometry UK." Retrieved 09/06/2014, from <http://www.flowcytometryuk.org/>.

Davis, C. (2014). "Enumeration of probiotic strains: Review of culture-dependent and alternative techniques to quantify viable bacteria." Journal of Microbiological Methods **103**: 9-17.

de Francesco, M., Jacobs, J. Z., Nunes, F., Serrano, M., McKenney, P. T., Chua, M.-H., Henriques, A. O. and Eichenberger, P. (2012). "Physical interaction between coat morphogenetic proteins SpoVID and CotE Is necessary for spore encasement in *Bacillus subtilis*." Journal of Bacteriology **194**(18): 4941-4950.

de Jong, I. G., Beilharz, K., Kuipers, O. P. and Veening, J.-W. (2011). "Live cell imaging of *Bacillus subtilis* and *Streptococcus pneumoniae* using automated time-lapse microscopy." Journal of visualized experiments: JoVE(53).

de Souza, R. D., Batista, M. T., Luiz, W. B., Cavalcante, R. C. M., Amorim, J. H., Bizerra, R. S. P., Martins, E. G. and de Souza Ferreira, L. C. (2014). "*Bacillus subtilis* Spores as Vaccine Adjuvants: Further Insights into the Mechanisms of Action." PLoS ONE **9**(1): e87454.

De Vries, Y. P. (2004). "The role of Calcium in bacterial spore germination." Microbes and Environments **19**: 199-202.

Dean, D. H. and Douthit, H. A. (1974). "Buoyant density heterogeneity in spores of *Bacillus subtilis*: biochemical and physiological basis." Journal of Bacteriology **117**(2): 601-610.

Déat, E., Blanquet-Diot, S. p., Jarrige, J.-F. o., Denis, S., Beyssac, E. and Alric, M. (2009). "Combining the dynamic TNO-gastrointestinal tract system with a Caco-2 cell culture model: Application to the assessment of lycopene and α -tocopherol bioavailability from a whole food." Journal of agricultural and food chemistry **57**(23): 11314-11320.

Deepika, G., Green, R. J., Frazier, R. A. and Charalampopoulos, D. (2009). "Effect of growth time on the surface and adhesion properties of *Lactobacillus rhamnosus* GG." Journal of Applied Microbiology **107**(4): 1230-1240.

Deepika, G., Karunakaran, E., Hurley, C. R., Biggs, C. A. and Charalampopoulos, D. (2012). "Influence of fermentation conditions on the surface properties and adhesion of *Lactobacillus rhamnosus* GG." Microbial Cell Factories **11**(116): 1475-2859.

Degnan, P. H. and Ochman, H. (2012). Illumina-based analysis of microbial community diversity New York, Nature Publishing Group.

Del Re, B., Sgorbati, B., Miglioli, M. and Palenzona, D. (2000). "Adhesion, autoaggregation and hydrophobicity of 13 strains of *Bifidobacterium longum*." Letters in Applied Microbiology **31**(6): 438-442.

Deng, Y. and Sun, M. (2011). "Complete genome sequence of *Bacillus subtilis* BSn5, a strain of plant-associated bacterium with antimicrobial activity to soil-borne plant pathogens." from <http://www.uniprot.org/uniprot/E8VHL4>.

di Giancamillo, A., Vitari, F., Bosi, G., Savoini, G. and Domeneghini, C. (2010). "The chemical code of porcine enteric neurons and the number of enteric glial cells are altered by dietary probiotics." Neurogastroenterology and Motility **22**(9): 1365-2982.

Díaz, M., Herrero, M., García, L. A. and Quirós, C. (2010). "Application of flow cytometry to industrial microbial bioprocesses." Biochemical Engineering Journal **48**(3): 385-407.

Dirix, G., Monsieurs, P., Dombrecht, B., Daniels, R., Marchal, K., Vanderleyden, J. and Michiels, J. (2004). "Peptide signal molecules and bacteriocins in Gram-negative bacteria: a genome-wide in silico screening for peptides containing a double-glycine leader sequence and their cognate transporters." Peptides **25**(9): 1425-1440.

Dragon, D. and Rennie, R. (2001). "Evaluation of spore extraction and purification methods for selective recovery of viable *Bacillus anthracis* spores." Letters in Applied Microbiology **33**(2): 100-105.

Dubnau, D. (1991). "Genetic competence in *Bacillus subtilis*." Microbiology and Molecular Biology Reviews **55**(3): 395-424.

Edwards, J., J. L., Busta, F. F. and Speck, M. L. (1965). "Thermal Inactivation Characteristics of *Bacillus subtilis* Spores at Ultrahigh Temperatures." Applied Microbiology **13**(6): 851-857.

EFSA (2010a). "EFSA event: meeting with stakeholders on scientific requirements for health claims related to gut and immune function.". from <http://www.efsa.europa.eu/en/events/event/nda101202.htm>.

EFSA (2010b). "Scientific Opinion on the safety and efficacy of Calsporin® (*Bacillus subtilis*) as a feed additive for piglets." EFSA Journal **8**(1): 1426.

Epstein, A. K., Pokroy, B., Seminara, A. and Aizenberg, J. (2011). "Bacterial biofilm shows persistent resistance to liquid wetting and gas penetration." PNAS **108**(3): 995-1000.

Errington, J. (2003). "Regulation of endospore formation in *Bacillus subtilis*." Nature Reviews Microbiology **1**(2): 117-126.

FAO/WHO (2002). Guidelines for the Evaluation of Probiotics in Food. London Ontario, Canada: 11.

Fields, R. D. (2013). "Map the other brain " Nature **501**: 25-27.

Fleming, H. P. and Ordal, Z. J. (1964). "Responses of *Bacillus subtilis* spores to Ionic environments during sporulation and germination." Journal of Bacteriology **88**: 1529-1537.

Fortnagel, P. and Freese, E. (1968). "Inhibition of aconitase by chelation of transition metals causing inhibition of sporulation in *Bacillus subtilis*." Journal of Biological Chemistry **243**(20): 5289-5295.

Furukawa, S., Narisawa, N., Watanabe, T., Kawarai, T., Myozen, K., Okazaki, S., Ogihara, H. and Yamasaki, M. (2005). "Formation of the spore clumps during heat treatment increases the heat resistance of bacterial spores." International Journal of Food Microbiology **102**(1): 107-111.

Furukawa, S., Watanabe, T., Koyama, T., Hirata, J., Narisawa, N., Ogihara, H. and Yamasaki, M. (2006). "Effect of high pressure carbon dioxide on the clumping of the bacterial spores." International Journal of Food Microbiology **106**(1): 95-98.

Garrett, T. R., Bhakoo, M. and Zhang, Z. (2008). "Bacterial adhesion and biofilms on surfaces." Progress in Natural Science **18**(9): 1049-1056.

Gilmore, M. E., Bandyopadhyay, D., Dean, A. M., Linnstaedt, S. D. and Popham, D. L. (2004). "Production of muramic delta-lactam in *Bacillus subtilis* spore peptidoglycan." Journal of Bacteriology **186**(1): 80-89.

Gitlin, I., Carbeck, J. D. and Whitesides, G. M. (2006). "Why are proteins charged? Networks of charge-charge interactions in proteins measured by charge ladders and capillary electrophoresis." Angew Chem Int Ed Engl **45**(19): 3022-3060.

Goldrick, S. and Setlow, P. (1983). "Expression of a *Bacillus megaterium* sporulation-specific gene during sporulation of *Bacillus subtilis*." Journal of Bacteriology **155**(3): 1459-1462.

González-Pastor, J. E. (2011). "Cannibalism: a social behavior in sporulating *Bacillus subtilis*." Fems Microbiology Reviews **35**(3): 415-424.

Gooding, K. M. and Regnier, F. E. (2002). HPLC Of Biological Macro- Molecules, Revised And Expanded, Taylor & Francis.

Gordon, D., Macrae, J. and Wheeler, D. (1957). "A *Lactobacillus* preparation for use with antibiotics." The Lancet **269**(6975): 899-901.

Gordon, N. C. and Wareham, D. W. (2010). "Antimicrobial activity of the green tea polyphenol (-)-epigallocatechin-3-gallate (EGCG) against clinical isolates of *Stenotrophomonas maltophilia*." International Journal of Antimicrobial Agents **36**(2): 129-131.

Gould, G. W. and Sale, A. J. H. (1970). "Initiation of germination of bacterial spores by hydrostatic pressure." Journal of General Microbiology **60**(3): 335-346.

Gregory, P. C., McFadyen, M. and Rayner, D. V. (1987). "The influence of gastrointestinal infusions of glucose on regulation of food intake in pigs." Quarterly Journal of Experimental Physiology **72**: 525-535.

Guillard, R. R. and Sieracki, M. S. (2005). "Counting cells in cultures with the light microscope." Algal culturing techniques: 239-252.

Guindulain, T., Comas, J. and Vives-Rego, J. (1997). "Use of Nucleic Acid Dyes SYTO-13, TOTO-1, and YOYO-1 in the Study of *Escherichia coli* and Marine Prokaryotic Populations by Flow Cytometry." Applied and Environmental Microbiology **63**(11): 4608-4611.

Gunasekera, T. S., Attfield, P. V. and Veal, D. A. (2000). "A flow cytometry method for rapid detection and enumeration of total bacteria in milk." Applied and Environmental Microbiology **66**(3): 1228-1232.

Guttenplan, S. B., Blair, K. M. and Kearns, D. B. (2010). "The EpsE flagellar clutch is bifunctional and synergizes with EPS biosynthesis to promote *Bacillus subtilis* biofilm formation." PLoS Genetics **6**(12): e1001243.

Hagen, C. A., Hawrylewicz, E. J. and Ehrlich, R. (1967). "Survival of microorganisms in a simulated martian environment: II. moisture and oxygen requirements for germination of *Bacillus cereus* and *Bacillus subtilis* var. *niger* spores." Applied Microbiology **15**(2): 285-291.

Hajela, N., Nair, G. B., Abraham, P. and Ganguly, N. K. (2012). "Health impact of probiotics - vision and opportunities." Gut Pathogens **4**(1): 1-6.

Hansen, C. (2014). "Swine Health & Nutrition." Retrieved 07/06/2014, from <http://www.chr-hansen.com/products/product-areas/animal-health-nutrition/swine-nutrition-health.html>.

Harding, S. and Johnson, P. (1986). "The Brownian diffusion of dormant and germinating spores of *Bacillus megaterium*." Journal of Applied Bacteriology **60**(3): 227-232.

Harding, S. E. and Johnson, P. (1984). "Quasi-elastic light scattering studies on dormant and germinating *Bacillus subtilis* spores." Biochemistry Journal **220**(1): 117-123.

Harrold, Z. R., Hertel, M. R. and Gorman-Lewis, D. (2011). "Optimizing *Bacillus subtilis* spore isolation and quantifying spore harvest purity." Journal of Microbiological Methods **87**(3): 325-329. doi: 310.1016/j.mimet.2011.1009.1014. Epub 2011 Oct 1014.

Harwood, C. R. (2001). *Bacillus subtilis* as a Model for Bacterial Systems Biology. eLS, John Wiley & Sons, Ltd.

Hayhurst, E. J., Kailas, L., Hobbs, J. K. and Foster, S. J. (2008). "Cell wall peptidoglycan architecture in *Bacillus subtilis*." Proceedings of the National Academy of Sciences **105**(38): 14603-14608.

Hayhurst, E. J., Kailas, L., Hobbs, J. K. and Foster, S. J. (2008). "Cell wall peptidoglycan architecture in *Bacillus subtilis*." PNAS **105**(38): 14603-14608.

He, G., Shankar, R. A., Chzhan, M., Samouilov, A., Kuppusamy, P. and Zweier, J. L. (1999). "Noninvasive measurement of anatomic structure and intraluminal oxygenation in the gastrointestinal tract of living mice with spatial and spectral EPR imaging." Proceedings of the National Academy of Sciences **96**(8): 4586-4591.

Henriques, A. O. and Moran, C. P., Jr. (2000). "Structure and assembly of the bacterial endospore coat." Methods. **20**(1): 95-110.

Hernlem, B. J. and Ravva, S. V. (2007). "Application of flow cytometry and cell sorting to the bacterial analysis of environmental aerosol samples." Journal of Environmental Monitoring **9**: 1317-1322.

Herruzo, R., Vizcaino, M. J. and Herruzo, I. (2010). "Efficacy of a new peracetic acid-based disinfectant agent ('Adaspor® ready to use')." Journal of Hospital Infection **74**(2): 192-193.

Hirota, R., Hata, Y., Ikeda, T., Ishida, T. and Kuroda, A. (2010). "The silicon layer supports acid resistance of *Bacillus cereus* spores." Journal of Bacteriology **192**(1): 111-116.

Hitchins, A. D., Gould, G. W. and Hurst, A. (1963). "The swelling of bacterial spores during germination and outgrowth." Journal of General Microbiology **30**(3): 445-453.

Hoa, N. T., Baccicalupi, L., Huxham, A., Smertenko, A., Van, P. H., Ammendola, S., Ricca, E. and Cutting, S. M. (2000). "Characterization of *Bacillus* species used for oral bacteriotherapy and bacterioprophylaxis of gastrointestinal disorders." Applied and Environmental Microbiology **66**(12): 5241-5247.

Hoa, T. T., Duc, L. H., Istatico, R., Baccigalupi, L., Ricca, E., Van, P. H. and Cutting, S. M. (2001). "Fate and dissemination of *Bacillus subtilis* spores in a murine model." Applied and Environmental Microbiology **67**(9): 3819-3823.

Holzapfel, W. H., Haberer, P., Snel, J. and Schillinger, U. (1998). "Overview of gut flora and probiotics." International Journal of Food Microbiology **41**(2): 85-101.

Hong, H. A., Duc le, H. and Cutting, S. M. (2005). "The use of bacterial spore formers as probiotics." FEMS Microbiology Reviews **29**(4): 813-835.

Hori, K. and Matsumoto, S. (2010). "Bacterial adhesion: From mechanism to control." Biochemical Engineering Journal **48**: 424-434.

Huang, J., Wang, L., Ren, N. and Juli, F. (1997). "Disinfection effect of chlorine dioxide on bacteria in water." Water Research **31**(3): 607-613.

Huang, J. M., La Ragione, R. M., Nunez, A. and Cutting, S. M. (2008). "Immuno-stimulatory activity of *Bacillus* spores." FEMS Immunology Medical Microbiology **53**(2): 195-203.

Huang, S. S., Chen, D., Pelczar, P. L., Vepachedu, V. R., Setlow, P. and Li, Y. Q. (2007). "Levels of Ca²⁺-dipicolinic acid in individual *Bacillus* spores determined using microfluidic Raman tweezers." Journal of Bacteriology **189**(13): 4681-4687. Epub 2007 Apr 4627.

Husmark, U. (1993). Adhesion mechanisms of bacterial spores to solid surfaces. Göteborg, Chalmers University of Technology.

Huyghebaert, G., Ducatelle, R. and Van Immerseel, F. (2011). "An update on alternatives to antimicrobial growth promoters for broilers." Veterinary Journal **187**(2): 182-188.

Ibrahim, S. A. and Bezkorovainy, A. (1993). "Inhabitation of *Escherichia coli* by *bifidobacteria*." Journal of Food Protection **56**(7): 713-715.

Igarashi, T. and Setlow, P. (2005). "Interaction between Individual Protein Components of the GerA and GerB Nutrient Receptors That Trigger Germination of *Bacillus subtilis* Spores." Journal of Bacteriology **187**(7): 2513-2518.

Invitrogen (2014, 2014). "Introduction to Flow Cytometry." Retrieved 09/06/2014, from http://media.invitrogen.com.edgesuite.net/tutorials/4Intro_Flow/player.html.

Isolauri, E., Sütas, Y., Kankaanpää, P., Arvilommi, H. and Salminen, S. (2001). "Probiotics: effects on immunity." The American Journal of Clinical Nutrition **73**(2): 444s-450s.

Israelachvili, J. N. (2011). Intermolecular and surface forces: revised third edition, Academic press.

Jagannath, A., Tsuchido, T. and Membré, J. M. (2005). "Comparison of the thermal inactivation of *Bacillus subtilis* spores in foods using the modified Weibull and Bigelow equations." Food Microbiology **22**(2-3): 233-239.

Jongenburger, I., Reij, M. W., Boer, E. P., Gorris, L. G. and Zwietering, M. H. (2010). "Factors influencing the accuracy of the plating method used to enumerate low numbers of viable micro-organisms in food." International Journal of Food Microbiology **143**(1-2): 32-40.

Józefiak, D., Kierończyk, B., Juśkiewicz, J., Zduńczyk, Z., Rawski, M., Długosz, J., Sip, A. and Højberg, O. (2013). "Dietary nisin modulates the gastrointestinal microbial ecology and enhances growth performance of the broiler chickens." PLoS One **8**(12): e85347.

Kararli, T. T. (1995). "Comparison of the Gastrointestinal Anatomy, Physiology, and Biochemistry of Humans and commonly used Laboratory Animals." Biopharmaceutics and Drug Disposition **16**: 351-380.

Keijser, B. J., Ter Beek, A., Rauwerda, H., Schuren, F., Montijn, R., van der Spek, H. and Brul, S. (2007). "Analysis of temporal gene expression during *Bacillus subtilis* spore germination and outgrowth." Journal of Bacteriology **189**(9): 3624-3634.

Kenny, M., Smidt, H., Mengheri, E. and Miller, B. (2011). "Probioites- do they have a role in the pig industry?" Animal **5**(3): 462-470.

Keserue, H.-A., Baumgartner, A., Felleisen, R. and Egli, T. (2012). "Rapid detection of total and viable *Legionella pneumophila* in tap water by immunomagnetic separation, double fluorescent staining and flow cytometry." Microbial Biotechnology **5**(6): 753-763.

Khan, M. M. T., Pyle, B. H. and Camper, A. K. (2010). "Specific and Rapid Enumeration of Viable but Nonculturable and Viable-Culturable Gram-Negative Bacteria by Using Flow Cytometry." Applied and Environmental Microbiology **76**(15): 5088-5096.

Khan, S. U. (2014). "Probiotics in dairy foods: a review." Nutrition & Food Science **44**(1): 71-88.

Khochamit, N., Siripornadulsil, S., Sukon, P. and Siripornadulsil, W. (2015). "Antibacterial activity and genotypic–phenotypic characteristics of bacteriocin-producing *Bacillus subtilis* KKU213: Potential as a probiotic strain." Microbiological Research **170**(0): 36-50.

Kim, H., Kang, Y., Beuchat, L. R. and Ryu, J. H. (2008a). "Production and stability of chlorine dioxide in organic acid solutions as affected by pH, type of acid, and concentration of sodium chlorite, and its effectiveness in inactivating *Bacillus cereus* spores." Food Microbiology **25**(8): 964-969.

Kim, J., Pitts, B., Stewart, P. S., Camper, A. and Yoon, J. (2008b). "Comparison of the antimicrobial effects of chlorine, silver ion, and tobramycin on biofilm." Antimicrob Agents Chemother **52**(4): 1446-1453.

Kindoli, S., Lee, H. A. and Kim, J. H. (2012). "Properties of Bac W42, a bacteriocin produced by *Bacillus subtilis* W42 isolated from Cheonggukjang." Journal of Microbiology and Biotechnology **22**(8): 1092-1100.

Kitis, M. (2004). "Disinfection of wastewater with peracetic acid: a review." Environment International **30**(1): 47-55.

Kleerebezem, M., Bongers, R., Rutten, G., de Vos, W. M. and Kuipers, O. P. (2004). "Autoregulation of subtilin biosynthesis in *Bacillus subtilis*: the role of the spa-box in subtilin-responsive promoters." Peptides. **25**(9): 1415-1424.

Knarreborg, A., Miquel, N., Granli, T. and Jensen, B. B. (2002). "Establishment and application of an in vitro methodology to study the effects of organic acids on coliform and lactic acid bacteria in the proximal part of the gastrointestinal tract of piglets." Animal Feed Science and Technology **99**(1-4): 131-140.

Knox, W. E., Stumpf, P. K., Green, D. E. and Auerbach, V. H. (1948). "The inhibition of sulfhydryl enzymes as the basis of the bactericidal action of chlorine." Journal of Bacteriology **55**(4): 451-458.

Kong, I.-S., Bates, T. C., Hulsmann, A., Hassan, H., Smith, B. E. and Oliver, J. D. (2004). "Role of catalase and oxyR in the viable but nonculturable state of *Vibrio vulnificus*." FEMS Microbiology Ecology **50**(3): 133-142.

Kong, L., Zhang, P., Yu, J., Setlow, P. and Li, Y.-q. (2010). "Monitoring the kinetics of uptake of a nucleic acid dye during the germination of single spores of *Bacillus* species." Analytical chemistry **82**(20): 8717-8724.

Kort, R., O'Brien, A. C., van Stokkum, I. H., Oomes, S. J., Crielaard, W., Hellingwerf, K. J. and Brul, S. (2005). "Assessment of heat resistance of bacterial spores from food product isolates by fluorescence monitoring of dipicolinic acid release." Applied and Environmental Microbiology **71**(7): 3556-3564.

Kos, B., Šušković, J., Vuković, S., Šimpraga, M., Frece, J. and Matošić, S. (2003). "Adhesion and aggregation ability of probiotic strain *Lactobacillus acidophilus* M92." Journal of Applied Microbiology **94**(6): 981-987.

Kunigk, L. and Almeida, M. C. B. (2001). "Action of peracetic acid on *Escherichia coli* and *Staphylococcus aureus* in suspension or settled on stainless steel surfaces." Brazilian Journal of Microbiology **32**: 38-41.

Kunst, F., Ogasawara, N., Moszer, I., Albertini, A., Alloni, G., Azevedo, V., Bertero, M., Bessieres, P., Bolotin, A. and Borchert, S. (1997). "The complete genome sequence of the gram-positive bacterium *Bacillus subtilis*." Nature **390**(6657): 249-256.

La Duc, M. T., Nicholson, W., Kern, R. and Venkateswaran, K. (2003). "Microbial characterization of the Mars Odyssey spacecraft and its encapsulation facility." Environmental Microbiology **5**(10): 977-985.

Langendijk, P. S., Schut, F., Jansen, G. J., Raangs, G. C., Kamphuis, G. R., Wilkinson, M. H. F. and Welling, G. W. (1995). "Quantitative fluorescence in situ hybridization of *Bifidobacterium* spp. with genus-specific 16S rRNA-targeted probes and its application in fecal samples." Applied and Environmental Microbiology **61**(8): 3069-3075.

Larsen, N., Nissen, P. and Willats, W. G. (2007). "The effect of calcium ions on adhesion and competitive exclusion of *Lactobacillus* ssp. and *E. coli* O138." International Journal of Food Microbiology **114**(1): 113-119.

Lawlor, P. G., Lynch, P. B., Caffrey, P. J., O'Reilly, J. J. and O'Connell, M. K. (2005). "Measurements of the acid-binding capacity of ingredients used in pig diets." Irish Veterinary Journal **58**(8): 447-452.

Lee, J. H., Shim, J. S., Chung, M. S., Lim, S. T. and Kim, K. H. (2009). "*In vitro* anti-adhesive activity of green tea extract against pathogen adhesion." Phytotherapy Research **23**(4): 460-466.

Lehtinen, J. (2007). Improvements in the assessment of bacterial viability and killing. Department of Biochemistry and Food Chemistry. Turku, Finland, University of Turku.

Leser, T. D., Knarreborg, A. and Worm, J. (2008). "Germination and outgrowth of *Bacillus subtilis* and *Bacillus licheniformis* spores in the gastrointestinal tract of pigs." Journal of Applied Microbiology **104**(4): 1025-1033. Epub 2007 Nov 1015.

Letourneau-Montminy, M. P., Narcy, A., Lescoat, P., Magnin, M., Bernier, J. F., Sauvant, D., Jondreville, C. and Pomar, C. (2011). "Modeling the fate of dietary phosphorus in the digestive tract of growing pigs." Journal of Animal Science **89**(11): 3596-3611. doi: 3510.2527/jas.2010-3397. Epub 2011 Jun 3516.

Leuschner, R. G. K. and Lillford, P. J. (1999). "Effects of temperature and heat activation on germination of individual spores of *Bacillus subtilis*." Letters in Applied Microbiology **29**: 228-232.

Lilly, D. M. and Stillwell, R. H. (1965). "Probiotics: Growth-promoting factors produced by microorganisms." Science. **147**(3659): 747-748.

Link, R. and Kováč, G. (2006). "The effect of probiotic BioPlus 2B on feed efficiency and metabolic parameters in swine." Biologia **61**(6): 783-787.

Liong, M. T. (2008). "Roles of probiotics and prebiotics in colon cancer prevention: Postulated mechanisms and in-vivo evidence." International Journal of Molecular Sciences **9**(5): 854-863. doi: 810.3390/ijms9050854. Epub 9052008 May 9050820.

Liu, H., Xu, W., Luo, Y., Tian, H., Wang, H., Guo, X., Yuan, Y. and Huang, K. (2011). "Assessment of tolerance to multistresses and in vitro cell adhesion in genetically modified *Lactobacillus plantarum* 590." Antonie van Leeuwenhoek **99**(3): 579-589.

Liu, J., Ledoux, D. R. and Veum, T. L. (1997). "*In vitro* procedure for predicting the enzymatic dephosphorylation of phytate in corn-soybean meal diets for growing swine." Journal of Agriculture and Food Chemistry **45**: 2612-2617.

Longworth, L. G. (1954). "Temperature dependence of diffusion in aqueous solutions." Journal of Physical Chemistry **58**: 770-773.

Löwgren, W., Graham, H. and Åman, P. (1989). "An in vitro method for studying digestion in the pig." British Journal of Nutrition **61**(3): 673-687.

Luu, S. and Setlow, P. (2014). "Analysis of the loss in heat and acid resistance during germination of spores of *Bacillus* species." Journal of Bacteriology **196**(9): 1733.

Mackowiak, P. A. (2013). "Recycling metchnikoff: probiotics, the intestinal microbiome and the quest for long life." Front Public Health **1**(52): 00052.

Mamane-Gravetz, H. and Linden, K. G. (2005). "Relationship between physiochemical properties, aggregation and u.v. inactivation of isolated indigenous spores in water." Journal of Applied Microbiology **98**(2): 351-363.

Marbouty, M., Saguez, C., Cassier-Chauvat, C. and Chauvat, F. (2009). "Characterization of the FtsZ-interacting septal proteins SepF and Ftn6 in the spherical-celled cyanobacterium *Synechocystis* strain PCC 6803." Journal of Bacteriology **191**(19): 6178-6185.

Marcinakova, M., Klingberg, T. D., Laukova, A. and Budde, B. B. (2010). "The effect of pH, bile and calcium on the adhesion ability of probiotic enterococci of animal origin to the porcine jejunal epithelial cell line IPEC-J2." Anaerobe **16**(2): 120-124.

Maris, P. (1995). "Modes of action of disinfectants " Scientific and Technical Review of the Office International des Epizooties **14**(1): 47-55

Marshall, B. J., Murrell, W. G. and Scott, W. J. (1963). "The Effect of Water Activity, Solutes and Temperature on the Viability and Heat Resistance of Freeze -dried Bacterial Spores " Journal of General Microbiology **31**: 451-460

Marshall, K., Stout, R. and Mitchell, R. (1971). "Mechanism of the initial events in the sorption of marine bacteria to surfaces." Journal of General Microbiology **68**(3): 337-348.

Marteau, P., Flouri, B., Pochart, J. P., Chastang, C., Desjeux, J. F. and Rambaud, J. C. (1990). "Role of the microbial lactase (EC 3.2.123) activity from yoghurt on the intestinal absorption of lactose: an in vivo study in lactase-deficient humans." Brazilian Journal of Nutrition **64**: 71-79.

Mathys, A., Chapman, B., Bull, M., Heinz, V. and Knorr, D. (2007). "Flow cytometric assessment of *Bacillus* spore response to high pressure and heat." Innovative Food Science & Emerging Technologies **8**(4): 519-527.

McClatchey, K. D. (2002). Clinical Laboratory Medicine, Lippincott Williams & Wilkins.

McKenney, P. T., Driks, A. and Eichenberger, P. (2013). "The *Bacillus subtilis* endospore: assembly and functions of the multilayered coat." Nature Reviews Microbiology **11**(1): 33-44. doi: 10.1038/nrmicro2921. Epub 2012 Dec 10 33.

McKenney, P. T. and Eichenberger, P. (2012). "Dynamics of spore coat morphogenesis in *Bacillus subtilis*." Molecular Microbiology **83**(2): 245-260. doi: 10.1111/j.1365-2958.2011.07936.x. Epub 02011 Dec 07 915.

Meador-Parton, J. and Popham, D. L. (2000). "Structural analysis of *Bacillus subtilis* spore peptidoglycan during sporulation." Journal of Bacteriology **182**(16): 4491-4499.

Merchant, H. A., McConnell, E. L., Liu, F., Ramaswamy, C., Kulkarni, R. P., Basit, A. W. and Murdan, S. (2011). "Assessment of gastrointestinal pH, fluid and lymphoid tissue in the guinea pig, rabbit and pig, and implications for their use in drug development." Eur J Pharm Sci **42**(1-2): 3-10.

Metzger, B. M. (1997). Genesis 18:8. Revised Standard Version of the Bible. CCAT. Philadelphia, National Council of Churches of Christ in America.

Miles, A. A., Misra, S. S. and Irwin, J. O. (1938). "The estimation of the bactericidal power of the blood." Epidemiology & Infection **38**(06): 732-749.

Miller, J. S. and Quarles, J. M. (1990). "Flow cytometric identification of microorganisms by dual staining with FITC and PI." Cytometry **11**(6): 667-675.

Mittal, K. L., Van Ooij, W. J. and Anderson, H. R. (1998). First International Congress on Adhesion Science And Technology---invited Papers: Festschrift in Honor of Dr. K.I. Mittal on the Occasion of His 50th Birthday, Taylor & Francis.

Moir, A. (2003). "Bacterial spore germination and protein mobility." Trends Microbiol. **11**(10): 452-454.

Monteiro, S. M. S., Clemente, J. J., Henriques, A. O., Gomes, R. G., Carrondo, M. J. T. and Cunha, A. E. (2005). "A procedure for high-yield spore production by *Bacillus subtilis*." Biotechnology Progress **21**(4): 1026-1031.

Möbeler, A., Köttendorf, S., Große Liesner, V. and Kamphues, J. (2010). "Impact of diets' physical form (particle size; meal/pelleted) on the stomach content (dry matter content, pH, chloride concentration) of pigs." Livestock Science **134**(1-3): 146-148.

Möbeler, A., Wintermann, M., Sander, S. J. and Kamphues, J. (2012). "Effect of diet grinding and pelleting fed either dry or liquid feed on dry matter and pH in the stomach of pigs and the development of gastric ulcers." Journal of Animal Science **90**: 343-345.

Muda, K., Aris, A., Salim, M. R., Ibrahim, Z., van Loosdrecht, M. C. M., Nawahwi, M. Z. and Affam, A. C. (2014). "Aggregation and surface hydrophobicity of selected microorganism due to the effect of substrate, pH and temperature." International Biodeterioration & Biodegradation **93**(0): 202-209.

Muir, R. and Kitchie, J. (1961). *Manual of Bacteriology*. J. Young. Edinburgh, Pentland.

Munoz, L., Sadaie, Y. and Doi, R. H. (1978). "Spore coat protein of *Bacillus subtilis*. Structure and precursor synthesis." Journal of Biological Chemistry **253**(19): 6694-6701.

Musovic, S., Oregaard, G., Kroer, N. and Sorensen, S. J. (2006). "Cultivation-independent examination of horizontal transfer and host range of an IncP-1 plasmid among gram-positive

and gram-negative bacteria indigenous to the barley rhizosphere." Applied and Environmental Microbiology **72**(10): 6687-6692.

Nakayama, M., Shimatani, K., Ozawa, T., Shigemune, N., Tomiyama, D., Yui, K., Katsuki, M., Ikeda, K., Nonaka, A. and Miyamoto, T. (2015). "Mechanism for the antibacterial action of epigallocatechin gallate (EGCg) on *Bacillus subtilis*." Bioscience, biotechnology, and biochemistry **79**(5): 845-854.

Nebe-von-Caron, G. (2008). "Standardisation in Microbial Cytometry." Cytometry Part A **75A**(2): 86-89.

Nebe-von-Caron, G. (2012). Personal Communication: FCM work on *Bacillus Subtilis* cells and spores. Cranfield.

Nebe-von-Caron, G., Stephens, P. and Badley, R. A. (1998). "Assessment of bacterial viability status by flow cytometry and single cell sorting." Journal of Applied Microbiology **84**(6): 988-998.

Nebe-von-Caron, G. (2009). "Standardization in microbial cytometry." Cytometry Part A **75**(2): 86-89.

Nebe von Caron, G. and Bongaerts, R. (2012). G-bead mixture instrument setup trial. Giga-bead mix protocol v2.1. Sharnbrook, Flow Cytometry UK: 6.

Nicholson, W. L. and Setlow, P. (1990). Sporulation, germination, and outgrowth. Sussex, John Wiley & Sons.

Novik, G., Sidarenka, A., Kiseleva, E., Kolomiets, E. and Dey, E. (2014). Probiotics. Biotransformation of Waste Biomass into High Value Biochemicals. S. K. Brar, G. S. Dhillon and C. R. Soccol, Springer New York: 187-235.

Nunez, R. (2001). "DNA measurement and cell cycle analysis by flow cytometry." Current Issues in Molecular Biology **3**(3): 67-70.

Ochi, K., Kandala, J. and Freese, E. (1982). "Evidence that *Bacillus subtilis* sporulation induced by the stringent response is caused by the decrease in GTP or GDP." Journal of Bacteriology **151**(2): 1062-1065.

Oh, Y. K. and Freese, E. (1976). "Manganese requirement of phosphoglycerate phosphomutase and its consequences for growth and sporulation of *Bacillus subtilis*." Journal of Bacteriology **127**(2): 739-746.

Oh, Y. K. and Nash, C. H. (1981). "Influence of pH on spore aggregation of *Streptosporangium brasiliense*." Folia Microbiol **26**(2): 164-166.

Oie, S., Obayashi, A., Yamasaki, H., Furukawa, H., Kenri, T., Takahashi, M., Kawamoto, K. and Makino, S. (2011). "Disinfection methods for spores of *Bacillus atrophaeus*, *B. anthracis*, *Clostridium tetani*, *C. botulinum* and *C. difficile*." Biological Pharmacy Bulletin **34**(8): 1325-1329.

ORFFA (2010). "Nutritional solutions for pigs, poultry and ruminants." Retrieved 07/06/2014, 2014, from <http://www.orffa.com/site/livestock-uk?OpenDocument&L1=LiveStock>.

Orrhage, K., Lidbeck, A. and Rafter, J. (1995). Influence of probiotics, *lactobacilli* and *bifidobacteria* on gastrointestinal disorders in adults. London, Taylor & Francis.

Paidhungat, M., Setlow, B., Daniels, W. B., Hoover, D., Papafragkou, E. and Setlow, P. (2002). "Mechanisms of induction of germination of *Bacillus subtilis* spores by high pressure." Applied and Environmental Microbiology **68**(6): 3172-3175.

Pandey, R., Ter Beek, A., Vischer, N., Smelt, J., Brul, S. and Manders, E. (2013). "Live cell imaging of germination and outgrowth of individual *Bacillus subtilis* spores; the effect of heat stress quantitatively analyzed with SporeTracker." PLoS One **8**(3): e58972.

Paredes-Sabja, D., Bond, C., Carman, R. J., Setlow, P. and Sarker, M. R. (2008). "Germination of spores of *Clostridium difficile* strains, including isolates from a hospital outbreak of *Clostridium difficile*-associated disease (CDAD)." Microbiology **154**(8): 2241-2250.

Paredes-Sabja, D., Setlow, P. and Sarker, M. R. (2011). "Germination of spores of Bacillales and Clostridiales species: mechanisms and proteins involved." Trends Microbiol **19**(2): 85-94.

Park, E., Lee, C., Bisesi, M. and Lee, J. (2014a). "Efficiency of peracetic acid in inactivating bacteria, viruses, and spores in water determined with ATP bioluminescence, quantitative PCR, and culture-based methods." Journal of Water and Health **12**(1): 13-23.

Park, H.-S., Schumacher, R. and Kilbane II, J. J. (2005). "New method to characterize microbial diversity using flow cytometry." Journal of Industrial Microbiology and Biotechnology **32**(3): 94-102.

Park, S. Y., Lee, H. U., Lee, Y. C., Kim, G. H., Park, E. C., Han, S. H., Lee, J. G., Choi, S., Heo, N. S., Kim, D. L., Huh, Y. S. and Lee, J. (2014b). "Wound healing potential of antibacterial microneedles loaded with green tea extracts." Materials Science and Engineering. C, Materials for Biological Applications **42**: 757-762.

Parkar, S. G., Flint, S. H., Palmer, J. S. and Brooks, J. D. (2001). "Factors influencing attachment of thermophilic bacilli to stainless steel." Journal of Applied Microbiology **90**: 901-908.

Parker, G. F., Daniel, R. A. and Errington, J. (1996). "Timing and genetic regulation of commitment to sporulation in *Bacillus subtilis*." Microbiology **142**(Pt 12): 3445-3452.

Partanen, K., Karhapää, M. and Siljander-Rasi, H. (2006). "Performance, carcass quality, and gastric alterations in fattening pigs fed additives containing formic acid either coated with sorbate or mixed with lactic acid." Agricultural and Food Science **15**: 324-339.

Paulse, A. N., Jackson, V. A. and Khan, W. (2007). "Comparison of enumeration techniques for the investigation of bacterial pollution in the Berg River, Western Cape, South Africa." Water SA **33**(2): 165-174.

Pedretti, S. (2013). "Probiotic Market: Up or Down?" Nutrafoods **12**: 18-19.

Pelczar, P. L., Igarashi, T., Setlow, B. and Setlow, P. (2007). "Role of GerD in germination of *Bacillus subtilis* spores." Journal of Bacteriology **189**(3): 1090-1098. Epub 2006 Nov 1022.

Pesce, G., Rusciano, G., Sasso, A., Isticato, R., Sirec, T. and Ricca, E. (2014). "Surface charge and hydrodynamic coefficient measurements of *Bacillus subtilis* spore by optical tweezers." Colloids and Surfaces B: Biointerfaces **116**(0): 568-575.

Picot, J., Guerin, C. L., Kim, C. L. V. and Boulanger, C. K. (2012). "Flow cytometry: retrospective, fundamentals and recent instrumentation." Cytotechnology **64**: 109-130.

Piggot, P. J. and Hilbert, D. W. (2004). "Sporulation of *Bacillus subtilis*." Current Opinion in Microbiology **7**(6): 579-586.

Pope, C. F., O'Sullivan, D. M., McHugh, T. D. and Gillespie, S. H. (2008). "A practical guide to measuring mutation rates in antibiotic resistance." Antimicrob Agents Chemother **52**(4): 1209-1214.

Posada-Urbe, L. F., Romero-Tabarez, M. and Villegas-Escobar, V. (2015). "Effect of medium components and culture conditions in *Bacillus subtilis* EA-CB0575 spore production." *Bioprocess and Biosystems Engineering* **38**(10): 1879-1888.

Powers, E. M. (1968). "Method for obtaining free bacterial spores of *Bacillus subtilis* var. *niger*." *Applied Microbiology* **16**(1): 180-181.

Ragkousi, K., Cowan, A. E., Ross, M. A. and Setlow, P. (2000). "Analysis of nucleoid morphology during germination and outgrowth of spores of *Bacillus* species." *J Bacteriol* **182**(19): 5556-5562.

Ramamurthy, T., Ghosh, A., Pazhani, G. P. and Shinoda, S. (2014). "Current perspectives on Viable but Non-Culturable (VBNC) pathogenic bacteria." *Frontiers in Public Health* **2**: 103.

Ranadheera, R. D. C. S., Baines, S. K. and Adams, M. C. (2010). "Importance of food in probiotic efficacy." *Food Research International* **43**(1): 1-7.

Rao, L., Xu, Z., Wang, Y., Zhao, F., Hu, X. and Liao, X. (2015). "Inactivation of *Bacillus subtilis* spores by high pressure CO₂ with high temperature." *International Journal of Food Microbiology* **205**: 73-80.

Ratnayake-Lecamwasam, M., Serror, P., Wong, K.-W. and Sonenshein, A. L. (2001). "*Bacillus subtilis* CodY represses early-stationary-phase genes by sensing GTP levels." *Genes and Development* **15**(9): 1093-1103.

Reimann, S., Grattepanche, F., Rezzonico, E. and Lacroix, C. (2010). "Development of a real-time RT-PCR method for enumeration of viable *Bifidobacterium longum* cells in different morphologies." Food Microbiology **27**(2): 236-242.

Reineke, K. (2013). Mechanisms of Bacillus spore germination and inactivation during high pressure processing. Prozesswissenschaften. Berlin, Technischen Universität Berlin. **Diplom – Ingenieur**: 170.

Reineke, K., Doehner, I., Schlumbach, K., Baier, D., Mathys, A. and Knorr, D. (2012). "The different pathways of spore germination and inactivation in dependence of pressure and temperature." Innovative Food Science and Emerging Technologies **13**: 31-41.

Ripamonti, B., Agazzi, A., Baldi, A., Balzaretto, C., Bersani, C., Pirani, S., Rebucci, R., Savioni, G., Stella, S., Stenico, A. and Domeneghini, C. (2009). "Administration of *Bacillus coagulans* in calves: recovery from faecal samples and evaluation of functional aspects of spores." Veterinary Research Communication **33**(8): 991-1001.

Risley, C. R., Kornegay, E. T., Lindemann, M. D., Wood, C. M. and Eigel, W. N. (1992). "Effect of feeding organic acids on selected intestinal content measurements at varying times postweaning in pigs." Journal of Animal Science **70**(1): 196-206.

Rosen, J. M., Woo, S. L. C., Holder, J. W., Means, A. R. and O'Malley, B. W. (1975). "Preparation and Preliminary Characterization of Purified Ovalbumin Messenger RNA from the Hen Oviduct." Biochemistry **14**(1): 69-78.

Ryu, J. H. and Beuchat, L. R. (2005). "Biofilm formation and sporulation by *Bacillus cereus* on a stainless steel surface and subsequent resistance of vegetative cells and spores to chlorine, chlorine dioxide, and a peroxyacetic acid-based sanitizer." Journal of Food Protection **68**(12): 2614-2622.

Šabatková, J., Kumprecht, I., Zobač, P., Suchý, P. and Čermák, B. (2008). "The probiotic Bioplus 2B as an alternative to antibiotics in diets for broiler chickens." Acta Veterinaria Brno **77**(4): 569-574.

Salminen, S., Deighton, M. and Gorbach, S. (1993). Lactic acid bacteria in health and disease. New York, Marcel Dekker.

Schrezenmeir, J. and de Vrese, M. (2001). "Probiotics, prebiotics, and synbiotics—approaching a definition." The American Journal of Clinical Nutrition **73**(2): 361s-364s.

Seale, R. B., Flint, S. H., McQuillan, A. J. and Bremer, P. J. (2008). "Recovery of spores from thermophilic dairy *Bacilli* and effects of their surface characteristics on attachment to different surfaces." Applied Environmental Microbiology **74**(3): 731-737. Epub 2007 Dec 2014.

Senesi, S. and Ghelardi, E. (2010). "Production, Secretion and Biological Activity of *Bacillus cereus* Enterotoxins." Toxins **2**: 1690-1703.

Setlow, P. (2012). Personal Communication: OD270 of DPA in *B. subtilis*. Farmington.

Setlow, B., Cowan, A. E. and Setlow, P. (2003). "Germination of spores of *Bacillus subtilis* with dodecylamine." Journal of Applied Microbiology **95**(3): 637-648.

Setlow, B., Loshon, C. A., Genest, P. C., Cowan, A. E., Setlow, C. and Setlow, P. (2002). "Mechanisms of killing spores of *Bacillus subtilis* by acid, alkali and ethanol." Journal of Applied Microbiology **92**(2): 362-375.

Setlow, B., Yu, J., Li, Y. Q. and Setlow, P. (2013). "Analysis of the germination kinetics of individual *Bacillus subtilis* spores treated with hydrogen peroxide or sodium hypochlorite." Letters in Applied Microbiology **57**(4): 259-265.

Setlow, P. (2003). "Spore germination." Current Opinion in Microbiology **6**(6): 550-556.

Setlow, P. (2006). "Spores of *Bacillus subtilis*: their resistance to and killing by radiation, heat and chemicals." Journal of Applied Microbiology **101**(3): 514-525.

Setlow, P. (2013). "Summer meeting 201--when the sleepers wake: the germination of spores of *Bacillus* species." Journal of Applied Microbiology **115**(6): 1251-1268.

Setlow, P. (2014). "The Germination of Spores of *Bacillus* Species: what we know and don't know." Journal of Bacteriology.

Shapiro, H. M. (2003). Practical Flow cytometry. Hoboken, John Wiley and Sons.

Shapiro, H. M. (2005). Practical Flow Cytometry, Wiley.

Shapiro, H. M. and Nebe-von-Caron, G. (2004). "Multiparameter Flow Cytometry of Bacteria." Methods in Molecular Biology **263**: 33-43.

Sharma, A., Gupta, S., Sarethy, I. P., Dang, S. and Gabrani, R. (2012). "Green tea extract: possible mechanism and antibacterial activity on skin pathogens." Food Chemistry **135**(2): 672-675.

Sharpe, J. and Wulff, S. (2005). "Small-Particle Analysis." Guide to Flow Cytometry: 69-75.

Shen, T., Bos, A. P. and Brul, S. (2009). "Assessing freeze–thaw and high pressure low temperature induced damage to *Bacillus subtilis* cells with flow cytometry." Innovative Food Science & Emerging Technologies **10**(1): 9-15.

Sheth, M., Parnami, S. and Bhide, M. (2012). "Colonization of Beneficial Microflora in the GUT of Indian Adult Females (35-50 yrs) as Affected by Dietary Fibre Intakes. ." Journal of Biomedical and Pharmaceutical Research **1**(3): 45-50.

Sifri, C. D. (2008). "Quorum sensing: bacteria talk sense." Clinical Infectious Diseases **47**(8): 1070-1076.

Silvaggi, J. M., Popham, D. L., Driks, A., Eichenberger, P. and Losick, R. (2004). "Unmasking novel sporulation genes in *Bacillus subtilis*." Journal of Bacteriology **186**(23): 8089-8095.

Smith, L. S., Wallace, L. and Rastogi, V. K. (2011). Studies on sporulation optimisation and characteristics of *Bacillus subtilis* spore quality. U. S. A. Research. Edgewood Chemical Biological Center, Development and Engineering Command.

Sorokulova, I. (2013). "Modern Status and Perspectives of Bacillus Bacteria as Probiotics. J Prob Health 1: e106. doi: 10.4172/2329-8901.1000 e106 Page 2 of 5 Volume 1• Issue 4• 1000e106 J Prob Health ISSN: 2329-8901 JPH, an open access journal administration in mice [51, 52]. Adjuvant properties of Bacillus bacteria were confirmed in many studies." Journal of Probiotic Health.

Spinosa, M. R., Braccini, T., Ricca, E., De Felice, M., Morelli, L., Pozzi, G. and Oggioni, M. R. (2000). "On the fate of ingested *Bacillus* spores." Research in Microbiology **151**(5): 361-368.

Stanley, N. R. and Lazazzera, B. A. (2004). "Environmental signals and regulatory pathways that influence biofilm formation." Molecular Microbiology **52**(4): 917-924.

Stocks, S. M. (2004). "Mechanism and use of the commercially available viability stain, BacLight." Cytometry A **61**(2): 189-195.

Stopa, P. J. (2000). "The flow cytometry of *Bacillus anthracis* spores revisited." Cytometry **41**(4): 237-244.

Sumeri, I., Arike, L., Adamberg, K. and Paalme, T. (2008). "Single bioreactor gastrointestinal tract simulator for study of survival of probiotic bacteria." Applied Microbiology and Biotechnology **80**(2): 317–324.

Swiecki, M. K., Lisanby, M. W., Shu, F., Turnbough, C. L., Jr. and Kearney, J. F. (2006). "Monoclonal antibodies for *Bacillus anthracis* spore detection and functional analyses of spore germination and outgrowth." Journal of Immunology **176**(10): 6076-6084.

Tam, N. K., Uyen, N. Q., Hong, H. A., Duc le, H., Hoa, T. T., Serra, C. R., Henriques, A. O. and Cutting, S. M. (2006). "The intestinal life cycle of *Bacillus subtilis* and close relatives." Journal of Bacteriology **188**(7): 2692-2700.

Tan, I. S. and Ramamurthi, K. S. (2014). "Spore formation in *Bacillus subtilis*." Environmental Microbiology Reports **6**(3): 212-225.

Tanghe, A., Van Dijck, P. and Thevelein, J. M. (2006). "Why do microorganisms have aquaporins?" Trends in Microbiology **14**(2): 78-85.

Tárnok, A. (2008). "SYTO Dyes and Histoproteins-Myriad of Applications." Cytometry Part A **73A**(6): 477-479.

Tavares, M. B., Souza, R. D., Luiz, W. B., Cavalcante, R. C., Casaroli, C., Martins, E. G., Ferreira, R. C. and Ferreira, L. C. (2013). "*Bacillus subtilis* endospores at high purity and recovery yields: optimization of growth conditions and purification method." Current Microbiology **66**(3): 279-285.

Thacker, P. A. and Baas, T. C. (1996). "Effects of gastric pH on the activity of exogenous pentosanase and the effect of pentosanase supplementation of the diet on the performance of growing-finishing pigs." Animal Feed Science and Technology **63**(1–4): 187-200.

Thanantong, N., Edwards, S. and Sparagano, O. A. (2006). "Characterization of lactic acid bacteria and other gut bacteria in pigs by a macroarraying method." Annals of the New York Academy of Sciences **1081**: 276–279.

Thompson, L. S., Beech, P. L., Real, G., Henriques, A. O. and Harry, E. J. (2006). "Requirement for the cell division protein DivIB in polar cell division and engulfment during sporulation in *Bacillus subtilis*." Journal of Bacteriology **188**(21): 7677-7685.

Torrallardona, D., Harris, C. I. and Fuller, M. F. (2003). "Pigs' gastrointestinal microflora provide them with essential amino acids." The Journal of nutrition **133**(4): 1127-1131.

Traag, B. A., Pugliese, A., Eisen, J. A. and Losick, R. (2013). "Gene conservation among endospore-forming bacteria reveals additional sporulation genes in *Bacillus subtilis*." Journal of Bacteriology **195**(2): 253-260.

Troussellier, M., Courties, C., Lebaron, P. and Servais, P. (1999). "Flow cytometric discrimination of bacterial populations in seawater based on SYTO 13 staining of nucleic acids." FEMS Microbiology Ecology **29**: 319-330.

Uccello, M., Malaguarnera, G., Basile, F., D'agata, V., Malaguarnera, M., Bertino, G., Vacante, M., Drago, F. and Biondi, A. (2012). "Potential role of probiotics on colorectal cancer prevention." BMC surgery **12**(Suppl 1): S35.

Ueckert, J., Breeuwer, P., Abee, T., Stephens, P., Nebe von Caron, G. and ter Steeg, P. F. (1995). "Flow cytometry applications in physiological study and detection of foodborne microorganisms." International Journal of Food Microbiology **28**: 317-326.

UniProt (2014, January 6, 2015). from <http://www.uniprot.org/uniprot/L8AJL5>.

Van Loosdrecht, M. C., Lyklema, J., Norde, W. and Zehnder, A. J. (1990a). "Influence of interfaces on microbial activity." Microbiological Reviews **54**: 75-87.

Van Loosdrecht, M. C. M., Norde, W. and Zehnder, A. J. B. (1990b). "Physical chemical description of bacterial adhesion." Journal of Biomaterials Applications **5**(2): 91-106.

van Melis, C. C., Nierop Groot, M. N. and Abee, T. (2011a). "Impact of sorbic acid on germinant receptor-dependent and -independent germination pathways in *Bacillus cereus*." Applied and Environmental Microbiology **77**(7): 2552-2554. doi: 2510.1128/AEM.02520-02510. Epub 02011 Jan 02528.

van Melis, C. C., Nierop Groot, M. N., Tempelaars, M. H., Moezelaar, R. and Abee, T. (2011b). "Characterization of germination and outgrowth of sorbic acid-stressed *Bacillus cereus* ATCC 14579 spores: phenotype and transcriptome analysis." Food Microbiology **28**(2): 275-283.

Van Oss, C. J., Chaudhury, M. K. and Good, R. J. (1988). "Interfacial Lifshitz-van der Waals and polar interactions in macroscopic systems." Chemistry Review **88**: 927-941.

Vasantha, N. and Freese, E. (1979). "The role of manganese in growth and sporulation of *Bacillus subtilis*." Journal of General Microbiology **112**(2): 329-336.

Veal, D. A., Deere, D., Ferrari, B., Piper, J. and Attfield, P. V. (2000). "Fluorescence staining and flow cytometry for monitoring microbial cells." Journal of Immunological Methods **243**(1-2): 191-210.

Vepachedu, V. R. and Setlow, P. (2007). "Role of SpoVA Proteins in Release of Dipicolinic Acid during Germination of *Bacillus subtilis* Spores Triggered by Dodecylamine or Lysozyme." Journal of Bacteriology **189**(5): 1565-1572.

Verma, N., Singh, N. A., Kumar, N. and Raghu, H. V. (2013). "Screening of different media for sporulation of *Bacillus megaterium*." Journal of Microbiology Research and Reviews **1**(4): 068-073.

Virto, R., Mañas, P., Álvarez, I., Condon, S. and Raso, J. (2005). "Membrane Damage and Microbial Inactivation by Chlorine in the Absence and Presence of a Chlorine-Demanding Substrate." Applied and Environmental Microbiology **71**(9): 5022-5028.

Vives-Rego, J., Resina, O., Comas, J., Loren, G. and Julia, O. (2003). "Statistical analysis and biological interpretation of the flow cytometric heterogeneity observed in bacterial axenic cultures." *Journal of Microbiological Methods* **53**: 43-50.

Vlamakis, H., Chai, Y., Beaugregard, P., Losick, R. and Kolter, R. (2013). "Sticking together: building a biofilm the *Bacillus subtilis* way." *Nature reviews. Microbiology* **11**(3): 157-168.

Vondruskova, H., Slamova, R., Trckova, M., Zraly, Z. and Pavlik, I. (2010). "Alternatives to antibiotic growth promoters in prevention of diarrhoea in weaned piglets: a review." *Veterinarni Medicina* **55**(5): 199-224.

Walker, R. and Buckley, M. (2006). Probiotic Microbes: The Scientific Basis. *American Academy of Microbiology*. Baltimore, Maryland, American Society for Microbiology.

Wallner, G., Amann, R. and Beisker, W. (1993). "Optimizing fluorescent in situ hybridization with rRNA-targeted oligonucleotide probes for flow cytometric identification of microorganisms." *Cytometry* **14**(2): 136-143.

Wang, D.-B., Yang, R., Zhang, Z.-P., Bi, L.-J., You, X.-Y., Wei, H.-P., Zhou, Y.-F., Yu, Z. and Zhang, X.-E. (2009). "Detection of *Bacillus anthracis* spores and vegetative cells with the same monoclonal antibodies." *PLoS One* **4**(11): e7810.

Want, A., Hancocks, H., Thomas, C. R., Stocks, S. M., Nebe-von-Caron, G. and Hewitt, C. J. (2011). "Multi-parameter flow cytometry and cell sorting reveal extensive physiological

heterogeneity in *Bacillus cereus* batch cultures." Biotechnology Letters **33**(7): 1395-1405.
doi: 1310.1007/s10529-10011-10566-z. Epub 12011 Mar 10522.

Warth, A. and Strominger, J. (1969). "Structure of the peptidoglycan of bacterial spores: occurrence of the lactam of muramic acid." Proceedings of the National Academy of Sciences **64**(2): 528-535.

Wilfart, A., Jaguelin-Peyraud, Y., Simmins, H., Noblet, J., van Milgen, J. and Montagne, L. (2007). "A step-wise in vitro method to estimate kinetics of hydrolysis of feeds." Livestock Science **109**(1-3): 179-181.

Wilfinger, W. W., Mackey, K. and Chomczynski, P. (1997). "Effect of pH and Ionic Strength on the Spectrophotometric Assessment of Nucleic Acid Purity." Biotechniques **22**(3): 474-481.

Wilson, W. W., Wade, M. M., Holman, S. C. and Champlin, F. R. (2001). "Status of methods for assessing bacterial cell surface charge properties based on zeta potential measurements." Journal of Microbiological Methods **43**(3): 153-164.

Winkelman, J. T., Blair, K. M. and Kearns, D. B. (2009). "RemA (Y1zA) and RemB (YaaB) regulate extracellular matrix operon expression and biofilm formation in *Bacillus subtilis*." Journal of Bacteriology **191**(12): 3981-3991.

Wuytack, E. Y. and Michiels, C. W. (2001). "A study on the effects of high pressure and heat on *Bacillus subtilis* spores at low pH." International Journal of Food Microbiology **64**(3): 333-341.

Wuytack, E. Y., Soons, J., Poschet, F. and Michiels, C. W. (2000). "Comparative study of pressure- and nutrient-induced germination of *Bacillus subtilis* spores." Applied and Environmental Microbiology **66**(1): 257-261.

Xing, Y., Li, A., Felker, D. L. and Burggraf, L. W. (2014). "Nanoscale structural and mechanical analysis of *Bacillus anthracis* spores inactivated with rapid dry heating." Applied and Environmental Microbiology **80**(5): 1739-1749.

Yang, C.-B., Li, A.-K., Yin, Y.-L., Huang, R.-L., Li, T.-J., Li, L.-L., Liao, Y.-P., Deng, Z.-Y., Zhang, J., Wang, B., Zhang, Y.-G., Yang, X., Peng, J. and Fan, M. Z. (2005). "Effects of dietary supplementation of cysteamine on growth performance, carcass quality, serum hormones and gastric ulcer in finishing pigs." Journal of the Science of Food and Agriculture **85**(11): 1947-1952.

Yardimci, O. and Setlow, P. (2010). "Plasma Sterilization: Opportunities and Microbial assessment Strategies in Medical Device Manufacturing." IEEE Transactions on Plasma Science **38**(4): 973-981.

Yi, X. and Setlow, P. (2010). "Studies of the commitment step in the germination of spores of *Bacillus* species." Journal of Bacteriology **192**(13): 3424-3433.

Young, S. B. and Setlow, P. (2003). "Mechanisms of killing of *Bacillus subtilis* spores by hypochlorite and chlorine dioxide." Journal of Applied Microbiology **95**(1): 54-67.

Zahavy, E., Fisher, M., Bromberg, A. and Olshevsky, U. (2003). "Detection of frequency resonance energy transfer pair on double-labeled microsphere and *Bacillus anthracis* spores by flow cytometry." Applied and Environmental Microbiology **69**(4): 2330-2339.

Zaman, M. S., Goyal, A., Dubey, G. P., Gupta, P. K., Chandra, H., Das, T. K., Ganguli, M. and Singh, Y. (2005). "Imaging and analysis of *Bacillus anthracis* spore germination." Microscopy Research Techniques **66**(6): 307-311.

Zeigler, D. R., Prágai, Z., Rodriguez, S., Chevreux, B., Muffler, A., Albert, T., Bai, R., Wyss, M. and Perkins, J. B. (2008). "The origins of 168, W23, and other *Bacillus subtilis* legacy strains." Journal of Bacteriology **190**(21): 6983-6995.

Zhang, J., Garner, W., Setlow, P. and Yu, J. (2011a). "Quantitative analysis of spatial-temporal correlations during germination of spores of *Bacillus* Species." Journal of Bacteriology **193**(15): 3765-3772.

Zhang, P., Garner, W., Yi, X., Yu, J., Li, Y. Q. and Setlow, P. (2010a). "Factors affecting variability in time between addition of nutrient germinants and rapid dipicolinic acid release during germination of spores of *Bacillus* species." Journal of Bacteriology **192**(14): 3608-3619. doi: 3610.1128/JB.00345-00310. Epub 02010 May 00314.

Zhang, P., Kong, L., Wang, G., Setlow, P. and Li, Y.-q. (2011b). "Monitoring the wet-heat inactivation dynamics of single spores of *Bacillus* species by using Raman tweezers, differential interference contrast microscopy, and nucleic acid dye fluorescence microscopy." Applied and Environmental Microbiology **77**(14): 4754-4769.

Zhang, P., Kong, L., Wang, G., Setlow, P. and Li, Y. Q. (2010b). "Combination of Raman tweezers and quantitative differential interference contrast microscopy for measurement of dynamics and heterogeneity during the germination of individual bacterial spores." Journal of Biomedical Optics **15**(5): 3494567.

Zhang, P., Liang, J., Yi, X., Setlow, P. and Li, Y.-q. (2014). "Monitoring of commitment, blocking, and continuation of nutrient germination of individual *Bacillus subtilis* spores." Journal of Bacteriology **196**(13): 2443-2454.

Zhang, Z., Jiang, B., Liao, X., Yi, J., Hu, X. and Zhang, Y. (2012). "Inactivation of *Bacillus subtilis* spores by combining high-pressure thermal sterilization and ethanol." International Journal of Food Microbiology **160**: 99-104.

Zhao, J., Krishna, V., Moudgil, B. and Koopman, B. (2008). "Evaluation of endospore purification methods applied to *Bacillus cereus*." Separation and Purification Technology **61**(3): 341-347.

Zhu, H., Hart, C. A., Sales, D. and Roberts, N. B. (2006). "Bacterial killing in gastric juice – effect of pH and pepsin on *Escherichia coli* and *Helicobacter pylori*." Journal of Medical Microbiology **55**(9): 1265-1270.

Zobell, C. E. (1943). "The effect of solid surfaces upon bacterial activity." Journal of Bacteriology **46**: 39-56.